PREDICTION OF THE IMMEDIATE EFFECT OF TRAFFIC ON FIELD SOIL QUALITIES

Ontvangen

2 8 JUNI 1994

UB-CARDEX

4095′

Promotor: ir. H. Kuipers
                   emeritus hoogleraar grondbewerking
Co-promotor: dr.ir. A.J. Koolen
                   universitair hoofddocent gronddynamica

P. Lerink

PREDICTION OF THE IMMEDIATE EFFECT OF TRAFFIC ON FIELD SOIL QUALITIES

Proefschrift

STELLINGEN

1. Als gevolg van het toepassen van brede lagedruk banden neemt de berijdingsintensiteit toe. Het nadelige effect van berijden op de fysieke bodemgesteldheid, gemeten in het spoor waar dit effect maximaal is, neemt daarbij af.

    Dit proefschrift.

2. Een nauwkeurig en handzaam instrument voor het bepalen van de vochttoestand van de bouwvoor is een onmisbaar hulpmiddel bij het kiezen van het juiste bewerkings-tijdstip en/of het voorspellen van de effecten van berijding.

    Dit proefschrift.

3. Voor het bepalen van het optimale bewerkingstijdstip is het te verwachten effect van berijding op de fysieke bodemgesteldheid het belangrijkste criterium.

    Dit proefschrift.

4. Bij het onderzoek van het verdichtingsproces van landbouwgrond door berijding bevindt de kennis van de bodemvervorming zich nog in een begin stadium.

    Dit proefschrift.

5. Bij verdichting van gestructureerde gronden als gevolg van berijding is het verband tussen het poriënvolume en de fysieke bodemgesteldheid niet eenduidig.

    Dit proefschrift.

6. Dit onderzoek heeft (opnieuw) aangetoond dat onze banden met Moeder Aarde niet van dien aard zijn dat wij ongelimiteerd druk op haar kunnen uitoefenen.

    H.J. van Dijk.

7. De tijd- en plaatsafhankelijke variabiliteit van de fysieke gesteldheid van de bouwvoor op perceelsniveau wordt vooral bepaald door de effecten van berijding.

8. Een auto werkt op zijn bestuurder als een morele kooi van Faraday.

9.   Het denkbeeldige weerstandspunt van een ploeg met lange risters ligt dichter bij het geploegde dan in het algemeen wordt aangenomen.

10.   Het feit dat jagers en vissers niet op gelijke voet bejegend worden komt vooral door het verschil in sociale status tussen beide groepen.

11.   Begripsvernauwing omvat al datgene dat te maken heeft met geestverarming na kennisverrijking. Aan begripsvernauwing ontsnappen alleen onderzoekers met hobby's.

W. Karsijns.

12.   De natuurlijke vruchtbaarheid, de geringe onkruiddruk en de goede vochthuishouding van de Nederlandse zavel- en kleigronden vormen een belangrijke basis voor duurzame landbouwsystemen.

voor Margriet

Abstract

Lerink, P. (1994)
Prediction of the immediate effect of traffic on field soil qualities. Ph.D. thesis, Department of Soil Tillage, Wageningen Agricultural University, The Netherlands, pp. 127, 22 figs, 16 tables, 129 refs, Dutch summary.

Field traffic by heavy machinery and transport vehicles is an integral part of modern arable crop production systems. The greater part of the field area is trafficked once or several times per year during the successive field operations. The traffic induced effect on the soil physical condition is often considered detrimental and must be minimized within the margins of practical and economical feasibility. The object of this study is to establish a strategy for prediction of the effects of traffic to be used on a farm scale.

The prediction method is based on a drastic limitation of the domain of prediction: a single field, two traffic systems, and two types of field operations. The effect of compaction by field traffic is expressed by so called soil qualities, i.e. soil physical properties which contain relevant information for the soil user. The soil condition at the time a certain field operation is performed is described by a single soil characteristic only: the gravimetric water content. Field traffic is characterized by the type of field operation and the type of traffic system. These characteristics are further described in terms of the tyre inflation pressure, the wheelload and the number of wheelings. The prediction functions, relating soil and traffic characteristics to the expected effect on soil qualities are established by means of a comparative method, and based on laboratory measurements on field compacted soil. The prediction functions are presented by means of extended M-P-V diagrams.

In the discussion of the experimental results, the significance of supplementary laboratory compaction methods are mentioned. Moreover, the extension of the prediction functions to situations beyond the domain considered in this study is briefly explored.

Additional keywords: soil compaction, field soil characteristics, traffic characteristics, prediction, physical soil properties.

CONTENTS

1 INTRODUCTION

The soil physical condition is only one of many factors determining the quality of agricultural field soils for crop production purposes. The physical condition of a field soil is not a constant, but changes continuously owing to man-induced and natural processes. In modern countries, the field activities by man are fully mechanized. In the Netherlands, scientific research on various aspects of soil-machine systems was started in 1959 by Emeritus Professor H. Kuipers at the Tillage Laboratory of the Wageningen Agricultural University.

Current knowledge of the mechanics of agricultural soil-machine interactions is systematically ordered by Koolen and Kuipers in their textbook "Agricultural Soil Mechanics" (1983). Soil-machine interactions are commonly divided into loosening processes and load bearing processes. Loosening processes are the result of soil engaging tillage tools, such as plough bodies, tines and discs. Koolen's dissertation "Soil Loosening Processes in Tillage; Analysis, Systematics and Prediction" (1977) reflects the comparatively high level of knowledge on soil loosening processes.

Load bearing processes are the result of surface applied loads by field traffic and certain tillage implements, such as rollers and packers. A comprehensive inventory of knowledge on the mechanics of load bearing processes was presented by Tijink in his dissertation entitled "Load Bearing Processes in Agricultural Wheel Soil Systems" (1988).

Knowledge on wheel-soil systems has resulted in a great number of prediction models. These models serve many purposes, such as to enhance the understanding of the principles governing wheel-soil interaction for scientific, advisory and educational purposes, to aid the design of agricultural tyres and machinery and to serve government policy. The object of this study is to establish a strategy for prediction on a farm scale.

Soil processes induced by field traffic are commonly denoted by the generic term "compaction". Owing to compaction, the soil physical condition changes in a manner often considered as undesirable. The physical condition of compacted soil can be described by a wide variety of soil physical properties. In prediction models

11

presented thus far, the effect of compaction on the soil physical condition is commonly expressed in terms of packing state properties, such as the dry bulk density and the pore space. In this study, information on the effect of compaction on these rather abstract quantities is extended with information on soil physical properties which describe the physical quality of a field soil as a growing and working medium. These soil properties are further denoted as "soil qualities". Examples of soil qualities are water and air conductivities, water retention characteristics and the penetration strength.

On the longer term, the effects of field traffic on the soil condition are impaired by the effects of natural soil processes. The study presented here only deals with the effects which are fully attributed to field traffic. These effects are referred to as the "immediate effects" of field traffic.

The world-wide concern about the adverse effects of field traffic, which are believed to cause a persistent degradation of the soil physical quality, has resulted in research on alternative traffic systems. A recent development are agricultural tyres featuring relatively low tyre to ground contact pressures. In the Netherlands, a multi-disciplinary research project was organized by the Institute of Agricultural Engineering (IMAG), in cooperation with the Wageningen Agricultural University (WAU), the Research Station for Arable Farming and Field Production of Vegetables (PAGV), the former Institute for Soil Fertility (IB) and the Winand Staring Centre for Integrated Land, Soil and Water Research (SC). The object of this research group was to investigate "The Perspectives of Reducing Soil Compaction by using a Low Ground Pressure Farming System". The research project was supported by the Directorate General for Agriculture of the European Community[1]. In 1984, a large scale field experiment was started on the IMAG experimental station "Oostwaardhoeve". The experiment ended in 1989. The study presented here was conducted within the framework established by this research project.
Research on various aspects of traffic-soil interaction has resulted in a number of publications in which the author of this thesis participated. Copies of these publications are inserted as appendices to this thesis. This thesis covers the contents of the distinct research projects and reflects their mutual coherence.

---

[1]Community Programme for the Coordination of Agricultural Research, Programme Land and Water Use Management, Research Contract N° 5910.

The development of a prediction method which is applicable on a farm scale raises a specific problem, being the scarcity of information on factors which control the effect of compaction. In chapter 3 "Introduction to the systematics of field traffic and the field soil condition" it is discussed how this problem can be overcome.

An arable field is trafficked several times per year. The occurrence of field traffic, the machinery that is involved and the factors which control the effect on the soil condition are dealt with in chapter 4, entitled: "Systematics of field traffic".

The effect of a specific traffic event on the soil condition depends on the soil condition at the time of traffic. Soil factors which control the traffic-induced effect on the soil condition, as well as their seasonal and inter-seasonal fluctuation are discussed in chapter 5, entitled: "Systematics of the field soil condition".

In order to develop a prediction method, three questions have to be answered: "What should be predicted"; "From what should be predicted" and; "How should be predicted". These questions are dealt with in chapter 6, entitled: "The method of prediction".

In chapter 7, the experiments are described to collect data required to transform a general prediction function into specific prediction functions and to verify the assumptions that underlie the prediction method. Chapter 7 is entitled: "Prediction functions based on observations on traffic compacted soil".

In chapter 8, entitled: "Laboratory simulation of the effects of compaction by field traffic", a laboratory method is discussed which aims to simulate the effects of field traffic on the soil condition and serves to support the analysis of the field experiments.

The prediction functions developed in Chapter 7 only apply to a limited domain. In chapter 9, entitled "The extensibility of the prediction method", it is discussed how the domain of prediction can be extended to situations for which the prediction functions are not explicitly defined.

Chapter 10 "Conclusion" includes a critical contemplation of the merits of the prediction method.

3   INTRODUCTION TO THE SYSTEMATICS OF FIELD TRAFFIC AND THE FIELD SOIL CONDITION

Compaction by field traffic is defined as the soil process induced by the load applied by running gear. The effect of compaction is a modified soil state in the zone of interference. Factors which control the effect of compaction are called process characteristics. These process characteristics refer to the initial soil state and to field traffic. Traffic-induced compaction is presented schematically in Fig. 1.
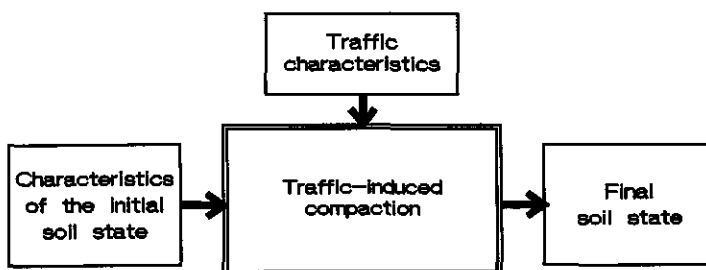
Fig. 1. Schematical presentation of traffic-induced compaction.

The effect of compaction, as a function of pertinent soil and traffic characteristics, can be expressed by the following equation:

$$Y = F(x_1, x_2, \ldots\ldots, x_n) \tag{1}$$

with:
    Y = the effect of compaction
    x_i = traffic and soil characteristics
    F = function relating Y to x_i

The reconnoitring phase of Agricultural Soil Mechanics revealed a large number of traffic and soil characteristics (x_i) pertinent in determining the effect of compaction. In the descriptive phase, several relationships and more sophisticated models (F) were established relating traffic and soil characteristics to the effect of

compaction. The effect of compaction (Y) is commonly defined in terms of packing state properties, such as the dry bulk density. The intellectual framework was based on deterministic concepts. The application of this field of knowledge for prediction on a routine base raises as a specific problem the large number of traffic and soil characteristics involved and the scarcity of easily accessible information on traffic and soil characteristics.

A key to unlock relevant information on traffic and soil characteristics is a system-approach to field traffic in agricultural practice. The significance of the system-approach is based on the order that underlies field traffic and the soil state during field traffic. Owing to this order, factors which control compaction are to a great extent system-defined. The system-approach drastically reduces the number and the variability of the process characteristics involved.

The global traffic-soil system is governed by three sets of variables, which refer to management, environment and soil, respectively. Factors related to management comprise amongst others the crop rotation, the cultivation system, the level of mechanization and the skill of the farm manager. Important environmental factors are the climate, the position on the landscape and the depth of the water table. Soil texture and structure are important soil factors.

On the next hierarchical level, the factors mentioned above are more or less intrinsic to the traffic-soil system. A sub-system within the global traffic-soil system which satisfies this condition is a single field, as a management unit, a geometrical unit within a given environment, and a soil unit with limited textural and structural variation.

In chapter 4 and 5, the systematics of field traffic and the field soil condition are analyzed within the homogeneous setting of factors related to management, environment and soil of a single field. In addition, system-defined soil and traffic characteristics will be identified.

4.1 Preliminary remarks

Prior, during and after the growing season a variety of field activities is carried out on an arable field in behalf of soil and crop management. The following activities can be distinghuised:
-        amelioration of the soil physical condition, including amelioration of the arable layer (primary tillage), seedbed and plantbed preparation (secondary tillage), and post harvest tillage (tertiary tillage);
-        amelioration of the soil fertility, including fertilizing and manuring;
-        sowing or planting;
-        crop nursery, such as weed control, pest control and ridging of potato beds;
-        harvesting, including transport;
-        crop residue treatments, such as straw chopping and bailing.

On modern farms, in countries with a high standard of living, these field activities are fully mechanized. Mechanized field practices which comprise one or a combination of these elemental activities are further referred to as field operations. Apart from the harvest, most field operations involve a single pass of a tractor with a mounted implement. In some occasions, tractor and implement form an integrated unit such as a combine harvester for cereal crops.

The analysis of the systematics of field traffic encompasses four items: the occurrence, the time and spatial aspects of field traffic and traffic characteristics. The occurrence of field traffic (§ 4.2) refers to the distinct field operations that are carried out on a field, including the type of machinery that is used. Some parts of a field are not trafficked at all, while other parts receive a great number of passes. The spatial distribution of field traffic is discussed in § 4.3. Factors which determine the planning of field operations are important with respect to the soil condition at the time of traffic, and will be dealt with in § 4.4. In § 4.5 an analysis is given of traffic factors which are pertinent in determining the effect of field traffic on the soil condition.

Despite a great degree of standardization, traffic systems differ from place to

place, on a national, regional and even local scale. Some factors which are responsible for this are: tradition, level of mechanization, farm size, soil type, type of crop rotation and climatical factors. In this study, the systematics of field traffic explicitly refers to the traffic system that was applied on the HGP/LGP-experimental field. This traffic system objects to be representative for the situation on 60 ha arable farms on medium textured soils in the Netherlands.

An important source of information for the analysis of the systematics of field traffic were the state-of-the-art reports and reviews by Barnes et al. (1971), Chancellor (1976), Soane et al. (1981a; 1981b; 1982), Taylor and Gill (1984), Soane (1985) and Håkansson et al. (1988).

4.2 The occurrence of field traffic

During a year, a number of field operations are performed before, during and after a growing season. The type of machinery that is involved, given a certain assortment of agricultural machinery or "level of mechanization", and given a certain farming system mainly depends on the soil type and the type of crop. The size of the machinery, i.e. the working width of implements, the maximum pay load of trailers and the engine power of tractors, is mainly determined by the farm size.

The respective field operations that are performed on a given field, including the type of machinery that is used, can be listed as a field operation record. The sequence of field operations corresponds with the cyclic nature of a crop rotation. A field operation record is thus determined by the soil type, the farm size, the crop rotation, the farming system and the level of mechanization. Apart from the soil type these factors are to a more or lesser extent variable in time. After decades of increasing tractor engine power, increasing working width of implements and increasing capacity of trailers, current developments are primarily meant to increase the effectiveness of a field operation and to facilitate the operation of tractors and implements.

Table 1 presents a list of field operations, including the machinery that is involved, which are carried out on the HGP/LGP experimental field. The crop rotation consists of ware potatoes, winter wheat, sugarbeet and onions. The management of the experimental field, in terms of the type of crop rotation, the farming system, the type of machinery and operational characteristics (such as the working depth

Table 1. Record of field operations on the experimental "HGP/LGP" field.

Field operation	Machinery
a) Potatoes	
fertilizing	tractor/fertilizer spreader
secondary tillage	tractor/rotary cultivator
planting	tractor/potato planter
crop nursery:	
ridging	tractor/inter row cultivator
spraying (herbicides)	tractor/sprayer
spraying (fungicides) 10x	
spraying (insecticides)	
harvest:	
chemical leaf killing	tractor/sprayer
defoliation, digging and	tractor/haulm topper/potato digger
loading	tractor/potato loader
transport	tractor/trailer
tertiary tillage	tractor/tine cultivator
primary tillage	tractor/rotary digger(/rotary cultivator/sowing machine)
b) Winter wheat	
secondary tillage/sowing	(tractor/rotary digger/)rotary cultivator/sowing machine
fertilizing 2x	tractor/fertilizer spreader
grass undersowing	tractor/sowing machine
crop nursery:	
spraying (herbicides)	tractor/sprayer
spraying (fungicides)	tractor/sprayer
harvest	combine harvester/straw chopper
spraying (herbicides)	tractor/sprayer
fertilizing	tractor/fertilizer spreader
primary tillage	tractor/reversible plough
c) Sugarbeet	
fertilizing	tractor/fertilizer spreader
secondary tillage	tractor/reciprocating harrow
sowing	tractor/precision sowing machine
crop nursery:	
spraying (herbicides) 2x	tractor/sprayer
mechanical weeding	tractor/hoe
harvest:	
defoliation and digging	tractor/leaf chopper/sugarbeet digger
loading	tractor/sugarbeet loader
transport	tractor/trailer
tertiary tillage	tractor/tine cultivator
primary tillage	tractor/reversible plough
d) Onions	
fertilizing	tractor/fertilizer spreader
secondary tillage	tractor/reciprocating harrow
sowing	tractor/precision sowing machine
crop nursery:	
spraying (herbicides) 2x	tractor/sprayer
spraying (fungicides) 6x	tractor/sprayer
mechanical weeding	tractor/hoe
harvest:	
defoliation/digging	tractor/adapted potato digger
loading	tractor/adapted potato loader
transport	tractor/trailer
manuring	tractor/slurry tank
tertiary tillage	tractor/tine cultivator
primary tillage	tractor/reversible plough

and the working speed), is typical for 60-ha crop farms in the Netherlands on medium textured soils.

4.3 Spatial aspects of field traffic

The regular features of the spatial distribution of field traffic are referred to as traffic patterns (Soane, 1985). A traffic pattern divides a field into three areas: two so called head lands of approximately 10 m width, which are positioned on the shortest sides of a rectangular field, and an area in between the head lands. The head lands are intensively trafficked for turning and transport purposes. The adverse effects of traffic on the head lands on the crop development are often visual. The traffic pattern on the area in between the head lands normally consists of parallel tracks. The position of these tracks follows from the wheel spacings and the effective working width. The tyre width determines the width of the tracks. Field traffic during sowing, crop nursery and the harvest of row crops is restricted to certain inter-row areas. The positions of the traffic patterns of field operations before and after the growing season are mutually independent. Despite this Lumkes (1984) found that a large number of the wheel passes are super-imposed.

Alternative traffic systems, designed to reduce the total field area covered with tracks, are the controlled traffic system and the zero-traffic system. According to the controlled traffic system, the traffic patterns of distinct field operations are synchronized. In the Netherlands, the perspectives of reducing the adverse effects of traffic-induced compaction by applying a controlled traffic system were studied by the "The Westmaas Research Group on Alternative Tillage Systems" (Boone, ed., 1984).

A zero-traffic system divides a field into production zones and permanent traffic lanes. Intensive experimentation was carried out on zero-traffic systems in the US (the former NTLM), Israel, Japan, the Netherlands (IMAG/PAGV), Germany and the UK (NIAE), using wide frame gantries and conventional agricultural machinery with extended wheel spacings. Reviews on zero-traffic systems are given by Taylor (1981) and Cooper et al. (1983). From a scientific point of view these experiments are of great importance as they provide a reference level for the quantification of the traffic induced effects on the soil condition and the crop production potential. So far, controlled traffic and zero traffic systems have not found acceptance in agricultural practice.

Table 2. Traffic intensity [-] of the distinct field operations of the HGP and LGP traffic systems.

Field operations	Traffic system	
	HGP	LGP
a) Potatoes		
fertilizing	0.08	0.11
secondary tillage	0.31	0.43
planting	0.16	0.23
crop nursery:		
ridging	0.16	0.23
spraying (12x)	0.02	0.03
harvest:		
chemical leaf killing	0.02	0.03
defoliation and digging	0.32	0.47
loading	0.44	0.55
transport	0.55	0.68
tertiary tillage	0.31	0.43
primary tillage	0.31	0.43
b) Winter wheat		
secondary tillage/sowing[*)]	-	-
fertilizing 2x	0.08	0.11
grass undersowing	0.16	0.23
crop nursery:		
spraying (2x)	0.02	0.03
harvest	0.17	0.23
spraying (herbicides)	0.02	0.03
fertilizing	0.08	0.11
primary tillage	0.63	0.78

[*)] secondary tillage and sowing were combined with primary tillage.

Field operations	HGP	LGP
c) Sugarbeet		
fertilizing	0.08	0.11
secondary tillage	0.24	0.33
sowing	0.08	0.12
crop nursery:		
spraying (2x)	0.02	0.03
mechanical weeding	0.08	0.12
harvest:		
defoliation and digging	0.16	0.23
loading	0.16	0.23
transport	0.28	0.34
tertiary tillage	0.31	0.43
primary tillage	0.63	0.78
d) Onions		
fertilizing	0.08	0.11
secondary tillage	0.24	0.33
sowing	0.11	0.16
crop nursery:		
spraying (8x)	0.02	0.03
mechanical weeding	0.08	0.12
harvest:		
defoliation and digging	0.32	0.47
loading	0.44	0.55
transport	0.55	0.68
manuring	0.12	0.12
tertiary tillage	0.31	0.43
primary tillage	0.63	0.78

A quantitative expression of the traffic pattern is the proportion of field area covered with wheel tracks. This characteristic of a traffic system is called the traffic intensity. Observations on the traffic intensity are reported by Arndt and Rose (1966), Eriksson et al. (1974), Voorhees (1977), Lumkes (1984) and Van de Zande (1991) and involved a variety of crops, cultivation systems and mechanization levels. Important conclusions were that the traffic intensity decreases at increasing size of farm machinery (working width and engine power) and that the traffic intensity of seed crops is low compared to root crops. The traffic intensities of the distinct field operations carried out on the HGP/LGP experimental field are given in Table 2 (data: Klooster, IMAG). The traffic intensities were calculated as the width of the widest tyre following a track divided by half the working width (small implement wheels were omitted).

From Table 2 the following general conclusions can be drawn:
1.   The traffic intensity of primary tillage, secondary tillage and the harvest of rootcrops is relatively high.
2.   The intensity of field traffic for seed crops is relatively low.
3.   Using wider tyres (LGP-traffic system) considerably increases the traffic intensity.

4.4 Time aspects of field traffic

For each crop a time table can be established, to schedule the distinct field operations that are involved. A time table thus consists of a sequence of time-intervals which indicate the timing of the distinct field operations for optimal crop production potentials under normal weather conditions. The setting of the distinct time-intervals primarily depends on the type of crop, the soil type, the climate and the growing stage. As far as the soil type is concerned, distinction is made between autumn-ploughed soils and soils which are ploughed in spring. Uncritically, soils with a clay content higher than 20% are classified as autumn-ploughed soils in the Netherlands (pers. comm. Van Ouwerkerk, 1990). The HGP/LGP experimental field is autumn-ploughed.
The time tables of the main field operations of the crops grown on the HGP/LGP experimental field are presented in Table 3.

The timing of a particular field operation by the farmer is, apart from the available time, based on the soil condition, the weather forecast and the date with reference

to the corresponding time-interval. The actual timing of a field operation determines the timeliness of a field operation.

In this context, the timing of field operations is of interest in relation to the corresponding soil condition. The importance of the soil condition in determining the timing of a field operation on a particular field depends on the type of field operation. Each field operation comprises a unique set of distinct soil-machine interactions. To this respect, distinction can be made between soil-wheel interaction and the interaction between the soil and the soil working implements. Soil working implements comprise implements that are explicitly designed for soil tillage, such as a plough and a tine cultivator, as well as soil working tools of equipment that implicitly involve some soil working, such as sowing coulters, discs of planting machines and the shares and sieve belts of harvest machinery for root crops.

Table 3. Optimal time intervals for some field operations in the Northern regions of the Netherlands (data: Klooster, IMAG).

Field operation	Crop			
	Potatoes	Winterwheat	Sugarbeet	Onions
secondary tillage	4 - 2/3[)]	10 - 2	4 - 1	3 - 4
sowing/planting	4 - 2/3	10 - 2	4 - 1	3 - 4
harvest	9 - 3/4	9 - 1	10 - 3/4	9 - 3
tertiary tillage	9 - 3/4		10 - 3/4	9 - 3
primary tillage	10 - 2	10 - 3	11 - 2	10 - 2

[)] month - week

In order to qualify the suitability of the field soil condition for a field operation, the terms "trafficability" and "workability" are used, which refer to soil-wheel interaction and the interaction of soil and soil working implements, respectively. Here, trafficability refers to soil factors which determine the mobility of a vehicle. The term workability is used to qualify the suitability of the soil for soil working.

In temperate regions, problems concerning the trafficability can occur when the soil strength does not permit high tractive forces, as in the case of ploughing and the harvest of root crops and maize under extremely wet soil conditions.

The timing of field operations which do not involve soil working, such as spraying operations and the harvest of seed crops, is virtually independent of the soil

condition in the corresponding time-interval as long as the field soil is trafficable. The timing of soil tillage operations, i.e. field operations that are explicitly meant for soil working, such as ploughing, seedbed preparation and the ridging of potato beds, is mainly based on the soil workability. At seedbed preparation and the ridging of potato beds, the soil workability refers to the ability of the more or less cohering topsoil layer to break into small structural elements, without smearing during the breaking process and the subsequent re-arrangement. The soil workability at ploughing refers to the ability of cohering soil to break into coarse fragments.

The timing of field operations which implicitly involve some soil working, such as sowing or planting and the harvest of root crops also depends on the soil condition, since the soil-tool interaction affects the quality of the work. Problems associated with soil-tool interaction are excessive sticking of soil on the sowing coulters and limited sievability under extremely wet soil conditions.

As will be detailed in § 5.4, the variability of the soil condition of a given field during the time-interval a certain field operation is preferably performed is governed by the soil water status. The range of soil water contents at which a field operation can be performed with a satisfying result depends on the type of field operation. Of the soil tillage operations, the range of soil water contents at which seedbed preparation can be carried out is relatively small as compared to the range of water contents at which the soil can be ploughed. In practical situations, ploughing is carried out as long as the field soil is trafficable. Field operations which implicitly involve soil working are carried out at a wide range of soil water contents as compared to seedbed preparation. The timing of field operations which do not involve soil working is less dependent of the soil water content as long as the soil is trafficable.

The range of water contents at which a field operation can be performed on a particular field may vary from year to year due to variation of the soil structure.

The range of soil water contents at which the respective field operations can be carried out, including the frequency of occurrence determines the number of workable days for the respective field operations and indicate the suitability of a field for soil management.

The opinion of the farmer on the suitability of the field soil condition for a particular

23

field operation is based on visual inspection and on touch. His reference system is experience. The effectiveness of this prediction method is based on the fact that, if a farmer decides to start a field operation, he can immediately verify the consequences. (Despite this, it is common experience that once a farmer starts a field operation he will only stop when the continuation is technically impossible. This may be associated to the farmers wish, and in some occasions, the need to treat a field as a whole at once). The scientific interest on soil-related aspects of the workability concerns among others the explanation of the soil physical phenomena governing workability (Koolen et al., 1987), the soil hydraulical factors governing workability (Van Wijk, 1987) and soil management factors affecting the number of workable days (Spoor and Godwin, 1984).

So far, machine-soil related aspects of the timing of field operations were discussed without considering the effects of the wheelings on the resulting soil condition. Although farmers are aware of the adverse effects of field traffic at wet soil conditions, they generally do not base the timing of field operations on limitation of these adverse effects. An exception to this rule is the timing of field operations that can be carried out on a frozen soil surface. For instance in the Netherlands, the spreading of fertilizer and the spreading of lime and manure at the end of the winter (February, March) are preferably performed on frozen ground.

In the absence of more detailed information, farmers base their opinion on the effects of field traffic on the soil condition on the rut depth, being the single available immediate indicator of the effect of field traffic. With the object to limit the adverse effects of field traffic by limiting the rut depth (and also to preserve field surface levelness), cage wheels or dual wheels are mounted on tractors with standard tyre equipment.

In Fig. 2 the actual timing of the main field operations on the HGP/LGP experimental field are schematically presented with reference to the optimum time intervals. From Fig. 2 it follows that:
1.   The time intervals for seedbed preparation, sowing/planting of potatoes, sugarbeet and onions partly overlap and span approximately four weeks.
2.   The actual timing of seedbed preparation, sowing/planting varied little between years.
3.   The actual timing of seedbed preparation, sowing/planting exceeded the optimal time intervals with approximately 2 weeks.
4.   The yearly timing of the harvest of root crops, as well as tertiary and

primary tillage varied considerably.
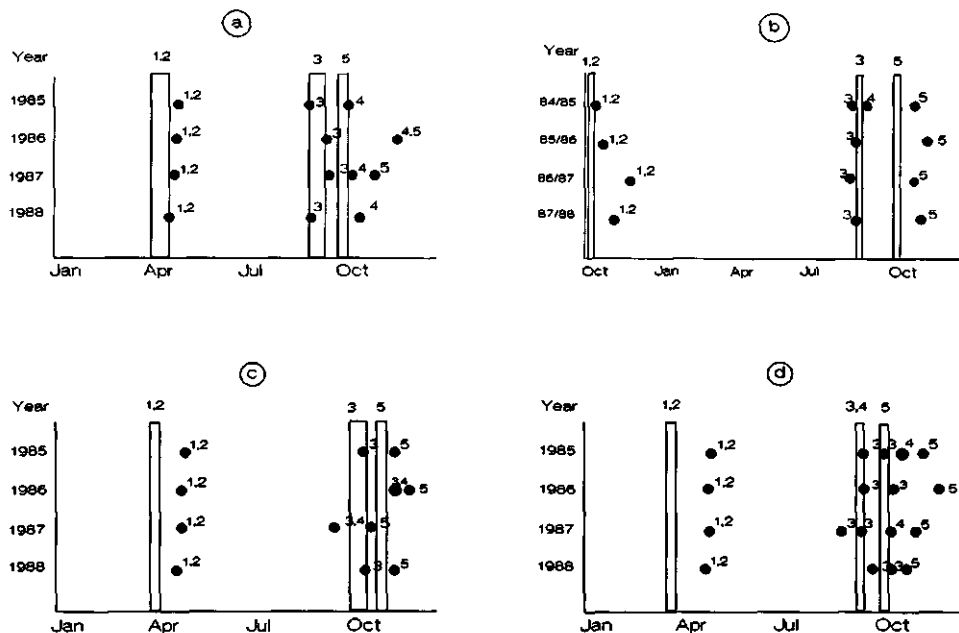
Fig. 2. *The actual timing of important field operations on the HGP/LGP experimental field. Bars indicate optimal time intervals (a: potatoes; b: winterwheat; c: sugarbeet; d: onions; 1: sec. tillage; 2: sowing/planting; 3: harvest; 4: tert. tillage; 5: primary tillage).*

The complexity of the management of the experimental field entails that the actual timing of field operations is based on organizational factors rather than on the suitability of the field soil. As a result, the yearly variation of the soil condition at the time a certain field operation is performed may be greater than in agricultural practice.

4.5. Factors determining the compaction capability of field traffic

4.5.1 Preliminary remarks

During the passage of a vehicle involved in a field operation load, and traction and

steering forces are transferred to the soil by pneumatic rubber tyres. In some countries, e.g. Russia and Italy, tracked vehicles are widely used. Occasionally, cage wheels are used in addition to tractor rear tyres. A detailed description of agricultural tyres, including tyre construction, size specifications and tread patterns, is given by Koolen and Kuipers (1983) and Tijink (1988).

Agricultural tyres are divided into driven and undriven tractor tyres and implement/trailer tyres. Important tyre properties are: maximum allowable wheel load, tyre size, inflation pressure, maximum travel speed and carcass strength. The mutual correlation between these properties is given in Table 4.

Table 4. Mutual correlation between tyre properties.

	wl	ts	ip	trs	cs
max. wheelload		+	+	-	+
tyre size	+		-	+	-
inflation pressure	+	-		+	-
max. travel speed	-	+	+		+
carcass strength	+	+	-	+	

For a given tyre (tyre size and carcass strength), the maximum wheelload and the maximum travel speed at varying tyre inflation pressure are specified by the tyre manufacturer.
Until recently, the choice of a tyre was predominantly based on its performance regarding load carrying, traction and steering. The growing concern about the adverse effects of field traffic on the soil condition emphasized the importance of tyre properties which are related to the effect on the soil condition.

Agricultural tyres transfer forces via the momentaneous tyre-soil contact surface to the soil mass. The tyre-soil interference can be uniquely described in terms of contact surface properties, including the dimensions and the stress state, the loading time and the number of load repetitions. Any factor affecting these properties also affects the stress regime in the soil mass and thus affects the compaction process to a more or lesser extent. Traffic factors which are pertinent in determining the nature of the contact surface and consequently the compaction process are further referred to as field traffic characteristics.

26

4.5.2 Traffic characteristics

Literature on soil-wheel systems reveals a great number of studies on the effect of distinct traffic characteristics on different aspects of the compaction process. Various methods of testing are applied, such as scale model testing, single wheel testing and full scale testing, using driven or undriven rigid wheels or commercial tyres. The tests are conducted on prepared soils in the laboratory or in outdoor soil bins, and in field situations resembling agricultural practice. The effects on the soil condition are measured directly, by observing the effects on relevant soil properties, or indirectly by stress measurements. To this latter respect, pressure gauges are mounted on the surface of rigid wheels or tyres, embedded in a rigid supporting surface or in the soil mass. From these sources, the following traffic characteristics are extracted and ordered with reference to vehicle, wheel, tyre and operational characteristics.

Vehicle characteristics: number of axles; factors controlling the dynamic weight distribution on the respective axles, such as the static weight distribution; implement factors determining the torque of driven wheels, such as the working width of soil working implements; axle widths and axle spacings;

Tyre characteristics: tyre inflation pressure; tyre dimensions (see Fig. 3a) such as the overall diameter (D), the rim diameter (d), the section width (b) and the section height (h), the aspect ratio (h/b); tyre construction properties (see Fig. 3b), including the number of plies (P) or the ply rating (PR), the direction of the plies (radial or cross ply), the type of tread pattern (tractor type, trailer/implement type);

Wheel characteristics: driven or undriven; towed or trusted; steered or non-steered;

Operational characteristics: working depth of implements; travel speed; weight of cargo; the effective working width; percentage wheel slip.

The significance of some important traffic characteristics in determining the compaction capability is explained here after.
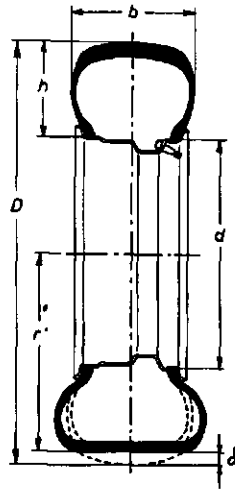
Fig. 3a. Tyre dimensions.
(b = tyre section width; D = overall tyre diameter; d = rim diameter; δ =
tyre deflection; h= tyre section height; r' = static loaded radius)(from Tijink,
1988).

radial ply   cross ply
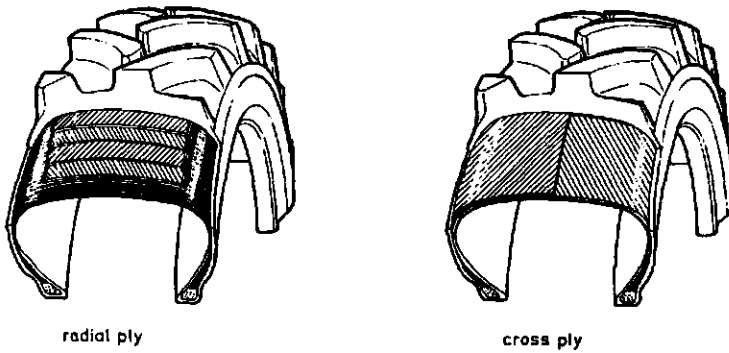
Fig. 3b. Tyre construction properties (from Tijink, 1988).

1. Inflation pressure
When a balloon, inflated at a certain pressure p_i is pushed with a force F against a rigid surface, it deflects and forms a circular contact surface. If the wall stiffness of the balloon is negligible, it follows that:

$$p_c = p_i \hspace{4cm} [2]$$
and:
$$A = F/p_i \hspace{4cm} [3]$$
with:

$\hspace{1cm} p_c$ = normal stress in the contact surface;

$\hspace{1cm} A$ = contact area.

The stresses in the contact surface are evenly distributed.

Conclusion: the normal stress in the contact surface equals the inflation pressure.

2. Load
When the force F is replaced by a force F', and F' > F, deflection and consequently the contact area increase. The stress in the contact surface remains however the same. Thus:

$$p_c' = p_i \hspace{4cm} [4]$$
$$A' = F'/p_i \hspace{4cm} [5]$$

Conclusions:
- the contact area increases as the load increases;
- the normal stress in the contact surface is independent of the load applied on the balloon.

3. Carcass stiffness
The effect of the carcass stiffness can be explained by replacing the balloon by a football. Due to the wall stiffness deflection decreases, hence:

$$A < F/p_i \hspace{4cm} [6]$$
$$p_c > p_i \hspace{4cm} [7]$$

Furthermore the stresses in the contact surface are no longer evenly distributed. To account for the carcass stiffness of agricultural tyres the following rule of thumb is proposed by Koolen and Kuipers (1983):

$$p_m \approx 1.3 * p_i \qquad\qquad [8]$$

with:

p_m = average normal pressure in the contact surface.

The carcass stiffness of tyres depends on the number of plies and the type of carcass construction (radial or cross ply).

4. Torque

When the surface is pulled aside, while the football is kept in place, tangential or shear stresses will develop in addition to the normal stress owing to F. The contribution of the shear stress is accounted for by the following rule of thumb (Koolen and Kuipers, 1983):

$$\sigma_1 \approx 1.5 * p_m \qquad\qquad [9]$$

or, by replacing p_m by p_i (eq. [8]):

$$\sigma_1 \approx 2 * p_i \qquad\qquad [10]$$

with:

σ_1 = first principal stress, i.e. the highest stress acting on an elemental soil volume near the contact surface.

The significance of σ_1 in compaction is dealt with in § 5.3.2.

In the literature, frequent use is made of equations proposed by Fröhlich (1934) to explain the relationship between contact surface characteristics and the stress state in the soil mass under a tyre. The Fröhlich equation applies to the stress distribution in a perfectly elastic medium loaded by a circular rigid plate. The local stress state is described in terms of the vertical normal stress σ_z. The following general rules are based on the Fröhlich equations:

1. σ_z gradually decreases with depth.
2.   At a given depth, σ_z attains its maximum value under the centre of the circular contact surface.
3.   The decrease of σ_z with depth depends on the size of the contact surface, i.e. the greater the contact surface the lower the decrease of σ_z with

depth. Rule of thumb:

$$\sigma_z = 1/2 * p_i, \text{ at } z = 1/2 * \text{tyre width} \qquad [11]$$

From 1 and 3 it follows that:
4. The stress state near the tyre-soil contact surface is predominantly determined by the tyre inflation pressure, and:
5. The stress state at greater depths, say at a depth of approximately half the tyre width, is predominantly determined by the wheel load. Both theoretical (Söhne, 1958) and experimental (Taylor et al., 1980; Blackwell and Soane, 1981) evidence exists, that the wheelload is an important factor in determining the compaction capability of a tyre at greater depths.

Combined stress measurements and stress computations (based on the Fröhlich equations) by among others Koolen et al. (1992), Van den Akker and Van Wijk (1986), Smith and Dickson (1984), Bolling and Söhne (1982), Gupta and Larson (1982) and Söhne (1953) confirm these general rules of thumb.

5. Repeated loading
The number of loading cycles may amount from two (e.g. during primary, secondary and tertiary tillage) to more than ten (e.g. during the harvest of potatoes). The effect of multiple loading cycles on the compaction process can be explained by considering the rut depth.

Under relatively dry soil conditions, the rut depth after repeated loading is primarily determined by the wheeling featuring the highest compaction capability (i.e. the highest wheelload and/or the highest inflation pressure). Under relatively wet conditions, each wheeling causes an increase of the rut depth and, consequently, a change of the soil state under the rut. Under intermediate soil moisture conditions, each successive wheeling causes an ever decreasing increase of the rut depth.

These phenomena can be explained in their turn by considering the change of the soil strength upon compactive loading. To this respect, distinction can be made between the strength hardening process type and the flowing type. Compaction of a dry soil mainly features volume reduction, i.e. an increase of the packing density of soil particles. The increase of the packing density is normally attended by an increase of the resistance to further volume reduction. This soil process is

31

referred to as the strength hardening process type (Koolen 1986). Compaction of a wet soil mainly features distortion or, in other words, flow, i.e. a rearrangement of soil particles without considerable volume reduction. As opposed to volume reduction, distortion is not attended by a considerable increase in soil strength. In § 5 the principles of the strength hardening and flowing processes are further detailed.

Studies on repeated loading are reported by Raghavan (1976), Braunack (1986) and Kayambo and Lal (1986).

6. Working speed
The driving speed is known to affect the compaction process (Baganz, 1963/64; Stafford and de Carvalho Mattos, 1981; Kuipers, 1986; Horn et al., 1989), especially in case the flowing process prevails. This is attributed to inertia forces and the delayed movement of water through the soil matrix. In agricultural practice, the driving speed of a given field operation varies little. Hence the working speed is, in this context, considered of minor importance.

Among scientists consensus exists on the fact that the tyre inflation pressure, the wheelload and the number of wheelings are the most important factors determining the compaction capability of field traffic. The tyre inflation pressure and the wheelload are commonly associated with topsoil and subsoil compaction, respectively.

A drastic reduction of the number of traffic characteristics can be achieved by considering only one set of farm machinery, with given operational characteristics (e.g. the working depth of tillage tools). In the following section the traffic characteristics of the machinery used on the HGP/LGP experimental field will be further specified.

4.5.3 Traffic characteristics of a given set of farm machinery

The comparison of traffic characteristics is based on the tyre inflation pressure, the wheelload and the number of wheelings.

Table 5 presents the tyre inflation pressures for different field operations and for the HGP and LGP traffic systems, respectively. Table 5 shows that the inflation pressure of the LGP traffic system is approximately half the pressure of the HGP

32

traffic system, with the exception of the trailer tyres. It is further concluded that the inflation pressure of field traffic after primary tillage and prior to the growing season is half the inflation pressure of other field operations. Again, the inflation pressure of trailer tyres forms an exception to this rule.

The static axle loads in round figures of tractors and implements are given in Table 6. With respect to the static axle loads, the HGP and LGP are comparable.

Table 5. Inflation pressure [kPa] of the HGP and LGP traffic systems for different field operations, tractors (T) and implements/trailers (I).

Field operation	Traffic system			
	HGP		LGP	
	T	I	T	I
fertilizing	80	-	40	-
secondary tillage	80	-	40	-
sowing/planting	160	160	80	80
crop nursery	160	160	80	80
harvest	160	240	80	80
tertiary tillage	160	-	80	-
primary tillage	160	-	80	-

Table 6 shows the relatively high axle loads of harvest operations in general and transport in particular. The static axle loads of primary, secondary and tertiary tillage operations are to a great extent comparable, and somewhat higher than axle loads at sowing/planting, crop nursery and spraying operations because of the heavier tractor being used. The difference of dynamic axle loads will be even higher owing to the considerable weight transfer on the tractor rear axle during the tillage operations.

33

Table 6. Static axle loads [Mg] of tractors (T) and implements/trailers (I), for different field operations and different crops. (F = front axle; R = rear axle).

Field operation	Crop			
	Potatoes	Winterwheat	Sugarbeet	Onions
fertilizing (empty container)	2.1 (TF) 4.3 (TR)			
sec. tillage	2.5 (TF) 3.1 (TR) 1.4 (I)		2.5 (TF) 3.1 (TR) 1.0 (I)	2.5 (TF) 3.1 (TR) 1.0 (I)
sowing/planting (container filled)	2.4 (TF) 1.4 (TR) 1.8 (I)		2.4 (TF) 1.4 (TR) 1.0 (I)	2.4 (TF) 1.4 (TR) 1.0 (I)
crop nursery: ridging	2.4 (TF) 1.4 (TR) 1.1 (I)			
hoeing			2.4 (TF) 1.4 (TR) 0.5 (I)	
spraying (empty container)	1.8 (TF) 2.9 (TR)	1.8 (TF) 2.9 (TR)	1.8 (TF) 2.9 (TR)	1.8 (TF) 2.9 (TR)
harvest:				
combine harvesting		6.9 (F) 2.06(R)		
digging	2.9 (TF) 2.1 (TR) 3.6 (I)		1.6 (TF) 5.8 (TR) 1.1 (I)	2.2 (TF) 2.1 (TR) 0.5 (I)
loading	2.9 (TF) 2.1 (TF) 3.6 (I)		2.0 (TF) 3.2 (TR) 1.9 (I)	2.9 (TF) 2.1 (TF) 3.6 (I)
transport (container filled)	2.0 (TF) 5.4 (TR) 5.4 (IF) 5.4 (IF)		2.0 (TF) 5.4 (TR) 5.4 (IF) 5.4 (IF)	2.0 (TF) 5.4 (TR) 5.4 (IF) 5.4 (IF)
tertiary tillage	2.4 (TF) 3.1 (TR)		2.4 (TF) 3.1 (TR)	2.4 (TF) 3.1 (TR)
primary tillage	2.4 (TF) 3.1 (TR)		2.4 (TF) 3.1 (TR)	2.4 (TF) 3.1 (TR)

Table 7 presents the number of wheelings per track (small implement wheels are omitted). Apart from the spraying and harvest operations most field operations result in two wheelings per track. The relatively large number of wheelings during the harvest operations for rootcrops is attributed to the passage of the different

tractor/implement combinations involved. The frequent use of the spraying tracks during the growing season of the root crops also results in a great number of wheelings per track.

Table 7. Number of wheelings per track for different field operations and different crops.

Field operation	Crop			
	Potatoes	Winterwheat	Sugarbeet	Onions
fertilizing	2	2	2	2
secondary tillage	2	2	2	2
sowing/planting	2	2	2	2
crop nursery:				
ridging	2			
hoeing			2 (2x)	2
spraying	2 (12x)	2 (3x)	2 (2x)	2 (8x)
harvest	20	2	22	22
tertiary tillage	2		2	2
primary tillage	2	2	2	2

4.6 Closing remarks on systematics of field traffic

In § 4.2 overall field traffic was decomposed into distinct field operations. The spatial distribution of the wheel tracks resulting from a given field operation was discussed in § 4.3. The spatial distribution was expressed in quantitative terms by the traffic intensity. In § 4.4 the distribution of the field operations in time was dealt with. It was shown that the timing of most field operations is restricted to well-defined time intervals. The relevance of these regular features of field traffic with respect to the yearly fluctuation of the soil state was mentioned. In § 4.5 an enumeration was given of traffic characteristics which are pertinent in determining the compaction capability of field traffic. It was stated that the tyre inflation pressure and the number of wheelings are important determinants of the degree of compaction of the topsoil, whereas the wheelload and the number of wheelings are considered as important determinants of subsoil compaction.

A further reduction of the number of traffic characteristics can be obtained by comparing the timing, the traffic intensity, the tyre inflation pressure, the wheelload

35

and the number of wheelings. From the data presented in the preceding paragraphs it can be concluded that the traffic characteristics of the following field operations are to a great extent comparable:
1.   Seedbed preparation for the respective root crops.
2.   Sowing and planting of the respective root crops.
3.   The harvest of the respective rootcrops.

The remaining traffic characteristics of a given set of farm machinery are thus:
-       the type of field operation;
-       the type of traffic system, i.e. HGP or LGP.

In Table 8 the field operations are chronologically ordered and further specified with respect to tyre inflation pressure, number of wheelings, range of axle loads and traffic intensity.

Table 8. Summary of important traffic characteristics of the HGP and LGP traffic systems.

Field operation	Tyre pressure [kPa]		No. of whee- lings	Stat. axle load [Mg]	Traff. intens. [-]	
	HGP	LGP	HGP/ LGP	HGP/ LGP	HGP	LGP
secondary tillage	80	40	2	2.5 - 3.1	0.3	0.4
sowing/planting	80	40	2	1.5 - 2.5	0.2	0.2
crop nursery:						
ridging (potatoes)	160	80	2	1.5 - 2.5	0.2	0.2
spraying	160	80	6 - 24	2 - 3	0.02	0.03
hoeing (sugarbeet)	160	80	2 - 4	1.5 - 2.5	0.1	0.1
harvest:						
rootcrops	160/240[1]	80	20	2.5 - 5.5	0.6	0.7
seed crops	160	80	2	2 - 7	0.2	0.3
tertiary tillage	160	80	2	2.5 - 3	0.3	0.4
primary tillage	160	80	2	2.5 - 3	0.6/0.3	0.8/0.4[2]

[1] tractor/implement (or trailer)
[2] ploughing/rotary digging

5.1 Preliminary remarks

In order to predict the effect of field traffic on the soil condition, information is required on the soil condition at the time a field operation is performed. The soil condition varies continuously in time and place owing to machine-induced and natural soil processes.

Machine-induced or, in other words, mechanical soil processes are commonly divided into loosening processes and compaction processes. Important natural soil processes are settlement after loosening, surface slaking by the impact of rain-drops, mechanical reinforcement by plantroots and freezing and thawing, wetting and drying, aging, and processes related with the activity of the soil flora and fauna. Both mechanical and natural soil processes are to a great extent season dependant by rules of field management and by nature, respectively.
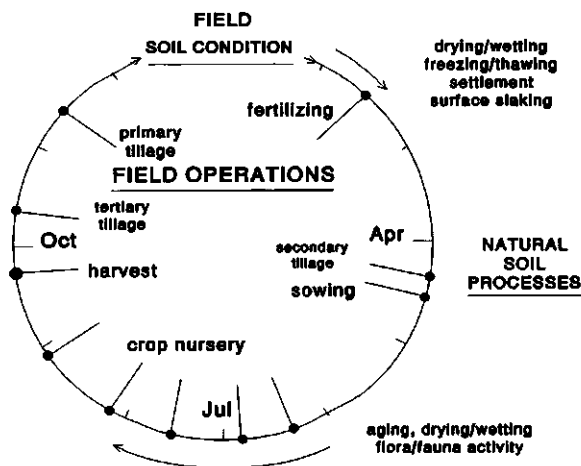

Fig. 4. The cyclical nature of the soil condition, machine-induced and natural soil processes.

The soil condition at the end of a cropping season becomes the starting point for the next cropping season; hence the soil condition features a cyclical nature, with a period of one year. The cyclical nature of the soil condition as a function of

important machine-induced and natural soil processes is outlined in Fig. 4. Similar schemes were proposed by Andersson et al. (1969), Soane (1985), Koolen (1987) and Bullock et al. (1988).

Knowledge on the significance of the variation of the soil condition in determining the effect of a given compactive treatment mainly concerns the soil strength in compaction, i.e. the soil compactibility. Information on the effect on soil physical properties which indicate the physical quality of a field soil for crop production, such as the water conductivity, water retention etc., still is fragmentary. To overcome this problem, it is assumed that the soil strength in compaction and the soil physical quality form a coherent system, i.e. the soil physical quality suffers progressively at decreasing soil strength in compaction. In the analysis of the systematics of the field soil condition, the soil strength properties in general and the compactibility in particular are used as a reference for the variation of the soil condition.

In the literature, various soil properties are used as strength indices. In § 5.2 these soil properties are ordered. In § 5.3 and § 5.4 the effects of important mechanical and natural soil processes are discussed with reference to the soil strength in compaction. In § 5.5 field soil characteristics which are pertinent in determining the effect of compaction by field traffic will be defined.

5.2 Strength related soil properties

Soil strength indices can be divided into soil properties which refer to the soil as a continuous medium and properties which consider the soil as a discreet system of the soil constitutive solid, water and air phases. Schafer and Johnson (1980) used the terms "behavioral properties" and "state properties", whereas Koolen and Kuipers (1983) used the terms "macro-factors" and "micro-factors". In the following, the notation proposed by Koolen and Kuipers is used.

5.2.1 Macro-factors

Well-known soil macro-factors which are used in connection with soil strength in compaction are: shear strength, cohesion and angle of internal friction (from classical soil mechanics); modulus of elasticity, Poisson's ratio, and viscosity (from rheology); tensile strength, compactibility index and others.

An important group of soil macro-factors are soil strength properties which are obtained from characterization processes (Koolen, 1977). Well known and standardized characterization tests are among others the cone-penetration test (Freitag et al., 1970), the plate-penetration test (Freitag et al. 1970), the Proctor test (Proctor, 1933), and the Atterberg consistency test (Atterberg, 1912). The strength determining macro-factors are commonly denoted as soil mechanical properties.

5.2.2 Micro-factors

On a microscopic level, the strength determining properties of the soil solid-water-air system refer to the nature of the soil solid phase, and to the proportions and distributions of soil particles, soil water and inter-particle bonds in a unit soil volume (Koolen and Kuipers, 1983).

Soil strength properties which refer to the nature of the soil solid components comprise the specific particle shapes, the size-weight distribution of soil particles, the type of the soil mineral components, and the type and weight fractions of other solid soil components, such as organic matter and calcium carbonate. As these properties are not affected by mechanical processes, they are referred to as soil intrinsic properties. In compaction studies, the intrinsic properties are commonly described by standardized textural classification systems, such as the USDA-texture triangle (Hillel, 1982), facultatively supplemented with the location, the type of clay mineral and weight fractions of other soil constitutive solid components.

Various studies are reported on the role of the soil intrinsic properties in determining the soil compactibility (Larson and Gupta, 1980; Van Wijk, 1984; Spivey et al., 1986; Beekman, 1987). The intrinsic properties of a field soil are relatively invariant in time and place. Information on the intrinsic properties of a field soil can be obtained from detailed soil maps.

For a soil with given intrinsic properties, the following strength determining extrinsic properties or, in other words, micro-factors can be distinguished:
- the proportion of soil particles in a unit soil volume, expressed as the dry bulk density (τ_d) [Mg/m^3] or, conversely, the bulk weight volume (Bwv) [m^3/Mg], the pore space (P) [%, v/v] and the void ratio (e) [-];
- the distribution of the soil particles, which is related to the pore size distribution;
- the proportion of soil water in a unit soil volume, expressed as the volumetric water content (Θ) [%, v/v] or the gravimetric water content (w)

[%, w/dry w];
- the distribution of soil water;
- the number of bonds at points of contact between soil particles apart from bonds by capillary forces, such as chemical bonds, Madelung forces and bonds formed by organic or anorganic cementing agents;
- the distribution of these bonds.

In the literature a great number of studies are reported on correlations between micro-factors and soil strength determining macro-factors. The micro-factors not only determine the soil strength, but are also closely related to soil properties which are descriptive of the soil physical quality, such as the water and air conductivity, water retention, thermal properties, root penetrability, thermal properties and others (Koolen, 1987).

The soil micro-factors of a field soil with given intrinsic properties vary within certain limits. Uncritically, the following ranges may be observed for medium to fine textured soils in temperate regions:
- pore space: 40 to 60% [v/v];
- dry bulk density: 1.10 to 1.60 [Mg/m^3];
- volumetric water content: 10 to 40% [v/v];
- gravimetric water content: 15 to 40% [w/dry w].

The distributions of water, air and inter-particle bonds in a unit soil volume are strongly related to the distribution of the soil particles. The distribution of soil particles in structured soils is more heterogeneous compared to the distribution of particles in non-structured soils. Likewise, a soil in a loose packing state is more heterogeneous compared to the same soil in a dense packing state.

In the following paragraphs the micro-factors will be extensively used to describe the effects of mechanical and natural soil processes.

5.3 Mechanical processes

As was stated before, mechanical soil processes can be divided into compaction and loosening. The occurrence of compaction or loosening depends on soil and load factors and will not be discussed here. Compaction and loosening are commonly associated with running gear and tillage implements, respectively.

5.3.1 Compaction processes

Upon loading by running gear, a soil element in the zone of interference deforms, i.e. it changes in shape and often decreases in volume. In Agricultural Soil Mechanics, fundamental treatises of soil stress and deformation behaviour are mainly based on continuum mechanics concepts. The physics of soil strength and the continuum physics of soil behaviour upon mechanical loading are still poorly understood (Snyder, 1987).
In continuum mechanics, the change in shape and volume of an elemental soil volume are expressed as deviatoric strain and volume strain, respectively. The soil volume is often converted into bulk packing state properties (Bwv, τ_d, P, e)[1].

Studies of the compaction process induced by the passage of a wheel or a number of wheelings usually account for volume strain only. The awareness that the effect on the soil condition, particularly of fine textured soils, could not always be attributed to volume strain only, increased the scientific interest in deformation behaviour and its associated effects on the soil physical condition. The significance of deformation was shown by Tijink et al. (1988, Appendix I). The authors investigated the deformation history of initially cubic soil elements under a wheeling, and concluded that: deformation was approximately radial symmetric; the principal strain directions rotated considerably ("kneading" deformation); and deviatoric strain dominated volume strain.

Based on the shape of stress-strain relationships, Koolen (1987) distinguished two distinct process-types in compaction: the strength hardening type and the flowing type.

Strength hardening

Strength hardening means that the resistance against deformation increases as deformation upon loading proceeds. The strength hardening process is thus self-impeding. Deformation stops when the compressive forces have reached an optimum. The increase of the soil strength is attributed to the increase of the soil packing density. For strength hardening processes it is assumed that volumetric

---

[1] If compactibility is described in terms of stress-strain relationships, then packing state properties, such as the bulk density and the pore space, should be considered as macro-mechanical quantities.

strain dominates deviatoric strain.

The strength hardening process type occurs under dry to moderately wet, loose to moderately dense (settled) soil conditions, and will result in relatively shallow ruts.

Compaction functions relating soil and load characteristics to the resultant bulk packing state are mainly based on this type of soil behaviour.

Flow

Soil flow occurs when a wet, saturated or near saturated, moderately dense clayey soil is subjected to compressive forces. As opposed to the strength hardening process type, soil flow is not self-impeding since volume reduction is negligible. Knowledge of the mechanics of flow mainly stems from Terramechanics, as flow is an important factor controlling the mobility of running gear. In Agricultural Soil Mechanics, soil flow received little attention (Koolen, 1987).

In practical situations, excessive flow may occur during spraying operations and the harvest of root crops under wet soil conditions. Multiple wheelings, using the same wheel track cause excessive rut formation. Owing to the lateral component of flow, the soil at the sides of a rut bulges up (Kuipers, 1968). This phenomenon can be used to identify the flow behaviour in field situations.

5.3.2   Stress factors determining the compactibility in strength hardening processes

The traffic-induced stress regime is usually composed of a number of loading cycles. The number of loading cycles equals the number of wheelings following the same wheel path. In continuum mechanics, the momentary state of stress in a point in the soil mass during a loading cycle is uniquely defined by the respective directions and sizes of the principal stress vectors $\sigma_1(t)$, $\sigma_2(t)$ and $\sigma_3(t)$.

The compactibility depends on the loading rate (El-Domiaty and Chancellor, 1970; Koolen and Kuipers, 1983). The sensitivity of the compactibility to kneading action is relatively high in soil with moderate quantities of particles of a very broad size range (Koolen, 1987). Multiple loading cycles with approximately equal loads cause small and ever decreasing volume reduction (e.g. Stone and Larson, 1980).

42

The most elaborate description of stress-strain relationships is based on Critical State Soil Mechanics (CSSM) concepts. Hettiaratchi (1987), using the tri-axial compression test (Fig. 5), showed that the volume of a soil element undergoing plastic (non-recoverable) deformation depends on the mean normal stress only:

$$v = \Gamma - \lambda \ln(\sigma_m) \qquad [12]$$

with:

v = soil volume

Γ, λ = soil strength parameters obtained from tri-axial compression tests

σ_m = mean principal stress = $(\sigma_1 + \sigma_2 + \sigma_3)/3$
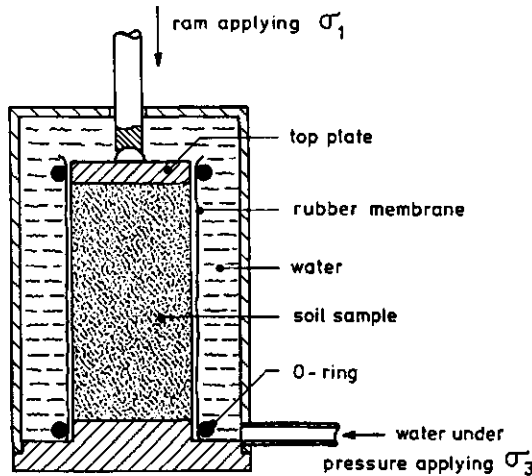

Fig. 5. Tri-axial compression test.

Koolen and Kuipers (1983) collected experimental evidence to show that the compaction capability of the stress regime under a wheeling mainly depends on the major principal stress (σ_1), hence:

$$v = f(\sigma_1, \Phi_i) \qquad [13]$$

with:

v = soil volume

43

σ_1 = major principal stress

Φ_i = soil strength parameters obtained from uni-axial compression
tests

f = compaction function

The compaction function can be determined by means of uni-axial compression tests (Fig. 6). In the literature, various formulae are used to describe the compaction function (f).
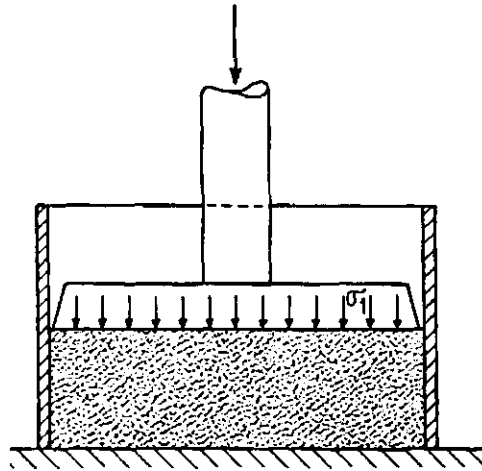
Fig. 6. Uni-axial compression test.

5.3.3 Soil factors determining the compactibility in strength hardening processes

Information on soil factors which are pertinent in determining the compactibility of a soil with given intrinsic properties mainly stems from uni-axial compression tests. Important soil characteristics are the water content and the state of pre-compaction.

Water content

Among scientists there is consensus on the dominant role of the soil water content in determining the compactibility (e.g. Soane, 1981a and b; Koolen, 1987 and Lafond et al., 1992). In order to quantify the water content, the gravimetric water content is preferred to the volumetric water content since the compactibility of initially loose soil is little sensitive to the initial soil volume.

44
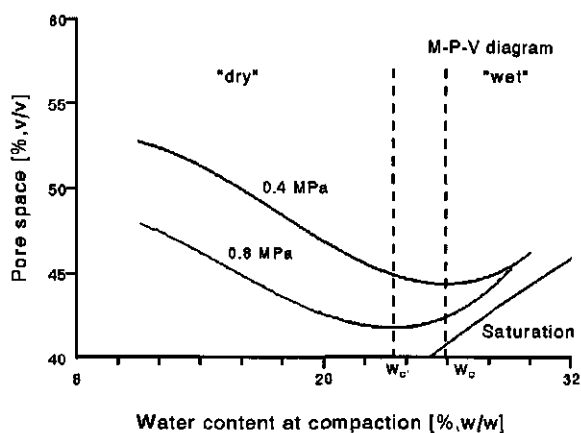
Fig. 7. M-P-V diagram.

The general shape of the curve expressing the resulting pore space (P) vs. the gravimetric water content at quick[2] uni-axial compaction with a given load is presented in Fig. 7. The diagram is called the M-P-V diagram (Moisture-Pressure-Volume diagram) (Koolen, 1987).

The curves are denoted as isobars since they refer to compaction with a certain compactive load. The sensitivity of the pore space to the gravimetric water content at compaction is expressed by the quotient dP/dw. Based on the value of this quotient, an isobar can be divided into two parts: a left part, with dP/dw < 0, and a right part, with dP/dw > 0. Compaction reaches a maximum where the curve parts meet. In accordance with Saini et al. (1983), the water content resulting in maximum compaction at a given compactive load is called the critical water content (w_c). At increasing compactive load, w_c decreases (see Fig. 7).

At a water content considerably lower than w_c, the compactibility is mainly attributed to the resistance to movement of the soil particles. At increasing water content at compaction, the resistance to particle movement is accompanied by the

---

[2] The term "quick compaction" does not refer to the rate of compaction but to the process that underlies volume reduction. At quick compaction, volume reduction occurs solely at the expense of soil air.

45

resistance to water flow and compression of entrapped air in a late stage of compression. These cumulative effects result in an increase of dP/dw in the part of the curve near to the bending point. The resistance to water flow partly explains the loading rate effect on the compactibility. The expansion of compressed air contributes to the immediate, or "elastic", rebound which is commonly observed after removal of the load. At a water content $w > w_c$, the compactibility is mainly determined by the water content and the volume fraction of entrapped air. For medium to fine textured soils, the volume fraction of entrapped air after unloading is approximately 5%. This fraction may amount to 10% for peaty soils.

The left, descending part of the isobar is called the "dry limb", while the right, rising part is called the "wet limb" of the isobar.

Assuming that the water content at compaction is the main factor determining whether a certain compactive load induces strength hardening or flow behaviour, then w_c can be used to identify the process type. Accordingly, the compaction process at water contents at the "dry" and "wet" sides of the isobar can be defined as strength hardening and flow, respectively. In the transition zone near the bending point, both processes will occur simultaneously.

The effectiveness of the uni-axial compression test in simulating compaction by field traffic at water contents $< w_c$ was shown by Dawidowski and Lerink (1990, Appendix III). The uni-axial compression test failed to simulate the soil behaviour at a water content $>> w_c$.
The significance of the type of compaction process in determining the effect on soil physical properties will be discussed in § 5.3.6.

Pre-compaction

When subjecting a dense or firm soil to compressive forces, the compressive stresses have to reach a threshold value to initiate further compaction. The dense or firm soil condition may be the result of compaction during a preceding field operation or caused by settlement. As far as the annually loosened arable layer concerns, the effect of field traffic will dominate the effect of settlement. In the subsoil the opposite holds. The firmness of the intermediate layer between the arable layer and the subsoil is the result of combined effects of settlement and field traffic.

The effect of pre-compaction on the shape of the uni-axial compaction curve can be demonstrated by including an unloading-reloading cycle during the compression of initially loose soil. The general shape of the uni-axial compression curve, with a unloading-reloading cycle, is given in Fig. 8.
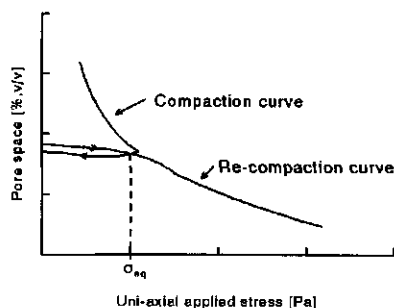
Pore space [%.v/v]

Compaction curve

Re-compaction curve

σ_{eq}

Uni-axial applied stress [Pa]

Fig. 8. Compaction curve with a unloading-reloading cycle.

A typical feature of the re-compaction curve soil is the knee-shaped transition zone. Settled soil (naturally compacted, consolidated) also shows a more or less clear knee-shaped transition zone. From the re-compaction curve, an equivalent pre-compaction stress σ_{eq} can be derived (Horn, 1980; Koolen, 1982). The equivalent pre-compaction stress indicates the stress threshold value that has to be exceeded to achieve further compaction. Measurements of σ_{eq} on field soils are reviewed by Koolen and Kuipers (1989). Field operations are separated by periods of time of variable duration (1 day to ca. 4 months). Meanwhile the soil strength changes owing to natural processes. Consequently the equivalent pre-compaction stress will deviate from the true pre-compaction stress.

In agricultural practice, compaction of re-compaction frequently occurs, owing to overlapping traffic-patterns (see also § 4.3). The significance of the state of pre-compactness in determining the effect of field traffic on the soil condition depends among others on the traffic characteristics of both field operations. If the traffic characteristics of the preceding field operation are comparable to the present situation, then the state of compactness will play a significant role. This situation occurs for instance at sowing/planting following seedbed preparation and in spraying tracks. The load-intensity of the harvest operations considerably surpasses the load intensity of the preceding field operations. Here, the state of pre-compactness will be of minor importance.

47

5.3.4 Stress factors determining the flowability

The rate dependency of the flowability contributes to the complexity of the stress-strain relationship. El Domiaty and Chancellor (1970) found that the flow behaviour of saturated Grimes clay satisfies the Bingham model. To initiate flow, the shear stress has to exceed a certain threshold value (ξ). During flow, the shear stress increases proportionally with the flow rate. In fluid mechanics this proportionality factor is called the viscosity (η).

In continuum mechanics, flow is denoted as deformation at constant volume or distortion. Distortional strains can be imposed on soil samples with the tri-axial compression apparatus. According to stress-strain theories, the maximum shear stress (τ_{max}) occurring in a soil sample during testing equals $\frac{1}{2}(\sigma_1 - \sigma_3)$. The degree of distortion can be expressed by ϵ_1, with:

$$\epsilon_1 = 1 - l_i/l_f \qquad\qquad [14]$$

with:

ϵ_1 = strain;
l_i = the initial length of the soil sample and;
l_f = the final length.

Dawidowski and Koolen (1987) and Dawidowski et al. (1990; Appendix II) distorted soil samples using the tri-axial test. The tests were run at various cell pressures. The authors found that the shear stress, expressing the flowability, was not sensitive to σ_3. Similar results were reported by Spoor and Godwin (1979). A possible explanation for this phenomenon is that the increase of σ_3 is entirely accounted for by the soil water pressure, while the forces between soil particles remain unaffected (Koolen and Kuipers, 1983). These findings suggest that the flowability is uniquely defined by soil factors, irrespective of the stress characteristics. In practical situations compressive stresses likely induce water transport over macroscopic distances owing to the overburden pressure. Consequently, some volume reduction will occur, and this may increase the resistance to flow.

5.3.5 Soil characteristics determining the flowability

Söhne (1952) reported that the flowability of wet clayey soils increased at increasing water content. For saturated Grimes clay, El Domiaty and Chancellor

(1970) found that the viscosity (η) was independent of the bulk density, while the threshold value (ξ) tended to increase with increasing bulk density.
Dawidowski and Koolen (1987) showed that the resistance to distortion increased at increasing water suction of near saturated Wageningen silty loam.

5.3.6 The effect of compaction on soil physical properties

So far, soil and stress factors were discussed which are pertinent in determining the macro-mechanical response of soil upon loading, in terms of volume reduction and distortion. In this paragraph the effects of compaction on soil physical properties will be discussed.

Extensive laboratory and field research is carried out on the effect of compaction on soil physical properties. Several such aspects have been reviewed by Cannell (1973) and Soane et al. (1981a,b, 1982). Compaction among others:
-        decreases the saturated water conductivity, while the unsaturated conductivity may either decrease or increase;
-        modifies the water retention characteristic;
-        decreases the air content at field capacity;
-        decreases the air permeability and the oxygen diffusity;
-        increases the penetration resistance;
-        increases the air-dry and oven-dry tensile strength.

These soil physical properties are in general dependant on the soil water status at testing. The water suction is often used as a reference base, unless the test method prescribes otherwise (as in the case of the saturated water conductivity and the air and oven dry tensile strength).

In a qualitative sense, the effect of compaction on soil physical properties can be explained from the change of the micro-factors which underlie compaction. The soil change on a microscopic scale is discussed using the concepts of stable/unstable behaviour, and dry/wet compaction (Koolen, 1987; Koolen and Kuipers, 1989).

Stable and unstable behaviour

Loose soil is heterogenous by nature, so that strong spots are separated by weaker spots. Upon compressive loading, compaction will first occur in a weak

49

spot, making it stronger so that another spot becomes the weakest. Compaction will thereforee stop at the first-mentioned spot and continue at the second spot. Eventually, compaction occurs throughout the entire soil mass subjected to compression. Processes having the tendency to occur throughout the soil mass are called stable processes. The opposite of stable behaviour is unstable behaviour. Unstable behaviour occurs when the effect of loading concentrates in one, weak spot. This tendency to concentrate ultimately leads to the development of fractures. The induction of unstable behaviour is the object of tillage operations.

An important feature of stable behaviour is the increase of the uniformity of the distribution of soil particles and, consequently, the uniformity of the pore size distribution. Sommer et al. (1972) and Bullock (1985), among many others, showed that compaction is at the expense of the larger sized pores, while the specific volume of smaller pores (< 30 μm) increases.

The increase of the proportion of soil particles in a unit volume, together with the increase of the uniformity of the distribution of particles in a unit volume are important factors explaining the observed effects on the macro-physical properties.

Dry/wet compaction

During field studies of the effect of traffic-induced compaction on soil physical properties and crop establishment, anomalies occurred which could not be attributed to differences in bulk packing state properties. A possible explanation for this is, that the compacted soil was sampled a while (hours, days) after compaction occurred, hence the water content at compaction was not known. McGarry (1987) observed that the effects of traffic were more detrimental when the soil was trafficked when wet than when dry.

Koolen (1976) studied the effect of uni-axial compaction at varying water content on some physical and mechanical properties of a medium textured soil. Prior to testing the effects, the compacted samples were equilibrated at three water suction levels (pF2, pF2.7 and air-dry). By comparing the effects of dry (w << w_c) and wet (w >> w_c) compacted samples the author showed that "wet" pre-compaction: increases shrinkage upon drying; increases the volumetric water content at pF2 and pF2.7; increases the re-compactibility (i.e. σ_{eq} decreases); and increases the unconfined compressive strength. These differences could not be attributed to differences of the bulk density only.

Akram and Kemper (1979) measured the saturated water conductivity on soil samples which were compacted at varying water content. The authors showed that

"wet" compaction resulted in a drastic reduction of the saturated water conductivity as opposed to "dry" compaction.

Dawidowski and Lerink (1990, Appendix III) found that the air content at pF2 decreases at increasing water content at uni-axial compaction to a certain state of compactness (P = 47 % [v/v]).

O'Sullivan (1992) showed an increase of the oven-dry tensile strength and the air permeability with an increasing water content at the time of compaction.

The detrimental effects of compaction of wet soil as compared to dry soil is attributed to the type of failure mechanism which underlies compaction. A cohering soil element may fail in a brittle or a compressive manner (Spoor and Godwin, 1979). A soil element exhibits brittle behaviour if it fails along a few well defined failure planes. The soil in between the failure planes behaves in a rigid manner. Failure that occurs along an infinite number of failure planes is termed compressive failure. Upon compressive failure, the internal structure of the soil element is deteriorated. Structure deterioration is variously termed dispersion (soil physics) or smearing (agronomy).

Although the concept of brittle and compressive failure was applied on macroscopic soil elements it can also be used to describe failure behaviour of small structural elements (Koolen and Kuipers, 1989). Brittle and compressive failure are examples of unstable and stable behaviour, but on the scale of small structural elements.

Whether aggregates will fail in a brittle or a compressive manner upon loading is not well understood. From the before mentioned experiments by Koolen (1976), it appears that the failure mechanism changes from brittle into compressive failure near the critical water content (w_c), when compacted at a given compacted load. A possible explanation for this is that the initially negative water pressure (water suction) during un-drained compaction changes into a positive, so called overburden pressure in the final stage of compaction of a moderately wet soil (Larson and Gupta, 1980). In the absence of internal capillary forces, the soil structural elements weaken and fail in a compressive manner.

Positive water pressures may occur in a near saturated state when pressure is built up in and transmitted from isolated air bubbles. This explains why the adverse

51

effects of compaction of wet soil may occur at water contents slightly lower than w_c (Koolen and Kuipers, 1989).

So far, the effects of compaction processes featuring mainly volume change were discussed. The effects of compaction processes featuring mainly deformation at constant volume (i.e. distortion) is still poorly documented. The major reasons are:
-       laboratory tests which impose large and controlled deformations on soil samples are expensive and time consuming;
-       the adverse effects of compaction have long been implicitly attributed to volume reduction, i.e. increase in packing density;
-       deformation in field situations is difficult to assess.

An important contribution on the agronomic significance of distortion was presented by Dawidowski and Koolen (1987). The authors deformed relatively wet, dense, undisturbed field samples with an initial height of 10 cm to a final height of 5 cm, using a tri-axial compression test. Deformation occurred at virtually constant volume. The test conditions were assumed to be representative for the situation occurring during compaction by field traffic at sugarbeet harvesting. The authors found an increase of the water suction, shrinkage and oven-dry tensile strength, while the saturated water conductivity drastically decreased. Similar results were reported by Dawidowski et al. (1990, Appendix II). These results suggest that the effects on soil physical properties of compaction processes featuring mainly distortion are comparable to the effects of "wet" compaction.

The range of distortional strains in a tri-axial test is limited. Lerink (1990, Appendix V) developed a simple and cheap kneading distortion apparatus, which allows virtually unlimited distortional strain. Dawidowski et al. (1990, Appendix III) showed that the effects of distortion in the kneading apparatus and the tri-axial apparatus were in close agreement.

5.3.7 Closing remarks on compaction

The soil water content of a soil with given intrinsic properties is the most important single soil characteristic in machine-induced compaction processes. The water content controls the process type, the soil strength during volume reduction and distortion, the micro-structural change upon compaction and inherently the effects on soil physical and mechanical properties.

5.3.8 Loosening processes

Loosening processes change cohering soil into a soil mass having little or no coherence. Considerable soil loosening occurs during primary (ploughing) and secondary (seed or plant bed preparation) and tertiary tillage. During ploughing the entire arable layer is loosened. Loosening during seedbed and plantbed preparation is restricted from approximately 3 cm (seedbed preparation) to approximately 7 cm (plantbed preparation). The main object of secondary tillage is to break the coarse structural elements into smaller fragments, and to level the soil surface. During tertiary tillage the soil is loosened to a depth of approximately 15 cm.

Relevant characteristics of a loosened soil are the absolute size and the size distribution of the structural elements and the strength of the structural elements. Uni-axial compression tests of medium textured soils by Tijink (1987) and Willat (1987) showed that the absolute size and the size distribution of loosely packed soil structural elements had little effect on the compactibility. Aggregate mixtures with a narrow size range were found to be more susceptible to compaction than aggregate mixtures with a wider size range. Sommer (1976) reported that the compactibility in static load uni-axial compression was negatively correlated with the pore space prior to testing. The effect of the initial pore space diminished at increasing load and water content at compaction. The results reported by Sommer (1976) agree with the earlier findings of Söhne (1952). The compactibility of aggregates is negatively correlated with the tensile strength of individual aggregates (Davies et al., 1973 and Braunack and Dexter, 1978).

Factors affecting the size and strength of the structural elements resulting from primary tillage are the water content at compaction during the harvest operations and the water tension at ploughing. Wet compaction during the harvest deteriorates soil structure as was discussed in § 5.3.6. Subsequent loosening by ploughing results in course, weak, unstable soil elements. During the winter and early spring the structure of autumn-ploughed soil will be modified by natural soil processes as will be discussed in § 5.4.

The significance of the soil water content as a determinant of the effect of tillage on soil physical properties was among others shown by Unger and Cassel (1991), Braunack and McPhee (1991) and Cresswell et al. (1991).

The compactibility of the loosened soil layer during seedbed preparation is considered of minor importance because of the shallow depth of this layer.

5.4 Natural soil processes

5.4.1 Preliminary remarks

The effects of natural processes superimpose on the relatively rigorous, abrupt changes of the soil condition during field operations. Natural soil processes are the result of the soil interaction with its physical, chemical and biological environment (Harris et al., 1966; Dexter 1991). Natural agents, acting as "driving forces" in natural processes comprise among others meteorological factors, such as precipitation, wind velocity, air temperature and radiation, and factors of biological origin, such as root activity (penetration, water extraction) and the activity of the soil macro and micro fauna, including earthworms and nematodes (burrowing and casting), bacteria and fungi (formation of cementing agents by decomposition of organic matter). As opposed to the change of the soil condition by machine-induced soil processes, the effects of natural processes occur continuously and relatively slow. Furthermore, the distinct natural processes are to a great extent interactive.
So far, little is known on the contribution of natural processes to the seasonal and inter-seasonal and spatial variation of soil strength properties (Douglas, 1986).

In § 5.4.2 the effects of some important natural soil processes on the strength determining micro-factors are briefly discussed. If information is available, the effects on macro-factors which are related to the soil strength in compaction are mentioned.

5.4.2 The effect of some important natural soil processes on the soil strength

The fluctuation of the water content

The water content of the arable layer changes continuously owing to infiltration and evaporation via the soil surface, drainage to and capillary flux from the subsoil, and water extraction by roots.

The water content is considered the most dynamic single property of a field soil.

Several case studies are conducted on the temporal variation of the soil water content. Bruce et al. 1977 reviewed the most comprehensive studies. These studies demonstrated the dynamic character of the soil water regime in the situations that were examined. Bruce et al. (1977) studied the hourly soil water regime at ten depth increments (0 - 15 cm) during a period of 8 days, of a vegetation free soil (sandy loam) in a humid area. Periods of high radiation were interrupted by 3 intermittent rainy spells. The authors found a marked diurnal variation of the water content at depths < 2 cm. The water content vs. time curve showed a sinusoidal shape, with a period of 1 day. The maximum and minimum water content occurred at 7 h 00 and 12 h 00, respectively. Similar observations were reported by Jackson et al. (1976). The fluctuation of the water content decreased at increasing depth. During the respective drying periods the average daily water content decreased considerably, especially in the depth interval of 2 - 8 cm. From the investigations by Bruce et al. (1977) followed, that the water content at field capacity in the period examined slowly decreased. The shape of the water content profile, the daily fluctuation of the water content profile and the decrease of the water content at field capacity described by the authors are considered as typical characteristics of the drying regime in springtime and summer in temperate regions.

Reid and Parkinson (1987) studied the winter water content regime of some heavy clay soils in the UK. After the prolonged wetting-up or recharging period, which may last until January, the water content remained virtually constant. The yearly variation of the water content in this time of the year was found unexpectedly low. The constancy of the winter water content is in agreement with the observations of Kay et al. (1985) on a clay loam soil in Canada. The longer term rise of the water content is defined as a wetting regime.

During four successive years, the water content at 0 - 4 cm and 4 - 8 cm depth was measured on one of the plots of the HGP/LGP experimental field. In Fig. 9 examples are given which are representative of the seasonal trends of the water content of the top soil. The levels of the curves as well as the daily fluctuation are primarily determined by the amount and temporal distribution of rainfall. Spoor and Godwin (1984) found that the level of the water content at field capacity in springtime was dependant on the amount of rainfall during the preceding winter.

From the experimental data available it is hypothesized that the yearly fluctuation of the water content, expressed by the water content at field capacity vs. time

55

curve, shows a sinusoidal shape. The maximum and minimum water contents occur during the winter and summer, respectively, while the soil is under a drying and wetting regime in the spring/summer and autumn/winter, respectively. The yearly trend of the water content at field capacity is the result of interactive effects of machine-induced and natural processes on the soil's ability to retain water against gravity. The daily water content in the spring, summer and fall may fluctuate considerably.
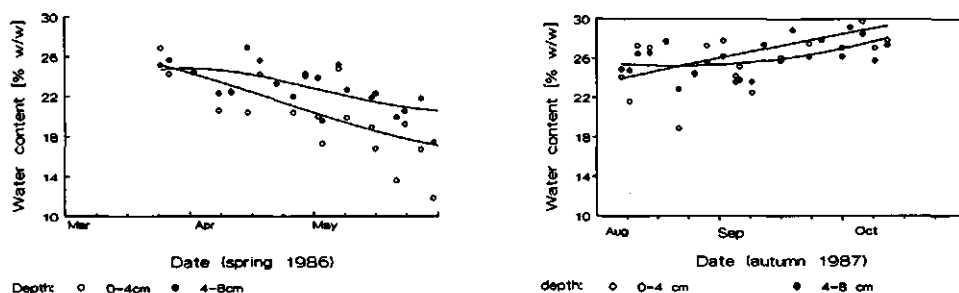

Fig. 9. Seasonal trends of the soil water content in spring and autumn.

Several models have been developed to assess the temporal field soil water regime (e.g. SWATRE, Feddes et al. 1978), using different sets of constants (e.g. soil texture and structure types, hydraulic properties, water retention curves), forcing variables (e.g. weather factors) and state variables (e.g. factors reflecting the seasonal change of the soil condition and the crop growth stage). These models are not yet applied on a routine base.

Little attention has been given to the spatial aspects of the surface soil water content. Van Wesenbeeck and Kachanoski (1988) found that the water content in a row under a corn crop was always lower than between the rows. Spoor and Godwin (1984) observed significant differences in soil water content between the ridge and depression areas on a fall ploughed field in spring, the depression areas being the wettest.

Soil strength as affected by wetting and drying

Subsequent wetting and drying cycles affect the soil strength in different ways. Cementing agents are re-distributed and brought in contact with soil particles as the soil dries. This being the major factor affecting the strength of non-swelling

56

soils (uncritically, soil with a clay content < 17 %). In swelling soils, structure formation by shrinking and swelling in response to drying and wetting is considered the most important single natural process (Towner, 1988).

The significance of structure formation by wetting and drying applies to disturbed soils, i.e. soils of which non-capillary bonds are disrupted and of which the natural heterogeneity of the spacial distribution of soil particles is transformed into a uniform distribution. The major cause of this poor soil structure in agricultural practice is traffic-induced compaction in general and wet compaction in particular.

Drying induces crack formation owing to non-uniform shrinkage. These cracks or fissures partly disappear during subsequent wetting, although they remain planes of weakness (Dexter, 1988). Swelling may also cause planes of weakness (Dexter et al. 1984).

Shrinking and swelling can be considered as unstable and stable behaviour, respectively. Shrinkage decreases the strength of weak spots by loosening, while relatively dense and strong spots become denser and stronger. Thus, shrinkage on drying increases the heterogeneity of the distribution of soil particles and in-herently soil air and water. Contrastingly, swelling weakens dense, strong spots and increases the strength of loose, weak spots.

In general, drying and wetting induce irreversible soil processes, which is among others reflected by the hysteresis loops of the water release/wetting curves. Croney and Coleman (1954) observed a decrease of the water content retained at low to intermediate water suction upon structure formation.

Several workers (Richardson, 1976; Utumo and Dexter, 1981a) reported aggregate formation upon wetting and drying of initially disturbed ("re-worked") soil specimen. Studies on the effects on strength properties refer to the friability (the drop shatter test, Utumo and Dexter, 1981a; Hadas and Wolf, 1984), the stability (the wet-sieving test, Bullock et al., 1985) and the aggregate crushing strength (Brazilian test, Utumo and Dexter, 1981). The general trend is, that subsequent drying and wetting increases the aggregate strength in these tests, although conflicting reports have been made (Chaney and Swift, 1986).

Limited information is available on the effect of structure formation on the soil strength in compaction. Braunack and Dexter (1978) found a decrease of the compactibility of beds of aggregates with increasing crushing strength. The authors used the water tension as a reference base for the water status. The decrease of the compactibility at increasing crushing strength upon successive drying and

wetting cycles may well be attributed to a decrease of the water content as reported by Croney and Coleman (1954).

Factors affecting the structure formation of a given field soil comprise weather factors which determine the number and amplitude of drying/wetting cycles, the rate of drying and wetting, and management factors which determine the degree of disturbance prior to wetting and drying, such as the type of crop (rootcrops or cereals), the water content during harvest operations and the water content at ploughing. In agricultural practice, it is common knowledge that the physical condition of a given field soil in spring among others depends on the amount of rainfall during the winter and early spring.
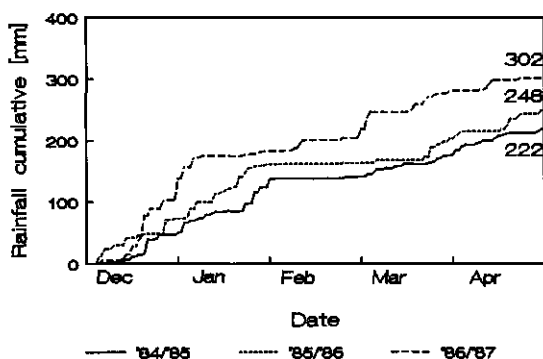
Fig. 10. Cumulative winter rainfall. (data: Klooster, IMAG).

In Fig. 10 the cumulative rainfall in the three successive years of experimentation are presented. Fig. 10 shows that winter '86/'87 was relatively wet compared to winter '84/'85 and '85/'86. This information will be used in § 7.6.3 as a possible explanation for anomalies in experimental data.

Aging

If a disturbed soil sample is kept at constant water content, it is usually found that some or all of the original strength is regained (Kemper et al., 1987; Utumo and Dexter, 1981). This phenomenon is called variously as aging, age-hardening, curing, strength regain or thixotropy. A number of different processes have been described which can contribute to aging. The most important of these are particle rearrangements and biological and chemical cementation (Dexter et al., 1988) and water suction equilibration (Koolen and Kuipers, 1983).

58

In the literature, several strength indices are used to assess strength regain, such as the stability in wet-sieving (Molope et al., 1985), probe penetration resistance (Dexter et al., 1988) and tensile strength and compactibility (Utumo and Dexter, 1981). They suggest that the strength regain decreases with time, until an equilibrium is reached at 1 to approximately 5 days after disturbance.

In agricultural practice, aging is of importance in case of field operations which follow each other in quick succession, such as sowing following seedbed preparation. Ojeniyi and Dexter (1979) recommended to allow the soil to rest for a few days before the next field operation is carried out.

Settlement

After the upheaval of the soil surface, which amounts to approximately 7 cm at a plough depth of 20 to 25 cm, the thickness of the arable layer gradually decreases owing to settlement. Kuipers and Van Ouwerkerk (1963) and Andersson and Håkansson (1966) measured the time dependant change of the thickness of the arable layer. The authors found that the upheaval at fall-ploughing virtually disappeared during levelling and compaction at seedbed preparation in spring. Rainfall increased the rate of settlement, while frost upheaval delayed settlement.

Kouwenhoven (1986) reviewed several factors influencing settlement of tilled soil, including settlement by gravity, weathering and shrinkage, the kinetic energy of precipitation and disintegration of aggregates weakened by moistening. Based on model studies on upheaval and subsequent settlement of tilled soils in a laboratory soil bin, Kouwenhoven (1986) concluded that the rate of settlement was mainly determined by the disintegration of soil particles by rain. The degree of settlement was positively correlated with the degree of upheaval and the working intensity (degree of crumbling) of the implement. Similar results, based on field studies, were reported by Spoor and Godwin (1984).

The increase of the bulk density upon settlement is a major factor affecting σ_{eq}, indicating the soil's susceptibility to further compaction (see § 5.3.3). Koolen and Kuipers (1989) observed that conventionally sized tractors, with tyres inflated at 40 kPa, caused very shallow rut depths during seedbed preparation. This indicates that σ_{eq} attains substantial values in situations which are normal for seedbed preparation.

Freezing and thawing

Based on the type of freezing process, distinction is made between in-situ freezing and ice-lens formation (Miller, 1980). Freezing processes featuring ice-lens formation are further divided into primary and secondary heaving, respectively. During primary heaving a single ice-lens is formed on the freezing front, while during secondary heaving a stack of discreet ice-lenses is formed. The expansion of the soil during primary and secondary heaving is attributed to migration of soil water from deeper soil layers to the freezing zone.

In-situ freezing is primarily associated with sandy soils. Medium textured (silty) soils are sensitive to ice-lens formation. In fine textured (clayey) soils freezing results in the formation of a large number of relatively small ice-lenses. In swelling soils, the formation of ice-lenses is accompanied by shrinkage of the surrounding soil by water extraction.

Kuipers and Van Ouwerkerk (1963) (Wageningen marine-clay) and Kay et al. (1985) (silt loam; clay loam) observed that autumn-ploughed soils quickly re-settled upon thawing and internal drainage and returned to near pre-freezing bulk-densities. The unstable nature of the pores formed by frost action appears to be in contrast to the characteristics of pores created by shrinkage and swelling under a drying regime. However, the collapsed pores remain planes of weakness, and will benefit the fragmentation of coarse soil structural elements upon drying and wetting during springtime tillage. In non-swelling silty soils, clod fragmentation by ice-lens formation is an important determinant of the soil friability in spring.

In agricultural practice, the positive effects of freezing/thawing in soil loosening processes is well known. The effect of structure formation by freezing and thawing on the soil strength in compaction is poorly documented. It may well be that the effect of freezing and thawing is accounted for by the soil water content.

In Fig. 11, the cumulative daily minimum temperatures of the three successive years of experimentation on the HGP/LGP experimental field are given. Only daily minimum temperatures < 0 degree celsius are accounted for. Fig. 11 shows that the number of days with minimum temperatures below zero degree celsius in winter '84/'85 and '85/'86 was considerably higher than in winter '86/'87. Again, this information will be used to explain anomalies in experimentation in § 7.6.3.
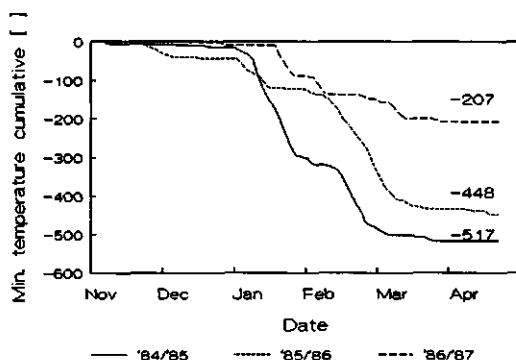
60

*Fig. 11. Winter temperature regime. Temperature sum of days with minimum
temperatures below zero degree celsius (data: Klooster, IMAG).*

5.5 Soil characteristics of a given field

In the preceding paragraphs, several factors which are known to affect the soil
condition and which may be relevant in compaction processes were briefly
discussed.

A great variety of soil properties are used to define the soil strength in compaction.
In § 5.2.1 and § 5.2.2 these properties were subdivided into macro and micro
factors. In § 5.3 the effects of mechanical compaction and loosening on the soil
condition were discussed. In § 5.3.1, compaction processes were subdivided into
the strength hardening and the flow process type. The effects of these compaction
processes on the soil condition were discussed using the concepts of dry and wet
compaction. It was shown that the water content at compaction plays an important
role in determining both the compactibility and the soil physical condition after
compaction.

The effect of pre-compaction on a subsequent compactive treatment was dealt
with in § 5.3.3. It was shown that compactive stresses have to exceed a threshold
value to initiate further compaction. Relevant properties describing the state of
mechanically loosened soil, such as size aspects and packing state of structural
elements may affect the compactibilty (§ 5.3.8). In § 5.4 some important natural
processes affecting the soil condition were mentioned. It was concluded that

61

knowledge of the effect of these processes on the compactibility in general and the change of the soil physical condition in particular is limited.

So far, the analysis of the variability of the field soil condition was restricted to distinct cause-effect relationships, and based on deterministic concepts. This approach revealed some information on the basic mechanisms controlling soil variation. In order to evaluate the interactive effect of these elemental processes on the spatial and temporal variation of the field soil condition, it is further assumed that the causes of variation are to a great extent system-defined. The system approach to soil variation greatly relies on the regular features of the management of a single field. A system approach to soil variation is not unique. Similar techniques are applied in other soil related disciplines (e.g. De Wit and Van Keulen, 1987; Van Lanen and Boersma, 1988).

The system approach to variation of the field soil condition

The objective of using a system approach is to dissolve soil variation into system-defined variation and system undefined or random variation. Here, the system applies to the homogeneous setting of a single field, a given cropping sequence, a given cultivation system and a given set of farm machinery.

Soil survey on the systematics of the variability of the soil strength is scarce (Douglas, 1986). Field studies mainly involve a relatively short period of time, with the maximum of one growing season. Variability is often evaluated by means of possible associations, whereas the question whether variation is system-defined or merely random by nature remains unanswered. In the near future, analysis of soil variation, using geo-statistical techniques coupled with causal relationships between pertinent forcing variables and soil properties may become a powerful method to enlighten soil variation.

The systematics of the field soil condition is further based on a number of assumptions. In this context, variation of the field soil condition implicitly refers to variation of the soil strength in compaction. The validity of the assumptions will be evaluated in § 7.

First assumption:
The intrinsic properties of the arable layer of a given field soil do not vary in time and place.

Objections:

In some regions in the Netherlands, the intrinsic properties of a given field soil vary considerably, despite the fact that spatial homogeneity is a major requirement for a field as a management unit. It can be stated however that the experienced farmer is aware of these spatial irregularities. The opinion of the farmer is an important criterion for selecting sites which represent the largest part of the field.

Second assumption:

Subsoil characteristics which are known to affect the arable layer, such as drainage characteristics and depth of the water table do not vary in place.

Objections:

Local variation of subsoil characteristics may exist. Again the experienced farmer is aware of these spatial differences.

Third assumption:

On the long term (decades), the field soil condition exhibits a dynamic equilibrium. Major factors controlling this equilibrium are the types of crop in the crop rotation and the level of mechanization.

Objections:

Both the cropping sequence and the level of mechanization change in time. The term "soil degradation" is used in connection with the assumed gradual decline of the soil physical quality (e.g. Greenland, 1981). The increase of the number of rootcrops in the cropping sequence and the increase of tractor power are considered as major causes.

Fourth assumption:

The annual variation of the field soil condition does not vary between years. Thus the temporal variation of the field soil condition exhibits a periodicity of one year (see Fig. 4).

Objections:

Inter-seasonal variation may occur owing to extreme weather variations, extreme soil conditions during the harvest of the preceding crop and the type of the preceding crop (rootcrop or cereal crop).

Fifth assumption:

The variation of the field soil condition in the period of time a certain field operation is performed can be fully attributed to the fluctuation of the water status.

Objections:
In wheel ruts formed during preceding field operations, the traffic induced effect on the soil condition may not be a unique function of the water content.

Sixth assumption:
The spatial variability of the field water content is system defined. Examples of system defined variation are:
- variation of the water content in and between plough ridges in springtime;
- variation of the water content in and between former wheel ruts.

Objections:
The system defined spatial variation of the soil water content may be super-imposed by variation owing to subsoil characteristics, the presence of a wind shield and spatial variation of the surface level. Again, the experienced farmer accounts for these anomalies.

From the assumptions mentioned above it follows that the water content at the time interval a certain field operation is performed is the most important soil characteristic. The water content is not system-defined and thus has to be assessed by measurement. Spatial variation of the soil water content is assumed to be largely system defined and acknowledged by the farmer. Additional factors which may cause significant inter-seasonal variation of the soil condition are:
- pre-compaction;
- weather regime in the winter and early spring;
- type of preceding crop (rootcrop or cereal crop);
- the soil condition during the preceding harvest operation ("dry" or "wet");
- the soil condition at ploughing ("dry" or "wet").

The effect of these factors on the soil condition will be partly accounted for by the soil water content. In § 7.6 the significance of these additional soil characteristics will be evaluated.

6   THE METHOD OF PREDICTION

6.1 Preliminary remarks

During each field operation, represented by a dot in Fig. 4, a unique set of interactions occur between the vehicle and the initial soil condition (Fig. 12a) giving rise to a new soil condition with new soil physical properties. The soil process resulting from soil-vehicle interaction is denoted as compaction. In Fig. 12b traffic induced compaction is further detailed. In § 4 and § 5, traffic and soil characteristics which control the compaction process have been evaluated. Soil characteristics were divided into micro-factors and strength determining macro-factors, their correlations (Fig. 12b, arrow A) were briefly discussed.

Two distinct compaction process shapes were distinguished: the strength hardening type and the flowing type. The soil behaviour upon compaction by traffic was discussed in terms of the continuum mechanics concepts of stress and strain, and the micro-scale physical phenomena underlying compaction. The correlations between these mechanical and physical phenomena were mentioned (Fig. 12b, arrow B).

With respect to the immediate effects of compaction on the soil condition it was discussed that bulk packing state properties are poor indices of the physical soil condition, since the relationship between these properties and soil qualities (Fig. 12b, arrow C) is in general not unique.

Prediction requires a prediction function (Fig. 12c) relating process characteristics to process effects. In § 6.2, methods to establish a prediction function will be reviewed, and examples will be given of prediction models presented in the literature. The method that will be used to establish a prediction function that suits the object of this study is presented in § 6.3.

6.2 Methods of prediction

Prediction methods can be divided into methods mainly based on knowledge of the mechanism of the process (analytical methods), methods mainly based on
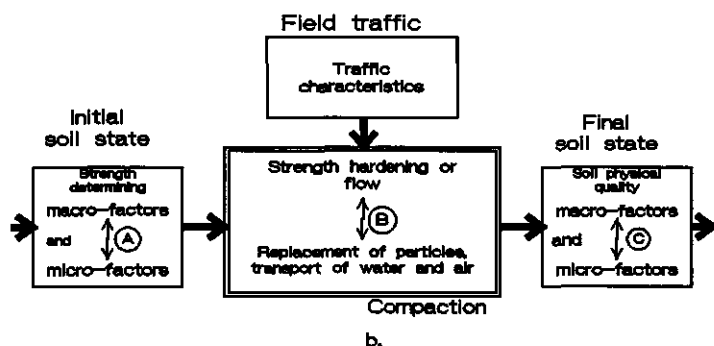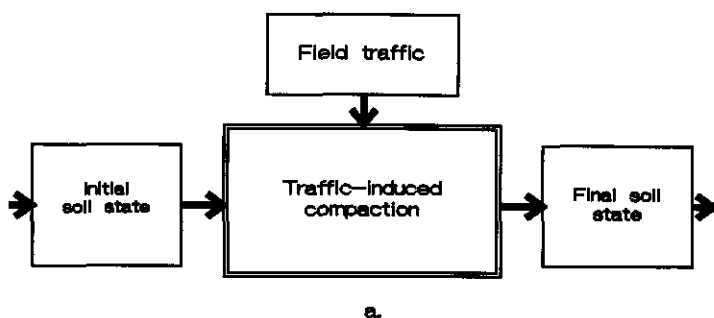
Fig. 12. Schematical presentation of traffic-induced compaction.

observations of relationships between process characteristics and process effects (empirical methods), and methods based on combinations of analytical and empirical methods. The latter called semi-empirical or composite methods (Koolen and Van Ouwerkerk, 1988).

Theories on traffic or wheel-induced compaction are often presented as models. These models are developed for different purposes such as:

- to enhance the understanding of the mechanism of the process;
- to aid vehicle and tyre design;
- to support advisory in agricultural practice.

In general, these compaction models are not appropriate for prediction on a routine base owing to their complexity and the difficulties encountered in obtaining reliable input-data.

Analytical methods

Analytical methods describing aspects of vehicle-soil interaction are often based on stress-strain relationships proposed by Boussinesq. Several such methods were reviewed by Yong et al. (1984) and Gupta and Allmaras (1987). It is to be expected that analytical procedures based on the Boussinesq solution, as well as empirical methods will be replaced by Finite Elements Methods (FEM). FEM (e.g. Vermeer, 1991) have far more possibilities to account for specific features of soil-wheel systems. The application of FEM for soil-wheel systems requires:
- adequate stress-strain relationships for agricultural soils. Such relationships are not yet available and validated. Results from the National Soil Dynamics Laboratory (NSDL, Auburn, Al.) are promising (Raper et al., 1992);
- relevant boundary conditions for soil-wheel systems and wheel properties;
- relationships between quantities describing the state of deformation of a soil element and quantities describing the soil quality of the deformed element.

In the Netherlands, research on soil-wheel systems based on FEM is carried out at the Tillage Laboratory of the Wageningen University since 1991.

Semi-empirical methods

Semi-empirical methods are based on calculated stress distributions in the tyre-soil interface and the soil profile and empirical stress-(volume-)strain relationships. Prediction methods which are based on these concepts are reported by Söhne (1953), Blackwell and Soane (1981), Smith (1985), Gupta and Larson (1982), Gameda et al. (1987), Van den Akker (1988) and Jacobsen and Dexter (1989).

Several methods to predict the stress distribution under surface applied loads are reviewed by Koolen and Kuipers (1983). The authors stated that the numerical summation procedure proposed by Söhne (1953) is the most detailed method and

67

likely gives the most accurate stress estimations. Empirical relationships for estimating the size of the contact area from data on tyre geometry are reviewed by Soane et al. (1981a,b).

Various empirical stress-volume strain relationships are applied in order to relate the predicted stresses to the resulting degree of compactness. Depending on the method of testing, distinction can be made between uni-axial compression tests and tri-axial compression tests. Other test variables are the compression rate, the sample preparation procedure (i.e. undisturbed field samples or laboratory prepared samples), sample dimensions and drainage conditions (drained or undrained).

Empirical methods

A large number of field experiments have been conducted in order to establish relationships between soil and traffic characteristics and the resultant soil condition. Several such studies are reviewed by Soane et al. (1981a,b). Prediction functions are presented as graphs, or equations derived from regression analysis. Often used soil and traffic characteristics which are considered to control compaction are the soil water content, the cone penetration resistance, the tyre inflation pressure, the wheelload and the number of wheel passes.

6.3 Closing remarks on existing prediction methods

Although existing models on traffic-induced compaction are useful in their own field of application, provided they are validated, they are considered here as unsuitable for prediction on a routine base. Important arguments for this statement are:

-    Existing prediction methods have in common, that the effect of compaction is expressed in terms of bulk packing state properties. As was indicated previously, bulk packing state properties are poor indicators of the effect of compaction on the physical condition of a soil as a working and growing medium. Gupta and Larson (1982) and Beekman (1985) extended laboratory compaction tests at varying load and water content with observations on relevant soil physical properties. However useful these methods may be for classifying the sensitiveness of a soil to the adverse effects of compaction, it is questionable whether the results effectively

resemble the effects in field situations.

-   Both analytical and semi-empirical models apply to idealized soil and traffic conditions and model validation has been undertaken to a very limited extent. Particularly anisotropic profiles impose large problems, and predictions based on uniform properties throughout must be handled with care (Smith, 1985). Tests are often confined to the same soil type and profile condition that was used to generate the prediction function (Soane, 1985). Koolen (1988) stated that stress estimations often lack sufficient accuracy.

-   Compaction models require detailed and accurate input-data on soil and traffic characteristics. In general, this information is not readily available, and indeed difficult to obtain (Plackett, 1985).

-   In § 5 it was discussed that the soil behaviour upon compaction can be divided into strength hardening and flow. It is questionable whether these distinct process shapes can be represented by a single model only.

Since analytical and semi-empirical methods are considered as inappropriate for prediction on a routine base, it was decided to establish a prediction theory which is based on empirical methods.

6.4 Prediction based on empirical methods

6.4.1 The prediction function (F)

Koolen (1977) divided empirical methods into comparative methods and methods based on known formulae and/or graphs.

Comparative methods

A comparative method can be applied even when the prediction function F is unknown. The comparative prediction method is based on the axiom that, if once has been observed that Y attains a certain value in a situation defined by the respective values of x_i, then Y will attain that particular value whenever the same

69

situation arises again, provided that Y is uniquely related to $(x_1.....x_n)$. Discrete relationships between Y and different sets of values of x_i can be converted into continuous relationships using formulae or graphs.

A well-known method to fit observations on relationships between Y and $(x_1.....x_n)$ by formulae or graphs is dimension analysis. Dimension analysis is particularly helpful if one has to deal with a large number of process characteristics. The application of dimension analysis is however restricted to test conditions which allow full control of the process characteristics which are involved, as in the case of laboratory scale model testing and single wheel testing.

Methods using known formulae or graphs

Prediction methods using empirical formulae or graphs are based on the assumption that the prediction function (F) is effectively represented by a known general formula or graph shape. A general formula can be transferred into a particular formula by means of numerical or statistical data processing methods. Limited graph data can be fit by an appropriate curve using a known graph shape. The conversion of a general formula or graph shape into a particular formula or graph may be referred to as calibration.
A typical example of using a known graph shape to establish a prediction function is given by Raghavan et al. (1976). The authors used the Proctor test and a static load compression test to develop a general graph expressing the dry bulk density as a function of the water content at compaction. The graph shape was subsequently used for curve fitting of graph data obtained from observations on field compacted soil from the same soil order.

Empirical formulae relating soil and traffic characteristics to soil qualities are entirely lacking. Raghavan et al. (1976) showed that laboratory compaction tests can be used to simulate traffic-induced effects on bulk packing state properties. Gupta and Larson (1982) and Beekman (1985) presented graphical relationships expressing the effect of laboratory compaction at varying load and water content on various soil qualities. However, the effectiveness of these laboratory compaction methods to simulate traffic-induced effects has not yet been validated.

From the absence of appropriate formulae or graphs relating traffic and soil characteristics to soil qualities it was decided to apply the comparative method to establish a prediction function.

70

Laboratory compaction tests can be of great help for developing a prediction function. It was thereforee decided to develop a laboratory compaction test meant to simulate compaction by field traffic. A detailed description of the laboratory test as well as its effectiveness in simulating the traffic induced effect on the soil condition is given by Dawidowski and Lerink (1990, Appendix III).

6.4.2 Where to predict from (x_i)

Empirical prediction methods are based on the assumption that the process effect (Y) is determined by a set of process characteristics (x_1.......x_n). The process characteristics have to satisfy the following requirements (Koolen, 1977):
-        Y must be a unique function of (x_1........x_n);
-        the sensitivity of Y to x_i must be appropriate.

A prediction function is unique when it only predicts one value of Y for each set of (x_1.....x_n). If not, other or additional process characteristics have to be taken into account.
The sensitivity of Y to x_i can be expressed by the quotient dY/dx_i. When this quotient equals near zero, x_i is apparently of minor importance and can be omitted. A high degree of accuracy of x_i is required when this quotient attains a high value. The objective of the study presented here is to develop a prediction method which is applicable on a routine base. Hence methods to assess x_i must be simple, and instruments, if required, must be cheap and easy to handle.

From § 4 and § 5 it followed, that traffic induced compaction is governed by a great variety of traffic and soil characteristics. Furthermore, these characteristics may attain a wide range of values. The development of a prediction function can be facilitated by reducing the number of process characteristics that are treated as variables, as well as their respective ranges. Reducing the number and ranges of process characteristics also puts restrictions on the field of application, or in other words the domain of prediction.

Limiting the domain of prediction

As was discussed in § 3, the major limitations of the domain of the prediction function considered here are that it only accounts for a single field and a given set of farm machinery. Traffic and soil characteristics which are pertinent in determining the immediate effect on soil qualities, within the limited domain defined

in § 3, were evaluated in § 4 and § 5. These characteristics comprised:
- traffic characteristics: the type of field operation;
    the traffic system (HGP or LGP);

- soil characteristics: the water content at compaction.

The domain defined by the traffic and soil characteristics mentioned above account for the effects of compaction throughout the entire zone of influence of the tracks resulting from a given field operation. The effects of compaction are not uniformly distributed throughout the zone of influence. Variation of the effects resulting from a given field operation occurs among tracks, along a track and within a cross sectional zone of influence underneath a track.

Relevant traffic factors causing variation among tracks are:
- tracks resulting from the passage of a single vehicle may be produced by different sets of wheelings, e.g. if the wheel paths of an implement do not overlap the wheel paths of the tractor;
- tracks resulting from a field operation involving more vehicles (e.g. at the harvest of root crops) may not, partly or completely overlap.

A change of the payload during traffic may cause variation of the effects of compaction along a track and among tracks produced by equal sets of wheelings (e.g. at spraying, fertilizing and harvesting).

Relevant soil factors causing variation of the effects among and along tracks are spatial variation of the soil water content and the effects of preceding traffic events.

A further limitation of the number of soil and traffic characteristics can be obtained by:
- considering maximum effects only;
- confining prediction to that part of the field which best represents the entire field;
- confining prediction to those tracks which best represent the majority of tracks resulting from a given field operation.

Measurements on compaction patterns in the cross sectional area under tracks were among others reported by Soane (1970), Raghavan et al. (1976), Raghavan

et al. (1977), Pollock et al. (1984), Gupta and Larson (1982) and Van den Akker and Lerink (1990). Based on these findings it is concluded that the maximum effect of traffic tends to occur near the vertical axis through the centre of the track. Maximum effects are further assumed in tracks that received the largest number of wheelings. The choice of the best representants of the field and the tracks is left to the opinion of the experienced farmer.

6.4.3 What to predict (Y)

In this section, soil properties which are descriptive of the physical condition of a given field soil, that are sensitive to compaction, and which contain relevant information for the user will be evaluated. The generic term "soil qualities" was proposed to denote soil physical properties which match these criteria.

In § 5 the concept of soil micro and macro factors was used as a classification system for soil strength related properties. The extension to account for a wider range of soil physical properties which are relevant for crop production was also discussed. Using micro factors to describe the soil condition after compaction is potentially attractive because of the limited number of factors which are involved.

The dry bulk density, or complementary, the total pore space, is the most important single determinant of the physical quality of traffic-compacted soil. However true this may be there is consensus among agronomists, that bulk packing state properties are unable to explain the perceived variation in for instance workability and crop development. Thus more information is needed to qualify the soil condition. Apart from the proportions of solids, water and air, micro factors are difficult or even impossible to assess. Therefore, macro factors will be used to qualify the soil condition.

Soil macro-factors which describe aspects of the soil physical quality can be ordered into three main groups:
1.   soil-crop factors, such as properties related with water transport and water capacity, aeration and root penetrability.
2.   soil-machine factors, such as properties related to trafficability and workability.
3.   soil-environment factors, such as properties related to erodibility and drainage.

73

Criteria for selection of soil qualities are principally user-defined. These user-defined criteria depend on many factors, such as:
- who is the user (a farmer, an extension worker or a scientist), and where is the information used for;
- which specific problems can be expected from compaction (e.g. limited root growth, erosion, or limited sievability at the harvest of root crops).

In this study, soil qualities are nominated which are appropriate to verify the effectiveness of the prediction method:
- the soil qualities should apply to various aspects of the physical soil quality;
- the soil qualities should be easy assessable and fit a coherent experimental scheme.

Based on these criteria, the following soil qualities were selected:
- pore space;
- air content at pF2;
- cone penetration resistance at pF2;
- air permeability at pF2;
- saturated water conductivity;
- oven-dry tensile strength.

7   PREDICTION FUNCTIONS BASED ON OBSERVATIONS ON TRAFFIC COMPACTED SOIL

7.1 Preliminary remarks

During three successive years (1985, 1986 and 1987) experiments were conducted to establish prediction functions relating traffic and soil characteristics to the immediate effects on soil qualities. The experiments involved field soil sampling and laboratory tests. The laboratory tests were conducted at the Tillage Laboratory of the Wageningen Agricultural University. Field soil sampling was performed on the HGP/LGP experimental field on the IMAG experimental station "Oostwaardhoeve".

Prior to evaluating the experiments which were carried out in behalf of this study (§ 7.3), the results (§ 7.4) and the discussion (§ 7.5), some information is given of the overall experimental lay-out of the HGP/LGP research project (§ 7.2).

7.2 Experimental lay-out of the HGP/LGP research project

In behalf of the HGP/LGP research project, a full-scale field experiment was designed on a 10 ha field on the IMAG experimental station "Oostwaardhoeve". The "Oostwaardhoeve" is situated in the Wieringermeer Polder, in the north-western part of the Netherlands. The experiment started in the autumn of 1984 and lasted five years. Detailed information on the overall experimental layout can be found in Vermeulen (ed., 1989).

Treatments

The main treatments comprised three traffic systems: a high-ground-pressure traffic system (HGP), a low-ground-pressure system (LGP) and a zero-ground pressure system (Z). The machinery used for the HGP and LGP treatments differed only with respect to the tyre equipment. The tyre equipment of the HGP traffic system resembled common practice on 60 ha arable farms in the Netherlands, at the time the experiment started (1984). The ground pressure levels for the LGP treatment were chosen in such a way that no harmful effects from

traffic were to be expected:

- at field operations in spring, before sowing, the mean ground pressure should not exceed 50 kPa;
- at other field operations, the mean ground pressure should not exceed 100 kPa.

Further criteria for selecting tyres which satisfy the mean ground pressure criterion are reported by Vermeulen et al. (1988). In Table 9, the tyre inflation pressure (p_i), mean ground pressure (p_m) and the major principal stress occurring near the tyre-soil contact surface (σ_1) for different field operations and traffic systems are given, p_m and σ_1 are calculated by means of the approximate formulae mentioned in § 4.

Table 9. Inflation pressure (p_i), mean normal ground pressure (p_m) and major principal stress (σ_1) of the HGP and LGP traffic systems [kPa], for various field operations.

Field operations	HGP			LGP		
	p_i	p_m	σ_1	p_i	p_m	σ_1
before sowing	80	100	160	40	50	80
other operations:						
tractors, combine	160	200	320	80	100	160
trailer, implements	240	300	480	80	100	160

As a reference, a zero-traffic system (Z) was also added to the experiment. In this study, the Z-treatment will not be further considered.

Experimental design

The experimental field was divided into four blocks, A, B, C and D (Fig. 13). Each block consisted of 6 plots. The size of the plots 1, 3, 4 and 6 was 50 x 100 m. The plots 2 and 5 were 6 x 100 m and were allocated to the Z traffic system. Two of the four remaining plots of each block were randomly assigned to the HGP traffic system. The remaining plots received the LGP traffic system. The size of the plots was big enough to perform the field operations on a practical scale, but restricted all traffic to the length direction of the plots. A rotation of four crops (cropping sequence: ware potatoes, winter wheat with undersown raygrass, sugar beet and
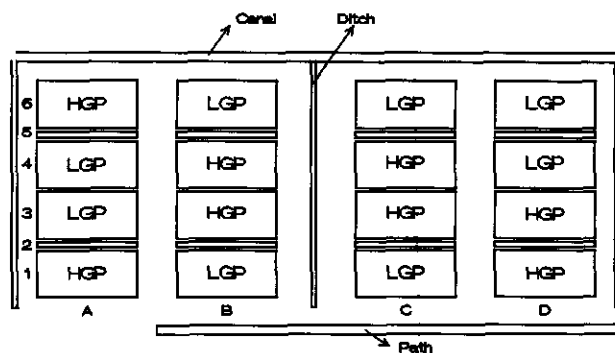
76

onions) was established on each block.

Fig. 13. Experimental design of the HGP/LGP experimental field.

At the start of the experiment, the crops were randomly assigned to the respective blocks. Soil and crop management, as well as the machinery involved, represented common practice on 60 ha arable farms on medium textured soils in the Netherlands. The respective field operations and the machinery involved were specified in Table 1.

Soil description

The marine sandy loam soil on the experimental station developed in the upper part of the Holocene sediment, and includes old marine clay and Almere and Zuyderzee deposits. The soils have AC-profiles and are classified as Typic Fluvaquents (Soil Survey Staff, 1975), or as Calcaric Fluvisols (FAO-UNESCO, 1974). In the Dutch classification system they are called Calcareous Polder Vague Soils with a loamy surface layer, mapping unit Mn25A (De Bakker, 1979). A soil taxonomic description of a representative pedon is presented in Table 10.

The arable layer ranged from sandy loam to clay loam (USDA classification). On average, the arable layer contained 23% clay (ranging from 14% to 35%), 32% silt, 44% fine sand and 1% coarse sand.

77

Table 10. Soil taxonomic description of a representative profile according to Soil Survey Staff (1975).

Horizon	Depth	Description
Ap	0-37	Very dark grey (5Y 3/1) with a weakly to moderately developed structure consisting of microporous, subangular blocky elements (0-13 cm depth) to angular blocky elements (13-17 cm depth) with diameters ranging from 2 to 10 mm: abrupt smooth boundary
C21g	37-45	Dark grey (5Y 4/1), heavy clay with a moderately developed structure, consisting of macroporous, angular blocky elements with diameters more than 20 mm: abrupt smooth boundary
C22g	45-78	Dark grey (5Y 4/1) clay with strongly developed compound prisms, composed of weakly developed, macroporous, angular blocky elements with diameters ranging from 10 to 20 mm. This horizon shows vertical cracks; common medium strong brown (7.5YR 5/6) stains around old roots; common thin strata of silt loam and loamy sand; gradual wavy boundary
C23g	78-135	Grey (5Y 5/1) clay with moderate, smooth compound prisms composed macroporous, weakly developed angular blocky elements with diameters more than 20 mm. This horizon contains many fossil roots and redbrown mottles; clear smooth boundary
CG1	135-150	Greenish grey (5GY 5/1) loam. The soil material is apedal, commonly contains shell fragments and belongs to the Pleistocene; gradual wavy boundary

All horizons are calcareous

Corresponding analytical data are given in Table 11.

Table 11. Analytical data of a Typic Fluvaquent.

Ho-rizon	Depth [cm]	Particle size distribution [%, w/w]					$CaCO_3$ [% w/w]	pH (KCl)	Org. matter [*] [% w/w]
		<2 μm	2-16 μm	16-50 μm	50-150 μm	>150 μm			
Ap	0-37	21.5	10.4	14.6	45.1	8.4	8.5	7.4	2.2
C21g	37-45	47.7	24.2	24.3	3.1	0.7	5.9	7.3	0.0
C22g	45-78	47.4	24.5	20.7	6.9	0.5	9.3	7.3	0.5
C23g	78-135	33.7	18.0	37.0	10.9	0.4	10.4	7.4	2.3

[*] Istscherekov-elementary

78

Among and within all plots large differences in soil composition occurred. In Fig. 14, information is given on the clay content of the arable layer. As a rule the subsoil contained more clay than the arable layer. Generally, the arable layer as well as the subsoil of blocks A and B contained less clay than blocks C and D. Within the blocks, the arable layer of the area near the canal contained more clay than the rest of the blocks. The experimental field was well drained with artificial drains placed at a distance of 11 m.
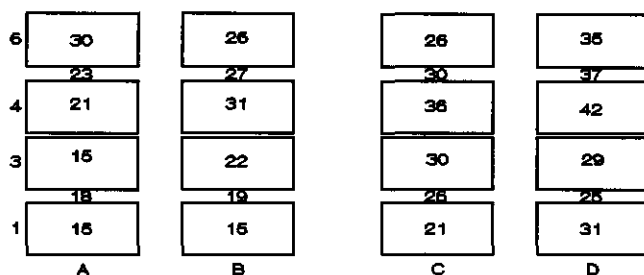

Fig. 14. Clay content (% w/w) of the arable layer near the middle of each plot (data: Kooistra, Winand Staring Centre).

7.3 Experimental methods

7.3.1 Choice of field operations and sampling locations

Field operations

The choice of the field operations which were used for developing prediction functions was primarily based on the traffic intensity, the time available for experimentation and the time required for experimentation. Using these criteria, seedbed preparation for the rootcrops and the harvest of the rootcrops were chosen. Seedbed preparation was chosen in favour of sowing because field sampling might have caused unacceptable damage to the seedbed. The harvest of root crops was selected because of the high traffic intensity, high axle loads, and the relatively high tyre inflation pressures.
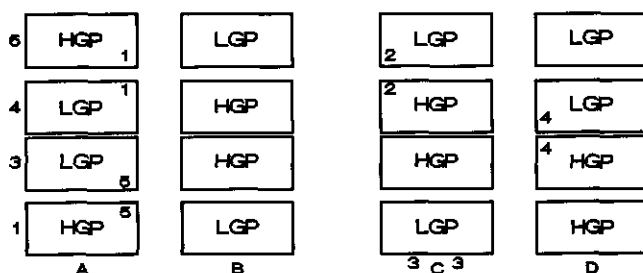
Sample locations

The prediction function presented in § 6 only accounts for a field soil with given

intrinsic properties. In order to minimize the effect of variation of the soil composition, it was decided to:

- choose sampling sites for corresponding HGP and LGP treatments as close as possible on neighbouring plots;
- choose sampling sites on plots with a clay content close to field average (≈ 26 % w/w).

For practical reasons it was not always possible to select sampling sites which met these conditions. The variability of the soil intrinsic properties was therefore not completely excluded. The consequences of introducing an extra variable are dealt with in § 7.4.1.

A small portion of the area of the respective plots already received field traffic at the time seedbed preparation was carried out. These trafficked areas were avoided for sampling since they did not represent the soil condition of the largest part of the plots. For the same reason, areas which received traffic during spraying operations were avoided at field sampling of the harvest treatments. In Fig. 15 the respective sampling sites are schematically presented.

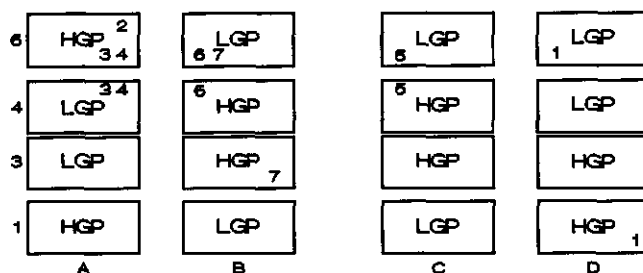Up: seedbed preparation; down: harvest operations

Fig. 15. Sample locations. Experiment numbers indicate respective locations.

80

7.3.2 Field sampling procedure

Field sampling procedure at seedbed preparation

After selecting a suitable location, using the conditions defined in § 7.3.1, two strips of 5 m were traced out with rods. These strips were situated in the length direction of the plot and marked the centrelines of tracks which were to be expected. Just before and immediately after traffic core samples were taken at 2-7 cm and 7-12 cm depth, the latter after removal of excess soil. Pre-traffic sampling was carried out while the field operation was in progress. After finishing pre-traffic sampling the sample locations were trafficked immediately. The tractor driver was instructed to travel over the marked strips and to stop half way the strips. After marking the positions of the rear tyres the implement was lifted and the tractor was advanced. The trafficked sections of $\approx$ 0.75 m between the rods marking the rear tyres and the tilled soil were used for core sampling.

All core samples were taken in metal cylinders with a sharpened edge (ϕ 76 or 81 mm, height 50 mm, wall thickness 1.5 mm). The inner side of the cylinders was oiled in order to minimize the possible harmful effects of soil-wall friction. The cylinders were pushed in the soil manually by means of an extension rod. For sampling after traffic a rubber hammer was needed. All core samples were trimmed to size with a sharp knife, covered underneath with 150 μm-maze nylon cloth, and stored in a closed wooden box. All handling was done with great care. Samples which appeared not representative were discarded.

The total number of core samples per treatment (HGP or LGP) thus amounted to 40; 20 samples before and 20 after traffic, 10 samples per depth layer. The number of core samples was determined by the time available for sampling and the total number of cylinders available.

Field sampling procedure at the harvest of rootcrops

After an appropriate location was chosen, a strip of 10 m length was traced out with rods. The strip represented the centreline of the track which would result from the passage of the harvest machinery (transport included). The strip was subsequently divided into 4 sections of equal length. The outer sections were used for core sampling before traffic, the middle sections were used for core sampling immediately after traffic. The sampling procedure of the harvest operations and seedbed preparation were further comparable.

Additional core samples were collected from untrafficked areas near the sampling sites of the harvest operations and seedbed preparation (sampling depths: 2 - 7 cm and 7 - 12 cm; ring size: ϕ x h = 120 x 50 mm; number: 5 at each depth layer). These core samples were used for laboratory compaction tests.

In Table 12 the sampling dates, sites and the type of crop grown in the preceding cropping season are listed.

Table 12. Sampling dates, sites and type of (preceding) crop.

Seedbed preparation					
Exp. no.	Date before	after	Plot HGP	LGP	Preceding crop
1	24-4-86	id.	A6	A4	sugarbeet
2	02-5-86	id.	C4	C6	onions
3	31-3-87	id.	C3	(edge)	potatoes
4	23-4-87	id.	D3	D4	w. wheat
5	27-4-87	id.	A1	A3	onions

Harvest operations					
Exp. no.	Date before	after	Plot HGP	LGP	Crop
1	26-07-85	id.	D1	D6	potatoes
2	30-10-85	id.	A6	–	sugarbeet
3	30-10-85	id.	A6	A4	sugarbeet
4	30-09-86	13-10-86	A6	A4	onions
5	03-10-86	id.	C4	C6	potatoes
6	06-11-86	id.	B4	B6	sugarbeet
7	15-09-87	01-10-87	B3	B6	onions

Deviations from standard sampling procedure

1.   Experiment no. 3 (seedbed preparation) was performed approximately one month earlier than usual, in order to gain time for an extra sampling session.

2.   Experiment no. 2 HGP (harvest) was repeated (exp. no. 3 HGP) after it became known that soil dredged from the canal was spread on the sides

82

of the plots bordering the canal.

3.   Digging and loading at the harvest treatments no. 4 and 7 were separated approximately two weeks in time. Accordingly pre-traffic and after-traffic sampling was separated by a time period of considerable duration.

7.3.3 Laboratory preparation and measurement methods

The smaller sized core samples were subjected to a series of measurements and preparations in order to assess:
-    total pore space: P;
-    field soil gravimetric water content, just before or immediately after compaction: w_f;
-    air content at pF2: $Ac_{(pF2)}$;
-    air permeability at pF2: $Ki_{(pF2)}$;
-    penetration strength at pF2: $Cl_{(pF2)}$;
-    saturated water conductivity: K_{sat};
-    oven-dry tensile strength: σ_t.

All core samples were kept in the metal cylinders until the tensile strength test. Pending a test, the core samples were stored in closed wooden boxes and kept at a cool place.
All samples were treated alike. As will be shown, the successive tests fitted a coherent experimental scheme. The sequence of tests and preparations ensured minimal mutual interference. Despite this, the results of the respective tests may be influenced to some extent by factors which are attributed to the experimental set-up, such as aging and drying/wetting. It can be reasoned however, that these effects are of minor importance compared to the effects of natural processes which occur in field situations. A high degree of standardization in scheduling, sample preparation and measuring was applied to minimize the disturbance due to the experimental set-up.

Scheme of measuring, preparation and storage

- Weighing   The ring samples were weighed the day after field sampling, to assess of w_f.

- Storage

83

- Equilibration   The ring samples were equilibrated at a matric suction of 10 kPa
                   (pF2) on a standard, sand-filled tension table (equilibration time:
                   3 days). A filter paper was placed between the sample and the
                   nylon cloth to ensure good contact.

- Weighing   After equilibration at pF2 the samples were weighed to assess
                   $Ac_{(pF2)}$.

- Air
  permeability   The air permeability was assessed using a constant pressure
                   permeameter (Perdok and Hendrikse, 1982).

- Storage

- Saturation   The samples were placed on a tension table installed at a tension
                   of 0 kPa. After an equilibration time of three days, water was
                   added on the surface of the tension table until the level was equal
                   to half the height of the cylinders (equilibration time: 3 days).

- Conductivity   The saturated water conductivity was assessed using the constant
                   head method (Klute and Dirksen, 1986). The samples had free
                   outflow underneath. The head varied from 1 to 4.5 cm, depending
                   on the conductivity. Half an hour equilibration time was given
                   before the measurements started. Since the conductivity
                   decreased in time, the average flow rate (Q [m^3/s]) was
                   determined over five successive time intervals. The duration of the
                   time intervals was variable, depending on the conductivity.

- Equilibration   The samples were equilibrated on a tension table at a tension of
                   10 kPa (equilibration time: 5 days).

- Penetrability   The penetration resistance was estimated by means of a needle
                   penetrometer (shaft: ϕ 0.8 mm, length 60 mm; conus: tip angle
                   30 °, ϕ-base 1.2 mm). The needle was attached to a force
                   transducer. The needle-force transducer assembly was mounted
                   on a universal material testing machine (Zwick). The penetration
                   rate was 25 mm/min. The penetration force and penetration depth
                   were continuously recorded on a XY-plotter. The testing machine

84

stopped automatically at a penetration depth of 4 cm. Penetrations were carried out in three-fold, at locations in between the centre and circumference of the sample surface.

- Storage

- Oven drying (105 °C; 3 days).

- Weighing   The oven dried samples were weighed, whereafter the soil cores were taken out of the cylinders. In general this could be done without disturbance of the slightly shrunken core. Sticking to the inner side of the ring was largely prevented by the oil film.

- Tensile
  strength   The diameter and length of each soil core were determined by means of a micrometer. The oven-dry tensile strength was assessed according to the Brasilian test (Kirkham et al., 1959). The force on the poles of the soil core was applied by the Zwick testing machine and was recorded continuously on a XY-plotter. Upon loading the force increased steadily until the moment of failure when it dropped sharply. The force at failure was read from the XY-plotter. After the cores were broken they were checked for irregularities, such as shell nests or plant litter.

- Weighing   Finally the metal ring was weighed to assess w_f and $Ac_{(pF2)}$.

7.3.4 Calculation and data processing

Calculation

The following formulae were used to calculate the respective soil properties.

- Pore space (P) [% v/v]:

$$P = (1 - (W_{dry} - W_{ring})/(\gamma_s \cdot V_{ring})) \times 100\%$$

with:

V_{ring} = ring volume [m³]
W_{dry} = weight of oven-dry core sample [Mg]

85

W_{ring} = weight of metal ring [Mg]

γ_s = specific density of soil particles [Mg/m^3]

- Gravimetric water content (w_f) [% w/w]:

$$w_f = (W_{wet} - W_{dry})/(W_{dry} - W_{ring}) \times 100\%$$

with:

W_{wet} = weight of core sample [Mg]

- Air content at pF2 (Ac(pF2)) [% v/v]:

$$Ac(pF2) = (1 - (W_{dry}-W_{ring})/(\gamma_s \cdot V_{ring}) - (W_{pF2}-W_{dry})/(\gamma_w \cdot V_{ring})) \times 100\%$$

with:

W_{pF2} = weight of core sample equilibrated at pF2 [Mg]

γ_w = specific density of water [Mg/m^3]

- Intrinsic air permeability at pF2 ($K_{i(pF2)}$) [m^2]:

$$K_{i(pF2)} = (V_a \times \eta_a \times h)/(p_a \times t \times A)$$

with:

V_a = volume of air passed through the core sample [m^3]

η_a = viscosity of air [Pa·s]

h = height of core sample [m]

p_a = pressure of air in the bell float [Pa]

t = time of air flowing [s]

A = sample cross sectional area [m^3]

V_a and p_a are given in the users manual of the test apparatus. The values of Ki were subsequently log-transformed.

- Saturated water conductivity (K_{sat}) [m/s]:

$$K_{sat} = Q/A \cdot \frac{L}{H_1 + L}$$

with:

H_1 = head [m]

Q = flow [m³/s]

L = height at soil sample [m]

K_{sat} was calculated of five successive time intervals (T_i) after a ½ hour equilibration time. It appeared that the log converted values of $K_{sat}(T_i)$ closely fitted a straight line when plotted vs. time. The parameters a and b defining a straight line were calculated using standard regression analysis. The value of b, representing $\log(K_{sat})$ at t = 0 (i.e. at the very beginning of water ponding) was subsequently used to assess $\log(K_{sat})$.

- Cone Index at pF2 $(CI_{(pF2)})$ [MPa]:

$$CI_{(pF2)} = F_p/A_c \times 10^{-6}$$

with:

F_p = penetration force [N]

A_c = base area of the cone [m²]

The penetration force F_p was obtained from the F_p vs. depth relationship as recorded by the XY-plotter. F_p was measured at penetration depths of 1, 2 and 3 cm. CI(pF2) was calculated as the average of three penetrations at three depths.

- Oven-dry tensile strength (σ_t) [MPa]:

$$\sigma_t = (2 \cdot F_t)/(\pi \cdot D_{dry} \cdot H_{dry}) \times 10^{-6}$$

with:

F_t = force at failure [N]

D_{dry} = diameter of oven-dry soil core [m]

H_{dry} = height of oven-dry soil core [m]

The bigger sized core samples were subjected to a uni-axial compression test. Force vs. piston displacement were recorded on a XY-plotter. Compression stopped automatically when a pressure of 0.4 MPa was reached. From the force vs. displacement curve porosities were calculated at 0.1, 0.2 and 0.4 MPa. Here, the porosity applies to the state of compactness before elastic rebound.

Data processing

Data on the respective soil properties of each set of corresponding core samples were averaged and standard deviations were calculated. Extreme values were discarded.

7.4 Results

7.4.1 Presentation

The results of the experiments are presented graphically by means of composite diagrams in Figs. 16, 17, 18 and 19. Each diagram presents the initial and final soil state, at a depth of 2-7 and 7-12 cm as a function of the field soil water content. The composite diagrams are further referred to as soil state diagrams. The M-P-V diagram is placed at the bottom of the soil state diagrams. The M-P-V diagram will be used extensively to explain the response of the respective soil qualities to compaction. The mean values of a series of tests on corresponding samples are rendered by symbols. Open and closed symbols refer to the initial and final soil state respectively.
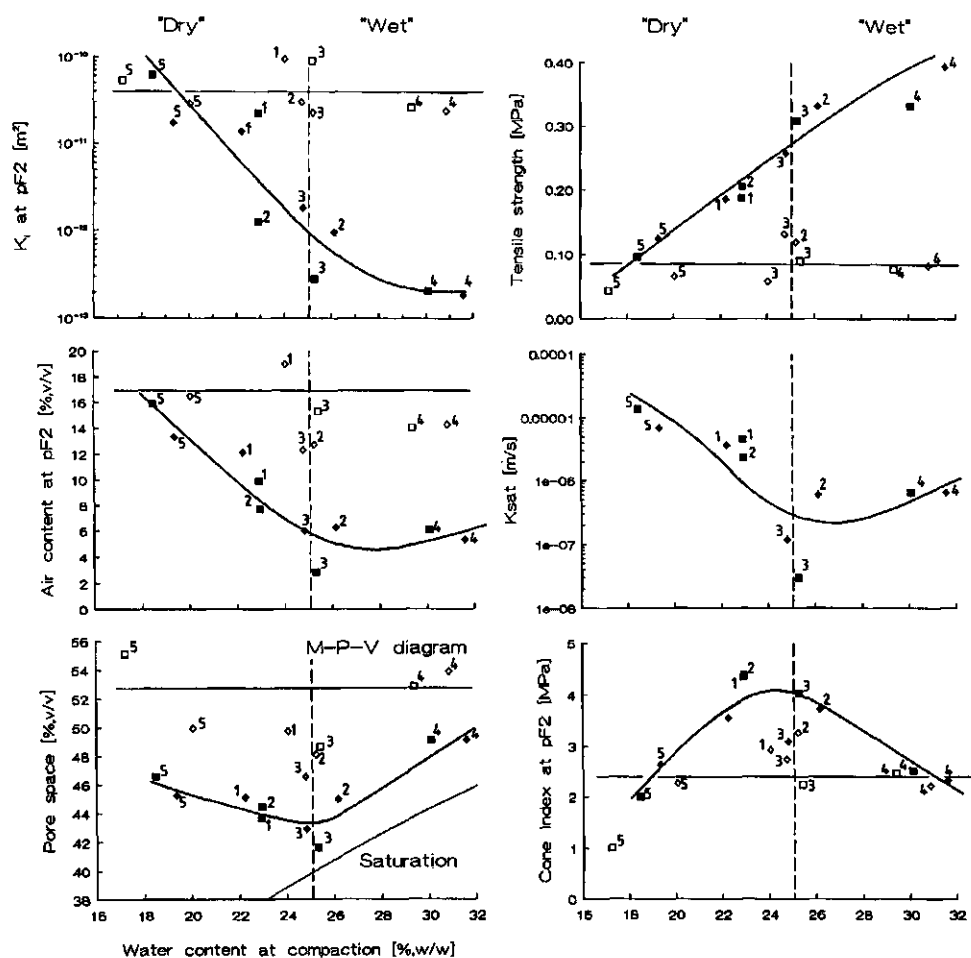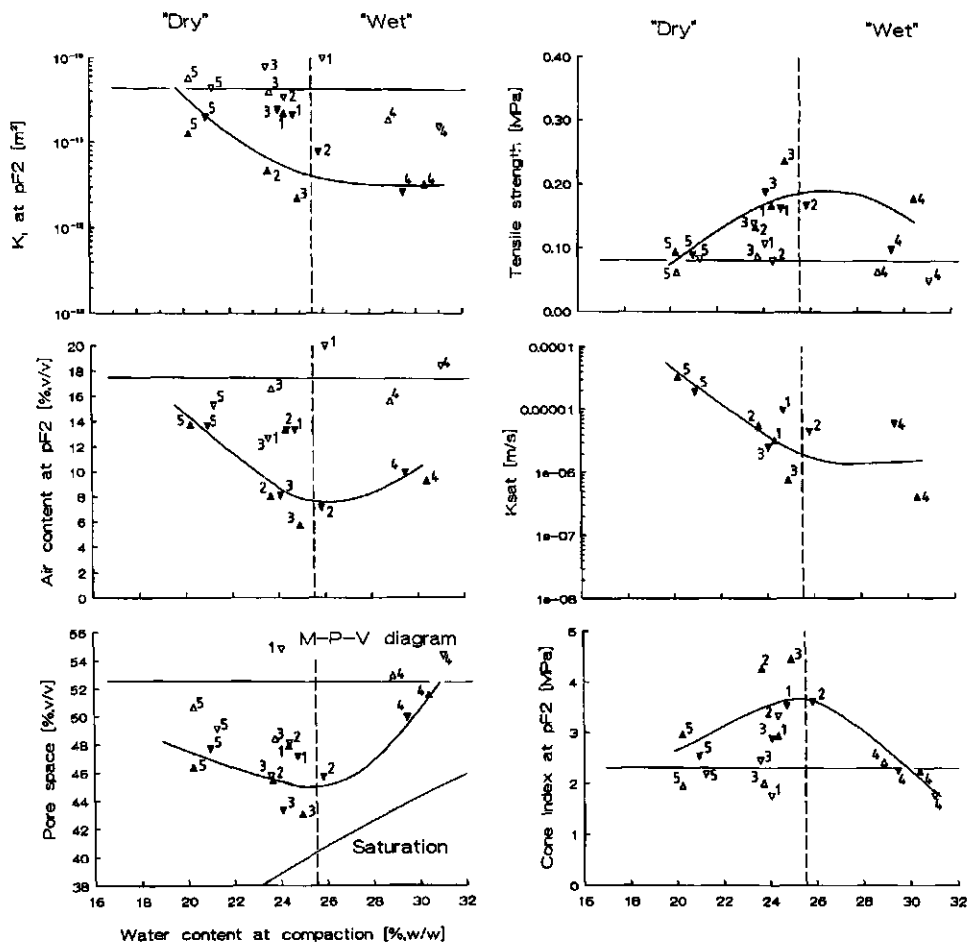
Fig. 16. Soil state diagram of HGP field traffic at seedbed preparation for rootcrops
(□ initial soil state at 2-7 cm depth, ◇ initial soil state at 7-12 cm depth; ■ final soil
state at 2-7 cm depth, ◆ final soil state at 7-12 cm depth; —— average initial soil
state at 2-12 cm depth; —— HGP-isobar at 2-12 cm depth; 1,2,... number of
experiment).

Fig. 17. Soil state diagram of LGP field traffic at seedbed preparation for rootcrops (△ initial soil state at 2-7 cm depth, ▽initial soil state at 7-12 cm depth; ▲ final soil state at 2-7 cm depth, ▼ final soil state at 7-12 cm depth; —— average initial soil state at 2-12 cm depth; —— LGP-isobar at 2-12 cm depth; 1,2,... number of experiment).
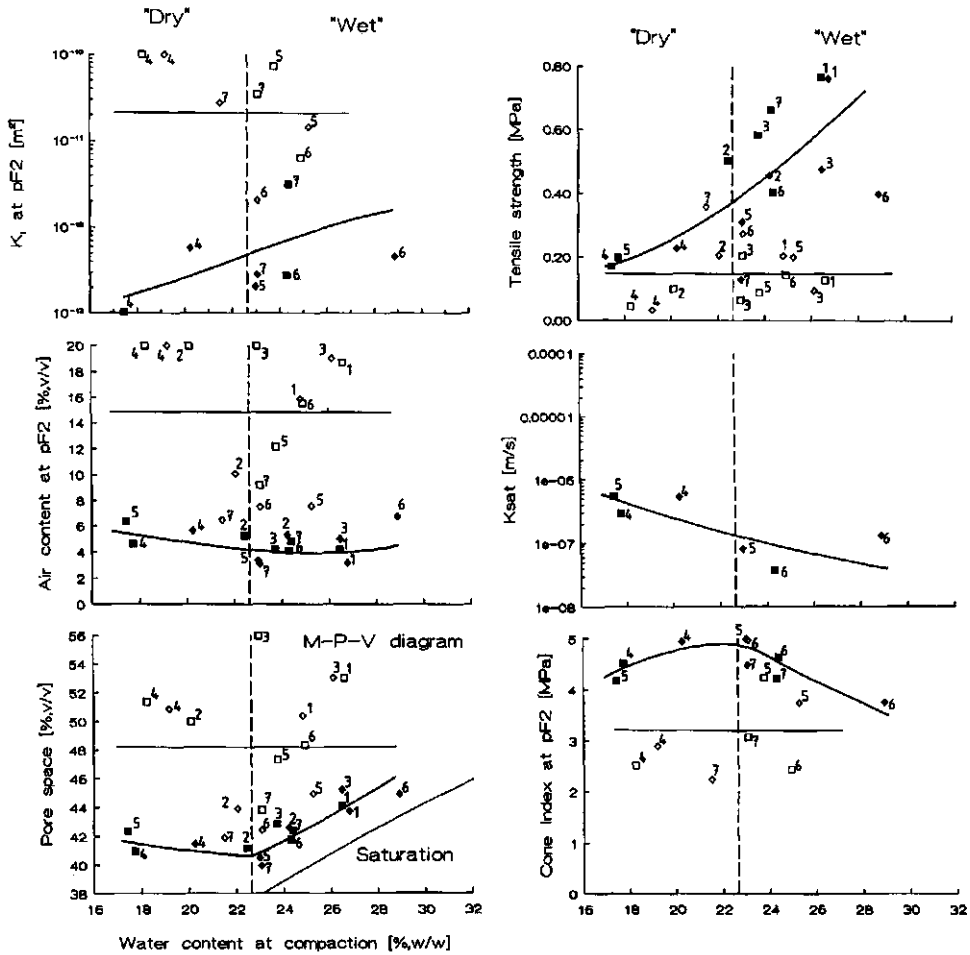
Fig. 18. Soil state diagram of HGP field traffic at the harvest of root crops
(◻ initial soil state at 2-7 cm depth, ◇ initial soil state at 7-12 cm depth; ■ final soil
state at 2-7 cm depth, ◆ final soil state at 7-12 cm depth; —— average initial soil
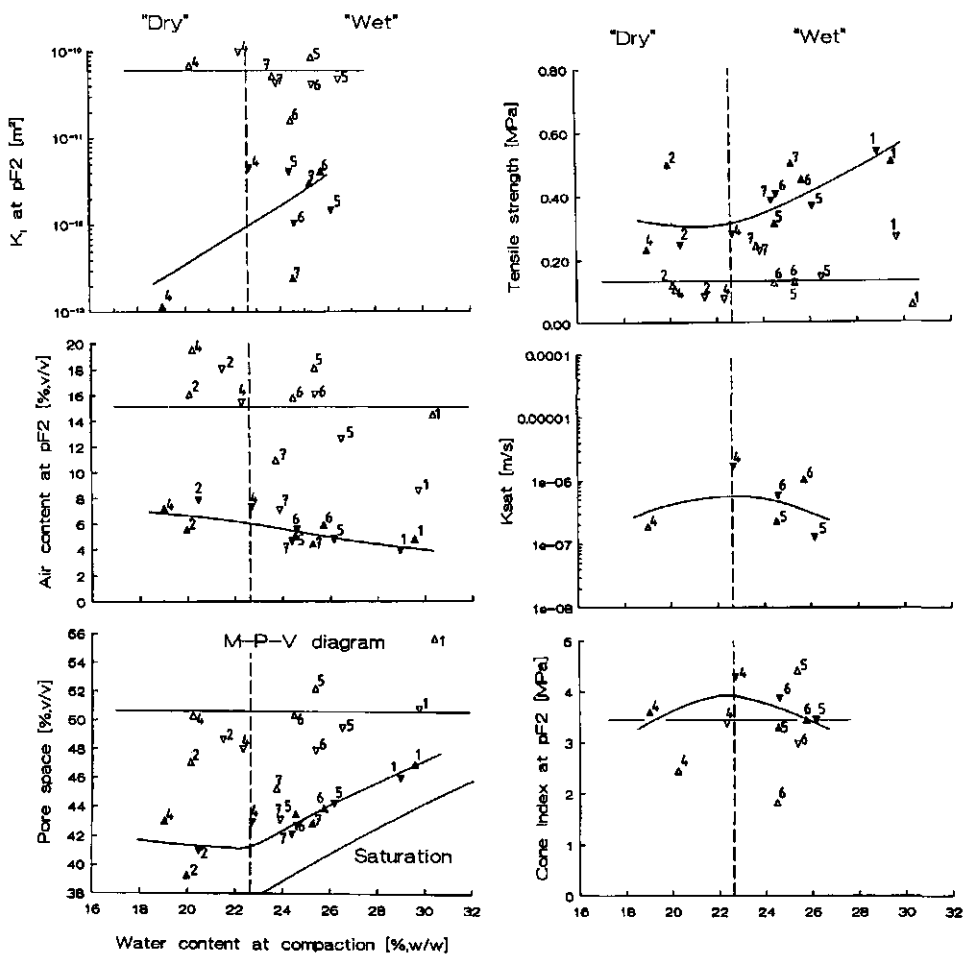state at 2-12 cm depth; —— HGP-isobar at 2-12 cm depth; 1,2,... number of
experiment).

91

Fig. 19. Soil state diagram of LGP field traffic at the harvest of root crops
(△ initial soil state at 2-7 cm depth, ▽initial soil state at 7-12 cm depth; ▲ final soil
state at 2-7 cm depth, ▼ final soil state at 7-12 cm depth; —— average initial soil
state at 2-12 cm depth; —— LGP-isobar at 2-12 cm depth; 1,2,... number of
experiment).

7.4.2 Estimation of the prediction function (F)

In order to establish a prediction function (F), the data symbols representing the final soil state are fitted with smooth, continuous curves. Each curve applies to a limited range of x_i and predicts a single soil quality only. The limited range of x_i consists of the variable water content at field traffic (w_f), a given field operation (seedbed preparation or harvest operation) and a given traffic system (HGP or LGP). From Figs. 16 to 19 it was inferred that the effect of depth was completely accounted for by the water content at compaction. Therefore, the symbols corresponding to the respective sample depths were fitted by a single curve.

The estimation of the shape and position of the curves is based on the assumption that the immediate effect of field traffic on a soil quality (Y) is a unique function of the process characteristics that were taken into consideration. Statistically this implies that the disturbance of Y-observed with respect to the prediction curve is attributed to the stochastic nature of Y.

The prediction curves are fitted by eye. Curve fitting by eye was preferred to curve fitting based on regression analysis since the data symbols could not be fitted properly by a common regression function. The complex shape of the curves is attributed to the distinct process types which underlie compaction at varying water content (see also § 5). The prediction curves are further denoted as isobars, since they refer to a specified compactive treatment. Maximum congruence was pursued between the HGP and LGP isobars.

The initial soil state was assumed to be independent of the water content at compaction and the depth of sampling. In Figs. 16 to 19 the initial soil state is presented by straight, horizontal lines, resembling the average initial soil condition.

7.5 Analysis

The analysis comprises:
- the effect of the water content at compaction on the final soil state, $Y(w_f)$ (§ 7.5.1);
- a comparison of the effects of the HGP and LGP traffic system, Y(traffic system) (§ 7.5.2);
- a comparison of the effects of the two field operations examined, Y(field operation) (§ 7.5.3).

93

The soil state diagrams show considerable deviation of the observed values of Y and the predicted values. In § 7.5.4 an analysis is given of the deviation.

7.5.1 The effect of the water content at compaction

The discussion on the effect of the water content at compaction is based on the M-P-V diagram and the soil quality diagrams, respectively.

M-P-V diagram

The isobars of the M-P-V diagrams in Figs. 16 to 19 clearly show two distinct curve parts. In accordance with the definitions stated in § 5.3.3, the left descending and the right rising parts are called the dry and wet limbs, respectively. The dry and wet zones of compaction are separated by a vertical line which intersects the X-axis at a critical water content resulting in maximum compaction. The critical water contents are given in Table 13.

Table 13. Critical water content for different field operations and traffic systems.

Field operation	Traffic system	Critical water content [% w/w]
seedbed preparation	HGP	25.1
seedbed preparation	LGP	25.6
harvest	HGP	22.6
harvest	LGP	22.6

With respect to the type of the compaction process, compaction in the "dry" and "wet" limbs were associated with strength hardening and flow, respectively. From the situations examined, it follows that compaction during seedbed preparation mainly features strength hardening, whereas at the harvest flow prevails.

At the time seedbed preparation was carried out, the water content at 2 - 12 cm depth lied mostly within the range of 18 to approximately 26 % [w/w]. Extreme wet situations (w_f = 29 to 32 % [w/w]) occurred in experiment number 5 of both the HGP and LGP treatments. The harvest operations were usually carried out at a slightly wider water content range w_f ≈ 17 to 27% [w/w]. An extreme wet situation occurred in experiment number 1 of the LGP treatment.

The sensitivity of the resultant pore space to compaction at increasing water content (dP/dw$_f$), along the dry limb of the isobar is markedly higher at seedbed preparation than at the harvest operation. The respective values for dP/dw$_f$ are approximately - 0.45 and - 0.25. A decrease of the sensitivity of P to w$_f$ at higher compactive efforts was also found in uni-axial compaction studies (e.g. Koolen, 1978).

The wet limbs of the isobars were estimated to run near parallel to the saturation line. The air-filled porosity at wet compaction equals approximately 4 to 6 % [v/v].

Soil quality diagrams

The vertical lines indicating the transition from dry into wet compaction in the M-P-V diagram are extended to the soil quality diagrams. At dry compaction during seedbed preparation, the change of the soil qualities at increasing water content at compaction is in line with the decrease in pore space, i.e. A$_c$(pF2), K$_i$(pF2) and K$_{sat}$ decrease at increasing water content at compaction, whereas Cl(pF2) and σ_t increase. The sensitivities of the soil qualities to the water content at compaction are: dA$_c$(pF2)/dw$_f \approx$ - 1.5; dlogK$_i$(pF2)/dw$_f \approx$ - 0.3; dCl(pF2)/dw$_f \approx$ 0.27; dlogK$_{sat}$/dw$_f \approx$ 0.28; dσ_t/dw$_f \approx$ 0.02

At wet compaction, the change of the soil qualities at increasing water content at compaction generally does not correspond to the change of the resultant pore space. Despite the increase of the pore space A$_c$(pF2), K$_i$(pF2) and σ_t remain virtually constant whereas K$_{sat}$ further decreases.

The soil quality diagrams of the harvest operations show that A$_c$(pF2), K$_i$(pF2) and K$_{sat}$ attain extremely low values and are virtually insensitive to the water content at compaction. The shape of the Cl(pF2)-isobar corresponds to the P-isobar in the M-P-V diagram. At dry compaction, σ_t slightly increases at increasing water content at compaction. At wet compaction, σ_t shows a marked increase despite the increase of the pore space. As opposed to A$_c$(pF2), K$_i$(pF2) and K$_{sat}$, σ_t appears to be a sensitive indicator of the detrimental effect of compaction under wet soil conditions (dσ_t/dw$_f \approx$ 0.04). The deterioration of the soil structure is attributed to soil flow. In view of the relatively deep wheel ruts, which may amount to approximately half the initial depth of the arable layer, it can be reasoned that flow was considerable.
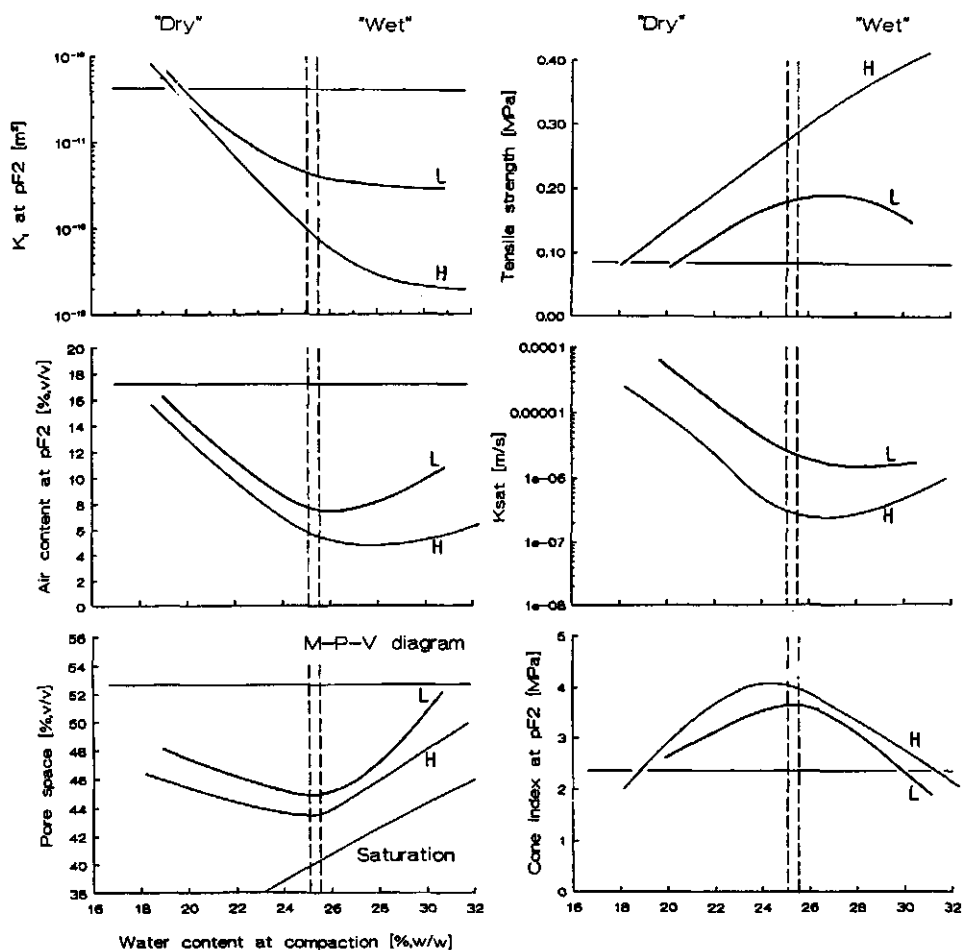
95

Fig. 20a. HGP and LGP isobars (seedbed preparation), —— average initial soil state at 2-12 cm depth, —— H = HGP isobar at 2-12 cm depth, —— L = LGP isobar at 2-12 cm depth.
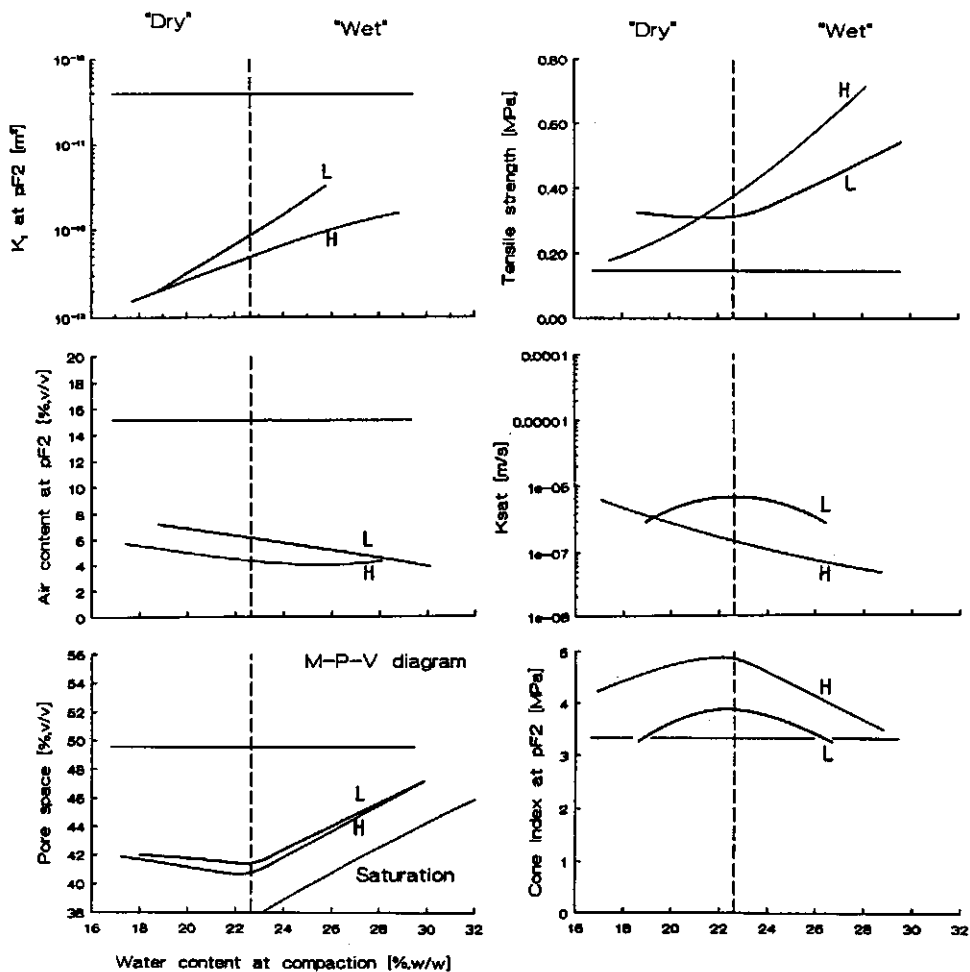
96

Fig. 20b. HGP and LGP isobars (harvest operation), —— average initial soil state at 2-12 cm depth, —— H = HGP isobar at 2-12 cm depth, —— L = LGP isobar at 2-12 cm depth.

7.5.2 The effect of the type of traffic system

In order to compare the effects of the HGP and LGP traffic systems, the isobars in the soil state diagrams in Figs. 16 to 19 are transferred to Figs. 20. The comparison of the effects of the HGP and LGP traffic systems are further based on the positions of the respective isobars. The shapes were considered as comparable.

The isobars in Fig. 20a (seedbed preparation) show a consistent effect of the type of traffic system. At dry compaction, the effect on the soil qualities of a decrease of the tyre inflation pressure from 80 to 40 MPa is comparable to the effect of a decrease of the water content at compaction of approximately 1 to 2 % [w/w]. The beneficial effect of the LGP traffic system in situations featuring wet compaction is considerably higher.

The effects of the HGP and LGP traffic systems at dry compaction during harvest (Fig. 20b) traffic are to a great extent comparable. At wet compaction, the oven-dry tensile strength of the HGP traffic system is markedly higher as compared to the LGP traffic system, and equivalent with an increase of the water content at compaction of approximately 3 % [w/w]. The sensitivity of the oven-dry tensile strength stresses the significance of this soil quality as an indicator of the soil physical state after wet compaction.

7.5.3 The effect of the type of field operation

Comparison of the effects of traffic during seedbed preparation and the harvest operation reveals that harvest traffic more frequently results in wet compaction. This phenomenon is not the result of higher water contents at harvest compaction, since the respective ranges of the water content at compaction are to a great extent comparable. The more frequent occurrence of wet compaction at harvest traffic is attributed to the higher compaction capability of harvest traffic owing to the higher tyre-soil contact pressures and a higher number of wheelings. The higher compaction capability causes the critical water content to decrease.

When comparing the effects of wet compaction resulting from seedbed preparation and harvest traffic it follows that the respective values of $A_c(pF2)$, $K_i(pF2)$ and K_{sat} are to a great extent comparable. This is explained by the fact that these soil qualities already draw near extreme values at compaction during seedbed

98

preparation.

The effect of the type of field operation at dry compaction is attributed to the lower level of the pore space in response to harvest traffic. The relationship between the pore space and some soil qualities at dry compaction is dealt with in § 7.6.2.

Using the effect on the oven-dry tensile strength as a reference-base it can be stated that the positive effect of the LGP traffic system is higher at seedbed preparations than at the harvest operations due to the fact that the positive effect of a single wheeling is diminished by the great number of wheelings involved in the latter case.

7.6 Analysis of factors causing disturbance

The prediction curves in Figs. 16 to 19, which express the expected values of soil qualities as a function of the water content at compaction, the type of field operation and the type of traffic system, and which apply to a limited domain, have to satisfy two important requirements.

Firstly, the prediction curves should be reliable. The prediction curves are reliable if they are fitted to experimental data of which:

1) the respective values of the soil characteristics lay within the range for which the prediction curve is defined;

2) the conditions of the limited domain are satisfied.

If the condition 1 and 2 are met, then the experimental data points in Figs. 16 to 19 can be considered to be of equal weight. In § 7.6.1 factors which may disturb the reliability of the prediction curve are discussed.

Secondly, a prediction function should be effective in prediction. A prediction function is effective in prediction, if for any set of values of x_i it predicts a value of Y (Y_{pr}) which matches the true value of Y (Y_{tr}). In § 7.6.2 factors which possibly affect the effectiveness of the prediction curves are evaluated.

7.6.1 The reliability of the prediction curves

The limited domain, as defined in § 3 and § 6.4.2 involved: 1) a single field; 2) a field soil with given intrinsic properties; 3) a given crop rotation; 4) a given set of farm machinery, and; 5) given working methods. During experimentation, variation occurred with respect to the field soil intrinsic properties and the working methods.

Variation of the soil intrinsic properties

The significance of the soil intrinsic properties in determining the effect of traffic on soil qualities is evident. The soil intrinsic properties not only affect the soil strength in compaction, but any soil physical property and consequently any soil quality. The interference of the variation of the soil intrinsic properties in prediction is twofold:
1) it undermines the reliability of the prediction functions, and;
2) it adversely affects the effectiveness of the prediction functions.
The latter will be dealt with in § 7.6.2.

In order to evaluate the variation of the soil intrinsic properties it is assumed that the effect of this variation on the traffic induced effects is a unique function of the clay content. From Figs. 14 and 15 follows that the clay content of the sampling sites belonging to seedbed preparation and harvest operations varied from approximately 21 to 30 % and 26 to 30 % [w/w], respectively.

The analysis of the effect of the clay content on the reliability of the prediction functions is based on the examination of the correlation between the water content at compaction (w) and the clay content (C) of the corresponding sampling sites. The significance of this examination lies in the fact that if (w) is correlated to (C) than the effect of the variation of the soil intrinsic properties on the prediction curves is systematic rather than stochastic. If no correlation exists than the variation of the soil intrinsic properties are considered to affect the effectiveness of the prediction functions rather than the reliability.

In Tables 14 and 15 the water content at compaction and the clay content of the corresponding plots are given. The clay fractions were presented in Fig. 14. The experiment numbers are ordered with increasing clay content.

From Tables 14 and 15 it follows that:
1.   At extremely low and high clay contents, the corresponding water contents at compaction are relatively low and high, respectively. This phenomenon agrees with common experience.

2.   At intermediate clay contents, there is no obvious correlation between the clay fraction and the water content at compaction. Hence it is concluded that the variation of the clay content does not interfere with the reliability

100

of the prediction functions.

3.   At seedbed preparation, there is no obvious correlation between the type of traffic system and the clay content. At the harvest operations, the average clay content of the HGP plots exceeds the average clay content of the LGP plots.

Table 14. Water content (w) at compaction and clay content (C) (seedbed).

Exp. no.	Traff. syst.	Plot	C [% w/w]	w(2-7cm) [% w/w]	w(7-12cm) [% w/w]
5	HGP	A1	15	18.46	19.35
5	LGP	A3	15	20.22	20.95
1	LGP	A4	21	24.33	24.72
3	HGP	C1	21	22.93	26.15
3	LGP	C1	21	24.91	24.06
2	LGP	C6	26	23.65	25.83
4	HGP	D3	29	30.09	31.59
1	HGP	A6	30	22.91	22.23
2	HGP	C4	36	22.93	26.15
4	LGP	D4	42	30.41	31.59

Table 15. Water content (w) at compaction and clay content (C) (harvest).

Exp. no.	Traff. syst.	Plot	C [% w/w]	w(2-7cm) [% w/w]	w(7-12cm) [% w/w]
3	LGP	A4	21	19.97	20.47
4	LGP	A4	21	19.02	22.70
7	HGP	B3	22	24.38	23.04
5	LGP	C6	26	24.53	26.15
6	LGP	B6	26	25.73	24.59
7	LGP	B6	26	25.26	24.38
2	HGP	A6	30	23.70	26.45
3	HGP	A6	30	22.43	24.22
4	HGP	A6	30	17.73	20.24
1	HGP	D1	31	26.44	26.76
6	HGP	B4	31	24.29	26.89
1	LGP	D6	33	29.56	28.95
5	HGP	C4	36	17.43	22.98

Seedbed preparation in experiment number 3 (Figs. 16 and 17) differed from other experiments with respect to the timing of the field operation. In experiment no. 3, seedbed preparation was carried out approximately four weeks earlier than usual. In Fig. 21 the compactibility in uni-axial compression of the soils in experiment 1 to 5 is presented by means of a M-P-V diagram. Fig. 21 is based on uni-axial compression tests on the bigger sized core samples (see also § 7.3.4). In Fig. 21 the porosities at uni-axial compression at 0.2 MPa are presented. The M-P-V diagram shows that the field soil in experiment no. 3 is relatively susceptible to compaction. A possible explanation for this phenomenon is that the field soil in experiment no. 3 did not favour the positive effects of the drying and wetting cycles in April.

The relatively high compactibility of the field soil in experiment no. 3 agrees with the positions of the corresponding data symbols in Figs. 16 and 17. The abnormal situation in experiment no. 3 may affect the reliability of the prediction functions.
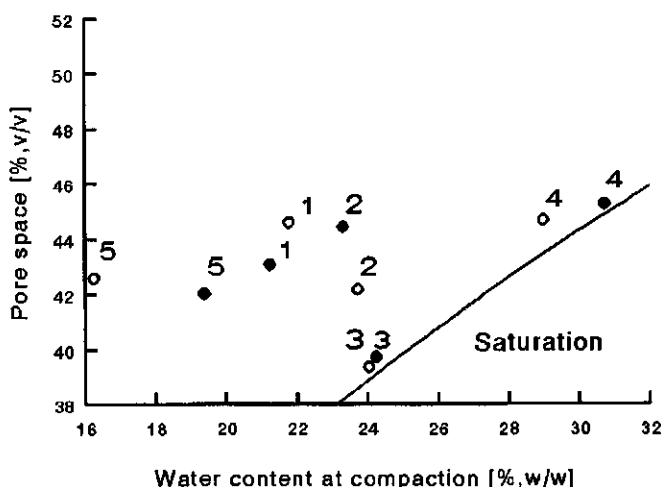

Fig. 21. M-P-V diagram of uni-axial compacted field soil samples. Uni-axial pressure: 0.2 MPa, closed and open dots refer to the HGP and LGP plots respectively (1,2 ....: experiment number).

102

The harvest operations in experiment no. 4 and 7 differed from the other harvest operations in that digging was not immediately followed by loading and transport. In both experiments, digging and loading/transport were separated approximately two weeks in time. From auxiliary measurements on water content vs. depth relationships, carried out immediately after digging and before loading/transport, it followed that the difference between the respective water contents at a given depth did not surmount 0.5 % [w/w] in both experiments. It is therefor concluded that the time delay did not affect the results.

7.6.2. The effectiveness of the prediction curves

The effectiveness of a prediction curve can be expressed by the deviation (Y_{dev}) between the predicted value of Y (Y_{pr}) and the true value of Y (Y_{tr}). Possible causes of deviation are:
- a process effect Y is not a unique function of the process characteristics which are taken into account;
- experimental errors, such as sampling, sample treatment and measurement errors;
- the soil inherent variability of intrinsic and extrinsic properties;
- the process effects are not sensitive to the process characteristics;
- other, unknown factors.

Sampling and measurement errors involve every individual core sample and are random by nature. The expectation of the error due to sampling and measurement of the mean of (n) observations is zero. The consequences of systematic errors due to sample treatments, such as storage, suction equilibration and saturation, and testing, such as the saturated water conductivity test, were minimized by pursuing a high degree of standardization. Core samples which obviously differed from others samples of the same order, e.g. owing to the presence of large holes, inclusion of plant litter or shell, were discarded. Although factors mentioned so far potentially contribute to deviation, they will not be further considered.
The variation of the soil intrinsic properties was already dealt with in § 7.6.1. In this paragraph the effect of variation of the soil intrinsic properties will be further specified.

In § 7.5.1 the sensitivity of the process effects to the process characteristics was discussed and will not be further detailed. In § 7.6.3, the significance of additional process characteristics will be evaluated.

103

The difference between Y_{pr} and Y_{tr} both concerns the pore space and the soil qualities. The deviation of the predicted pore space (P_{pr}) from the true pore space (P_{tr}) is the result of variation of the soil compactibility or variation of the compaction capability (note: in this context the pore space is considered a macro-mechanical soil property).

A variation of the compaction capability stems from the difference among the implements used for seedbed preparation (reciprocating harrow, rotary harrow, rotary cultivator) and the harvest (potato digger, onion digger, sugarbeet digger), and from varying working methods (driving speed, working depth, harvest methods). As compared to the variance of the soil compactibility, the variance of factors determining the compaction capability is considered to be of minor importance. Hence the deviation of P_{pr} from P_{tr} is attributed to variation of the soil compactibility. Possible causes of this variance will be discussed in § 7.6.3.

The significance of the variance of the compactibility follows from the sensitivity of the soil qualities to the pore space (note: in this context the pore space is considered a micro-factor). In Fig. 22 the soil qualities are plotted vs. the pore space. The graph data only refer to dry compaction and involves both traffic systems and both field operations. Fig. 22 shows that the pore space at dry compaction is an important determinant of the soil qualities. For simplicity the data symbols are fitted by straight lines, using standard regression techniques.

The sensitivities of the soil qualities to the pore space at dry compaction are: $dA_c/dP \approx 1.39$; $dlogK_i/dP \approx 15.27$; $dCl/dP \approx -0.29$; $dK_{sat}/dP \approx 10.56$; $d\sigma_i/dP \approx -0.012$. From the sensitivity of the soil qualities to the pore space at dry compaction it is concluded that the deviation of the predicted values of the soil qualities from the true values can be largely attributed to the variance of the soil compactibility. Therefore, the analysis of factors causing deviation is confined to factors which underlie the variance of the compactibility.

The significance of the variance of the compactibility to explain the deviation of the soil qualities only applies to the strength hardening process type. If soil mainly exhibits flow upon compaction, compactibility has lost its meaning and must be replaced by flowability. As opposed to the compactibility, the M-P-V diagram does not give information on the flowability. Therefore, the variance of the soil qualities at wet compaction cannot be related to the variance of the flowability. In the absence of a profound base, deviation at wet compaction is not further analyzed.
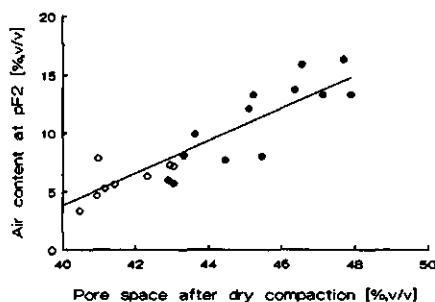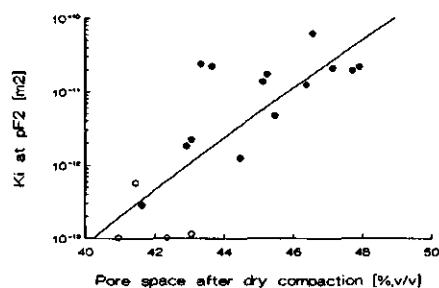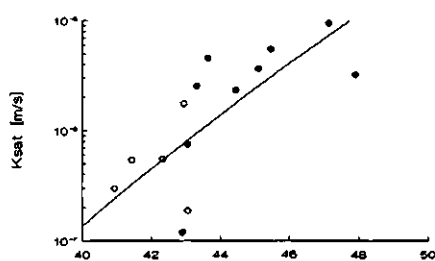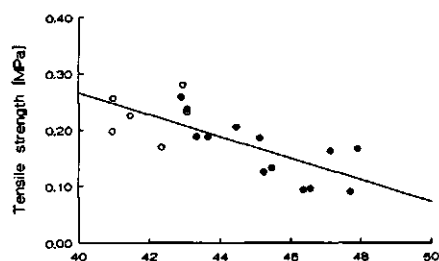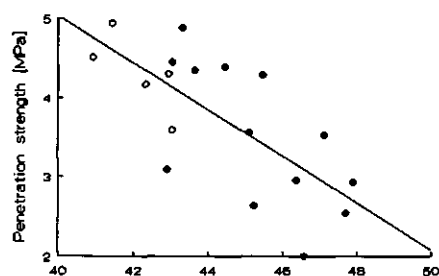
Fig. 22. Relationship between pore space and soil qualities of dry compacted soil
(open dots: harvest operations; closed dots: seedbed preparation).

105

7.6.3 Variance of the compactibility

Deviation of P_{pr} from P_{tr} at dry compaction indicates that, within the limited domain of prediction, the compactibility is not a unique function of the gravimetric water content at compaction. Thus, in order to increase the effectiveness of the prediction functions, additional process characteristics have to be taken into account. A detailed inquiry, based on statistical concepts, of factors causing variance of the compactibility lies beyond the scope of this study. In the following, some factors which potentially contribute to deviation will be evaluated. Additional characteristics may involve soil properties which are descriptive of the initial soil state and factors which are known to cause inter-seasonal variation of the initial soil state. Of both groups examples will be given.

Soil properties

1. The initial pore space

The initial pore space at seedbed preparation and the harvest varied considerably and approximately ranged from 45 to 60 % and 42 to 56 %, respectively. The M-P-V diagrams of Figs. 16 to 19 show that, in general, the initial and final pore space are positively correlated. It can be reasoned that the sensitivity of the final pore space to the initial pore space depends on factors which determine the initial state of compactness. To this respect, distinction can be made between mechanical pre-compaction and natural consolidation.

2. Intrinsic soil properties

The spatial heterogeneity of the intrinsic properties of the experimental field is only one of many factors which control the spatial variability of the field soil. Other factors comprise subsoil characteristics, the altitude of the soil surface, the type and timing of field operations and others. The effect of the perceived variation of the intrinsic properties can only be studied in case of a spatial homogeneous setting of these supplementary factors. The experiment presented here does not satisfy this condition. Thus the question of the effect of the variance of the soil intrinsic properties on the effectiveness of the prediction functions remains unsolved. In view of the relatively large variation of the intrinsic properties of the experimental field it is expected that the effectiveness of prediction functions obtained from observations on "real" field soils surmount the effectiveness of the

prediction functions which are established in this study.

Other factors

Factors which are considered here as relevant in determining the inter-seasonal variation of the field soil state at seedbed preparation are:
1) the type of crop grown during the preceding growing season;
2) the soil condition at the harvest of the preceding crop;
3) the soil condition at primary tillage;
4) weather factors.

In Table 16, a qualitative expression is given of the effects of the distinct factors on the field soil state at the time seedbed preparation is normally carried out.

A "+" notation is used if a decrease of the soil compactibility is to be expected.
A "-" notation is used to express the opposite.
If no effect is to be expected, a "+/-" notation is used.

Preceding crop

Table 2 showed that the traffic intensity of rootcrops is markedly higher than the traffic intensity of seedcrops. This difference is mainly caused by harvest traffic. Since intensive traffic will result in a poorer soil physical condition, the effects of rootcrops and seedcrops are expressed by a "-" and "+" notation, respectively.

Table 16. The effect of some relevant factors in determining the compactibility at seedbed preparation.

Exp. no.	clay cont.	pre-crop	soil cond. harvest	soil cond. prim. till.	sum winter rainfall	sum winter temp.	sum
1.	+/-	-	+/-	-	+	+	+/-
2.	+/-	-	+/-	-	+	+	+/-
3.	+/-	-	+/-	-	+/-	+	-
4.	+	+	-	+	+/-	+	+
5.	-	-	+/-	+	+/-	+	+/-

Soil condition at the harvest

The effect of harvest traffic is represented by a "-" sign if traffic was carried out under relatively wet soil conditions ($w_f << w_c$), causing wet compaction. A "+" notation indicates dry compaction ($w_f << w_c$). (Information on the soil water content was obtained from Klooster, IMAG).

Soil condition at primary tillage

The effect of primary tillage is represented by a "+" notation if the field operation was performed under relatively dry soil conditions resulting in intensive fracture formation during tillage. A "-" notation indicates a wet soil condition resulting in limited fracturing of the cohering soil mass. (Information on the soil water content was obtained from Klooster, IMAG).

Winter rainfall

Excessive rainfall during the time in between primary tillage and seedbed preparation adversely effects the soil structure. The cumulative winter rainfall was presented in Fig. 10. Fig. 10 showed that the winter rainfall in 1986/1987, prior to experiments no. 4 and 5 was somewhat higher than in the corresponding period in 1985/1986.

Winter temperatures

Intermittent freezing/thawing has a positive effect on the soil physical condition. Fig. 11 showed that the temperature regimes of the winters prior to the experiments (1985/1986, 1986/1987) were to a great extent comparable, featuring relatively many frost days. In Table 16 this situation is represented by a "+" notation for all experiments.

In Table 16, the respective effects were summed, assuming the effects being of equal weight and additive. Despite this rather crude approach, it appears that the outcome of the effect-summation procedures is in agreement with the relatively poor and good initial and final soil conditions in experiment number 3 and 4, respectively.

8   LABORATORY SIMULATION OF THE EFFECTS OF COMPACTION BY FIELD TRAFFIC

The establishment of prediction functions would be greatly facilitated if the effects of compaction by field traffic could be adequately simulated by laboratory compaction tests. Dawidowski and Lerink (1990, Appendix III) applied the quick uni-axial compaction test on prepared soil samples. The compaction tests were run at various uni-axial loads and water contents. The effects of compaction were quantified in a way comparable to the study presented here. The authors compared the soil state diagrams of traffic and laboratory compacted soil and concluded that the effect of traffic-induced compaction can be adequately simulated by the quick uni-axial compaction test, provided that the levels of the isobars are field-calibrated. The degree of similarity decreased at higher water contents at compaction.

The differences between the effects of traffic-induced and laboratory compaction can be attributed to:
-    expulsion of water during testing;
-    field traffic not only induces uni-axial strain, but also lateral expansion (Tijink et al. 1989, Appendix I);
-    compaction by field traffic is the result of a number of loading cycles; at laboratory testing only one loading cycle was applied;
-    differences in compression rates;
-    the actual value of σ_1 in field situations is not known. Furthermore, σ_1 may depend on the initial soil state;
-    at laboratory testing samples of prepared soil are used.

Dawidowski and Lerink (1990, Appendix III) used prepared soil samples in order to standardize the initial soil state, and because the size of the soil structural elements and holes would otherwise be too big and too varying to give representative and reproducible results. The practical benefits of a standardized sample preparation procedure are beyond doubt. However in some cases it may be inevitable to fall back on undisturbed field samples.

The soil behaviour in the uni-axial compaction test only approximates the true process in the field. In order to optimize the simulation procedure more information

is required on the soil structural changes on a microscopic scale in relation to the macroscopic effect, i.e. volume strain, deformation and distortion. It may well be true that uni-axial compaction underestimates the actual strains on a microscopic scale.

The uni-axial compaction test not properly simulates the effects of traffic in situations were wet compaction prevails. Here, the tri-axial compaction test (Dawidowski et al. 1990, Appendix II) and the distortion apparatus (Lerink, 1990, Appendix V) are useful alternatives. Since volume reduction is considered here of minor importance, moisture-pressure-volume (M-P-V) diagrams should be replaced by moisture-pressure-distortion (M-P-D) diagrams. Further research is required to set the boundary conditions for testing, such as the deformation rate and the cell pressure of the tri-axial apparatus. The calibration of a M-P-D diagram by field experiments imposes a specific problem, being the obscurity of the degree of deformation in the zone of influence. Perhaps deformation can be related to the rut depth (see also Tijink et al., 1990, Appendix I).

The prediction functions presented in § 7 only apply to a limited domain: a single field, a given set of farm machinery, two field operations and two traffic systems. In this section it is discussed how the domain of prediction can be extended in order to account for a greater range of soil and traffic characteristics.

Field soils on a given farm or on a range of farms may vary with respect to soil type, drainage condition and field management. The soil state diagram, based on uni-axial compaction tests, is a powerful tool to classify the sensitivity of these field soils to dry compaction. A similar technique was proposed by Gupta and Larson (1982).

The tyre inflation pressure and the wheelload can be used as a reference base in order to extend the domain of prediction to other types of farm machinery and traffic systems. This extension relies on the accuracy of predicted stress distributions in the soil mass and stress-volume strain relationships (see also Koolen et al., 1992, Appendix VI).

Other field operations which are relevant in determining the field soil quality, because of the traffic intensity and the compaction capability, are spraying and primary tillage (ploughing). Spraying operations differ from other field operations in that frequent use is made of the spraying tracks. Table 7 showed that the spraying tracks may receive up to 24 passages, each separated by a period of time of variable duration. The effect of a spraying operation is expected to be greatly dependant on the effect of preceding operations. This factor makes prediction cumbersome.

The effect of field traffic at ploughing is of limited interest since compaction by the over-land wheels is immediately followed by the loosening action of the plough. Prediction of the effect of in-furrow wheels requires a different approach, which accounts for the nature of the plough pan and the effects of excessive slip.

To increase the extensibility of the prediction method, reliable information is required on relationships between wheel characteristics and the stress distribution in the zone of influence. Especially for the flow-type compaction process this information still is scarce. It is to be expected that Finite Element Methods (FEM) will help to enlighten this complex field of soil-wheel interaction.

10   CONCLUSION

Of those factors adversely affecting the physical condition of the arable layer of agricultural soils, field traffic is by far the most important. The intensity of field traffic, in terms of load transfer and frequency in place and time justifies the scientific interest in general and the need for adequate prediction techniques in particular.

Prediction is the ultimate form of knowledge and, inherently, the most uncertain form of knowledge. An effective way to reduce this uncertainty is to limit the domain of prediction by reducing the number and range of the process characteristics that have to be treated as variables. The major limitations of the domain of prediction in this study are the single field and the given set of farm machinery.

The occurrence of field traffic is not chaotic but indeed well-defined by rules of soil and crop management practices. The same applies, be it to a lesser extent, to the field soil condition at the time a field operation is to be performed. The discernment of the regular, systematic features of field traffic and the field soil condition at the time of field traffic forms an important base for the method of prediction proposed in this study.

Based on the analysis of the systematics of field traffic and the field soil condition, it was hypothesized that the soil condition of a field soil with given intrinsic properties can be uniquely defined by a single property, being the gravimetric water content at compaction. Likewise, it was expected that the traffic intensity of the machinery used for seedbed preparation and the harvest of root crops, respectively, are comparable.

During the passage of a wheel, an elemental soil volume in the zone of interference deforms and often reduces in volume. Most prediction methods proposed so far only take volume reduction into consideration. The change of the physical soil quality however may not be uniquely related to the degree of volume reduction. This is attributed to the deterioration of the soil structure due to deformation. In this study, information on the effect on the pore space is extended by information on soil physical properties which contain relevant information for the

112

user. The prediction functions, relating the water content at compaction to the expected effect on the soil qualities, are presented graphically by means of extended M-P-V diagrams.

The results, based on laboratory tests on field compacted soil, confirm the significance of the soil water content in determining the effect of compaction by a given field operation. Of the many factors possibly undermining the effectiveness and reliability of the prediction functions, the variation of the soil intrinsic properties of the plots on the experimental field was considered the most important.

The single field validity of the prediction function presented in this study drastically restricts the applicability on a routine base. Laboratory simulation of the effects of compaction and standardized stress measurement techniques are considered useful to classify the susceptibility of field soils to compaction and the compaction capability of agricultural machinery, respectively.

The importance of distortional strains in determining the effect on the physical condition of wet compacted soil emphazizes the need for adequate stress-strain theories. It is expected that Finite Element Methods (FEM) will help to enlighten this complex field of soil-wheel interaction.

Het voorspellen van de onmiddellijke effecten van berijding op bodemkwaliteiten.

Bij het gebruik van de bodem voor akkerbouwmatige produktie doeleinden is de fysieke toestand van de bouwvoor continu aan veranderingen onderhevig. Deze veranderingen zijn een gevolg van mechanische en natuurlijke processen. Mechanische processen worden vaak onderverdeeld in verdichtende en losmakende processen (§ 1). De verdichtende processen zijn vooral het gevolg van het berijden van de bodem tijdens gemechaniseerde veldwerkzaamheden ten behoeve van gewasverzorging en grondbewerking.

Verdichting door berijding is een bijkomend gevolg van de veldwerkzaamheden en als zodanig onbedoeld en vaak zelfs ongewenst. Als gevolg van de hoge lasten die op de bodem worden overgedragen en de hoge berijdingsfrequentie zijn de effecten van berijding op de fysieke bodemtoestand ingrijpend en grootschalig.

Het kunnen voorspellen van de effecten van berijden is een onderdeel van de studie naar een doelmatig en ecologisch verantwoord bodembeheer. Het doel van deze studie is het ontwikkelen van een strategie voor het voorspellen van de berijdingseffecten op basis van eenvoudig toegankelijke procesgrootheden. De globale opzet van deze studie is in § 2 kort uiteen gezet.

Het effect van berijden hangt af van een groot aantal factoren, zoals blijkt uit verkennende en verklarende studies die aan dit onderzoek ten grondslag liggen. De waarde van deze zogenaamde procesgrootheden, welke betrekking hebben op de voertuigen en werktuigen die deel uitmaken van het veldverkeer en de bodemtoestand op het moment van berijden, wordt in vergaande mate bepaald door het teeltsysteem. Om toegang te krijgen tot de anderszins moeilijk kwantificeerbare procesgrootheden wordt in deze studie een systeem-benadering van het veldverkeer en de bodemtoestand toegepast (§ 3).

Teeltsystemen verschillen van land tot land, van regio tot regio, van bedrijf tot bedrijf en zelfs van perceel tot perceel. Oorzaken hiervan zijn bijvoorbeeld het klimaat, de grondsoort, de grootte van het bedrijf en het kleigehalte van de bouwvoor. Teneinde het aantal procesgrootheden tot hanteerbare proporties terug

te brengen is in deze studie gekozen voor een voorspellingsmethode met een één-perceelsgeldigheid. Impliciet worden daarbij het teeltsysteem, het machinepark en de grondsoort als onveranderlijke grootheden verondersteld. De één-perceelsgeldigheid is in deze studie de belangrijkste beperking van het domein van de voorspellingsmethode (§ 3).

Een nadere analyse van het berijdingssysteem op een gegeven perceel leert, dat de aard van de veldwerkzaamheden en het tijdstip waarop deze werkzaamheden worden uitgevoerd, vooral worden bepaald door de gewasrotatie (§ 4). Naar de berijdingsintensiteit kan men daarbij onderscheid maken tussen graangewassen en rooivruchten. De werkbreedte van de te onderscheiden veldwerkzaamheden bepaalt vervolgens het sporenpatroon op het veld. De bandspanning, de wiellast en het aantal spoorvolgende wielen worden, gegeven het type bewerking, als belangrijkste grootheden beschouwd die bepalend zijn voor het verdichtingsvermogen.

De verandering van de bodemtoestand als gevolg van berijding wordt aangeduid met de algemene term verdichting. Tijdens het verdichtingsproces onder een passerend wiel verandert een eindig volume-elementje grond in volume en van vorm. Onder droge omstandigheden overheerst volume-verandering, terwijl verdichting onder natte omstandigheden vooral gepaard gaat met vormverandering ofwel stroming. Het eind-volume van een gewichtseenheid grond en de mate van stroming als gevolg van een zekere belasting worden aangeduid met de algemene term verdichtingsgevoeligheid.

De verdichtingsgevoeligheid van de bouwvoor van een gegeven perceel verandert voortdurend als gevolg van elkaar aanvullende mechanische en natuurlijke processen (§ 5). Zowel de mechanische als de natuurlijke processen hebben in eerste benadering een cyclisch karakter, met een periode van één jaar. Een nadere beschouwing leert, dat in een gegeven tijdsbestek waarin een bepaalde bewerking wordt uitgevoerd, de fluctuatie van de verdichtingsgevoeligheid in belangrijke mate wordt bepaald door de fluctuatie van de vochttoestand van de bouwvoor. Op basis hiervan is vervolgens aangenomen dat de tussen-jaarlijkse fluctuatie van de verdichtingsgevoeligheid van de bouwvoor, in de periode dat een bepaalde bewerking wordt uitgevoerd, wordt bepaald door één grootheid: de vochttoestand van de bouwvoor.

Voor het beschrijven van de bodemgesteldheid, onmiddellijk volgend op een

115

berijding, is in deze studie gekozen voor een reeks bodem-fysische eigenschappen welke betrekking hebben op afzonderlijk aspecten van de fysieke bodemtoestand en welke gevoelig zijn voor verdichting door berijding (§ 6). Deze bodem-fysische eigenschappen worden bodemkwaliteiten genoemd. Voor het creëren van een voorspellingsfunctie, d.w.z. een functie die een verband legt tussen de bodem- en berijdingsgrootheden enerzijds en het effect op de bodemkwaliteiten anderzijds, is de zogenaamde vergelijkende methode toegepast. De vergelijkende methode berust op het axioma, dat een te voorspellen grootheid telkens dezelfde waarde aanneemt wanneer zich eenzelfde situatie voordoet zoals beschreven door de bekende grootheden, mits de onbekende grootheid éénduidig bepaald wordt door de bekende grootheden.

Gedurende een periode van 3 jaar zijn grondmonsters genomen vlak voor en direct na berijdingen tijdens veldwerkzaamheden op een proefveld op het IMAG-proefbedrijf "de Oostwaardhoeve". Het proefveld maakte deel uit van een interdisciplinair onderzoeksproject: "Perspectives of reducing soil compaction by using a low-ground-pressure traffic system". De bodemkwaliteiten zijn bepaald aan de hand van laboratorium metingen. De resultaten van de waarnemingen zijn grafisch weergegeven door middel van zogenaamde bodemtoestands diagrammen (§ 7). Door het verbinden van de discrete meetresultaten door vloeiende curven zijn continue voorspellingsfuncties gevormd. De curven, die de relatie weergeven tussen het vochtgehalte tijdens berijding en het onmiddellijke effect op de bodemkwaliteiten, hebben betrekking op twee groepen bewerkingen (de zaai- en pootbedbereiding en de oogst van rooivruchten) en twee berijdingssystemen (het gangbare hogedruk en het lagedruk berijdingssysteem).
De resultaten onderschrijven het belang van het vochtgehalte bij het bepalen van het berijdingseffect op de bodemkwaliteiten.

Uni-axiale persproeven, uitgebreid met metingen aan bodemkwaliteiten, kunnen een belangrijke bijdrage leveren aan het ontwikkelen van voorspellingsfuncties (§ 8). Uitgebreide uni-axiale persproeven kunnen tevens worden toegepast voor het classificeren van de verdichtingsgevoeligheid van verschillende gronden. Tenslotte kunnen uitgebreide uni-axiale persproeven een rol spelen bij het overdragen van voorspellingsfuncties met een één-perceelsgeldigheid naar situaties die buiten het domein van de voorspellingsfuncties liggen (§ 9). De waarde van de simulatie van het effect van berijding door uni-axiale persproeven beperkt zich tot verdichtingsprocessen waarbij volume verandering overheerst. Voor situaties die vooral gekenmerkt worden door stroming bieden tri-axiale persproeven

116

perspectieven. Drukcelmetingen onder voertuigen, gecombineerd met formules waarmee het spanningsverloop in de bodem onder banden geschat kan worden, kunnen worden toegepast voor het classificeren van het verdichtingsvermogen van verschillende berijdingssystemen.

Aan het verdiepen van de kennis omtrent het stromingsgedrag van grond onder banden kan Finite Element Methods (FEM) een bijdrage leveren.

REFERENCES

Akram M, Kemper WD (1979) Infiltration of soils as affected by the pressure and water content at the time of compaction. Soil Sci. Soc. Am. J., 43: 1080-1086. American Society for Testing Materials (A.S.T.M.) (1964) Book of standards, II. Am. Soc. Test. Materials, PA, pp. 206-213.

Andersson S, Håkansson I (1966) Structure dynamics in the top soil. Grundförbättring, 3: 191-288.

Arndt W, Rose CW (1966) Traffic compaction of soil and tillage requirement. J. Agric. Eng. Res., 11: 170-187.

Atterberg A (1912) Die Konsistenz und die Bindigkeit der Böden. Intern. Mitt. Bodenk., 2: 149-189.

Baganz K (1963/64) Spannungs- und Verdichtungsmessungen im Boden bei verschiedenen Fahrgeschwindigkeiten. Archiev für Landtechnik, 4: 35-45.

Barnes KK, Carleton WM, Taylor HM, Trockmorton RI, Vanden Berg GE (eds) (1971) Compaction of agricultural soils. ASAE, St. Joseph, USA, 471 p.

Beekman F (1987) Soil strength and forest operations. Ph.D. Thesis, Agricultural University, Wageningen, The Netherlands, 168 p.

Blackwel PS, Soane BD (1981) A method of predicting bulk density changes in field soils resulting from compaction by agricultural traffic. J. Soil Sci., 31: 51-65.

Bölling I, Söhne W (1982) Der Bodendruck schwerer Ackerschlepper und Fahrzeuge. Landtechnik, 37: 54, 56-57.

Boone FR (ed)(1984) Experiences with three tillage systems on a marine loam soil. II: 1976-1979. Agric. Res. Reports 925, Pudoc, Wageningen, 263 p.

Braunack MV, Dexter AR (1978) Compaction of aggregate beds. In: Emerson WW, Bond RD, Dexter AR (eds), Modification of soil structure. John Wiley.

Braunack MV, McPhee JE(1991) The effect of initial soil water content and tillage implement on seedbed formation. Soil Tillage Res., 20: 5-17.

Bruce RR, Thomas AW, Harper LA, Leonard RA (1977) Diurnal soil water regime in the tilled plow layer of a warm humid climate. Soil Sci. Soc. Am. J., 41: 455-460.

Bullock P, Newman ACD, Thomasson AJ (1985) Porosity aspects of the regeneration of soil structure after compaction. Soil Tillage Res., 5: 325-341.

Bullock MS, Kemper WD, Nelson SD (1988) Soil cohesion as affected by freezing, water content, time and tillage. Soil Sci. Soc. Am. J., 52: 770-776.

Cannell RQ (1973) Some effects of soil compaction on root growth. NIAE Subject Day, Mechanical Behaviour of Agricultural Soils, February 22nd, 1973.

Chancellor WJ (1976) Compaction of soil by agricultural equipment. University of California, Bull. 1881, 53 p.

Chaney K, Swift RS (1986) Studies on aggregate stability. I. Re-formation of soil aggregates. J. Soil Sci., 37: 329-335.

Cooper AW, Trouse AC, Dumas WT, Williford JR (1983) Controlled traffic farming; a beneficial cultural practice for southern US agriculture. ASAE Paper No. 83-1547, ASAE, St. Joseph, MI 49085.

Cresswell HP, Painter DJ and Cameron KC (1991) Tillage and water content effects on surface soil physical properties. Soil Tillage Res., 21: 67-83.

Croney D, Coleman JD (1954) Soil structure in relation to soil suction. J. Soil Sci., 5: 75-84.

Danfors B (1974) Compaction in the subsoil. Transl. from Spec. Bull. S.24, Swedish Institute of Agricultural Engineering, Ultuna, Sweden, 91 p.

Davies DB, Finney JB, Richardson SJ (1973) Relative effects of tractor weight and wheelslip in causing soil compaction. J. Soil Sci., Vol. 24, 3: 399-409.

Dawidowski JB, Koolen AJ (1987) Changes in soil water suction, conductivity and dry strength during deformation of wet undisturbed samples. Soil Tillage Res., 9: 169-180.

Dawidowski JB, Lerink P (1990) Laboratory simulation of the effects of traffic during seedbed preparation on soil physical properties using a quick uni-axial compression test. Soil Tillage Res., 17: 31-45.

Dawidowski JB, Lerink P, Koolen AJ (1990) Controlled distortion of soil samples with reference to soil physical effects. Soil Tillage Res., 17: 15-30.

De Bakker H (1979) Major soils and soil regions in the Netherlands. Junk, The Hague/Pudoc, Wageningen, 203 p.

De Wit CT, Van Keulen H (1987) Modeling production of field crops and its requirements. Geoderma, 40: 253-265.

Dexter AR (1988) Advances in characterization of soil structure. Soil Tillage Res., 11: 199-238.

Dexter AR, Horn R, Kemper WD (1988) Two mechanisms for age-hardening of soil. J. Soil Sci., 39: 163-175.

Dexter AR, Kroesbergen B, Kuipers H (1984) Some mechanical properties of aggregates of top soils from the IJsselmeer polders. 2. Remoulded soil aggregates and the effects of wetting and drying cycles. Neth. J. Agric. Soil Sci., 32: 215-227.

Dexter AR (1991) Amelioration of soil by natural processes. Soil Tillage Res., 20:

87-100. Douglas JT (1986) Effects of season and management on the vane shear strength of a clay top soil. J. Soil Sc., 37: 669-679.

El-Domiaty AM, Chancellor WJ (1970) Stress-strain characteristics of saturated clay soil at various rates of strain. Trans. ASAE, 13: 685-690.

Eriksson J, Håkansson I, Danfors B (1974) Effect of soil compaction on soil structure and crop yields. Swedish Institute of Agricultural Engng. Bull. 354, 101 p.

Feddes RA, Kowalik PJ, Zaradny H (1978) Simulation of field water use and crop yield. Simulation Monograph. Wageningen, Pudoc, 1978, 189 p.

Freitag DR, Schafer RL, Wismer RD (1970) Similitude studies of soil machine systems. Trans. ASAE, 13: 201-213.

Fröhlich OK (1934) Druckverteilung im Baugrunde. Springer Verlag, Wien.

Gameda S, GSV Raghavan, E McKyes, Theriault R (1987) Subsoil compaction in a clay soil. I. Cumulative effects. Soil Tillage Res., 10: 113-122.

Gupta SC, Allmaras RR (1987) Models to assess the susceptibility of soils to excessive compaction. Advances in Soil Science, 6: 65-100.

Gupta SC, Larson WE (1982) Modelling soil mechanical behaviour during tillage. In: Unger P, Van Doorn PM Jr, Whisler FD, Skidmore AAEL (eds), Symposium on Predicting Tillage Effects on Soil Physical Properties and Processes. Am. Soc. of Agron., Spec. Publ. 44, Madison, WI, pp. 151-178.

Greenland DJ (1981) Soil management and soil degradation. Soil Sci. J., 32: 301-322.

Håkansson I, Voorhees WB, Riley H (1988) Vehicle and wheel factors influencing soil compaction and crop response in different traffic regimes. Soil Tillage Res., 11: 239-282.

Hadas A, Wolf D (1984) Soil aggregates and clod strength dependence on size, cultivation and stress load rates. Soil Sci. Soc. Am. J., 48: 1157-1164.

Harris RF, Chesters G, Allen ON (1966) Dynamics of soil aggregation. In: Norman AG (ed) Adv. Agron., 18: 107-169.

Hettiaratchi DRP (1987) A critical state soil mechanics model for agricultural soils. Soil Use Management, 3: 94-105.

Hillel D (1980) Fundamentals of Soil Physics. Academic Press, New York, NY, 413 p.

Horn R (1980) Eine Methode zur Ermittlung der Druckbelastung von Böden anhand von Drucksetzungsversuchen. Z. f. Kulturtechnik und Flurbereinigung, 22: 20-26.

Horn R, Blackwell PS, White R (1989) The effect of speed of wheelings on soil stresses, rutdepth and soil physical properties in an ameliorated

Transitional Red Brown Earth. Soil Tillage Res., 13: 353-364.

Jakobsen BF, Dexter AR (1989) Prediction of soil compaction under pneumatic tyres. Soil Tillage Res., 26: 107-119.

Kay BD, Grant CD, Groenevelt PH (1985) Significance of ground freezing on soil bulk density under zero tillage. Soil Sci. Soc. Am. J., 49: 973-978.

Kemper WD, RC Rosenau, Dexter AR (1987) Cohesion development in disrupted soils as affected by clay and organic matter content and temperature. Soil Sci. Soc. Am. J., 51: 860-867.

Kirkham D, De Boodt MF, De Leenheer L (1959) Modulus of rupture determination on undisturbed soil core samples. Soil Sci., 87: 141-144.

Klute A, Dirksen C (1986) Hydraulic conductivity and diffusity: Laboratory methods. In: Klute A (ed) Methods of soil analysis. Part 1, Physical and Mineralogical Methods, 2nd edition, Number 9, ASA/SSSA, Madison, Wisconsin USA, pp. 687-732.

Koolen AJ (1976) Mechanical properties of precompacted soil as affected by the moisture content at precompaction. In: Proc. 7th ISTRO Conf., Sweden, paper 20.

Koolen AJ (1977) Soil loosening processes in tillage analysis, systematics and predictability. Ph.D. Thesis, 159 p. Meded. Landbouwhogeschool Wageningen 77-17.

Koolen AJ (1978) The influence of a soil compaction process on subsequent soil tillage processes. A new research method. Neth. J. Agric. Sci., 40: 167-182.

Koolen AJ (1982) Precompaction stress determination on compacted soil. In: Proc. 9th ISTRO Conf., Osijek, Yugoslavia, pp. 225-230.

Koolen AJ, Kuipers H (1983) Agricultural soil mechanics. Advanced Series in Agricultural Sciences 13, Springer Verlag, Berlin, Heidelberg, etc., 241 p.

Koolen AJ (1987) Deformation and compaction of elemental soil volumes and effects on mechanical soil properties. Soil Tillage Res., 10: 5-19.

Koolen AJ, Boekel P, Perdok UD, Van Wijk ALM (1987) Bewerkbaarheidsgrenzen en hun bodemfysische achtergrond. Themadag "Werkbaarheid en tijdigheid", May 13, Wageningen, The Netherlands, PAGV verslag nr. 64, pp. 22-40.

Koolen AJ, Van Ouwerkerk C (1988) Pedotechnique - Inventory of predictive methods, and unlocking of relevant input data. In: Proc. 11th ISTRO Conf., Edinburgh, Scotland, Vol. 2: 721-726.

Koolen AJ, Kuipers H (1989) Soil deformation under compressive forces. In: Mechanics and related processes in structured agricultural soils (Eds.: WE

Larson, GR Blake, RR Allmaras, WB Voorhees, SC Gupta). NATO ASI Series, Serie E: Applied Sciences, Vol. 172: 37-53, Kluwer, Dordrecht.

Koolen AJ, Lerink P, Kurstjens DAG, Van den Akker JJH, Arts WBM (1992) Prediction of aspects of soil-wheel systems. Soil Tillage Res., 24: 381-396.

Kouwenhoven JK (1986) Model studies on upheaval and reconsolidation of tilled soils in a laboratory soil bin. Soil Tillage Res., 8: 289-302.

Kuipers H, Van Ouwerkerk C (1963) Total pore estimations in freshly ploughed soil. Neth. J. Agric. Sci., Vol. 11, no.1, p.45-53.

Kuipers H (1968) Entgegengesetzte Effekte von Reifen und Bodenbearbeitung. Berichte des Internationalen Symposiums, 13-15 Juni 1968, Warna, pp. 59-65.

Kuipers H (1986) Soil compaction in arable farming. Trans. XIII Congress ISSS, 13-20 August, Hamburg, Vol. 5: 310-327.

Lafond J, Angers DA, Laverdière MR (1992) Compression characteristics of a clay soil as influenced by crops and sampling dates. Soil Tillage Res., 22: 233-241.

Larson WE, Gupta SC (1980) Estimating critical stresses in unsaturated soils from changes in pore water pressure during confined compression. Soil Sci. Soc. Am. J., 44: 1127-1132.

Lerink P (1990) The kneading distortion apparatus. Technical Note, Soil Tillage Res., 17: 173-179.

Lumkes LM (1984) Traffic intensity. In: Boone FR (ed) Experiences with three tillage systems on a marine loam soil. II: 1976-1979. Agric. Res. Reports 925. Pudoc, Wageningen, p. 12-23.

McGarry D (1987) The effect of soil water content during land preparation on aspect on soil physical condition and cotton growth. Soil Tillage Res., 9: 287-302.

Miller RD (1980) Freezing phenomena in soils. In: Hillel D (ed) Applications of soil physics. Academic Press, New York.

Molope MB, Grieve IC, Page ER (1985) Thixotropic changes in the stability of molded soil aggregates. Soil Sci. Soc. Am. J., 49: 979-983.

Ojeniyi SO, Dexter AR (1979) Soil factors affecting the macro-structures produced by tillage. Trans. ASAE, 22: 339-343.

O'Sullivan MF (1992) Uniaxial compaction effects on soil physical properties in relation to soil type and cultivation. Soil Tillage Res., 24: 257-269.

Perdok UD, Hendrikse LM (1982) Workability test procedure for arable land. In: Proc. 9th ISTRO Conf., Osijek, Yugoslavia, pp. 511-519.

Plackett CW (1985) A review of force prediction methods for off-road wheels. J.

Agric. Engng. Res., 31: 1-29.

Pollock D, Perumpral JV, Kuppusamy T (1984) Multipass effects of vehicles on soil compaction. Paper No. 84-1054 presented at the winter meetings of the ASAE, Chicago, IL.

Proctor RR (1933) Fundamental principles of soil compaction. Eng. News Record, 111: 245-248,286-289,348-351.

Raghavan GSV, McKyes E, Stemshorn E, Gray A, Beaulieu B (1977) Vehicle compaction patterns in clay soil. Trans. ASAE 20: 218-220,225.

Raghavan GSV, McKyes E, Chassé M (1976) Soil compaction patterns caused by off-road vehicles in Eastern Canadian agricultural soils. J. Terram., 13: 107-115.

Raper RL, Johnson CE, Bailey AC, Burt AC, Block WA (1992) Predicting soil stresses beneath a rigid wheel. Paper no. 9201101 presented at Ag. Eng. 92, Uppsala, Sweden, 1992, pp. 12.

Reid I, Parkinson RJ (1987) Winter water regimes of clay soils. J. Soil Sci., 38: 473-481.

Saini GR, Chow TL and Ghanem I (1984) Compactibility indexes of some agricultural soils of New Brunswick, Canada, pp. 33-38.

Schafer RL, Johnson CE (1980) Changing soil condition - The soil dynamics of tillage. In: Prediction of tillage effects on soil physical properties and processes. ASA, Madison Wisconsin USA, pp. 13-28.

Smith DLO, Dickson JW (1984) On the contributions of ground pressure and vehicle mass to soil compaction for vehicles carrying high and low payloads. SIAE Departemental Note no. SIN/411.

Smith DLO (1985) Compaction by wheels: a numerical model for agricultural soils. Soil Sci. J., 36: 621-632.

Snyder VA (1987) Mechanical equilibrium in externally loaded unsaturated granular similar media. Soil Sci. Soc. Am. J. 51:1413-1424.

Soane BD (1970) The effects of traffic and implements on soil compaction. J. Proc. Inst. Agric. Eng., 25: 115-126.

Soane BD, Blackwell PS, Dickson JW, Painter DJ (1981a) Compaction by agricultural vehicles: A review. I. Soil and wheel characteristics. Soil Tillage Res., 1: 207-237.

Soane BD, Blackwell PS, Dickson JW, Painter DJ (1981b) Compaction by agricultural vehicles: A review. II. Compaction under tyres and other running gear. Soil Tillage Res., 1: 373-400.

Soane BD, Dickson JW, Campbell DJ (1982) Compaction by agricultural vehicles: A review III. Incidence and control of compaction in crop production. Soil

Tillage Res., 2: 3-36.

Soane BD (1985) Traction and transport systems as related to cropping systems. Proc. Int. Conf. Soil Dynamics, Auburn AL, 5: 863-935.

Söhne W (1952) Die Verformbarkeit des Ackerbodens. Grundl. Landt., 3: 51-59.

Söhne W (1953) Druckverteilung im Boden und Bodenverformung unter Schlepperreifen. Grundl. Landtechnik, 5: 49-63.

Söhne W (1958) Fundamentals of pressure distribution and soil compaction under tractor tyres. Agric. Engng., 39: 279-281, 290.

Soil Survey Staff (1975) Soil Taxonomy. A basic system of soil classification for making and interpreting soil surveys. Handbook, 436. USDA, U.S. Govt. Print. Off., Washington, D.C., 754 p.

Sommer C, Stoinev K, Altemüller HJ (1972) Das Verhalten vier verschiedener Modelböden unter vertikaler Belastung. Landbauforschung Völkenrode, 22(1): 45-56.

Sommer C (1976) Ueber die Verdichtungsempfindlichkeit von Ackerböden. Grundl. Landt., 26: 14-23.

Spivey LD, Busscher WJ, Campbell RB (1986) The effect of texture on strength of South-Eastern Coastal Plain soils. Soil Tillage Res., 6: 351-363.

Spoor G, RJ Godwin (1979) Soil deformation and shear strength characteristics of some clay soils at different moisture contents. J. Soil Sci., 30: 483-498.

Spoor G, RJ Godwin (1984) Influence of autumn tilth on soil physical conditions and timing of crop establishment in spring. J. Agric. Engng. Res., 29: 265-273.

Stafford JV, de Carvalho Mattos P (1981) The effect of forward speed on wheel-induced soil compaction: Laboratory simulation and field experiments. J. Agric. Engng. Res., 26: 333-347.

Stone JA, Larson WE (1980) Rebound of five one-dimensionally compressed unsaturated granular soils. Soil Sci. Soc. Am. J., 44: 819-822.

Taylor JH, Burt EC, Bailey AC (1980) Effect of total load on subsurface soil compaction. Trans. ASAE, 23: 568-570.

Taylor JH (1981) A controlled-traffic system using a wide frame carrier. In: Proc. 7th Int. Conf. ISTVS, Calgary, Canada 1: 385-409.

Taylor JH, Gill WR (1984) Soil compaction: state of-the-art report. J. Terramechanics, 21: 195-213.

Tijink FGJ (1988) Load bearing processes in agricultural wheel-soil systems. Ph.D. Thesis, Agricultural University, Wageningen, The Netherlands, 173 p.

Tijink FGJ, Lerink P, Koolen AJ (1988) Summation of shear deformation in stream tubes in soil under a moving tyre. Soil Tillage Res., 12: 323-345.

Towner GD (1988) The influence of sand- and silt-size particles on the cracking during drying of small clay-dominated aggregates. J. Soil Sci., 39: 347-356.

Unger PW, DK Cassel (1991) Tillage implement disturbance effects on soil properties related to soil and water conservation: a literature review. Soil Tillage Res., 19: 363-382.

Utumo WH, Dexter AR (1981a) Tilth mellowing. J.Soil Sci., 32: 187-201.

Utumo WH, Dexter AR (1981b) Soil friability. J.Soil Sci., 32: 203-213.

Utumo WH, Dexter AR (1982) Changes in soil aggregate water stability induced by wetting and drying cycles in non-saturated soils. J. Soil Sci., 33: 623-637.

Van de Zande JC (1991) Computed reconstruction of field traffic patterns. Soil Tillage Res., 19: 1-15.

Van den Akker JJH, Van Wijk ALM (1985) A model to predict subsoil compaction due to field traffic. In: Monnier G, Goss MJ (eds) Soil compaction and regeneration. Proc. Workshop Soil Compaction, Avignon, pp. 69-84.

Van den Akker JJH (1988) Model computation of subsoil stress distribution and compaction due to field traffic. In: Proc. 11th ISTRO Conf. Edinburgh, Scotland, Vol. 1: 403-408.

Van den Akker JJH, Lerink P (1990) Verandering van bodemkwaliteiten door berijding. Themadag Management Bodemstructuur, Werkgroep Technische Aspecten van de Grondbewerking, NRLO, pp. 25-44.

Van Lanen HAJ, Boersma OH (1988) Use of soil-structure type data in a soil-water model to assess the effects of traffic and tillage on moisture deficit, aeration and workability of sandy loam and clay loam soils. In: Proc. 11th ISTRO Conf., Edinburgh, Scotland, pp. 415-420.

Van Wesenbeeck IJ, Kachanoski RG (1988) Spatial and temporal distribution of soil water in the tilled layer under a corn crop. Soil Sci. Soc. Am. J. 52: 363-368.

Van Wijk ALM (1984) Physical soil degradation: Analysis, modeling and effects of soil compaction due to field traffic in modern agriculture. Institute for Land and Water Management Research, internal note no. 1524.

Van Wijk ALM (1987) Effect van grondsoort en ontwatering op de bewerkbaarheid en tijdigheid in het voorjaar. Themadag Bewerkbaarheid en Tijdigheid, May 13, Wageningen, The Netherlands, PAGV verslag nr. 64, pp. 86-103.

Vermeer PA (ed.)(1991) PLAXIS, finite element code for soil and rock plasticity. Balkema, 1991, 99 p.

Vermeulen GD, Arts WBM, Klooster JJ (1988) Perspective of reducing soil

compaction by using a low ground pressure farming system: selection of wheel equipment. In: Proc. 11th ISTRO Conf., Edinburgh, Scotland, Vol.1, pp. 329-344.

Vermeulen GD (ed) (1989) Unpublished Report, IMAG, Wageningen, 1989, 118 p.

Voorhees WB (1977) Soil compaction. Nature of the problem. Conservation Tillage Research and Needs, 1977.

Willatt ST (1987) Influence of aggregate size and water content on compactibility of soil using short-time static loads. J. Agric. Engng. Res., 37: 107-115.

Yong R, Fattah EA, Skiadas N (1984) Vehicle traction mechanics. Elsevier Science Publishers, Amsterdam, 307 p.

CURRICULUM VITAE

Peter Lerink was born on October 7th, 1956 in Arnhem (The Netherlands).

From 1975 to 1983 he studied Agricultural Engineering at the Wageningen Agricultural University. His main subjects were agricultural mechanical engineering and soil dynamics.

From 1985 to 1988 he worked as a research fellow at the Department of Soil Tillage, Wageningen, on the study of soil compaction in field operations.

Since 1990 he is appointed in a research and development function of Rumptstad Industries, manufacturer of agricultural machineries.

APPENDICES

Summation of Shear Deformation in Stream Tubes in Soil under a Moving Tyre

F.G.J. TIJINK*, P. LERINK** and A.J. KOOLEN

Tillage Laboratory of the Wageningen Agricultural University, Diedenweg 20, 6703 GW Wageningen (The Netherlands)

ABSTRACT

Tijink, F.G.J., Lerink, P. and Koolen, A.J., 1988. Summation of shear deformation in stream tubes in soil under a moving tyre. *Soil Tillage Res.*, 12: 323-345.

Deformation of a silt loam and a silty clay loam, induced by a moving tyre, was measured and analysed using the theory of large strains in 3 dimensions. Tyre dimensions were half those of current large agricultural trailer tyres and the initial soil depth was half the thickness of the arable layer in agricultural fields. Rut depths were 39.5 and 28.9% of the initial soil-layer thickness. Within the tyre width, soil porosity was reduced from 48 and 50% to 44.1 and 43.8%, and the natural largest principal strain was 0.642 and 0.440. The strain of volume elements was approximately radial-symmetric, while the principal directions rotated considerably. Deviatoric strain dominated over volumetric strain.

INTRODUCTION

The deformation of soil under a tyre in soil–vehicle systems is not only of interest in relation to the development of rolling resistance and pull force, but also because it changes the soil qualities of importance in soil use. Undisturbed soil that is being approached by a tyre may be considered to be composed of small elemental volumes, cubes, arranged in such a way that their angular points form a 3-dimensional cubic grid of horizontal layers of cube rows parallel to the direction of wheel travel. Rut formation and slip will be accompanied by deformation of volume elements near the tyre. The deformation of a volume element starts as soon as it enters the zone influenced by the tyre, and deformation stops as soon as the element leaves the zone of influence. During the time that such an element is in this zone, its degree of deformation generally increases with time. An element that has passed the zone is in a

---

*Present address: Institute of Agricultural Engineering (I.M.A.G.), Wageningen, The Netherlands.
**Author to whom correspondence should be addressed.

deformed state, with a degree of deformation dependent on soil factors, tyre factors and soil–vehicle system factors. The deformation that the volume element has endured has changed the element condition on a micro-level, and thus has also changed soil qualities such as: water retention, air content at field capacity, water and gas conductivities, thermal properties, root penetration resistance, erodibility, shrinkability, as well as soil mechanical properties (compactability, deformability, breakability, soil-material friction and adherence; Koolen, 1987). Studies concerning the effects on soil qualities require a different description of the degree of deformation of a volume element than studies concerning rolling resistance and pull force.

Deformation investigations usually have been concentrated on one or only very few aspects of deformation, such as deformation measurements needed to establish stress fields from strain fields (Perumpral et al., 1971) or strain rate fields (Yong et al., 1984), or compaction patterns. Also, they have often been confined to soil that moved in only vertical planes in the direction of travel (plane strain condition). This article presents a deformation investigation in which the course of deformation of volume elements was measured and expressed in measures that are expected to be closely connected with the change in soil micro-condition and qualities, without the limitation of plane strain.

FLOW AND DEFORMATION

Flow analysis

Soil near a tyre can be considered as a continuum that flows with respect to a space reference system. If properties and flow characteristics at each position in space remain invariant with time, the flow is called steady flow. A time-dependent flow, on the other hand, is called unsteady flow. Often, a steady flow may be derived from an unsteady flow field by changing the space reference. For instance, the unsteady flow pattern created by a tyre moving over initially undisturbed soil at constant speed V_0 relative to a reference xy (Fig. 1a) can be transformed to a steady flow in reference $\xi \eta$ (Fig. 1b) fixed to the wheel axis by superimposing a velocity V_0 on the entire flow field of Fig. 1a.

Flows can be presented graphically with streamlines. These lines are drawn so as to be always tangent to the velocity vectors of soil particles in a flow (see Fig. 1). For steady flow, the orientation of the streamlines will be fixed, and soil particles will proceed along stream paths coincident with the streamlines. Streamlines proceeding through the periphery of a very small area dA at some time t will form a tube, called stream tube (see Fig. 1b). According to the definition of the streamline, there can be no flow through the walls of the stream tube. As in steady flows the stream tubes are fixed, the small black volume element fixed to the undisturbed soil in Fig. 1b will just flow through the indicated stream tube, its lateral sides coinciding with the stream tube wall.
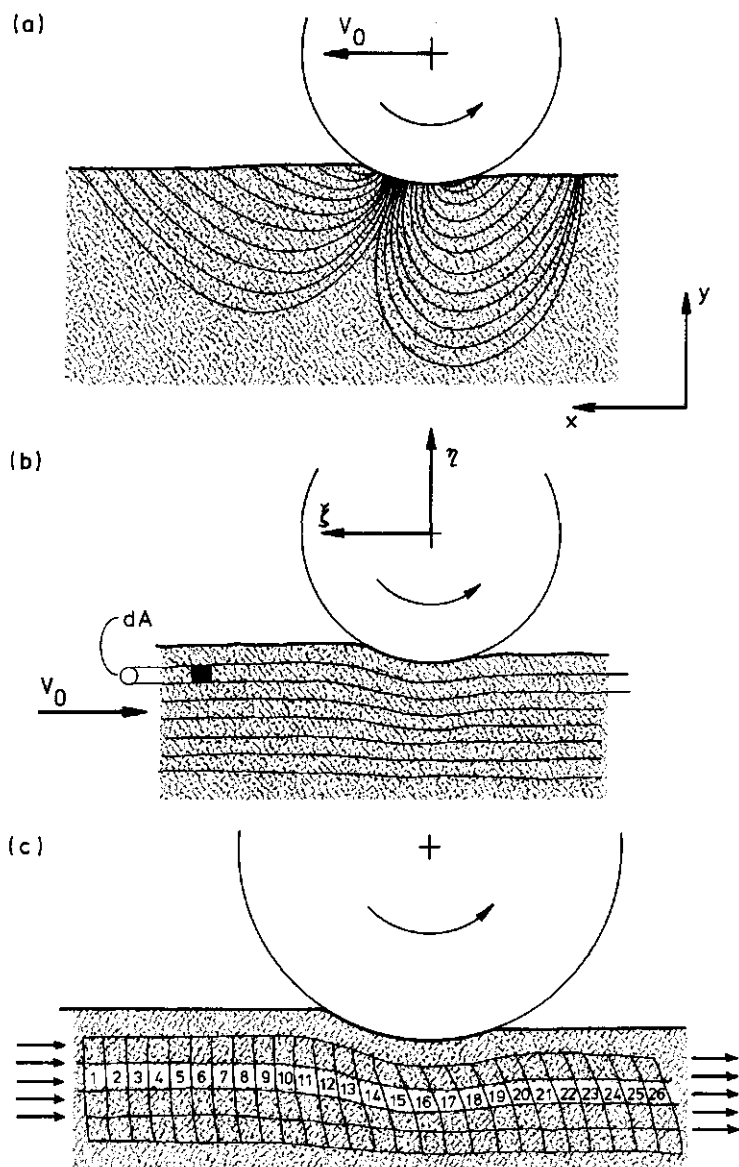
Fig. 1. Stream lines in a soil-wheel system. Unsteady flow in (a) is changed into steady flow in (b) by changing from xy to $\xi\eta$-reference. A stream tube is indicated in (b). Subsequent positions of a volume element moving through a stream tube are numbered in (c).

Here, the element will move initially as a rigid body, deform in the curved part of the stream tube, and again move as a rigid body when it has left the wheel's sphere of influence. Volume elements flowing through one and the same stream tube in a steady flow field behave identically. Because the vertical plane through

the centre of the wheel in the direction of travel is a plane of symmetry, the flow pattern on one side of this plane is the mirror image of the pattern at the other side of the plane.

Fig. 1c shows subsequent, numbered stages of deformation of a small initially cubic soil element passing through a stream tube in a steady flow field. The time interval between two successive stages has been selected so that it equals the original soil element length divided by the velocity of the untouched soil. Because the picture of Fig. 1c presents a steady flow, its determination is relatively easy. Although the picture as such is not an instantaneous picture, it can be obtained from an instantaneous picture of the soil interior, provided with an internal grid, when taken at the moment the wheel is passing by. The reason for this is, of course, that all successive volume elements behave identically.

For many flowing materials, deformation will not influence properties of the volume element material, as in the case of water, or only induce reversible changes, as in the case of air. When soil is deformed, however, one must expect deformation-induced structural changes that make the physical properties of the element change greatly. The soil physical effect of the deformation endured by the volume element in Fig. 1c cannot be determined uniquely by merely comparing its final shape (Position 21) with its initial shape (Position 9), because the final shape can be obtained from the initial shape via an infinite number of different "deformation paths". But, theoretically, there is always a unique "shortest path" to arrive at a given shape from another given shape. When two shapes are compared, between which only little deformation has occurred (for instance Nos. 15 and 16 in Fig. 1c), it may be stated that the "true" path resembles the "shortest" path. Therefore, a large deformation path can be dealt with by dividing the deformation into a number of small steps of small deformation, calculating relevant quantities for each step on the basis of the "shortest"-path assumption, and, finally, adding up the relevant quantities. It appears that the sum found is independent of the step number chosen, provided the steps are small.

An important question is, what are the relevant quantities that must be summed to obtain the most useful relationship between deformation sum and soil physical effect? This question cannot be answered yet. This article therefore concentrates on quantities that are directly connected with the measurements and significantly change as deformation progresses.

Analysis of homogeneous strain

In volume-element deformation studies it is very convenient to select the element small enough that the flow in a small domain containing the element may be assumed to be homogeneous. Straightness and parallelism of small line elements in the domain are then conserved during deformation. When the vol-

ume element is cubic initially, homogeneity means that the element transforms to a non-cubic rectangular block or a parallelepiped, and its deformation can be completely recorded by following 4 angular points of the body, not all lying in one plane.

Fig. 2a shows a very small volume element moving through a stream tube. A small domain containing the initially cubic element is supposed to undergo homogeneous deformation and the stream tube is straight, so that in the drawing plane the element deforms from a square (labelled i) to a rectangle (labelled f), its height changing from l_i to l_f. Two intermediate positions, close to each other, are indicated, one occurring at time t, the other an infinitesimally small time interval dt later. The relative vertical compression, $d\epsilon_l$, in time dt is:

$$d\epsilon_l = \frac{l_t - l_{t+dt}}{l_t}$$

if decrease in length is taken as positive.

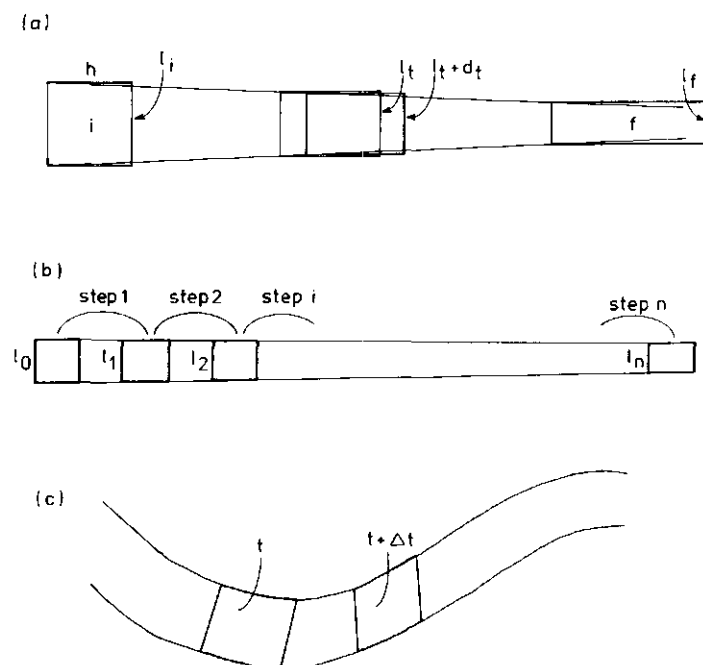The total relative vertical compression occurring between positions i and f is

Fig. 2. Refers to the definitions of incremental and natural strain of a volume element moving through a stream tube. (a) Change of element in straight tube in small time interval. (b) Changes in large time intervals. (c) Change in curved tube.

135

$$\int_{\text{position } i}^{\text{position } f} d\epsilon_l$$

which is known as true or natural vertical strain, indicated by $\bar{\epsilon}_l$ (where the subscript refers to the line element considered). Obviously,

$$\bar{\epsilon}_l = -\int_{l_i}^{l_f} \frac{dl}{l} = \ln\left(\frac{l_i}{l_f}\right)$$

The so-called large, or technical, vertical strain between positions i and f is defined as

$$\epsilon_l = \frac{l_i - l_f}{l_i}$$

It can easily be shown that

$$\bar{\epsilon}_l = -\ln\,(1 - \epsilon_l)$$

When the deformation path is divided into n small but finite steps, with vertical strain $(\varDelta\epsilon_l)_j$ in step j, then

$$\bar{\epsilon}_l \approx \sum_{j=1}^{n} (\varDelta\epsilon_l)_j$$

if the steps selected are small enough. This approximation is inaccurate if steps are relatively large. The inaccuracy is eliminated when incremental strains are expressed as natural incremental strains. Clearly, for the large steps in Fig. 2b:

$$\varDelta\bar{\epsilon}_1 + \varDelta\bar{\epsilon}_2 + \ldots + \varDelta\bar{\epsilon}_n = \ln\frac{l_0}{l_1} + \ln\frac{l_1}{l_2} + \ldots + \ln\frac{l_{n-1}}{l_n} = \ln\frac{l_0 l_1 l_2 \ldots l_{n-1}}{l_1 l_2 \ldots l_n} = \ln\frac{l_0}{l_n} = \bar{\epsilon}_l$$

So:

$$\bar{\epsilon}_l = \sum_{j=1}^{n} (\varDelta\bar{\epsilon}_l)_j$$

The above approach can be applied to any line element of the body, e.g. side h, and to volume changes.

Usually in soil, a flow as in Fig. 2a involves compaction and lateral expansion (perpendicular to the drawing plane). It means that the largest change in length occurs in the vertical direction. Important is the question of what deformation quantity relates most to the effect on physical soil properties. Is it volume change, or $\bar{\epsilon}_l$, or $\bar{\epsilon}_h$, or a certain stage in the course of deformation, or are there even interactions? Most likely it is $\bar{\epsilon}_l$, because it reflects the amount of soil

particle movement best; lateral expansion and volume change partly compensate each other, and lateral expansion is distributed over more directions.

Generally, a stream tube is not straight, but curved, as in Fig. 2c. An initially cubic volume element will deform to a parallelepiped, which changes continuously when travelling through the stream tube. The shapes at time t and a short time-interval Δt later, are presented in Fig. 2c. It may be assumed that the situation at $t+\Delta t$ has developed from the situation at t through: a translation of the body centre of gravity, followed by, firstly, so-called principal strains in principal directions, and after this, a rotation of the element (so-called rigid-body rotation).

The strain of a line element during Δt is called a principal strain if there exist line-elements normal to the considered line-element at t, that remain normal to that line-element during Δt. Directions of line elements undergoing principal strain are called principal directions. According to strain theory, a homogeneous deformation generally has 3 principal directions, all mutually perpendicular. The largest linear strain in the body occurs in one of the principal directions and is denoted by $\Delta \epsilon_1$. The smallest, denoted by $\Delta \epsilon_3$, occurs in another principal direction, while $\Delta \epsilon_2$ is the principal strain in the remaining principal direction. As $\Delta \epsilon_1$, $\Delta \epsilon_2$, and $\Delta \epsilon_3$ refer to one deformation 'step', they are often called incremental principal strains. If rotation in Δt is small, directions of line elements of the body are not influenced significantly by the rotation in time-interval Δt. Then, the principal directions defined by the above decomposition of the change in Δt may be considered as 'true' principal directions occurring during Δt. If rotation in Δt is large, the principal strain directions in the decomposition of the change in shape between t and Δt have little physical meaning.

Mathematically, the shape of the volume element in Fig. 2c at $t+\Delta t$ is a linear transformation of the shape at t. Using linear algebra, principal strains, principal directions and angle of rotation can be calculated from the angular points of both parallelepipeds. Calculation procedures for 2-dimensional homogeneous deformation have been given in detail by Koolen and Kuipers (1983). A brief description of procedures applying to the 3-dimensional case is presented as an appendix at the end of this article.

Just as $\bar{\epsilon}_l$ was found to be pertinent in the flow in Fig. 2a, the natural largest principal strain, $\Sigma \Delta \bar{\epsilon}_1$, is expected to relate strongly to the soil physical changes of flows in curved stream tubes. Rigid body rotation in relation to orientation of principal directions needs further inspection. When the element travels through the curved stream tube, a continuous rigid body rotation takes place, as well as a continuous rotation of the principal directions. If both rotations are not equal, the element experiences principal strains of which the directions rotate during the deformation process. It is still unknown to what extent this will result in a soil physical effect different from that of identical principal strains having constant directions relative to the element.

The assumption of homogeneous flow in volume elements, made in the previous section, is never entirely correct if the angular points of the elements are measured coordinates of tracers in experiments. This is because of experimental errors, soil heterogeneity and the fact that tracers buried in soil never form a grid with infinitesimally small meshes. As a consequence, measured angular points never formed exactly parallelepipeds, and correction procedures had to be developed. These procedures refer to estimating the volume of an element,
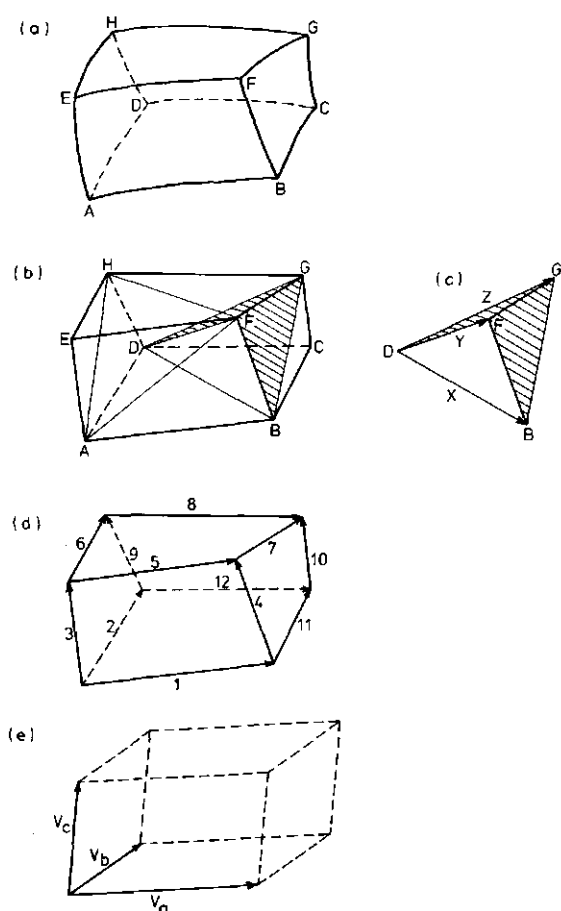
Fig. 3. Experimental strain analysis. (a) True (unknown) shape of convex element. (b) Approximation by a non-convex element, which is divided into tetraeders (c) to calculate volume. Approximation (d) with straight lines between angular points is transformed into parallelepiped (e). Finally, shape (e) is blown or shrunk to the estimated volume to obtain a parallelepiped that fits (a) well.

138

establishing a parallelepiped shape that fits the shape of an element well and dealing with data scatter.

Because of the above-mentioned reasons, the true shape of a deformed grid element defined by measured positions of angular points is not a parallelepiped but a so-called convex body (Fig. 3a). It means that its volume is not uniquely defined by the coordinates of its angular points. To estimate the volume of the body two simplifying assumptions were made: (1) the edges of the body are straight lines; (2) each of the 6 surfaces of the body is considered to be composed of two planes, intersecting at the connecting line between two opposite angular points of the surface.

In this way, a figure as presented in Fig. 3b is obtained. The shape and size of the new, non-convex body depend on the choice of the connecting lines between two opposite angular points. In principle, $2^6 = 64$ configurations are possible. Here, a fixed configuration has been selected, being the one presented in Fig. 3b. In this way, diagonals of corresponding planes between adjoining bodies coincide, and the sum of all individual volumes of assumed elements will equal true total volume of all real elements. The volume of the non-convex body can easily be calculated after recognizing that it is composed of 6 tetraeders (using diagonal DF in Fig. 3b). It is known that the volume of tetraeder DBGF (Fig. 3c) defined by vectors $\mathbf{X}(\mathbf{x}_1, \mathbf{x}_2, \mathbf{x}_3)$, $\mathbf{Y}(\mathbf{y}_1, \mathbf{y}_2, \mathbf{y}_3)$, $\mathbf{Z}(\mathbf{z}_1, \mathbf{z}_2, \mathbf{z}_3)$ can be calculated using

$$\text{Volume DBGF} = 1/3 \begin{vmatrix} \mathbf{x}_1 & \mathbf{x}_2 & \mathbf{x}_3 \\ \mathbf{y}_1 & \mathbf{y}_2 & \mathbf{y}_3 \\ \mathbf{z}_1 & \mathbf{z}_2 & \mathbf{z}_3 \end{vmatrix}$$

Applying the same procedure to the remaining tetraeders (AEFH, ADFH, ADFB, DFGH, BCGD) and adding the results, the volume of element ABCDEFGH is obtained.

A volume element such as in Fig. 3a, the volume of which has been estimated in the way mentioned above, can be 're-shaped' into a parallelepiped which fits the original element well, using the following procedure.

(1) Define vectors $\mathbf{V}_1$, $\mathbf{V}_2$, ..., $\mathbf{V}_{12}$ between measuring points of the element, as indicated in Fig. 3d. Denote three non-parallel edges of a well-fitting parallelepiped by vectors $\mathbf{V}_a$, $\mathbf{V}_b$, $\mathbf{V}_c$ (Fig. 3e).

(2) The direction of $\mathbf{V}_a$ is selected as equal to the direction of the vector-sum of $\mathbf{V}_1$, $\mathbf{V}_5$, $\mathbf{V}_8$ and $\mathbf{V}_{12}$, the size of $\mathbf{V}_a$ is selected as equal to $\frac{1}{4}|\mathbf{V}_1 + \mathbf{V}_5 + \mathbf{V}_8 + \mathbf{V}_{12}|$. Thus,

$$\mathbf{V}_a = \tfrac{1}{4}(\mathbf{V}_1 + \mathbf{V}_5 + \mathbf{V}_8 + \mathbf{V}_{12})$$

(3) Similarly, $\mathbf{V}_b$ and $\mathbf{V}_c$ are calculated, and the parallelepiped of Fig. 3e is obtained.

(4) Finally, this parallelepiped is expanded or shrunk uniformly in all direc-

tions as much as is needed to obtain a volume equal to the estimated volume of the element in Fig. 3a.

The end result is a parallelepiped that fits well, as desired, and is used in further data processing.

Owing to the experimental problems described at the start of this section and the correction procedures involved, each volume element will show a certain amount of deformation after data processing, even when the element has not been loaded. Specifically, carrying out a strain-analysis according to the Analysis of homogeneous strain always results in finite values of rotation angle, principal strains and principal directions, even if no deformation has occurred. Mean values of each of the incremental principal strains and of incremental rotation angle, found for undeformed volume elements, are called the initial scatter level. Ideally, in the case of steady flow, elements in the same stream tube that have come to rest after deformation would be identical. Calculated rotation and strain increments for these elements should be zero. However, owing to the experimental problems and correction procedures, non-zero increments are always found. When these increments are expressed as a mean for ideally identical elements, they are referred to as the final scatter level. Deformation will always cause additional scatter as soil is always heterogeneous to some extent. Therefore, the final scatter level is higher than the initial scatter level. Initial scatter levels were calculated by applying the strain-analysis procedure to the elements in the outer, upper stream tubes, which were apparently unchanged. Each tube contained 16 elements, so these levels could be calculated from 2×15 elements. Final scatter levels were calculated by applying the procedure to four element long tube ends behind the tyre under the rut. Two tubes of each of the three tube layers were under the rut, so final scatter levels could be calculated from $2 \times 3 \times 4$ elements. The scatter level was so high that often only special approaches allowed conclusions to be drawn from the measured data. These approaches will be explained in detail where the measured results are presented and discussed (in the Results and discussion section).

EXPERIMENTAL PROCEDURE

Measurements were made in Schinnen silt loam and Wageningen silty clay loam, both being described in Koolen (1972). Soil brought in from the field was deep-frozen, dried slightly, and passed through a sieve of mesh size 10 mm. Then the water content was adjusted by moistening. After a certain equilibration time, a portable test bin (1.5-m long and 0.5-m wide) was filled with 21 equal portions. The total amount of soil required for each bin was calculated so that a final soil height of 150 mm after compression to the desired porosity would be obtained. Each portion was poured into the bin at a predetermined location to achieve uniform distribution of loose soil in the bin. After the soil

140

had been smoothed, the porosity was adjusted to the desired level with a large compression machine described in Tijink and Koolen (1985). This machine can compress the soil in a bin uniaxially through a very large compression plate that has the same length and width as the inside of the bin. The Schinnen soil was prepared at a moisture content of 26.21% (w/dry w) and a porosity of 48% (v/v). The Wageningen soil was prepared to a moisture content of 26.99% (w/dry w) and a porosity of 50% (v/v).

After the above soil preparation, a vertical, round steel needle with a diameter of 6.0 mm and a flat bottom was forced into the soil down to the bin bottom and drawn back carefully, so that a continuous vertical hole was created. This was repeated at distances of 5 cm so that the holes in the soil surface formed a square grid of rows of holes with centre-to-centre distances of 5 cm in longitudinal and transverse directions of the soil bin. Subsequently, in each hole, a small steel ball was pushed to the bin bottom using a very thin needle, and more balls to depths of 5.00, 10.00 and 14.75 cm less than the depth of the lowest ball. This was possible because ball diameters were slightly greater than hole diameter, so that on one hand balls could be brought into the holes with a thin needle, and on the other hand balls did not fall from their own weight to greater depths than desired. The highest balls were just below the soil surface. In this way, the soil was provided with an internal 3-dimensional grid having tracers in the grid points in the form of steel balls. The grid element size was always $5 \times 5 \times 5$ cm, except for the upper layer where grid elements were $5 \times 5 \times 4.75$ cm.

A tyre was run a certain distance in the marked soil using the wheel–soil test facility described in Tijink and Koolen (1985). In these experiments, the soil was moved and not the wheel axis. The wheel was suspended in a rigid frame constructed over rails attached to the rail foundation. Soil bins, prepared in a separate building, were transported by hydraulic crane to a carriage which could be pulled along the rails by an electrically-powered cable winch. The linear dimensions of the tyre used were about half those of current large agricultural trailer tyres. The depth of the soil in the bins was 150 mm, that is about half the thickness of the arable layer in agricultural fields. The carriage with the soil bin was moved under the frame construction and rut formation started as soon as the tyre contacted the soil. After a rut of a certain length was formed, the wheel was raised suddenly by letting the tyre climb against an inclined rigid plate, positioned a little above the soil surface. Wheel raising was assumed to be fast enough for the soil not to change during removal of the wheel, so that the final state of deformation reflects steady flow. Both tests were run with a 'Vredestein', agricultural trailer and implement tyre of the following specifications: (1) tread; 'grooved implement (GI)'-type, having 4 circumferential, 6-mm deep, grooves with an outer width of 8 mm and an inner width of 6 mm; (2) tyre size, 7.00–12 (tyre width 187 mm, diameter 667 mm); (3) ply rating, 4; (4) rated load at 1.5 bar inflation pressure, 490 kg. In the tests, the tyre

inflation pressure was 1.5 bar, and the wheel was ballasted so that a vertical load of 497 kg was exerted on the soil. Forward speed was 0.25 m s^{-1}.

After rut formation, the deformation pattern was recorded by measuring spatial coordinates of all steel balls while removing the deformed soil carefully. Care was taken that ball positions were not disturbed before being measured. Use was made of a vertical measuring needle that could move along calibrated guides in 3 orthogonal directions. The measured grid for the Schinnen soil is partly presented in Fig. 4. In this figure, connecting lines have been drawn between grid points in order to visualize volume elements. Each grid element is labelled using i- , j- , and k-numbers as indicated in Fig. 4. The hatched element, for instance, is labelled $i=10, j=1, k=2$. Likewise, stream tubes, element layers etc. may be referred to using these numbers. Fig. 4 also defines the orientation of an xyz-reference system. This sytem will be used to present and discuss directional aspects in the following section. Data processing started with calculating 'new', well-fitting parallelepipeds from the measured elements following the procedures outlined in Experimental strain analysis. Next, deformation quantities were calculated for each new body (i, j, k). The 'true-path' method analysed the strain of element (i, j, k) from the shape of (i, j, k) and the shape of the element $(i-1, j, k)$ in the same stream tube. The 'shortest-path' method calculated strain values from the shape of (i, j, k) and the shape of the element $(i=1, j, k)$ being the first element in stream tube (j, k).
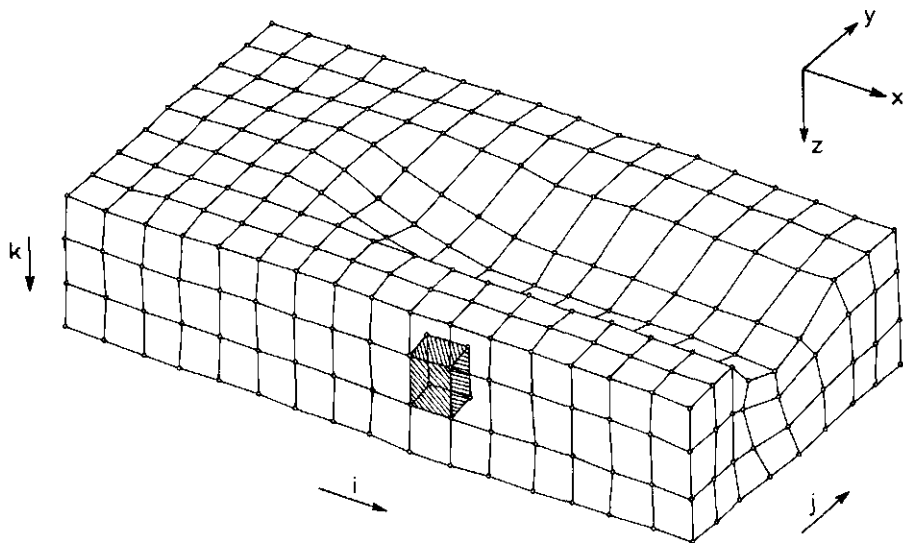

Fig. 4. Elements in steady flow field under a tyre in Schinnen soil (tyre not shown). Element positions are indicated by i, j, k. xyz-reference indicates directions.

142

RESULTS AND DISCUSSION

Results for the Schinnen silt loam are presented in Figs. 5–10 and Table 1. The 6 inner stream tubes ($(i, 4, 1)$, $(i, 4, 2)$, $(i, 4, 3)$, $(i, 5, 1)$, $(i, 5, 2)$, $(i, 5, 3)$)), which were under the tyre, did not differ much. Fig. 5 shows the calculated volumes of the elements in these 6 tubes, as a function of position in the tube

TABLE 1

Schinnen soil. Ultimate natural largest principal strain ($\bar{\epsilon}_1$) calculated according to the shortest-path assumption, and ultimate volume change (Δ vol%), and their standard deviations. j and k are defined in Fig. 4

|	j							
	1	2	3	4	5	6	7	8
$k=1$								
$\bar{\epsilon}_1$	0.068	0.062	0.245	0.427	0.491	0.275	0.074	0.045
std	0.016	0.013	0.011	0.020	0.019	0.012	0.009	0.026
Δ vol%	100.75	104.50	102.75	87.75	84.25	103.25	101.00	100.00
std	1.09	2.18	2.17	1.30	2.59	3.83	2.92	0.71
$k=2$								
$\bar{\epsilon}_1$	0.136	0.149	0.297	0.516	0.502	0.279	0.162	0.114
std	0.011	0.010	0.010	0.010	0.016	0.011	0.009	0.004
Δ vol%	97.50	95.25	90.00	95.75	97.00	91.00	96.50	100.50
std	1.50	1.09	1.00	1.02	1.23	2.24	1.66	0.87
$k=3$								
$\bar{\epsilon}_1$	0.148	0.141	0.264	0.450	0.426	0.212	0.134	0.113
std	0.008	0.011	0.010	0.014	0.018	0.013	0.012	0.007
Δ vol%	99.00	100.75	97.75	96.50	97.50	100.25	100.75	103.50
std	0.71	0.83	2.28	1.80	2.87	2.86	2.59	0.87
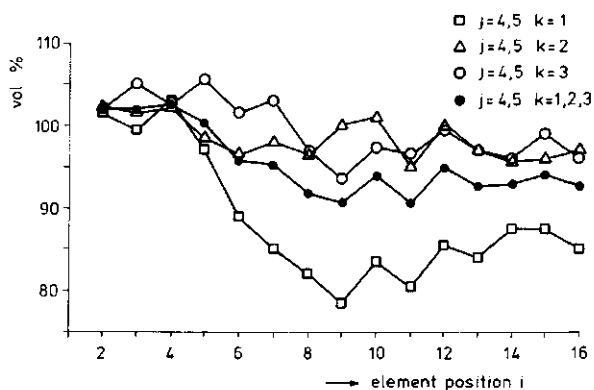
Fig. 5. Schinnen soil. Volume change in the stream tubes under the tyre. Curve through closed dots indicates mean values. i, j, k are defined in Fig. 4.
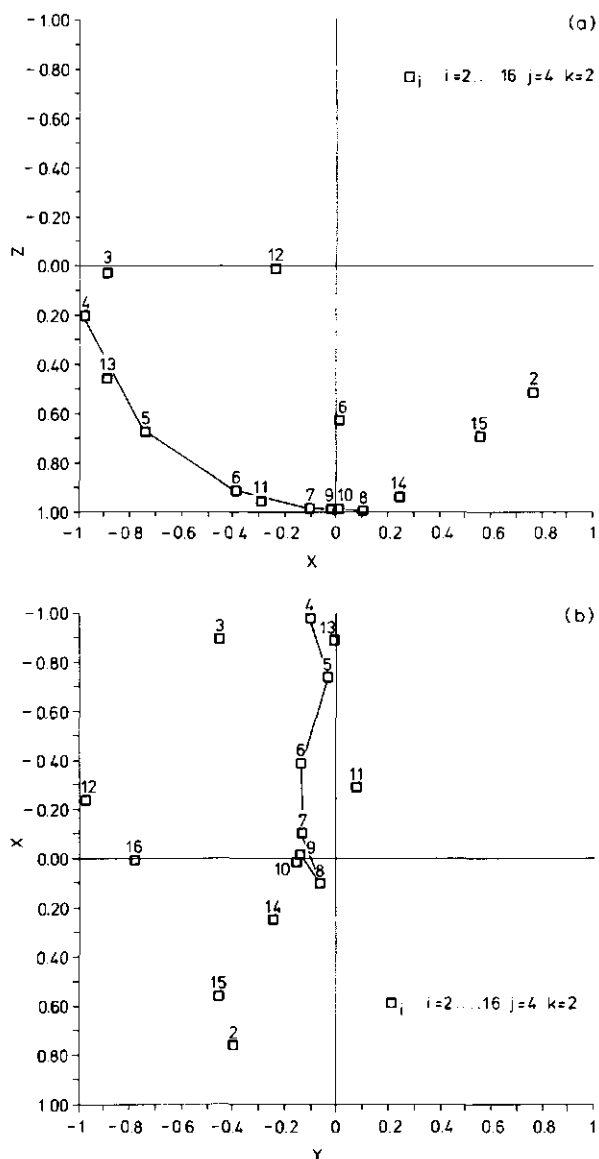
Fig. 6. Schinnen soil. Projections in the xz-plane (a) and the xy-plane (b) of unit directional vectors representing directions of incremental largest principal strain in a stream tube under the tyre. Numbers at the points refer to i. i, j, k and x, y, z are defined in Fig. 4.

(i-number). The volumes are expressed as a percentage of the volumes of the respective undeformed ($i=1$) elements. Calculated volume reduction in the upper 2 tubes is substantially higher than in the lower 4 tubes. This is partly due to soil having moved into the grooves of the tyre tread. The mean curve for the 6 tubes shows that there are 3 distinct phases of volumetric strain:
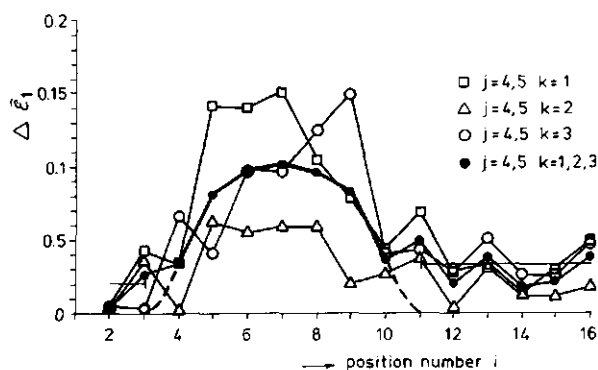
Fig. 7. Schinnen soil. Natural incremental largest principal strain in the stream tubes under the tyre. Curve through closed dots indicates mean values. Horizontal lines are scatter levels. Extended bell-shaped curve represents "true" values. i, j, k are defined in Fig. 4.
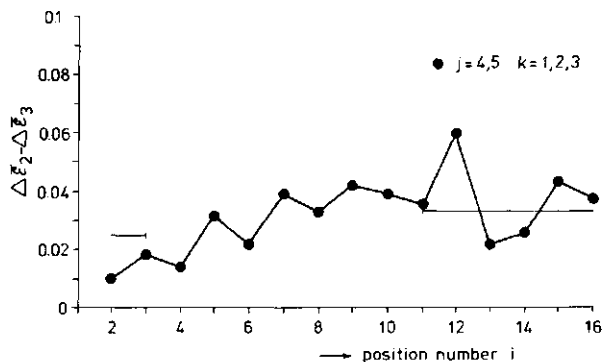

Fig. 8. Schinnen soil. Natural incremental intermediate principal strain minus natural incremental smallest principal strain in the stream tubes under the tyre. Curve through closed dots represents mean values. Horizontal lines are initial and final scatter levels. i, j, k are defined in Fig. 4.
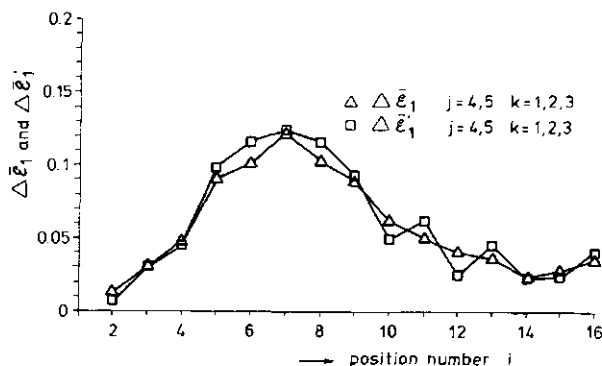
Fig. 9. Schinnen soil. Natural incremental largest principal strain components of total strain increment and of the deviatoric part of total strain increment, each averaged over stream tubes under the tyre. i, j, k are defined in Fig. 4.
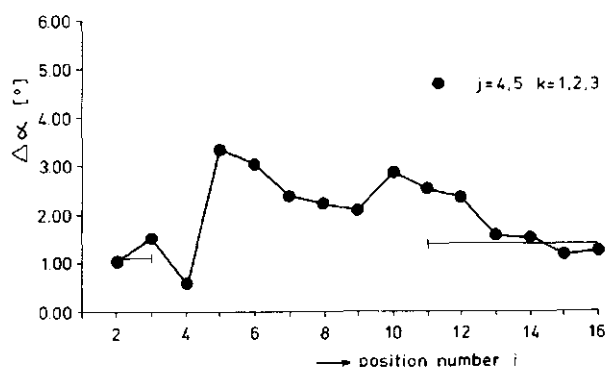
145

Fig. 10. Schinnen soil. Incremental rigid-body rotation in the stream tubes under the tyre. Curve through closed dots indicates mean values. Horizontal lines are scatter levels. i, j, k are defined in Fig. 4.
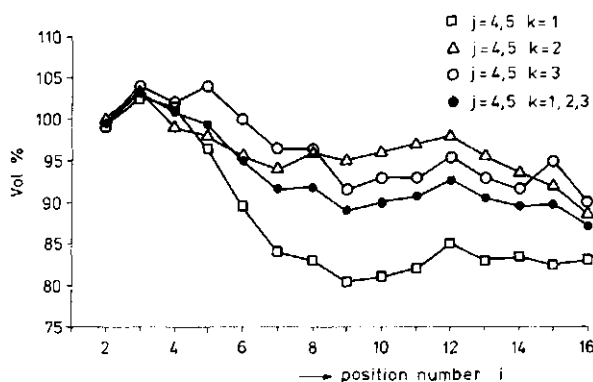

Fig. 11. Wageningen soil. Volume change in the stream tubes under the tyre. Curve through closed dots indicates mean values. i, j, k are defined in Fig. 4.

initially, volumetric expansion ($i=2, 3, 4$), followed by compaction ($i=5, ...,$ 10), and, finally, a slight expansion ($i=11, 12$). Figs. 5-10 show results obtained by the true-path method for the Schinnen soil. Direction of the natural, incremental, largest principal strain ($\Delta \bar{\epsilon}_1$-direction) has been expressed as a unit vector in the orthogonal xyz reference system defined in Fig. 4. By definition, the length of a unit vector is 1. The orientation of such a unit vector can be visualized by projecting its tip onto the xz plane under the condition that the origin of the vector is in the origin of the system. Projections of the unit $\Delta \bar{\epsilon}_1$-directional vectors for the element positions in the stream tube ($j=4$, $k=2$) are shown in Fig. 6a. Positions i are indicated by the numbers at the points shown. Theoretically, a line can be drawn that connects sequential pro-
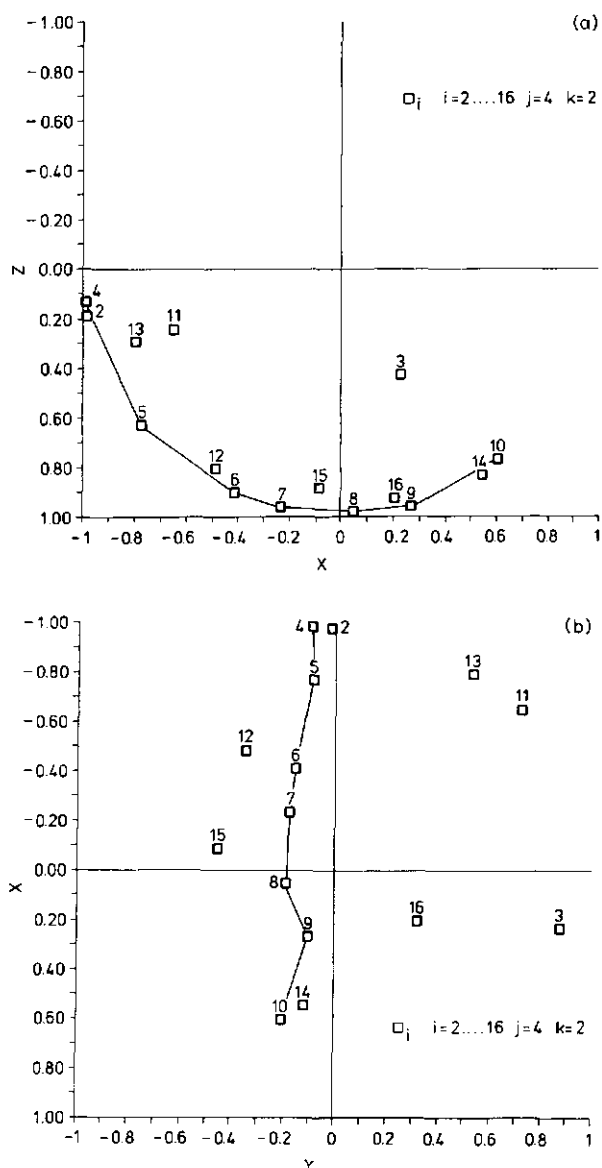
146

Fig. 12. Wageningen soil. Projections in the xz-plane (a) and the xy-plane (b) of unit directional vectors representing directions of incremental largest principal strain in a stream tube under the tyre. Numbers at the points refer to i. i, j, k and x, y, z are defined in Fig. 4.

jections in the graph. Where this line is not smooth, the projections show no true $\Delta\bar{\epsilon}_1$-directions, but only scatter. Where the line is smooth, it presumably presents true $\Delta\bar{\epsilon}_1$-directions and shows how the $\Delta\bar{\epsilon}_1$-direction changes from
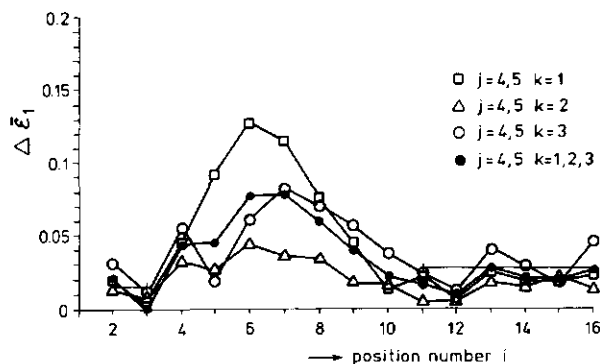
Fig. 13. Wageningen soil. Natural incremental largest principal strain in the stream tubes under the tyre. Curve through closed dots indicates mean values. Horizontal lines are scatter levels. Extended bell-shaped curve represents "true" values. i, j, k are defined in Fig. 4.
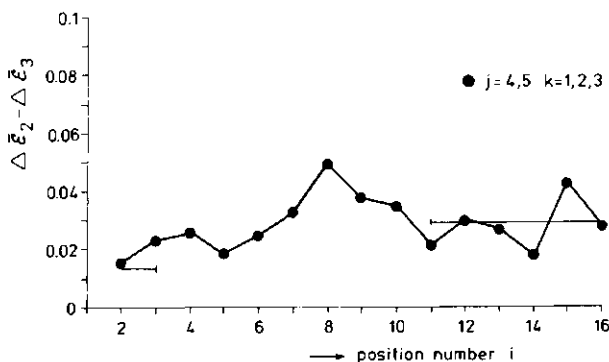

Fig. 14. Wageningen soil. Natural incremental intermediate principal strain minus natural incremental smallest principal strain in the stream tubes under the tyre. Curve through closed dots represents mean values. Horizontal lines are initial and final scatter levels. i, j, k are defined in Fig. 4.

position to position in the stream tube. Smoothness occurs for positions $i = 4 \ldots 10$, so that the $\varDelta\bar{\epsilon}_1$-directions presented for these positions may be considered as true. The smooth, true part of the connecting line has been drawn. It shows that the $\varDelta\bar{\epsilon}_1$-direction of a moving element rotated considerably as the element progressed through the stream tube. Fig. 6b shows the projections in the xy plane of the same directional vectors. $\varDelta\bar{\epsilon}_1$-directions for the positions in stream tubes $(j = 4, k = 1)$ and $(j = 4, k = 3)$ over and under the considered tube were very similar to those presented in Fig. 6. The natural incremental largest principal strain, $\varDelta\bar{\epsilon}_1$, of the elements in the 6 inner stream tubes is plotted against the position in the tube in Fig. 7. The curve through the closed dots presents the mean value in the 6 tubes for positions with the same i-number, and thus applies to the large stream tube $(j = 4, 5, k = 1, 2, 3)$. The horizontal straight lines are the initial and final scatter levels of $\varDelta\bar{\epsilon}_1$. To eliminate scatter level, the following procedure was applied.
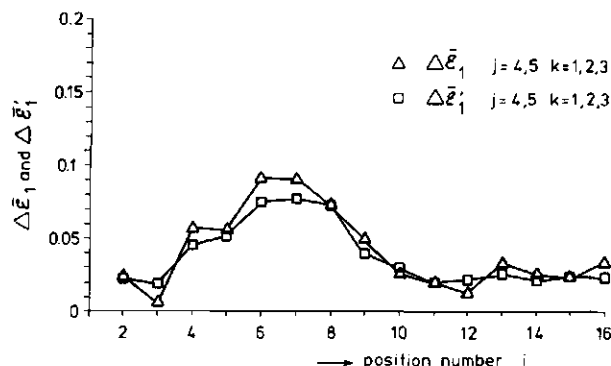
148

Fig. 15. Wageningen soil. Natural incremental largest principal strain components of total strain increment and of the deviatoric part of total strain increment, each averaged over stream tubes under the tyre. i, j, k are defined in Fig. 4.
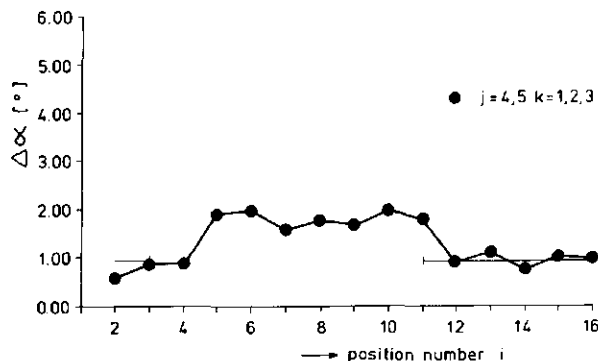

Fig. 16. Wageningen soil. Incremental rigid-body rotation in the stream tubes under the tyre. Curve through closed dots indicates mean values. Horizontal lines are scatter levels. i, j, k are defined in Fig. 4.

(1) The positions i where elements were significantly influenced by the wheel are determined from the bell-shape of the mean curve in Fig. 7.

(2) The scatter level of $\Delta\bar{\epsilon}_1$ is assumed to reduce to zero as soon as the direction of $\Delta\bar{\epsilon}_1$ is physically unique and determined correctly. It was shown in Fig. 6 that both conditions are satisfied for positions $i = 4 \ldots 10$.

(3) The true relationship between $\Delta\bar{\epsilon}_1$ and position is constructed from (1) and (2). For this, the true part of the bell-shaped mean curve between positions $i = 4$ and $i = 10$ is extrapolated to the horizontal coordinate axis to obtain a bell-shape that just covers all positions where elements were influenced significantly ($i = 3 \ldots 11$).

After completing the true curve, the total natural largest principal strain, $\tilde{\epsilon}_1$, averaged over the 6 inner stream tubes, is calculated by reading $\tilde{\epsilon}_1$-values from this curve at the positions $i = 3 \ldots 11$, and adding these values:

149

TABLE 2

Wageningen soil. Ultimate natural largest principal strain (ϵ_1) calculated according to the shortest-path assumption, and ultimate volume change (Δ vol%) and their standard deviations. j and k are defined in Fig. 4

	j							
	1	2	3	4	5	6	7	8
$k=1$								
$\bar{\epsilon}_1$	0.026	0.044	0.215	0.336	0.385	0.214	0.114	0.050
std	0.006	0.003	0.011	0.020	0.007	0.013	0.004	0.021
Δ vol%	100.50	100.25	99.25	85.75	80.25	95.75	99.50	99.50
std	1.50	0.43	1.30	1.30	0.83	2.60	1.12	1.50
$k=2$								
$\bar{\epsilon}_1$	0.074	0.107	0.193	0.334	0.326	0.214	0.114	0.050
std	0.013	0.013	0.005	0.019	0.031	0.013	0.004	0.021
Δ vol%	97.75	95.75	93.75	92.00	92.75	89.00	94.25	98.25
std	2.86	0.43	1.30	1.30	2.59	1.00	0.43	1.79
$k=3$								
$\bar{\epsilon}_1$	0.070	0.089	0.174	0.238	0.237	0.173	0.10	0.061
std	0.015	0.004	0.013	0.003	0.006	0.005	0.016	0.007
Δ vol%	92.00	93.50	92.25	91.75	93.00	92.00	93.50	95.50
std	3.39	1.12	1.79	1.92	1.87	2.24	2.06	2.29

$$\bar{\epsilon}_1 = \Sigma \Delta \bar{\epsilon}_1 = 0 + 0.045 + 0.098 + 0.116 + 0.124$$

$$+ 0.116 + 0.093 + 0.050 + 0 = 0.642$$

Fig. 8 gives $\Delta \bar{\epsilon}_2 - \Delta \bar{\epsilon}_3$ for the elements in the 6 inner stream tubes as a function of position in the tube. Initial and final scatter levels of $\Delta \bar{\epsilon}_2 - \Delta \bar{\epsilon}_3$ are presented as horizontal lines in the figure. Comparing $\Delta \bar{\epsilon}_2 - \Delta \bar{\epsilon}_3$ in the 6 inner tubes with the scatter level of $\Delta \bar{\epsilon}_2 - \Delta \bar{\epsilon}_3$ shows that usually $\Delta \bar{\epsilon}_2 \approx \Delta \bar{\epsilon}_3$. This means that, as a first approximation, element deformation was radial–symmetric.

It is known from strain theory that, theoretically, homogeneous strain can be divided into a deviatoric strain part and a volumetric strain part. Applying this division to the largest principal strain ϵ_1 it is found that

$$\epsilon_1' = \epsilon_1 - \tfrac{1}{3}\epsilon_v$$

if strains are small. ϵ_1' is the (imaginary) largest principal strain of the deviatoric strain and volumetric strain $\epsilon_v = \epsilon_1 + \epsilon_2 + \epsilon_3$. The results may be extended to small natural strain increments:

$$\Delta \bar{\epsilon}_1' = \Delta \bar{\epsilon}_1 - \tfrac{1}{3}\Delta \bar{\epsilon}_v$$

$\Delta\bar{\epsilon}_v = \Delta\bar{\epsilon}_1 + \Delta\bar{\epsilon}_2 + \Delta\bar{\epsilon}_3$. $\Delta\bar{\epsilon}_1'$ was calculated from $\Delta\bar{\epsilon}_1$, $\Delta\bar{\epsilon}_2$ and $\Delta\bar{\epsilon}_3$ for each element in the 6 inner tubes using the above formula. Fig. 9 presents $\Delta\bar{\epsilon}_1'$ as well as $\Delta\bar{\epsilon}_1$, each averaged over the 6 inner tubes, as a function of position in the tube. It can be seen that $\Delta\bar{\epsilon}_1'$ and $\Delta\bar{\epsilon}_1$ are nearly equal, which means that deviatoric strain dominated over volume change in this experiment. Fig. 10 shows, for the elements in the 6 inner tubes, incremental rigid body rotation $\Delta\alpha$ as well as mean values, and initial and final scatter levels.

The true curve has been obtained by a procedure similar to that used in obtaining the true $\Delta\bar{\epsilon}_1$. Comparing this graph with the graph for $\Delta\bar{\epsilon}_1$-directions (Fig. 6) shows that rotation of the $\Delta\bar{\epsilon}_1$-direction was much greater than rigid body rotation. So the elements have experienced rotation of principal directions.

The shortest-path method results showed that the deformation rate was very small for positions $i = 13$, 14, 15 and 16 in all stream tubes. Therefore, elements in these tube parts were considered to be outside the zone of wheel influence, and calculated shortest-path strain values were averaged over these positions for each tube. These mean values, together with their standard deviations, are presented in Table 1. It can be seen from the table that the assumption that the outer upper tubes are not influenced is not entirely correct. However, the error in computed scatter levels in the true steps method is extremely small. The shortest-path results were compared with the true steps results using the results of both methods for the 6 inner tubes. As previously explained, the true steps method calculated $\bar{\epsilon}_1 = 0.642$ for these tubes. The shortest path $\bar{\epsilon}_1$ from Table 1, averaged over the ends of the 6 inner tubes, is 0.469. So, the true steps $\bar{\epsilon}_1$ was the shortest path $\bar{\epsilon}_1$ multiplied by 1.37.

Results for Wageningen silty clay loam are presented in Figs. 11–16 and Table 2. For the 6 inner stream tubes in this soil, $\bar{\epsilon}_1$ was 0.440 by the true steps method and 0.309 by the shortest-path method, the ratio being 1.42.

The behaviour of Wageningen soil was very similar to that of the Schinnen soil. Deformations in the Wageningen soil were smaller than in the Schinnen soil. This is related to differing rut depths, which were 4.25 and 6.10 cm, respectively. Deviatoric strain dominated less over volume change in the Wageningen than in the Schinnen soil.

CONCLUSION

The degree of deformation of soil volume elements affected by a tyre has been analysed and expressed numerically. Such procedures are needed where relationships between soil–tyre system characteristics and deformation intensity are to be evaluated. Tyre size, thickness of the loose soil layer, and rut depth proportions in the reported investigation are very usual. Quantitative information on the degree of deformation is needed where field soil deformation is to be simulated with measuring equipment such as the triaxial apparatus. In the tests reported, the natural largest principal strain calculated for the

true deformation path was 40% higher than that calculated according to the shortest-path assumption.

APPENDIX

Algebraic analysis of 3-dimensional homogeneous strain

A parallelepiped in a 3-dimensional orthogonal coordinate system can be represented by a $(3,3)$ matrix $\mathbf{B}$, if one angular point of the parallelepiped coincides with the origin of the system. $\mathbf{Be}^1$, $\mathbf{Be}^2$, $\mathbf{Be}^3$ (the columns of $\mathbf{B}$) are the parallelepiped edges that meet in the origin ($e^1 = (1, 0,0)^t$), $e^2 = (0, 1, 0)^t$, $e^3 = (0, 0, 1)^t$). Consider two elements: $\mathbf{B}_f$ developed from $\mathbf{B}_i$. Let the $(3,3)$ matrix $\mathbf{T}$ be given by $\mathbf{B}_f = \mathbf{TB}_i$. Matrix $\mathbf{T}$ is found by solving the matrix equation

$$\mathbf{B}_f^t = \mathbf{T}^t \mathbf{B}_i^t$$

using Gauss-elimination with row-pivoting. $\mathbf{T}$ has to be decomposed according to $\mathbf{T} = \mathbf{RS}$, where $\mathbf{R}$ represents a rotation and $\mathbf{S}$ is a symmetrical matrix, representing deformation. It is known from linear algebra that every (m, n) matrix $\mathbf{A}$ $(m \geqslant n)$ can be written as

$$\mathbf{A} = \mathbf{U}\Delta\mathbf{V}^t, \text{ with } \mathbf{U}^t\mathbf{U} = \mathbf{V}^t\mathbf{V} = \mathbf{I}_n$$

Δ is a diagonal matrix with, on its diagonal, the so called singular values of $\mathbf{A}$, which satisfy

$$\delta_1 \geqslant \delta_2 \geqslant ...\delta_n \geqslant 0$$

This singular value decomposition is carried out for matrix $\mathbf{T}$, according to Golub and Reinsch (Wilkinson and Reinsch, 1971). Then,

$$\mathbf{T} = \mathbf{U}\Delta\mathbf{V}^t = (\mathbf{U}\mathbf{V}^t) \ (\mathbf{V}\Delta\mathbf{V}^t)$$

It can be reasoned that $\mathbf{U}\mathbf{V}^t$ is the desired rotation matrix $\mathbf{R}$ and $\mathbf{V}\Delta\mathbf{V}^t$ the desired deformation matrix $\mathbf{S}$. It is clear that the columns of $\mathbf{V}$ are eigenvectors of $\mathbf{S}$ and the numbers δ_1, δ_2, δ_3 are eigenvalues of $\mathbf{S}$. The three eigenvector directions are the principal directions. The corresponding natural principal strains are calculated using the relationship

natural principal strain $= -\ln$ (eigenvalue),

where decreases in length are taken as positive. Angle of rotation is calculated from **R**.

REFERENCES

Koolen, A.J., 1972. Mechanical behaviour of soil by treatment with a curved blade having a small angle of approach. J. Agric. Eng. Res., 17: 355–367.
Koolen, A.J., 1987. Deformation and compaction of elemental soil volumes and effects on mechanical soil properties. Soil Tillage Res., 10: 5–19.
Koolen, A.J. and Kuipers, H., 1983. Agricultural Soil Mechanics. Advanced Series in Agricultural Sciences, 13. Springer Verlag, Heidelberg, 241 pp.
Perumpral, J.F., Liljedahl, J.B. and Perloff, W.H., 1971. The finite element method for predicting stress distribution and soil deformation under a tractive device. Trans. Am. Soc. Agric. Eng., 14: 1184–1188.
Tijink, F.G.J. and Koolen, A.J., 1985. Prediction of tire rolling resistance and soil compaction, using cone, shear vane, and a falling weight. In: Proc. Int. Conf. Soil Dynamics, 17–19 June, 1985, Auburn, AL, vol. 4, pp. 800–813.
Wilkinson, J.H. and Reinsch, C., 1971. Linear Algebra, Handbook for Automatic Computation, Vol. 2. Springer Verlag, Heidelberg, pp. 134–151.
Yong, R.N., Fattah, E.A. and Skiadas, N., 1984. Vehicle traction mechanics. Developments in Agricultural Engineering, 3. Elsevier Scientific Publishing Company, Amsterdam/Oxford/New York, 307 pp.

Controlled distortion of soil samples with reference to soil physical effects

J.B. Dawidowski*, P. Lerink and A.J. Koolen**

Tillage Laboratory, Agricultural University, Diedenweg 20, 6703 GW Wageningen (The Netherlands)

(Accepted for publication 30 January 1990)

ABSTRACT

Dawidowski, J.B., Lerink, P. and Koolen, A.J., 1990. Controlled distortion of soil samples with reference to soil physical effects. *Soil Tillage Res.*, 17: 15–30.

A simple soil distortion apparatus, developed by the second author, is able to impose very large distortional strains on soil samples. Its action was compared with the well-known triaxial test, for natural major principal strains up to 0.69, larger values being beyond the capability of the triaxial apparatus. Comparison included measurements of strain field homogeneity, yield stress, and soil physical properties after distortion. Agreement between both test methods was good.

INTRODUCTION

Nearly pure distortion (deformation without volume change) of soil occurs on many occasions in agriculture, e.g. in ploughing and trafficking of wet, dense soil and in puddling flooded land for rice growing. The significance of this type of soil reaction is that it consumes energy and that it will change soil properties to either better or worse conditions. Being able to simulate homogeneous distortion of a soil volume element is needed in soil physics, soil tillage, agricultural engineering, and agronomy research. Presently, two apparatuses that can distort agricultural soil in a controlled way are available: the triaxial apparatus, and the distortion apparatus developed by Lerink (1990).

The triaxial apparatus is widely known (Bishop and Henkel, 1964). A cylindrical sample of wet, dense soil, usually having a height of 10 cm and a diameter of 5 cm, is enclosed by rigid top and bottom plates and a cylindrical rubber membrane (Fig. 1a). A rigid transparent cylinder (the cell) is placed over the enclosed sample and filled with water. The water in the cell is pres-

---

*Present address: Institute of Agricultural Mechanization of the University of Agriculture, Szczecin, Poland.
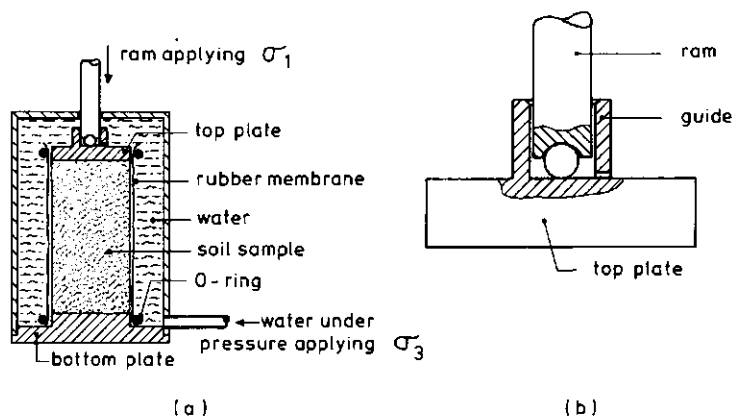**Author to whom correspondence should be addressed.

Fig. 1. (a) Triaxial apparatus for deforming soil samples and measuring soil deformability. (b) Detail showing top plate with guide.

surized to a constant cell pressure, σ_3. A loading ram is then moved downward at constant speed to deform the sample. The degree of deformation at any moment can be expressed by the natural vertical strain

$$\bar{\epsilon}= -\ln\left(1 -\frac{\Delta l}{l_0}\right) \tag{1}$$

where l_0=initial sample height and Δl=decrease in sample height due to the ram movement. During the test, the force exerted by the ram on the sample (F) is continuously measured as a function of Δl. The vertical normal stress σ_1 on the sample is due partly to F and partly to σ_3. σ_1 can be calculated at any time as:

$$\sigma_1 =\frac{F}{A}+\sigma_3 \tag{2}$$

where A is the surface area of the horizontal sample cross section. Since sample volume only changes slightly, A can be approximated by

$$A=\frac{A_0\times l_0}{l_0-\Delta l} \tag{3}$$

where A_0 equals $(\pi/4)$ times the square of the initial sample diameter. The volume change of the sample during deformation can be determined by measuring the water that is displaced from the cell through the water-supply tube.

A recent development is the distortion apparatus (Lerink, 1990). Wet, dense soil in a rigid cylinder on a rigid base is covered by an annulus that fits in the cylinder, and a piston that fits in the annulus (Fig. 2). The soil sample has a diameter of 98.5 mm and an initial height of 35.4 mm. A loading ram is moved
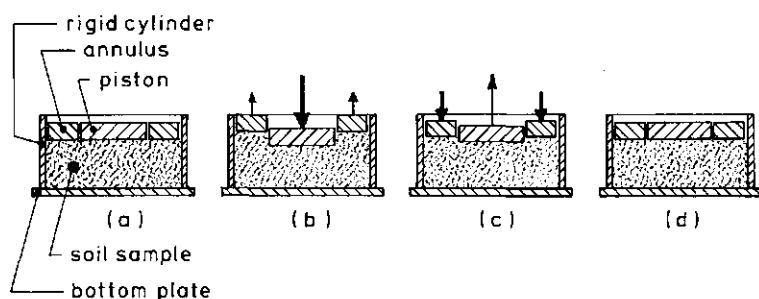
155

Fig. 2. Soil sample in distortion apparatus. (a) Situation at the start of a deformation cycle. (b) Deformation by piston-down movement. (c) Deformation by annulus down movement. (d) Situation after deformation cycle.

downward at constant speed to press the piston into the sample over a certain distance Δl. When that distance has been reached the piston load is removed and the annulus is moved downward by the loading ram at the same speed until a flush sample surface has been retained. This loading cycle can be repeated a number of times. During the test, the force (F) exerted by the ram when the piston is moved downward is continuously measured as a function of Δl. The force needed to move the annulus downward is not measured because it is irrelevant owing to the large frictional forces between the annulus and cylinder in this part of the loading cycle. Lerink assumed that the deformation field under the piston and the deformation field under the annulus were both homogeneous though not the same: the absolute value of the largest strain in the field under the piston is vertical and twice the assumed absolute value of the horizontal strain; the absolute values of the major and minor principal strains in the field under the annulus are assumed to be equal. Lerink selected apparatus dimensions so that the maximum principal strain in the field under the piston nearly equals the maximum principal strain in the field under the annulus (Lerink, 1990). Thus, if initial soil height is l_0 and the piston maximum downward movement in the soil is Δl, the natural major principal strain is:

$$\bar{\epsilon} = - (n_p + n_a)\ln\left(1 - \frac{\Delta l}{l_0}\right) \qquad (4)$$

where n_p and n_a are the numbers of applied piston and annulus impressions, respectively.

The triaxial apparatus has a limited deformation capability ($\bar{\epsilon}_1 = 0.69$ at maximum). The test is expensive. The amount of deformation that the feasible and relatively cheap distortion apparatus can impose on the soil is practically unlimited. There are further differences between both apparatuses. Stress–strain relationships may differ because the distortion apparatus

acts discontinuously. Both tests involve interfering shear stresses between soil and solid boundaries, but this interference is probably greater with the distortion apparatus than with the triaxial apparatus. Real homogeneity in the assumed homogeneous strain fields in the distortion apparatus may be very poor. σ_3 on a soil volume element in the distortion apparatus cannot be selected at will, but is determined by the soil-apparatus system. For a cohesive, non-hardening, non-softening soil with a zero angle of internal friction, σ_1 in the soil under the annulus during a piston-down stroke equals $2\ c$, (where c is cohesion) ideally, because this soil part undergoes unconfined compression in this test stage. Because σ_1 under the annulus equals σ_3 under the piston, σ_1 in the soil under the piston then equals $2\ c + 2\ c = 4\ c$, so that the piston force will equal $4\ c$ multiplied by piston area. Similar considerations apply to the annulus down stroke. The fact that either the piston or the annulus is unloaded during testing implies that ($\sigma_3 = 0$) zones always exist, in which brittle (unstable) failure may occur. A future development may include the possibility to impose an extra load on the upward moving annulus or piston, in order to increase stress levels in the soil.

This article reports an investigation in which the triaxial test and the distortion test were compared with respect to strain field homogeneity, stress–strain curve, and a number of soil physical effects.

EXPERIMENTAL PROCEDURE

Strain analysis experiment

Moist, medium-textured soil material was compressed in a 25×25 cm^2 soil bin under a compression plate (Blanken, 1987). After removing the bin the soil block was cut along a central plane into two parts with a large knife. Then, the cutting plane of one part was provided with a square grid of coloured glass beads. Bead diameter and mesh size were 1 mm and 7.6 mm, respectively. Subsequently, block parts were assembled again, imposing a small pressure perpendicular to the plane of cut, and a new sample was taken with a steel cylinder in such a way that a soil cylinder with grid beads in one plane through the cylinder axis was obtained. This cylinder, with dimensions required by the distortion apparatus, was deformed in this apparatus by one piston compression over a distance equal to 0.2 times the initial height. The deformed grid was recorded by measuring planar coordinates of the beads while removing the soil carefully. Care was taken that bead positions were not disturbed before being measured.

Physical properties after deformation

Sample preparation

We made the following requirements for the soil condition prior to deformation in the triaxial or distortion apparatus: deformation should occur without change in soil volume which requires a relatively dense soil; initial soil physical properties should be similar to a well-structured field soil. It was assumed that uniaxial compaction of strong aggregates with a water content "at the dry side of the compaction isobar" (Dawidowski and Lerink, 1990), followed by wetting could result in the desired soil condition. We read the desired soil physical properties from (Soane et al., 1982): (1) penetration resistance should not be greater than 0.8–1MPa; (2) air conductivity should not be smaller than 150 mm h^{-1}, which corresponds to an air permeability $K_i = 6.6 \times 10^{-12}$ m^2 (log $K_i = -11.2$ m^2); (3) the limiting value of water conductivity is 50 mm day^{-1}, log $K_{sat} = -6.2$ m h^{-1}; (4) air-filled porosity at field capacity (soil water tension = 10 kPa) should not be smaller than 10%. Dawidowski and Lerink (1990) presented a moisture–pressure–volume diagram measured in uniaxial compression, extended with soil physical properties. We used the same soil type and followed the same preparation procedure as these authors. Using the desired soil physical property values that are given above we read from the diagram presented by Dawidowski and Lerink that the soil condition aimed for could be obtained by uniaxial compression to 0.6 MPa at a soil water content of 20.5% (wt/dry wt). According to the diagram, only the resulting air permeability would be slightly less than the value aimed for.

The soil that was used in our experiments was Slootdorp sandy loam soil. Characteristics of this soil have been presented by Dawidowski and Lerink (1990). The soil was collected in autumn 1986. After the soil had been deep-frozen, it was successively: air dried to a moisture content at which the cracked soil clods were easily crumbled; gently crushed by hand into smaller sized aggregates; air dried in a drying room to minimum attainable moisture content; sieved to remove particles smaller than 0.6 mm and particles larger than 8 mm; wetted. Special care was paid to avoid mechanical and physical destruction of the aggregates during the wetting procedure. The total amount of soil was divided into small portions that were spread thinly in a narrow band on a wooden plate. Water was added by spraying a fine mist of a weight of water needed to obtain a water content of 20.5% (wt/dry wt). The wetted portions were collected in a plastic box and stored for 1 week to equilibrate. Steel cylinders were filled with prepared soil by spooning. Soil in these cylinders was compacted by uniaxial compression to 0.6 MPa. The amount of soil that was added to the cylinders is determined by the requirement that the effect of soil–metal friction on the effective compactive stress within the soil sample should be minimal. To satisfy this requirement, Koolen (1974)

showed that the ratio of the sample diameter to the sample height during testing should preferably not be greater than two. Soil cylinders intended for triaxial tests were made by compacting 125 g soil in 50 mm diameter cylinders. The resulting soil cylinder height was 35.4 mm. In order to obtain an initial sample height suitable in the triaxial tests (about 10 cm), three soil cylinders were placed one above another when these tests were performed, so that the initial sample height in triaxial testing was always $3 \times 35.4 = 106$ mm. Soil cylinders intended for distortion tests were made by compacting 500 g soil in 98.5 mm diameter cylinders. The resulting soil height was 35.4 mm. After uniaxial compaction all samples were saturated and subsequently equilibrated to the required water tension on a sand box.

Deformation in triaxial apparatus

Soil cylinders of an appropriate initial size were deformed in a triaxial apparatus at a ram speed of 8.33 mm s^{-1} giving a strain rate of approximately 0.09 s^{-1}. Water displacement to or from the cell through the water supply tube was measured using a paraffin volume gauge (Bishop and Henkel, 1964, p. 208). The connection between the ram and the top plate is shown in Fig. 1b. To prevent the top plate from tilting when subjecting samples to large strains, the top plate is provided with a guide into which the ram fits (Bishop and Henkel, 1964, p. 37). Two series of samples were deformed in the machine. Samples of the first series which were all at a water tension of 3.1 kPa, were deformed to different levels of maximum (vertical) natural strain: 0.1, 0.2, 0.3, 0.4 and 0.5. Each strain level was realized at three different confining pressures σ_3: 100, 200 and 300 kPa. Samples of the second series, which were at a water tension of 10 kPa, were deformed to the same range of strain levels, but only at a confining pressure $\sigma_3 = 200$ kPa. So, in total, $5 \times 3 + 5 \times 1 = 20$ triaxial tests were performed.

Deformation in distortion apparatus

Ram speed was selected so as to obtain the same strain rate as in the triaxial tests. During all piston down strokes, we let the piston travel a distance of 3.54 mm through the soil, which is 10% of the initial height of the soil samples. All samples deformed in the distortion apparatus were at a water tension of 3.1 kPa. Samples were deformed to different sums of piston down strokes and annulus down strokes, in such a way that the following levels of maximum natural strain were realized: 0.114, 0.208, 0.328, 0.445, 0.538, 0.685, 0.892.

Soil physical properties measurements

After treatment with triaxial or distortion apparatus, soil water tension prevailing immediately after unloading, saturated water conductivity, air perme-

159

ability at a water tension of 10 kPa, and tensile strength after oven-drying were measured.

Soil water tension immediately after unloading was measured using a small ceramic tensiometer needle. The time between removal of the load and insertion of the needle into a soil sample depended upon the type of test. That time never exceeded 5 min in the case of triaxial tests, and was always smaller than 4 min in the case of distortion tests.

After the measurements with the needle, the samples were partially drained for 2 days on a sand box at 25 kPa to harden them. This hardening strengthened the deformed samples enough to allow taking new subsamples from them. The triaxially deformed, barrel-shaped, samples were halved using a wire saw. A new subsample having a diameter of 50 mm and a height of 25 cm was taken from each sample-half by carefully pressing a greased steel cylinder with a sharpened cutting edge into the soil, simultaneously removing superfluous soil outside the cutting edge by means of a sharp blade. Subsamples taken from samples deformed in the distortion apparatus, using cylinders that were also sharpened and greased, also had diameters of 50 mm, but their heights were equal to the heights of the original samples.

Saturated water conductivity, air permeability at a water tension of 10 kPa, and soil tensile strength in an oven-dry condition were measured on the subsamples following the same procedures as used by Dawidowski and Lerink (1990).

RESULTS AND DISCUSSION

The deformed grid, which has been measured in the strain analysis experiment and which reflects the degree of homogeneity of the deformation field under the piston in the distortion apparatus test, is presented in Fig. 3 together with its undeformed shape. From the initial and final shapes of the grid elements, following the calculation procedure presented in the Appendix of
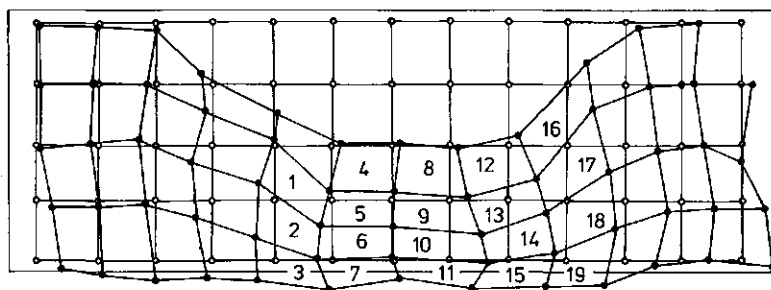

Fig. 3. Marking grid in sample, before and after a piston impression by the distortion apparatus. Strain values of numbered grid elements are given in Table 1. (Some distortion at sample circumference occurred when sample holder was removed.)

160

TABLE 1

Maximum relative shortening ϵ_1 and minimum relative shortening ϵ_3 of deformed soil elements indicated in Fig. 3

Element	ϵ_1	ϵ_3	Element	ϵ_1	ϵ_3	Element	ϵ_1	ϵ_3
1	0.40	−0.17	8	0.11	0.00	14	0.71	0.10
2	0.75	0.07	9	0.44	−0.20	15	0.58	0.07
3	0.54	0.07	10	0.61	−0.27	16	0.31	−0.80
4	0.32	0.03	11	0.63	−0.10	17	0.46	−0.51
5	0.45	−0.02	12	0.28	0.07	18	0.24	−0.21
6	0.53	−0.07	13	0.45	0.00	19	0.39	−0.01
7	0.65	0.05						

Koolen and Kuipers (1983), maximum relative shortening ϵ_1 and minimum relative shortening ϵ_3 were calculated for each element (see Table 1). Element numbers in the table refer to the grid element numbers in Fig. 3. If we leave the strongly deformed element 16 out of consideration, the mean $\epsilon_1 = 0.47$ and the standard deviation of $\epsilon_1 = 0.06$. Comparing these values with the natural strain $\bar{\epsilon}_1$ for all soil under the piston calculated as 0.51 using eqn. (4), it may be concluded that the homogeneity assumption used in the introduction is justified. After inspection of the entire deformed grid it may also be concluded that, relative to the deformation of the soil under the piston, large parts of the soil under the annulus are only slightly deformed.

Figure 4a presents stress–strain relationships measured in the triaxial tests. The curves for the samples at a water tension of 3.1 kPa show that measured σ_1 does not depend on the level of applied σ_3, which means that the soil angle of internal friction ϕ is zero. The figure also shows that soil strength increases with initial water tension. Stress–strain relationships measured during piston down strokes in the distortion apparatus differ from those measured in triaxial tests: the distortion apparatus curves ever increase with piston depth and curve tangent modulus increases with depth from the very start of piston travel. The latter phenomenon does not apply to early piston down strokes: here curve tangent modulus decreases initially, and starts to rise with depth after a significant amount of piston travel. Figure 4b, applying to the reported tests which all had a piston down travel of 3.54 mm in the soil during each piston down stroke, presents maximum vertical stress measured at the end of piston down strokes as a function of natural vertical strain. Because the soil angle of internal friction ϕ appeared to be zero, cohesion (c) can be estimated from the triaxial test results (Fig. 4a) as well as from the distortion test results (Fig. 4b). This will be done for the samples that initially were at a water tension of 3.1 kPa. Figure 4a shows that, at the largest degree of deformation obtained in the triaxial tests, $\sigma_1 - \sigma_3$ was 0.086 MPa, which implies that, ac-
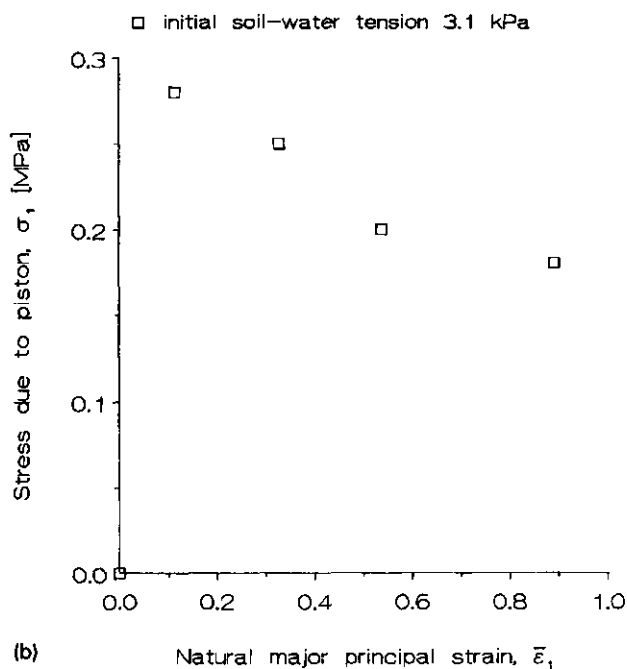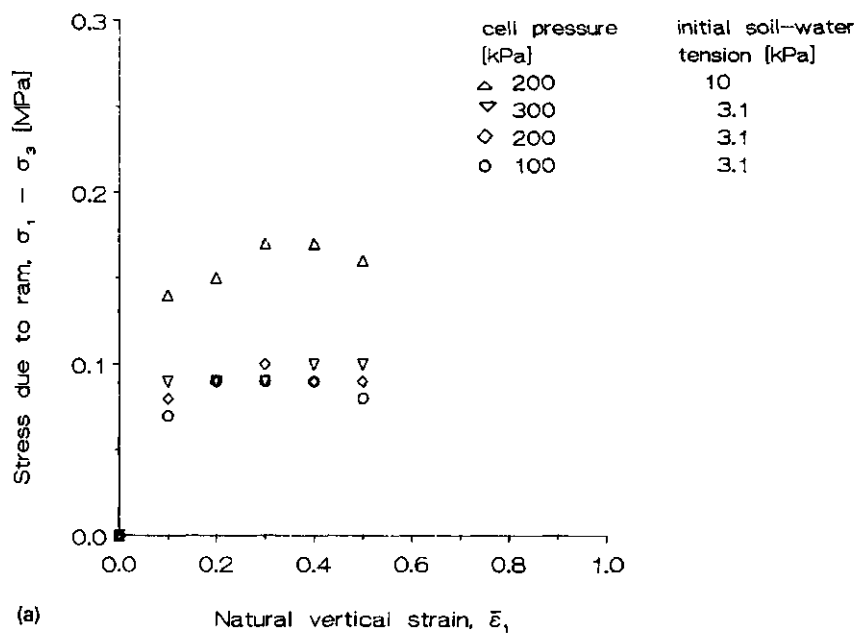
Fig. 4. Stress–strain relationships measured in (a) triaxial or (b) distortion apparatus.

cording to $c = \frac{1}{2}(\sigma_1 - \sigma_3)$ if $\phi = 0$, c equals 0.043 MPa in the case of the triaxial tests. Figure 4b gives a σ_1 value of 0.18 MPa for the largest degree of deformation with the distortion apparatus. According to the relation $\sigma_1 = 4c$, derived for this apparatus in the Introduction, this estimates c as 0.045 MPa. The relatively high σ_1 values measured in the distortion apparatus at small and intermediate strain values may be due to interfering soil–metal shear stresses and soil stress heterogeneity. These probably vanish at great soil strains owing to the smear effect of expelled water and the rearrangement of soil particles, respectively.

Porosities after the deformation treatments differed by -1 to $+2\%$ from those before deformation. Measured porosity increase tended to be higher for the distortion tests than for the triaxial tests. Soil physical properties as affected by different degrees of deformation in the triaxial or distortion apparatus are presented in Figs. 5–8. Figure 5 presents soil water tension after unloading. Figure 6 applies to saturated water conductivity. Figure 7 shows air permeability at a water tension of 10 kPa. Figure 8 gives soil tensile strength measured on oven-dry samples. The influences of σ_3 and initial water tension on the measured soil qualities can be seen from the triaxial test results. σ_3 did not affect the soil qualities. The soil water tension before deformation affected the water tension and the air permeability at a water tension of 10 kPa, and probably also the oven-dry tensile strength.

The distortion apparatus results can be compared with the triaxial apparatus results for an initial soil water tension of 3.1 kPa. It can be seen that, for most physical properties, the measured property value at any given degree of deformation is independent of the type of apparatus used, i.e. effects of a certain deformation with the distortion apparatus are the same as with the triaxial apparatus. The results are also similar to the effects of deforming wet, dense, undisturbed samples measured by Dawidowski and Koolen (1987). Deviating and unexpected results were the measured soil water tensions after unloading in the distortion apparatus (Fig. 5b). These values were in agreement with the other water tension measurements when read immediately after inserting the measuring needle. However, with the distortion apparatus, the needle reading was not constant with time, but dropped continuously until a value close to that for the undeformed sample was reached. Water tension–deformation relationships which have been measured 2 and 4 min after unloading, and which are presented in Fig. 5b, demonstrate the rate of water tension decrease. We hypothesized that this decrease was caused by water transport from the soil under the annulus to the soil under the piston. Soil mass under the annulus is relatively large compared with mass under the piston, and has a mean water tension that is little affected because large parts are only slightly deformed (see Fig. 3), so that it probably acts as a buffer for water tension. If the hypothesis is true, water tension cannot decrease after deformation when distortion is severe enough to make the soil under the pis-
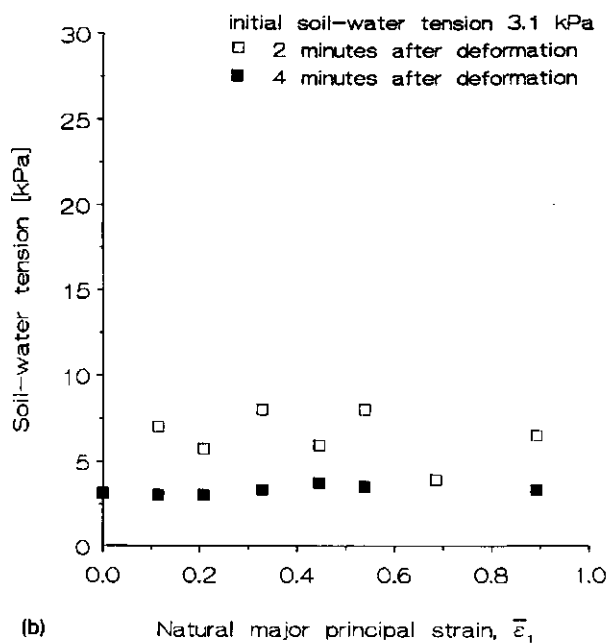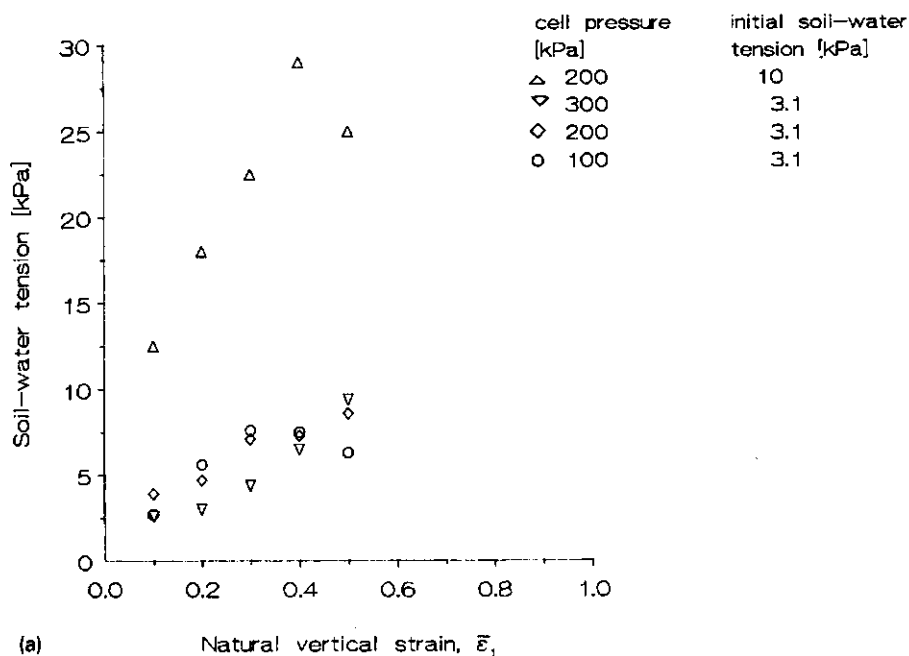
Fig. 5. Soil water tension after distortion as a function of degree of distortion imposed by (a) triaxial or (b) distortion apparatus.

cell pressure   initial soil-water
[kPa]   tension [kPa]

△ 200   10
▽ 300   3.1
◇ 200   3.1
○ 100   3.1

-2

-3

-4

-5

-6

Log Ksat [ms⁻¹]

0.0   0.2   0.4   0.6   0.8   1.0

(a)

Natural vertical strain, $\bar{\varepsilon}_1$

□ initial soil-water tension 3.1 kPa

-2

-3

-4

-5

-6

Log Ksat [ms⁻¹]

0.0   0.2   0.4   0.6   0.8   1.0

(b)
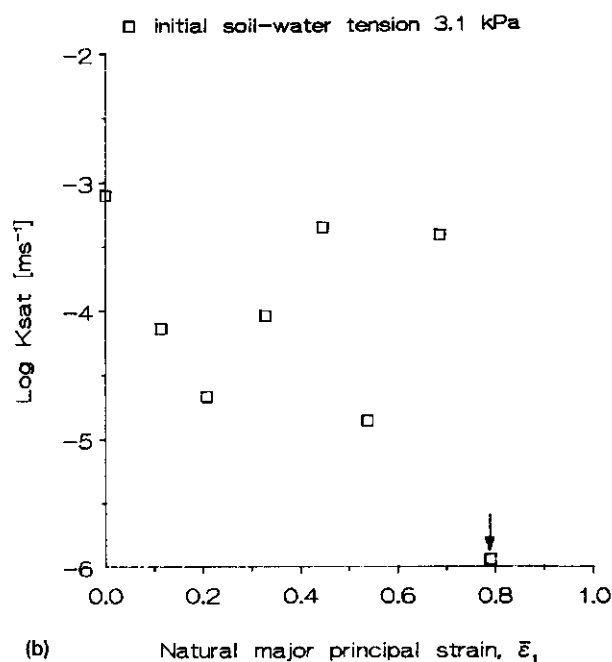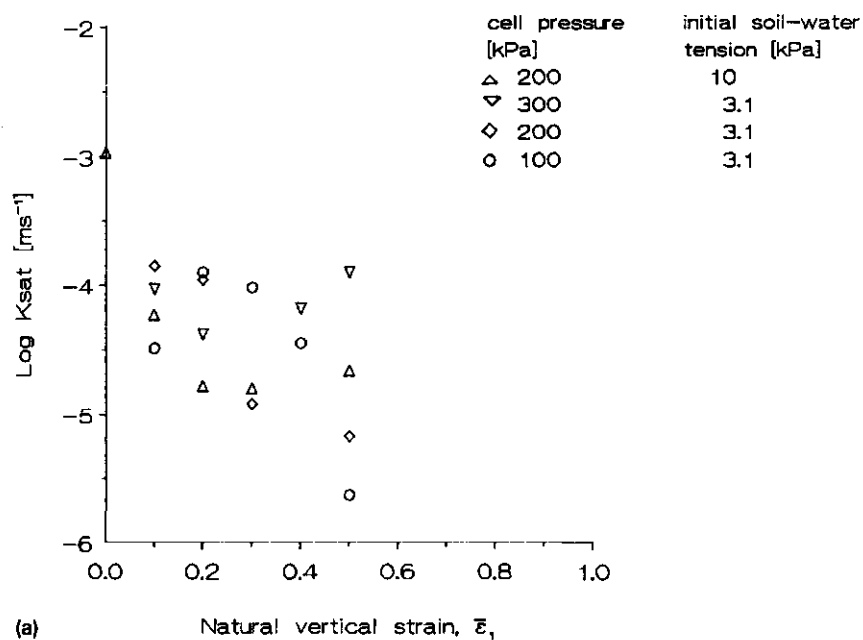
Natural major principal strain, $\bar{\varepsilon}_1$

Fig. 6. Saturated water conductivity after distortion as a function of degree of distortion imposed by (a) triaxial or (b) distortion apparatus.
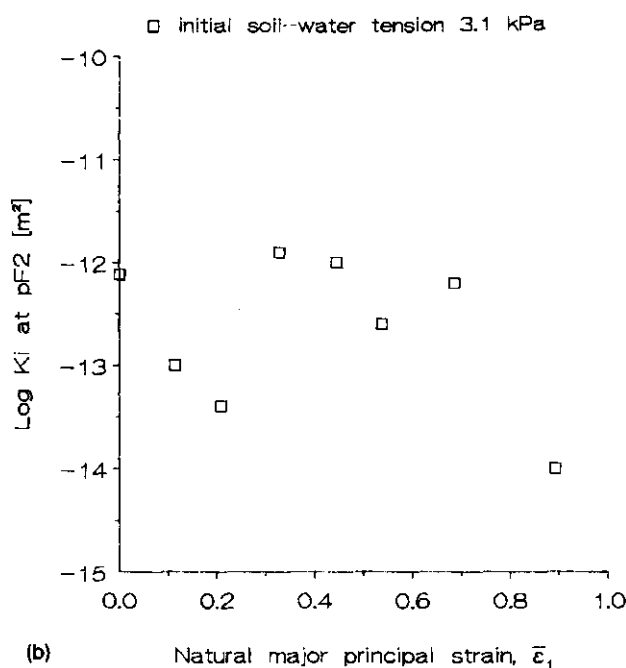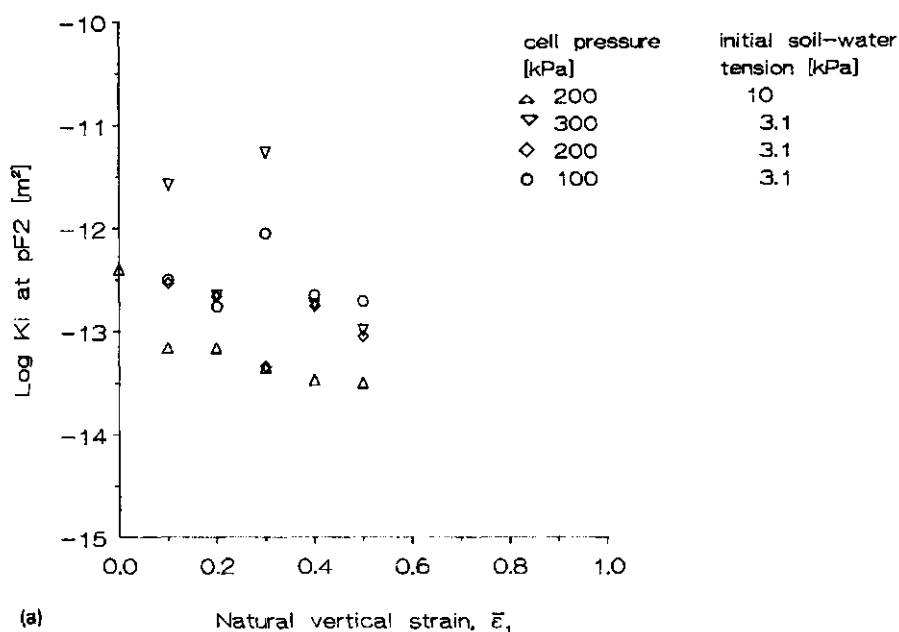
Fig. 7. Air permeability (measured at a water tension of 10 kPa) after distortion as a function of degree of distortion imposed by (a) triaxial or (b) distortion apparatus.
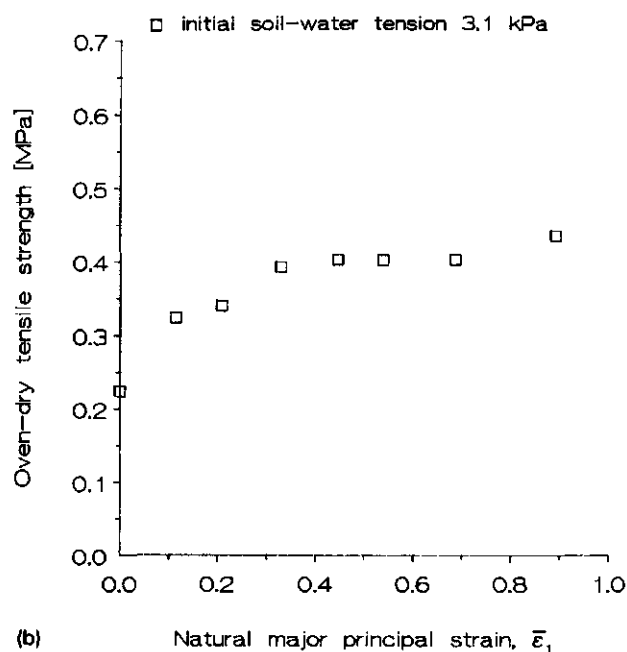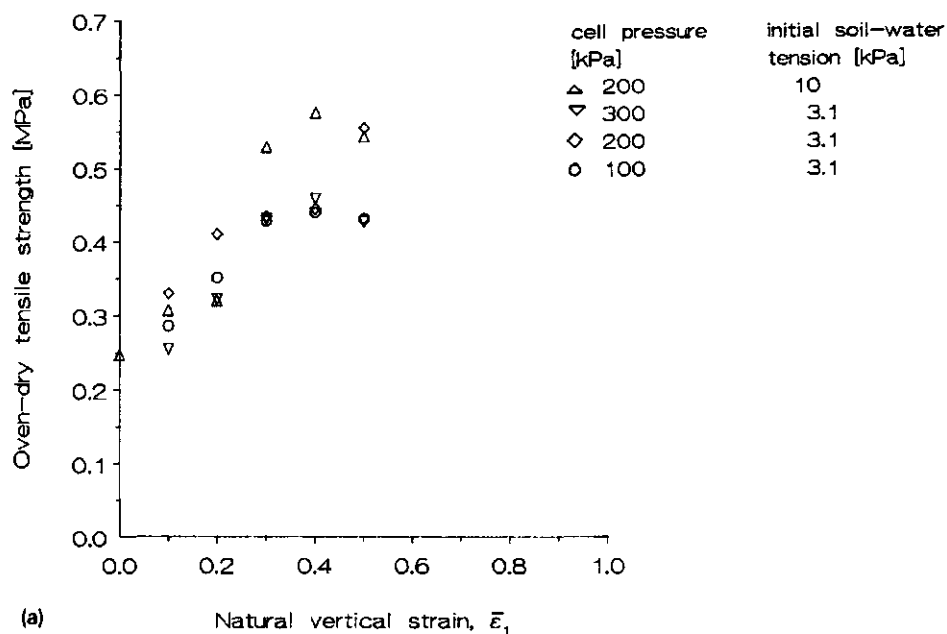
166

Fig. 8. Tensile strength (measured after oven-drying) after distortion as a function of degree of distortion imposed by (a) triaxial or (b) distortion apparatus.

ton impermeable for water. A few additional tests in which treatment consisted of one, very long, piston down stroke confirmed the hypothesis. Scatter in measured water conductivities and air permeabilities was always large (Figs. 6 and 7), which is probably inherent to these types of tests. It is generally believed that a triaxial apparatus measures soil elemental behaviour best and deforms soil samples homogeneously. Resemblance between the triaxial test results and the distortion apparatus results was satisfactory. The distortion apparatus may be considered as a useful development because no other apparatus is able to impose the very large soil strains occurring in a number of field operations in a controlled and quantifiable way.

CONCLUSION

Using a wet, dense cohesive soil with zero angle of internal friction a simple distortion apparatus developed by P. Lerink was compared with a triaxial apparatus. Comparison included measurements of strain field homogeneity, stress–strain curves, and soil physical properties after distortion: soil water tension after unloading, saturated water conductivity, air permeability at a water tension of 10 kPa, and dry tensile strength. Strain in the measuring zone of the distortion apparatus was homogeneous. Although stress levels were not the same, both sets of apparatus measured similar yield stresses and had similar effects on the soil physical properties. These similarities could occur because, with a zero angle of soil internal friction, not only the strains but also the shear stresses were similar in the measuring zone. Because the sample zone outside the measuring zone is distorted less, water tension differences may occur between the measuring and outer zones, which may induce water transport in the sample after the distortion treatment. The distortion apparatus provides an inexpensive and quick method to deform dense, wet soil samples to large and quantifiable extents. Degree of deformation has been expressed as the natural major principal strain.

REFERENCES

Bishop, A.W. and Henkel, D.J., 1964. The Measurement of Soil Properties in the Triaxial Test. Edward Arnold, London, 228 pp.
Blanken, L.C., 1987. Naar een model voor het gedrag van grond onder belasting. Unpublished thesis. Tillage Laboratory, Wageningen Agricultural University, Wageningen, 76 pp.
Dawidowski, J.B. and Koolen, A.J., 1987. Changes of soil water suction, conductivity and dry strength during deformation of wet undisturbed samples. Soil Tillage Res., 9: 169–180.
Dawidowski, J.B. and Lerink, P., 1990. Laboratory simulation of the effects of traffic during seedbed preparation on soil physical properties using a quick uni-axial compression test. Soil Tillage Res., 17: 31–45.
Koolen, A.J., 1974. A method for soil compactibility determination. J. Agric. Eng. Res., 19: 271–278.

Koolen, A.J. and Kuipers, H., 1983. Agricultural Soil Mechanics. Advanced Series in Agricultural Sciences, 13. Springer, Heidelberg, 241 pp.

Lerink, P., 1990. The kneading distortion apparatus. Soil Tillage Res., 17: 173–179.

Soane, B.D., Dickson, J.W. and Campbell, D.J., 1982. Compaction by agricultural vehicles: a review. III. Incidence and control of compaction in crop production. Soil Tillage Res., 2: 3–36.

Laboratory simulation of the effects of traffic during seedbed preparation on soil physical properties using a quick uni-axial compression test

J.B. Dawidowski[1] and P. Lerink[2]

Tillage Laboratory of the Wageningen Agricultural University, Diedenweg 20, 6703 GW, Wageningen (The Netherlands)

ABSTRACT

Dawidowski, J.B. and Lerink, P., 1990. Laboratory simulation of the effects of traffic during seedbed preparation on soil physical properties using a quick uni-axial compression test. *Soil Tillage Res.*, 17: 31–45.

A quick uni-axial compression test was applied to simulate the effect of traffic during seedbed preparation on the soil condition. The soil type was "Slootdorp" sandy clay loam. The effect on the soil condition was quantified by the following soil physical properties: total pore space; saturated water conductivity; air content at pF2; air permeability at pF2; penetrability at pF2; and oven-dry tensile strength. The compression tests were run at various uni-axial loads and moisture contents. The relationships between the respective soil physical properties and the moisture content at compression, as a function of the uni-axial load, were presented graphically by means of a composite diagram. The relationships were compared with those obtained from observations on traffic-compacted soil. Good agreement was found between the shape of the curves. A calibration method was discussed in order to use the quick uni-axial compression test, extended with measurements on soil physical properties for predictive purposes.

INTRODUCTION

Relationships on soil compaction as a function of relevant soil and load characteristics have in common, that the effect on the soil condition is expressed by bulk packing state properties (e.g. dry bulk density, total pore space and void ratio). There is now increasing awareness that more detailed infor-

---

[1]Present address: Institute of Agricultural Mechanization of the University of Agriculture, Szczecin, Poland.
[2]Author to whom correspondence should be addressed.

mation is required, in order to evaluate the significance of mechanical compaction to soil use and, eventually, to optimize soil management. Koolen (1987) introduced the term soil qualities, as a generic term for soil physical properties which are relevant for soil use. Soil qualities of agricultural soils refer to water and air conductivities, water and air storage capacities, thermal properties and strength properties, such as compactibility, breakability and penetrability.

Knowledge on the effects of traffic on soil qualities mainly stems from field studies. The first attempt to assimilate observations on soil qualities of traffic-compacted soil into coherent relationships was presented by Lerink (1990). Laboratory studies on the effect of compaction on soil qualities are reported by Gupta and Larson (1982), Dawidowski and Koolen (1987) and Beekman (1987) among others. However, information on the effectiveness of laboratory-compaction methods simulating the traffic-induced effect on the soil condition is scarce (Gupta and Allmaras, 1986).

The objectives of this study were to determine the effect on soil qualities of laboratory compaction at varying load and moisture content, and to compare the results with the effect of compaction by field traffic during seedbed preparation. Information on the effect of compaction by field traffic was obtained from Lerink (1990).

THEORETICAL CONSIDERATIONS

A laboratory compression method, aimed to simulate the true process effects effectively, has to satisfy two fundamental requirements. Firstly, the method should account for the process characteristics which are known to control the process effects. Secondly, the laboratory compaction process should be compatible with the traffic-induced compaction process, in that both processes are governed by similar physical phenomena. These aspects of laboratory simulation are detailed below. Laboratory simulation assuredly presents partial incompatibilities, which will be indicated in the text.

The laboratory compression method

Soil physical properties of a given soil are a function of the soil state at a micro level. Relevant soil micro-factors comprise the proportions and distributions of solid particles and water in a unit volume, and the number, type and distribution of inter-particle bonds (Koolen, 1987). When an elemental soil volume is loaded by transient wheelings, it simultaneously changes in shape (pure deformation or deformation at constant volume) and in volume (pure compression or, complementary, pure compaction). On a micro level, solid particles, air and water are redistributed, inter-particle bonds are broken and new bonds are formed. It is commonly assumed that the rapid loading by transient wheelings does not cause soil water transport over macroscopic dis-

171

tances, hence volume reduction is solely at the expense of the air-filled pore space and thus volume reduction occurs at constant gravimetric moisture content.

The effects of pure deformation and pure compaction on soil micro-factors are to some extent comparable, in that both processes result in redistribution of the solid particles, water and air, and in rupture of inter-particle bonds. The question arises: is it necessary to take deformation into account in order to simulate the traffic-induced effect on soil qualities? To answer this question, reference is made to the concept of "wet" and "dry" compaction (Koolen, 1987). Dry compaction occurs when volume reduction upon loading is limited by the increase of the soil compressive strength. At wet compaction, the volume reduction upon loading is limited by entrapped soil water. In practical situations, wet compaction will be accompanied by considerable deformation, resulting in deep ruts and bulging-up of the sides of the ruts. Since deformation at virtually constant volume affects soil qualities (Dawidowski and Koolen, 1987), it was concluded that laboratory compression tests should account for large deformations when loading results in wet compaction.

When a soil volume is dry compacted, it is hypothesized that the effect on soil qualities is mainly caused by volume reduction. This hypothesis is supported by the fact that soil physical properties in general are very sensitive to small changes in bulk packing density. Additional effects of deformation are assumed to be of minor importance. Compaction by field traffic at seedbed preparation mainly features dry compaction (Lerink, 1990). A simple compression test, primarily designed to impose volume strain on soil samples, is the uni-axial compression test (Koolen and Kuipers, 1983). In this study, the uni-axial compression test was used to simulate the effects of dry compaction.

Load characteristics

Relevant characteristics of the loading cycles on an elemental soil volume under transient wheelings are the loading rate, the absolute and relative values of the principal stress components at any one moment and the number of loading cycles (i.e. the number of wheels following the same path).

Compaction by wheelings is typified as "quick" compaction. Quick compaction explicitly refers to the physical phenomena underlying compaction. The main characteristic of quick compaction is that water transport does not occur over macroscopic distances. The adverse effect of local pressure build-up in pore water on the stability of soil aggregates is discussed by Larson and Gupta (1980). The compression rate at uni-axial testing should be at least of the same order of magnitude, in order to simulate the physical phenomena featuring traffic-induced compaction. Koolen (1987) estimates the vertical strain rate of a soil volume element in the arable layer being approximately 0.6 s^{-1}, in case of a volume reduction of 20%, and assuming that the vertical strain starts at a distance of 50 cm in front of the nearing tyre–soil contact

172

surface and stops when the tyre–soil contact surface arrives above the soil element. Uni-axial compression at compression rates resulting in quick compaction is denoted as quick uni-axial compression.

The maximum value of the first principal stress ($\sigma_1\text{max}$) acting on a soil element during a wheeling is known to be an important determinant of the resultant degree of compaction (Koolen and Kuipers, 1983). Repeated loading with approximately equal loads causes some, but ever decreasing additional volume reduction (Koolen, 1987). Since methods to calculate the stresses under wheelings lack sufficient accuracy (Koolen and Kuipers, 1988), it was decided to characterize the stress regime of a specific vehicle–soil system by the uni-axially applied stress (σ_{eq}) which results in the same effect on the soil qualities. The laboratory compression tests were therefore run at various loads to ensure that the effects of compaction resulting from the traffic events which were used for comparison were covered.

Soil characteristics

The plough layer of medium to fine textured soils in the spring consists of a loose assembly of coarse structural units. The volume of soil samples which are suitable for laboratory compression tests is small compared with the size of these units. Small samples of loosely packed, coarse units are poor representatives of the field soil condition. Furthermore, the behaviour in compaction is severely disturbed by the rigid sample surroundings. It is therefore common practice to reduce the scale of the soil units and pores. Scale reduction reduces the average size and the size distribution of the soil units and pores, giving an increase of the structural homogeneity of the soil. Thus, a relatively small number of replicates suffices to assess accurately the soil response to laboratory compression.

Preparation of the field soil for laboratory testing by scale reduction probably distorts the similarity of the soil response to compaction. Knowledge on the effect of scale reduction on the soil response to compaction is fragmentary. Tijink (1988) showed, that the absolute size of soil aggregates had little effect on the compactibility at uni-axial compression. However, mixtures of aggregates with a narrow size range behaved differently in compaction compared with mixtures with a broad size range. The effect of the aggregate size distribution on the compactibility was also found by Willatt (1987).

The soil moisture status is the major determinant of the soil response to compaction. The soil moisture status both affects the compactibility and the micro-structural change during compaction (Lerink, 1990). In temperate regions, the soil moisture status at shallow depths may show considerable daily and even hourly fluctuations. In compaction studies, the soil moisture status is commonly quantified by the gravimetric moisture content.

EXPERIMENTAL PROCEDURE

Soil preparation for laboratory compression

The soil used for experimentation was collected in the summer of 1986 from an experimental field of the IMAG-experimental station "Oostwaar- dhoeve", Slootdorp, The Netherlands. The experimental field was allocated to the research project entitled: "Perspective of reducing soil compaction by using a low ground pressure (LGP) traffic system". The soil type is detailed in Table 1. After freezing and thawing, to promote crack formation, the coarse soil units were successively: dried to a moisture content at which the soil units could be easily crumbled; gently crushed by hand into smaller sized frag- ments; air dried in a drying room; and sieved (mesh size: 1 mm^2) in order to remove the dust fraction from the aggregate fraction. The weight fractions of some size fractions of the resulting aggregate mixture are listed in Table 2. The method of size reduction described here ensures minimal damage of the internal structure of the aggregates.

The total amount of prepared soil was divided into 11 portions of equal weight. Each portion was wetted to the desired moisture content, ranging from 10 to 30% (w/w), in steps of 2%. Special attention was paid to avoid me- chanical destruction of the aggregates during the wetting procedure. There- fore, each portion was sub-divided into smaller portions which were spread thinly on a wooden plate. A calculated amount of water was added by spray-

TABLE 1

Some intrinsic properties of "Oostwaardhoeve" sandy clay loam

Fraction	% w/w
Clay fraction	30
Sand fraction	40
Organic matter content	2
CaCO$_3$ content	6

TABLE 2

Weight fractions of some size fractions of the prepared soil

Size fraction (mm)	Weight fraction (% w/w)
0.6–1	11
1–2	29
2–4	56
4–8	4

ing a fine mist of water. The wetted sub-portions were subsequently collected in plastic boxes, sealed and stored for one week to equilibrate.

The wetting procedure of soil portions with a desired moisture content higher than 22% was carried out in two steps. At first, the soil portions were wetted to 22% and after a week water was supplemented to obtain the desired moisture contents.

Sample preparation

Prepared soil was added to steel cylinders (diameter, 81 mm; height, 50 mm) by spooning, giving a loose packing state. The amount of soil added to the cylinders was equivalent to 200 g of oven-dry soil. The pore space prior to testing depended on the moisture content and ranged from 60% to approximately 70% at increasing moisture content. The sample height was approximately 40 mm, giving a sample diameter to height ratio of approximately 2.

Uni-axial compression

The universal material testing machine that was used for uni-axial compression is shown in Fig. 1. Prior to testing, a soil sample in a steel ring
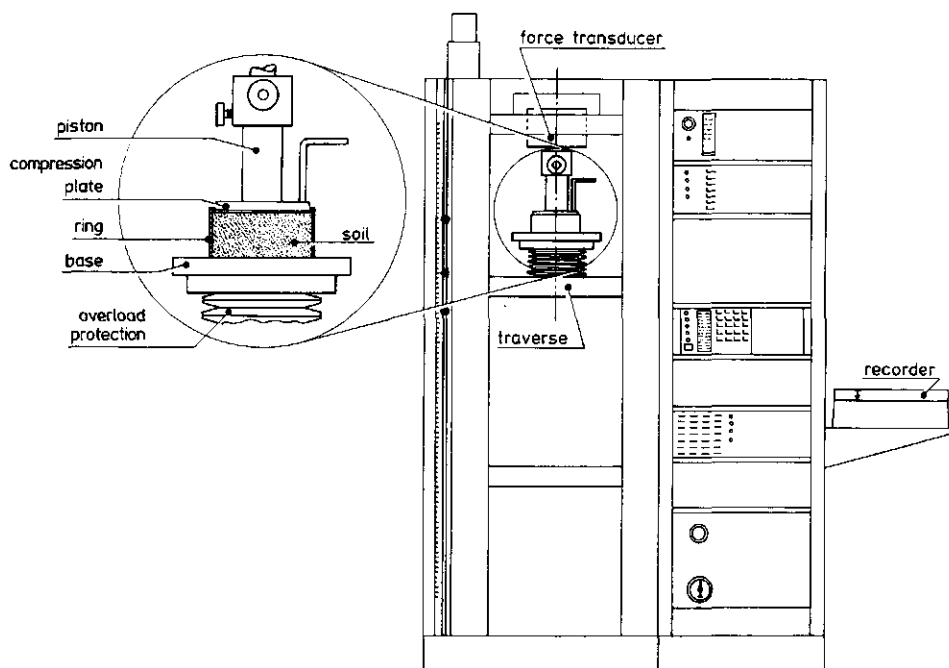

Fig. 1. The universal material testing machine.

175

with a closely fitting compression plate was placed on the traverse. At testing, the traverse moved with a constant speed upwards. The piston force and the displacement of the traverse were simultaneously recorded. The maximum error of measurement of the height of the compacted samples was ± 0.1 mm, which is equivalent to about $\pm 0.5\%$ (v/v) in pore space. The soil samples were compressed until a maximum pressure of 0.1, 0.2, 0.4, 0.6 and 0.8 MPa, respectively, including four replications. The total number of soil samples thus amounted to 11 (moisture contents) $\times$ 5 (uni-axial pressures) $\times$ 4 (replicates) $= 220$ samples.

The movement of the traverse stopped automatically when the pre-adjusted maximum force was reached. After the force dropped to reach a state of equilibrium, the traverse was moved downward. After a quarter of an hour, which was sufficient to stop the soil from rebounding, the height of the sample was determined by moving the traverse upward until a force of 10 N was exerted by the piston. The total pore space was calculated from the dry weight and the volume of the compressed sample.

The maximum traverse speed of the universal material testing machine was 16.7 mm s^{-1} (1000 mm min^{-1}). For practical reasons, the traverse speed was adjusted to 8.3 mm s^{-1} (500 mm min^{-1}), giving a vertical strain rate of approximately 0.2 s^{-1}.

The effect on soil qualities

After compaction, each soil sample was subjected to a series of tests, in order to determine the following soil properties: saturated water conductivity; air permeability; penetrability; air-filled pore space and oven-dry tensile strength. As these properties are generally a function of the soil moisture status, they were determined at the moisture content near field capacity (i.e. at pF2 for medium textured soils in The Netherlands) unless the test method prescribes otherwise (as in the case of saturated water conductivity and oven-dry tensile strength).

Prior to the saturated water conductivity test, the soil samples were placed on a sand box and slowly saturated by adjusting the water tension from 1 kPa to 0 kPa. The saturated water conductivity (K_{sat}) was measured using the constant head method (Klute, 1965). The samples were then drained to equilibrium at a tension of 10 kPa ($\approx$ pF2) and weighed to obtain the air content at pF2. The intrinsic air permeability (K_i(pF2)) was measured using a constant head permeameter (Perdok and Hendrikse, 1982). Of each set of four replicates, two samples were subjected to a penetration test (cone needle with top angle 30°; base diameter 2 mm; penetration rate 0.8 mm s^{-1}; number of replications per sample, 5).

After oven drying, the samples were weighed and the intact soil cores were

taken out of the steel cylinders. The oven-dry tensile strength was determined using the "Brazilian test" (Kirkham et al., 1959).

Data processing

The numerical results of the measurements of the respective soil qualities of each set of four replicates were averaged, except for the saturated water conductivity (K_{sat}) and the intrinsic air permeability ($K_i(pF2)$) which are
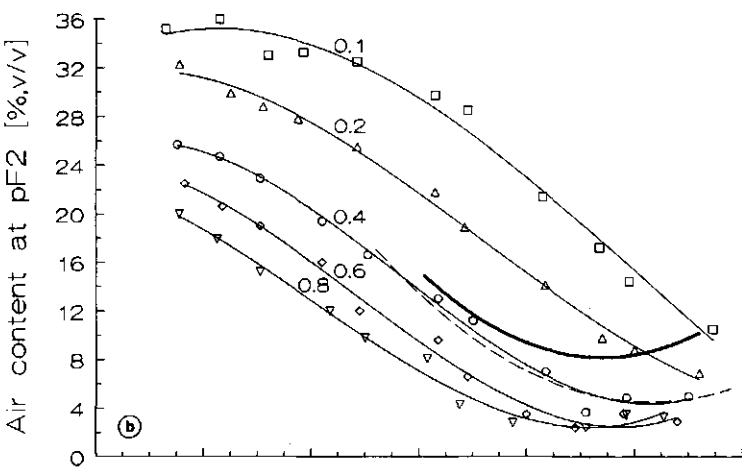

Fig. 2a, b.

177

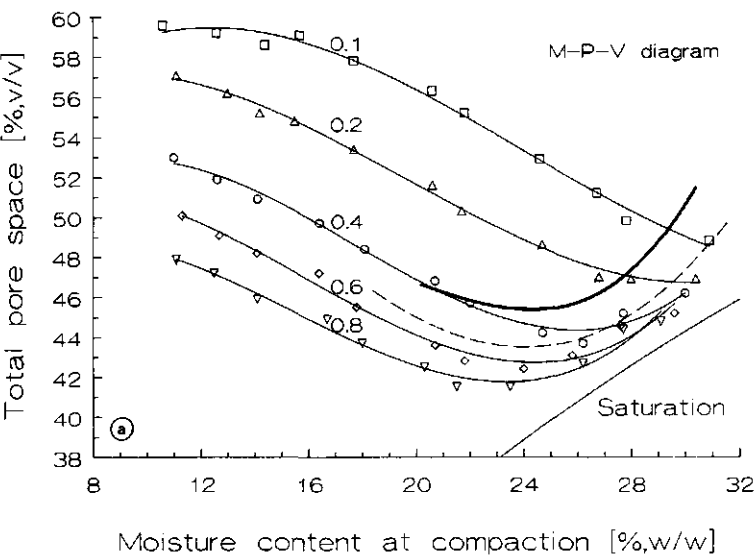expressed as log-means. The penetrability was calculated from the quotient of the mean vertical force during penetration and the cone base area.

Compaction by field traffic

The experimental field on the "Oostwaardhoeve" was divided into two main plots. Management of both plots resembled regular field management on 60 ha sized farms in The Netherlands. The field operations on both plots were
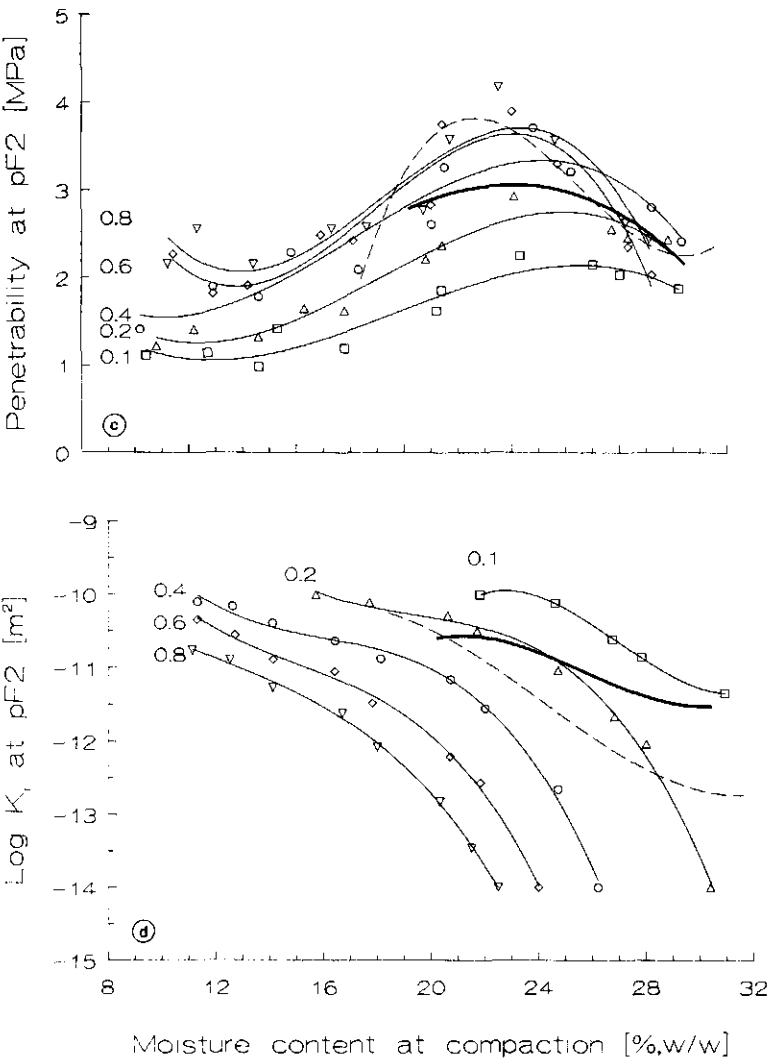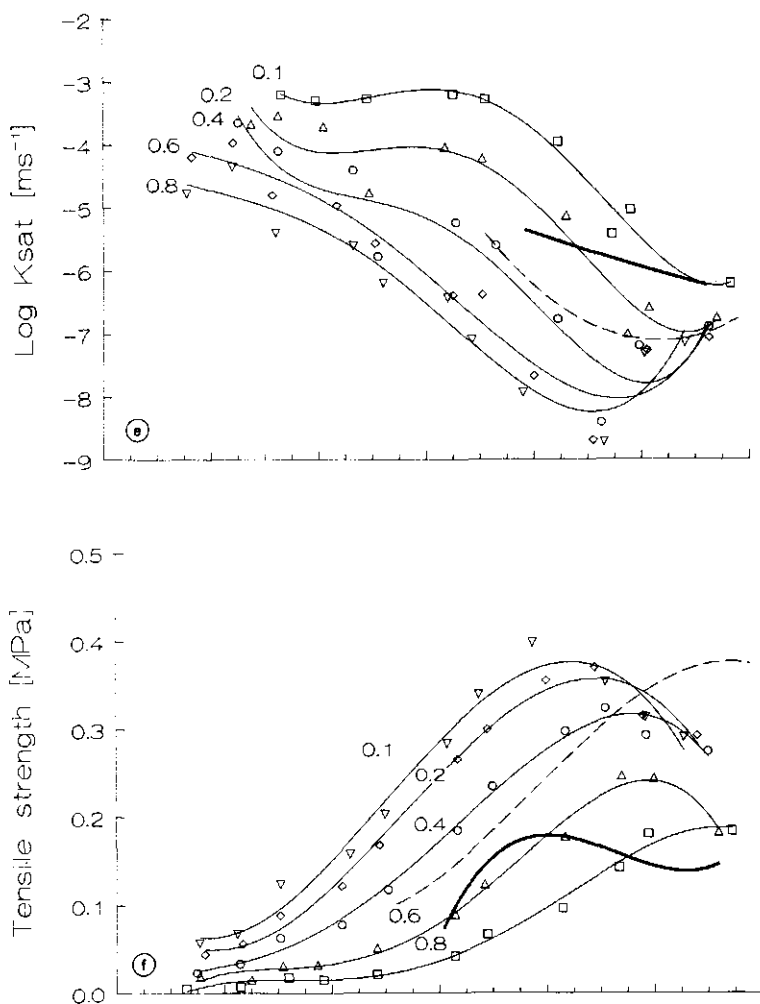

Fig. 2c, d.

Fig. 2. Composite diagram of the effects of laboratory and traffic-induced compaction on (a) total pore space, (b) air content at pF2, (c) penetrability at pF2, (d) air permeability at pF2, (e) saturated water conductivity and (f) oven-dry tensile strength, as a function of the gravimetric moisture content at compaction. 0.1, ..., 0.8 indicate the pressure at uni-axial compression (MPa), and are represented by the same symbols throughout. The heavy line indicates the LGP traffic system. The dotted line the HGP system.

carried out by the same type of machinery. The wheeled vehicles used on the LGP (low ground pressure) and HGP (high ground pressure) plot were equipped with tyres featuring low ground contact pressure and high ground contact pressure, respectively.

In three successive years, core samples were collected at a depth of 2–12 cm under the centreline of wheel ruts resulting from field traffic during seedbed preparation. The soil samples were collected immediately after the passage of the vehicles. The tyre inflation pressures of the LGP and HGP traffic system were 40 and 80 kPa, respectively (on modern farms in The Netherlands, a tyre pressure at seedbed preparation of about 100 kPa is common practice). The soil samples were subjected to the same series of tests as the uni-axially compressed soil samples. For a detailed description of the effects of traffic on field soil qualities, reference is made to Lerink (1990).

RESULTS

The effects of laboratory and traffic-induced compaction on the soil qualities are presented graphically by means of a composite diagram (Fig. 2). The horizontal and vertical axes refer to the gravimetric moisture content at compaction and the distinct soil qualities, respectively. Each symbol represents the average of four replicates, except for the penetrability. Here, each symbol represents the average of five measurements on two samples of each set of four replicates. The respective symbols are fitted by second or third order polynomials, whichever fitted the best. Since the respective curves represent equal uni-axial pressure, they are referred to as "isobars". The curves referring to the effects of compaction by field traffic were obtained from Lerink (1990).

In the diagram expressing the intrinsic air permeability, extreme high (log $K_i(pF2) > -10$ m^2) and extreme low (log $K_i(pF2) < -14$ m^2) values were omitted.

DISCUSSION

The discussion is focussed on two items: (1) the effect of uni-axial compaction of prepared soil on soil qualities as a function of the moisture content at compaction and the uni-axial pressure; (2) comparison of the effects of compaction by field traffic during seedbed preparation and the effects of laboratory compaction of prepared soil.

The effects of uni-axial compaction

The effect of compaction on the total pore space as a function of the gravimetric moisture content at compaction and the compactive load is expressed by the M–P–V diagram. The significance of the M–P–V diagram in agronomics is two-fold. Firstly, it is expected that the M–P–V diagram will play

an important role where soils are to be classified on the basis of their compactibility (Koolen, 1987). The compactibility is reflected by the positions of the isobars. Secondly, the shape of the isobars demonstrates the effect of the moisture content at compaction on the compactibility. The M–P–V isobar can be divided into two parts: a left part, where the compactibility increases with increasing moisture content at compaction, and a right part, where the compactibility decreases with increasing moisture content. The left and right part of the isobar refer to dry and wet compaction, respectively. The curve parts conjoin at a moisture content resulting in maximum compaction. The moisture content resulting in maximum compaction decreases at increasing compactive load.

The shape of the isobars expressing the effect on the respective soil qualities is to a great extent congruent with the isobars in the M–P–V diagram. The general trend is, that the isobars change progressively at increasing moisture content at compaction and reach an extreme value at the moisture content resulting in maximum compaction. The penetrability deviates from this general trend in that the isobars reach an optimum at a moisture content at compaction that is slightly lower than the moisture content at maximum compaction. This is especially true at uni-axial loads lower than 0.6 MPa. A further increase of the moisture content at compaction modifies the soil qualities in accordance with the increase in pore space.

The effect of the moisture content at compaction on the soil micro-structural change is visualized by comparing the soil qualities of soil samples which were compacted to the same degree of compactness at varying moisture content. Figures 3a and b illustrate the effect on the air content at pF2 and the oven-dry tensile strength, respectively, of soil samples compacted to 47% pore space at varying moisture content. The bivalent role of the moisture content at compaction on soil qualities thus involves the effect on the compactibility and the effect on the micro-structural change during compaction. Compaction studies of Akram and Kemper (1979) confirm this.

Comparison of the effects of laboratory compaction and compaction by field traffic

When comparing the shapes of the isobars corresponding to laboratory and traffic-induced compaction, respectively, it appears that they are to a great extent congruent. This implies that the traffic-induced compaction process is effectively simulated by the quick uni-axial compression test and that the gravimetric moisture content at compaction is the dominant soil characteristic controlling the effects of compaction. Deformation, which increases at increasing moisture content at compaction by field traffic, apparently has a minor effect on the compactibility and the resultant soil qualities, even when the soil is wet compacted. This can be explained from the fact that the relatively
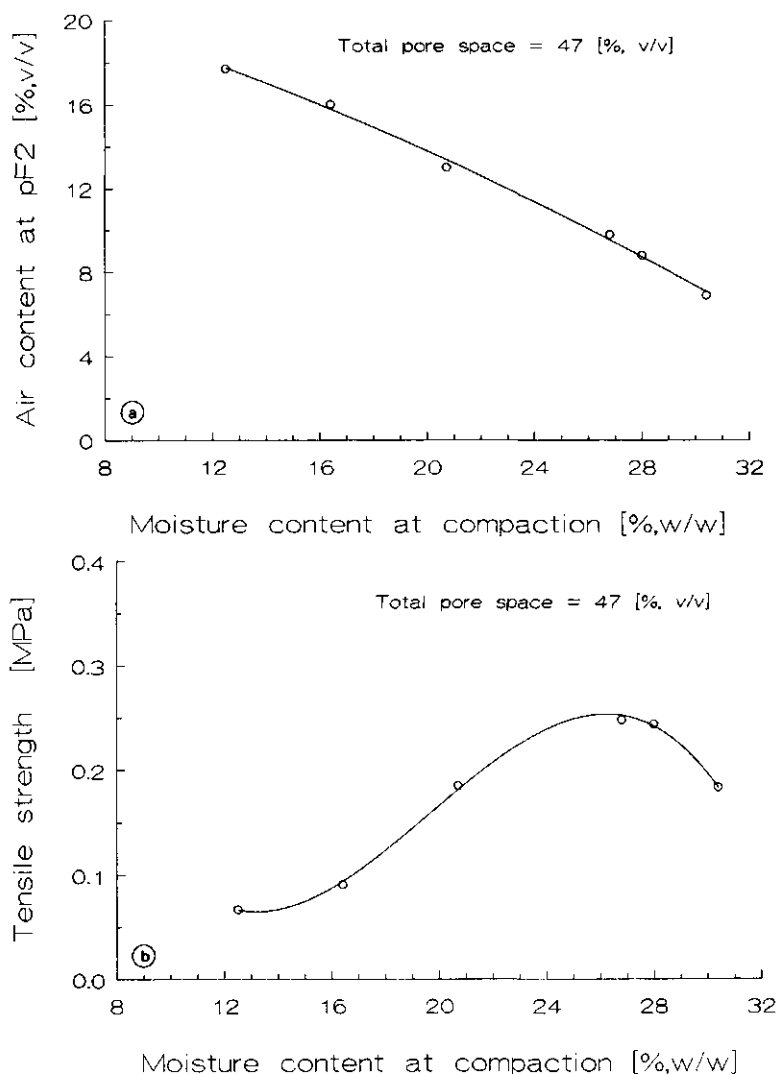
Fig. 3. The effect of uni-axial compaction to 47% pore space on (a) the air content at pF2 and (b) the oven-dry tensile strength, as a function of the gravimetric moisture content at compaction.

low compressive loads, as well as the small number of loading cycles featuring field traffic at seedbed preparation, will not induce large distortional strains. This is in agreement with the shallow ruts that were formed by both the LGP and the HGP traffic system. From observations on the effects of compaction at harvesting, featuring higher inflation pressures and loading by up to 15 wheels, it followed that the effects of wet compaction could no longer be adequately simulated by uni-axial compression.

When comparing the positions of the isobars of traffic and laboratory compacted soil, respectively, it follows, that the load characteristics of both the LGP and HGP traffic system cannot be represented by a single value of σ_{eq} in quick uni-axial compression. For example, the isobars expressing the effect of the LGP and HGP traffic system on the resultant total pore space correspond with σ_{eq} equals approximately 0.35 and 0.5 MPa, respectively, whereas the effect on the air content at pF2 correspond with σ_{eq} equals approximately 0.25 and 0.4 MPa, respectively. This discrepancy is primarily attributed to the differences between the structure of the field soil and the reconstituted structure of the soil prepared for laboratory compression.

CONCLUSIONS

The effect of compaction by field traffic at varying moisture content on soil physical properties can be adequately simulated by the quick uni-axial compression test on prepared soil samples, provided that compaction does not involve large distortional strains. The relationships obtained from laboratory compression, extended with measurements on soil qualities, are qualitative in nature rather than quantitative. When the extended M–P–V diagram is used for predictive purposes, a calibration procedure is required, in order to assess the respective values of σ_{eq} of the isobars which represent the traffic-induced effects on the soil qualities. Since the shape of the isobars can be effectively predicted using the extended uni-axial compression test, a relatively small number of observations on field-compacted soil samples suffices. The extended M–P–V diagram can further give detailed information on the susceptibility of field soils to the adverse effects of compaction.

REFERENCES

Akram, M. and Kemper, W.D., 1979. Infiltration of soils as affected by the pressure and water content at the time of compaction. Soil Sci. Soc. Am. J., 43: 1080–1086.
Beekman, F., 1987. Soil strength and forest operations. Ph.D. Thesis Wageningen Agricultural University, The Netherlands, 168 pp.
Dawidowski, J.B. and Koolen, A.J., 1987. Changes of soil water suction, conductivity and dry strength during deformation of wet undisturbed samples. Soil Tillage Res., 9: 169–180.
Gupta, S.C. and Allmaras, R.R., 1986. Models to assess the susceptibility of soils to excessive compaction. University of Minnesota, St. Paul, MN 55108, pp. 65–100.
Gupta, S.C. and Larson, W.E., 1982. Modeling soil mechanical behaviour during tillage. In: P. Unger, D.M. Van Doren Jr., F.D. Whisler and E.L. Skidmore (Editors), Symposium on Predicting Tillage Effects on Soil Physical Properties and Processes. Am. Soc. Agron., Madison, WI, Spec. Publ. 44, pp. 151–178.
Kirkham, D., De Boodt, M.F. and De Leenheer, L., 1959. Modulus of rupture determination on undisturbed soil core samples. Soil Sci., 87: 141–144.
Klute, A., 1965. Laboratory measurement of hydraulic conductivity of saturated soil. In: C.A.

Black, D.D. Evans, J.L. White, L.E. Ensminger and F.E. Clark (Editors), Methods of Soil Analysis, Part I. Physical and Mineralogical Properties, Including Statistics of Measurement and Sampling. Am. Soc. Agron., Madison, WI, Agronomy, 9: 210–221.

Koolen, A.J., 1987. Deformation and compaction of elemental soil volumes and effects on mechanical properties. Soil Tillage Res., 10: 5–19.

Koolen, A.J. and Kuipers, H., 1983. Agricultural Soil Mechanics: Advanced Series in Agricultural Sciences 13, Springer, Heidelberg, 241 pp.

Koolen, A.J. and Kuipers, H., 1988. Soil deformation under compressive forces. In: W.E. Larson, G.R. Blake, R.R. Allmaras, W.B. Voorhees and S.C. Gupta (Editors), Mechanics and Related Processes in Structured Agricultural Soils. Proc. ARN, St. Paul, MN, pp. 37–52.

Larson, W.E. and Gupta, S.C., 1980. Estimating criteria stress in unsaturated soils from changes in pore water pressure during confined compression. Soil Sci. Soc. Am. J., 44: 1127–1132.

Lerink, P., 1990. Prediction of the immediate effect of traffic on field soil qualities. Soil Tillage Res., 16: 153–166.

Perdok, U.D. and Hendrikse, L.M., 1982. Workability test procedure for arable land. In: Proc. 9th Conf. Int. Soil Tillage Res. Org. (ISTRO), Osijek, Yugoslavia, pp. 511–519.

Tijink, F.G.J., 1988. Load-bearing processes in agricultural wheel-soil systems. Ph.D. Thesis Wageningen Agricultural University, The Netherlands, 173 pp.

Willatt, S.T., 1987. Influence of aggregate size and water content on compactibility of soil using short-time static loads. J. Agric. Eng. Res., 37: 107–115.

184

Prediction of the Immediate Effects of Traffic on Field Soil Qualities

P. LERINK

Wageningen Agricultural University, Tillage Laboratory, Diedenweg 20, 6703 GW Wageningen (The Netherlands)

ABSTRACT

Lerink, P., 1990. Prediction of the immediate effects of traffic on field soil qualities. *Soil Tillage Res.*, 16: 153-166.

Based on the comparative prediction method, a prediction function was developed, which relates pertinent soil and traffic characteristics to the immediate effect of traffic on the field soil condition. The effect on the field soil condition is expressed in terms of a number of soil physical and mechanical properties, which are relevant to soil use and which are referred to as soil qualities. The prediction function is based on a limited domain, in order to restrict the number of soil and traffic characteristics that have to be taken into account, and to limit the range of values they can attain. The prediction function is presented graphically by means of composite diagrams.

INTRODUCTION

To establish a framework for a discussion on the development of a prediction function which predicts the immediate effect of traffic on the field soil condition, prediction is illustrated by the following conceptual relationship:

$$Y = F(x_1, \ldots, x_n) \tag{1}$$

where:
Y = the immediate effect on the field soil condition:
F = the prediction function;
x_i = soil and traffic characteristics that are pertinent in determining the effect on the field soil condition.

Prediction methods which have been proposed so far (reviewed by Soane et al., 1981b) have in common, that the effect of traffic on the soil condition is expressed by packing state properties, such as pore space and dry bulk density. During the last decade there has been increasing awareness that these packing state properties do not adequately describe the detrimental effect of compac-

tion by traffic (Soane, 1985). A major factor that undermines the suitability of packing state properties to quantify the traffic-induced effect on the soil condition is, that soil physical and mechanical properties that refer to the soil as a continuum, are generally not uniquely determined by the packing state properties only. These soil properties, such as water and gas conductivities, water storage capacity and penetrability, are more rationally related to the suitability of the soil for crop production.

Furthermore, macro-packing state properties are not sensitive indicators of the change of the soil condition by compaction. Voorhees et al. (1978) found that compaction by controlled wheel traffic increased the bulk density by 20% or less, whereas the penetration resistance was increased by as much as 400%.

Intensive field and laboratory research has been carried out to observe a great variety of effects of single traffic and soil characteristics on the resulting soil condition (Barnes et al., 1971; Chancellor, 1976; Soane et al., 1981a,b, 1982). Until now, knowledge based on such observations has never been assimilated into a coherent prediction method. The main reason for the absence of prediction methods based on observation may well be the difficulties that are encountered when dealing with the large number of traffic and soil characteristics involved, as well as the wide range of values they can attain.

The objective of this paper is to present a prediction method, which is based on observations, to predict the immediate effects of traffic on soil physical and mechanical properties that are pertinent with respect to soil use for crop production.

THE EFFECT OF TRAFFIC ON SOIL CONDITION

The immediate effect of the traffic-induced compaction process on soil condition can be quantified in terms of various soil properties using different measurement methods. The soil properties which are pertinent in describing the soil condition are primarily determined by the user of the information, i.e. the farmer. Furthermore, quantitative information on the soil condition after field traffic may serve as input data for soil water models (Van Lanen and Boersma, 1988) and crop production models (De Wit and Van Keulen, 1987). Soil properties which are pertinent with respect to soil use, and which are affected during a field operation, are further referred to as soil qualities (Koolen, 1987). Soil qualities include soil physical and mechanical properties that refer to workability, trafficability, gas, water and heat conductivity, root penetrability, water storage capacity, erodibility and stability.

Soil physical and mechanical properties are generally dependent on the soil moisture status. A complete description of the soil condition requires the determination of the soil qualities at a range of soil moisture contents or moisture suctions. As a matter of course this is virtually impossible. It was therefore decided to measure the soil qualities at a moisture content that corresponds with field capacity, i.e. at a matric water potential of -10 kPa (pF2) unless

the measurement technique prescribes otherwise (as in the case of the saturated water conductivity and the oven-dry tensile strength).

THE PREDICTION FUNCTION

Prediction methods that are based on observations can be divided into methods using empirical formulae or graphs and comparative methods (Koolen and Kuipers, 1983). Prediction methods using empirical formulae or graphs assume that the prediction function (F) can be described by a known general formula or graph shape.

Theoretically, a prediction function relating traffic and soil characteristics to the resulting soil qualities may be composed of empirical formulae that estimate the stresses occurring in the soil mass under a transient wheeling, and of observations on the soil qualities of a soil which has been compacted in the laboratory at a range of stress levels. This approach, including both empirical formulae and observations, has become known as the composite method (Koolen and Van Ouwerkerk, 1988).

With respect to estimating soil stress, Koolen and Kuipers (1989) state that currently available methods have a poor accuracy. Information on the effect of laboratory compaction on soil qualities is available from the literature (Akram and Kemper, 1979; Gupta and Larson, 1982; Beekman, 1987). However, evidence that these compaction tests, which involve uni-axial compression of prepared soil samples, adequately simulate the traffic-induced effect on the field soil condition is lacking.

The effect of large deformations, which are likely to occur under wet soil conditions, on soil qualities of a silty clay loam was studied by Dawidowski and Koolen (1987). These authors concluded, that deformation at constant volume had a marked effect on soil qualities. Hence, laboratory compaction tests which do not allow large deformations, such as the uni-axial compression test, do not adequately simulate the traffic-induced effect on the soil condition, when compaction is accompanied by large deformations.

Because detailed information on the relationship between traffic and soil characteristics and the effect on soil qualities is lacking, it may be concluded that prediction must be based on the comparative method.

THE COMPARATIVE METHOD

Even when the prediction function (F) is unknown, eqn. (1) can still be used as a prediction method. If once it has been observed that a particular set of values of x_i is related to a particular value of Y, it can be reasoned that Y will attain that value again, whenever the same situation, defined by the particular set of values of x_i, occurs again, provided that Y is uniquely determined by the set of values of x_i. A typical prediction function can be developed by

multiple observations of the relationships between different sets of values of the process characteristics (x_i) that are taken into account and the process effects (Y).

The overall domain of prediction comprises different field operations, including different types of farm machinery and tyre equipment, and field soils featuring different soil types and varying soil conditions. Limitation of the domain of prediction is required in order to limit the number of traffic and soil characteristics that have to be taken into account and the range of values that can be attained by these characteristics. In this study, the domain of prediction was limited to a single field, two types of field operations (seedbed preparation and the harvest of root crops), a single set of farm machinery and two types of tyre equipment, which are further referred to as traffic systems.

The traffic-induced effect on the soil condition of an arbitrary soil volume in the zone of influence under the wheel rut, depends on the position of the soil volume relative to the center line of the wheel rut. Furthermore, the traffic pattern resulting from a particular field operation may be composed of different tracks, originating from different wheelings with varying axle loads. It was decided to confine the range of prediction to the maximum effects on the resulting soil qualities of the soil mass in the zone of influence under the respective wheel ruts. It was expected that these maximum effects would occur under the centre line of the wheel ruts at a depth of 0 to about 12 cm, i.e. in the upper half of the trafficked arable layer. Furthermore, it was expected that the maximum effects would occur under wheel ruts resulting from the largest possible number of wheelings, including maximal axle loads.

TRAFFIC AND SOIL CHARACTERISTICS

Traffic and soil characteristics have to be identified that are pertinent in determining the effect on the soil condition (Y) in terms of soil qualities. The effectiveness of the comparative method to predict a value of Y that matches the observed value, depends on whether the effect on the soil qualities is uniquely determined by the traffic and soil characteristics that have been taken into account.

Traffic characteristics

On a microscopic scale, soil properties that are pertinent in determining the soil qualities of a soil with given intrinsic properties are: the proportion of soil particles in a unit volume; the spatial distribution of the soil particles; the proportion of soil water in a unit volume; the spatial distribution of soil water; the non-capillary bonds between the soil particles and the spatial distribution of the inter-particle bonds. These properties are further referred to as soil micro-factors (Koolen, 1987). When a soil is subjected to a mechanical process,

its micro-factors and inherently the soil qualities change, owing to redistribution of soil particles and soil water and rupture of inter-particle bonds. When the soil is considered as a continuum, the response to loading of an elemental soil volume within this continuum can be described in terms of deformation, which may be accompanied by volumetric strain, and/or failure. It can be reasoned that the soil response in terms of these continuum mechanical concepts is closely related to the effects on the soil micro-factors. From this it is inferred that traffic characteristics that determine the soil response in terms of deformation and/or failure are also pertinent in determining the effect on soil qualities.

If soil qualities are uniquely related to the proportion of soil particles in a unit volume, as may be true in the case of pure cohesionless sands, then traffic characteristics must be selected that are pertinent in determining the resulting volume of a loaded elemental soil volume. Koolen and Kuipers (1983) concluded that a stress system causing compaction can be effectively characterized by the first principal stress (σ_1). However, as stated before, evidence exists that the effect on the soil qualities not only depends on the volume change but also on the degree of deformation. Hence traffic characteristics that are pertinent in determining the degree of deformation have to be included.

From this brief discussion on traffic characteristics it follows that a detailed quantitative characterization of field traffic is far beyond comprehension. However, traffic characteristics that determine the soil response in terms of continuum mechanics concepts are in their turn completely defined by the type of machinery and tyre equipment, the tyre inflation pressure, the payload in the case of transport or the working depth in the case of tillage, and the driving speed. These characteristics are further used to characterize field traffic.

Soil characteristics

Pertinent field soil characteristics have to be identified to allow the prediction function to be unique. The uniqueness of the prediction function implies that the soil qualities resulting from a specific compactive treatment are identical, whenever the field soil condition at compaction is defined by a particular set of values of the soil characteristics.

In the course of time, the soil condition of a field soil is a continuous function of natural and man-induced processes. Important "driving forces" for natural processes, such as root growth and weather factors, as well as man-induced processes feature an annual cycle by nature and by rules of field management, respectively. Therefore, it is hypothesized that the soil condition of a particular field is largely determined by the time of year. In moderate climates, an important soil factor that deviates from this annual trend is the soil moisture status at shallow depths, which fluctuates daily and even hourly. The soil moisture status of a field soil can be easily and effectively quantified by the gravi-

189

metric moisture content as a function of depth. The significance of the gravimetric moisture content in determining the effect of mechanical compaction processes on the resultant soil qualities is twofold. Firstly, in the literature there is consensus on the dominant role of soil moisture content in determining the compactibility of a soil with given intrinsic properties (Soane et al., 1981a). It is emphasized that, apart from practical reasons, the gravimetric moisture content is preferred to the soil volumetric moisture content, since the soil compactibility at stress levels that are likely to occur in the vicinity of wheels of agricultural equipment is independent of the volume that was occupied by a given amount of dry soil prior to compaction (Tijink, 1988). Secondly, soil moisture content at compaction affects the failure mechanism that enables soil particles and soil water to redistribute. Dry soil structural elements crack upon loading, whereas wet elements exhibit plastic deformation. At moisture contents in between these extreme conditions, soil structural elements will exhibit both failure mechanisms. The type of failure mechanism that prevails can be derived from compaction studies by Koolen (1978) and Akram and Kemper (1979), by comparing the effects of compaction to equal dry bulk densities at varying moisture content. These studies show that the effects on pertinent soil physical and mechanical properties of "wet" compacted soil markedly deviate from the effects of "dry" compacted soil.

The characterization of the soil condition of a field soil by a single property, i.e. the gravimetric moisture content as a function of depth, may not completely account for the effects of calamities, such as extreme weather conditions and the long-term effects of field operations that are carried out under extremely wet or dry soil conditions. These calamities may disturb the cyclic character of the field soil condition to such an extent that the effect on the soil condition of a particular field operation is not uniquely defined by the gravimetric moisture content.

In conclusion, eqn. (1) can be rewritten as

$$Y = F(x_1, x_2, x_3) \tag{2}$$

where:
Y = the effect on soil condition in terms of soil qualities;
F = the prediction function according to the comparative method;
x_1 = the moisture content at compaction;
x_2 = the type of field operation;
x_3 = the type of traffic system

The domain of prediction is limited to a single set of farm machinery, two traffic systems and two field operations (i.e. seedbed preparation and the harvest of rootcrops). The range of prediction is confined to the maximum effects on the soil condition.

The objective of experimentation was to collect data that would enable the development of a typical prediction function and to verify the assumptions that underlie the prediction method. The prediction function is based on a large number of observations of the relationship between different sets of values and entities of the soil and traffic characteristics, respectively, and the immediate effect on the soil condition. In this study, the effect on the soil condition is expressed by the following soil qualities: air content at pF2, air permeability (Ki) at pF2, cone penetrability at pF2, saturated hydraulic conductivity (K_{sat}) and oven-dry tensile strength.

Prediction of the immediate effects of traffic on the soil condition fits within the framework established by research-project 319 of the Institute of Agricultural Engineering (IMAG, Wageningen, The Netherlands) entitled: "Perspective of reducing soil compaction by using a low ground pressure (LGP) traffic system; interrelationships between tyre pressure, state of compactness and crop performance". In the context of this multi-disciplinary project, a long-term field experiment, designed to monitor the effects on soil and crop condition at three levels of contact pressure (including a high ground pressure (HGP) traffic system, a low ground pressure (LGP) traffic system and a zero-traffic system), was started in autumn 1984 at the IMAG-experimental farm "Oostwaardhoeve", at Slootdorp, The Netherlands. The experimental field was divided into four main plots of 2 ha. Crop rotation (ware potatoes–winter wheat–sugarbeet–onions) was randomly assigned to the main plots. The main plots were subdivided into four sub-plots, two of which were randomly assigned to the LGP traffic system and the remaining two to the HGP traffic system (the zero-traffic sub-plots are not discussed here). Experimental field management involved farm machinery and work methods (driving speed and working depth) typical of 60-ha arable farms in The Netherlands.

On both the LGP plots and the HGP plots, the type of machinery used to perform a particular field operation as well as the working methods were identical. Therefore, field traffic can be characterized by referring to the traffic systems (LGP and HGP) and the type of field operation. The tyre pressures

TABLE 1

Inflation pressure levels (kPa) applied in the experiment

	HGP	LGP
Uncontrolled traffic before sowing/planting	80	40
Other operations	160	80
Trailer and implement tyres	240	80

as a function of the traffic system and the type of field operation were adjusted according to Table 1 (Vermeulen et al., 1988).

The soil type of the arable layer ranged from sandy loam to clay loam; the organic-matter content and the calcium carbonate content amounted to 1.5–2.0% (w/w) and 5–10% (w/w), respectively.

Experimental method

In three successive years, experiments have been carried out to quantify the soil response to field traffic at seedbed preparation and the harvest of root crops. The effect on soil condition was determined at two depth intervals (2–7 cm and 7–12 cm) below the centre line of the wheel ruts. The experiments comprised field sampling and laboratory tests.

Field sampling

Immediately after rut formation, the soil was sampled at two depths (2–7 cm and 7–12 cm) below the centre line of the rut using 50-mm high and 76-mm diameter stainless steel soil sampling rings. The sample locations were randomly distributed within a section of 5 m rut length. It is assumed that this sampling procedure presents mutually independent observations. The locations of the sampling sections on the trafficked plots were arbitrarily chosen, on the condition of maximum payload when transport was involved, and a maximum number of wheelings.

TABLE 2

Laboratory tests

Treatment	Measurement	Method
	Moisture content and porosity, immediately after compaction	
Equilibration at pF2	Moisture and air content at pF2; intrinsic air permeability at pF2	(Perdok and Hendrikse, 1982)
Saturation	Saturated water conductivity	Constant head method (Black, 1965)
Equilibration at pF2	Cone penetrability	Cone angle: 30°; base diameter: 1.2 mm; penetration rate: 25 mm min^{-1}
Oven drying	Tensile strength	Brazilian test (Kirkham et al., 1959)

Laboratory tests

Each core sample was subjected to a standard series of measurements. The successive treatments and measurements are listed in Table 2. The numerical results of measurements performed on samples belonging to the same set were averaged, except for the results of the measurements of saturated water conductivity and intrinsic air permeability, which are presented as log means and anti-log converted log means, respectively. The penetration resistance is expressed as the cone index, being the quotient of the mean vertical force during penetration and the cone-base area ([MPa]).

RESULTS

The effect of traffic on the respective soil qualities (Y_{obs}) as a function of the gravimetric moisture content at compaction, the type of field operation and the type of traffic system is presented graphically by means of composite diagrams. These diagrams are shown in Figs. 1 and 2, and refer to field traffic at seedbed preparation for root crops and to field traffic at the harvest of these root crops, respectively. The composite diagrams include the effect of traffic on the total pore space.

The prediction function (F) that relates the predicted values of the resulting soil qualities (Y_{pr}) to the moisture content at compaction (x_1) for the distinct field operations (x_2) and traffic systems (x_3) is expressed as a series of curves. The prediction curves are fitted by eye.

The graphical relationship between the gravimetric moisture content at "quick" compaction and the resulting total pore space has become known as a moisture–pressure–volume (M–P–V) diagram (Koolen, 1987). The M–P–V curves plotted in Figs. 1 and 2 show that at increasing moisture content, the total pore space decreases, levels off until a more or less distinct minimum value is reached and increases again. The moisture content at which the total pore space starts to increase again, and which corresponds with a minimum value of the M–P–V curve, separates the compaction process into "dry" compaction and "wet" compaction. By definition, "dry" compaction refers to a compaction process which does not feature a limitation of the compactibility by entrapped air and water. Consequently, "wet" compaction refers to a compaction process which features a limitation of the compactibility by entrapped air and water. In the diagrams presented in Figs. 1 and 2, vertical lines that intersect the moisture content axis separate "dry" from "wet" compaction for both the HGP and the LGP traffic system.

At "dry" compaction, the soil qualities are negatively correlated to the moisture content at compaction, i.e. higher moisture contents result in less desirable soil qualities. At "wet" compaction, the saturated water conductivity, the air permeability at pF2 and the air content at pF2 have very low values and
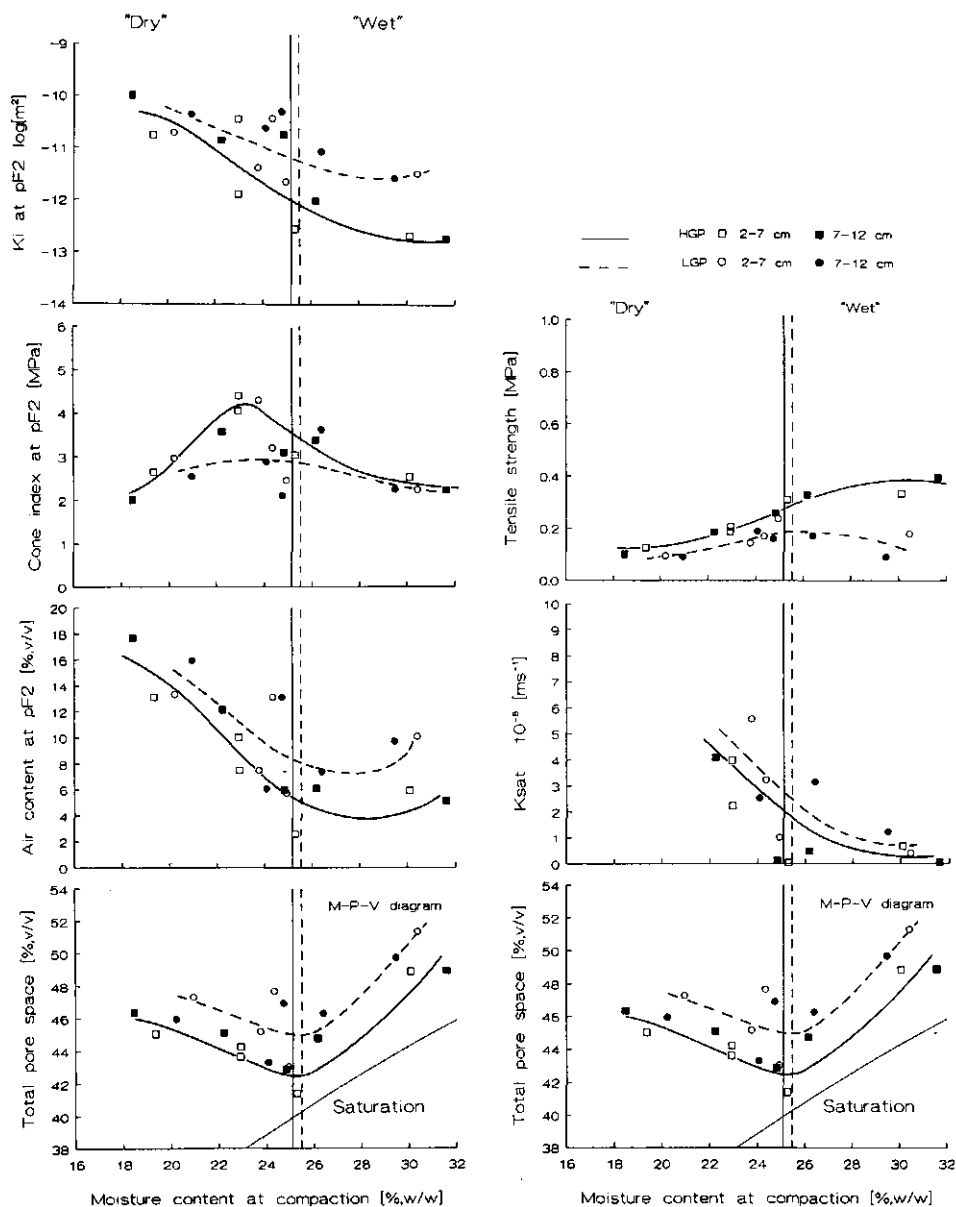
193

Fig. 1. Composite diagram of the immediate effect of field traffic at seedbed preparation on soil qualities as a function of the soil moisture content at compaction.

are virtually independent of the moisture content at compaction, despite the fact that the total pore space increases at increasing moisture content. The
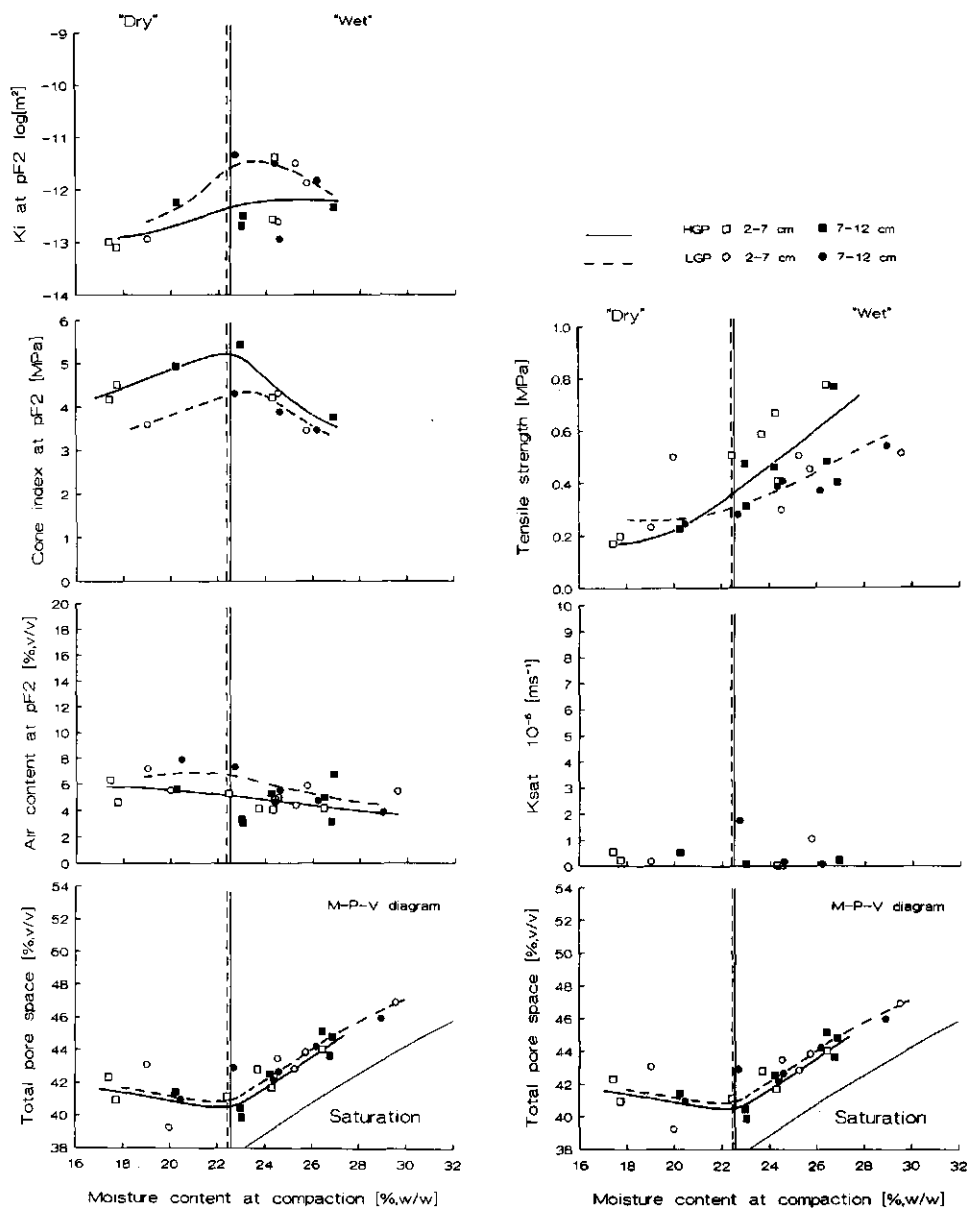
194

Fig. 2. Composite diagram of the immediate effect of field traffic at the harvest of root crops on soil qualities as a function of the soil moisture content at compaction.

tensile strength appears to be a useful indicator of the structural deterioration at "wet" compaction. At increasing moisture content at compaction the increase of the oven-dry tensile strength may be attributed to increasing defor-

195

mation at constant volume, which is in agreement with the findings of Dawi-
dowski and Koolen (1986).

The comparison of the effects of the HGP and the LGP traffic system on
the resulting soil condition is based on the relative positions of the respective
prediction curves. At seedbed preparation, the HGP traffic system results in a
higher degree of compactness and less desirable soil qualities as compared with
the LGP traffic system. The gravimetric moisture content resulting in maxi-
mum compaction is slightly lower for the HGP traffic system as compared with
the LGP traffic system. The degree of compactness resulting from field traffic
at the harvest of the root crops is the same for the HGP and the LGP traffic
system. The effect of the type of traffic system on the soil qualities is clearly
represented by the oven-dry tensile strength.

DISCUSSION

The effectiveness of a prediction method primarily depends on the following
criteria: does the prediction method provide useful information; does the pre-
diction method meet the desired accuracy; is the prediction method practicable.

At present, no generally accepted standards are available that quantitatively
describe optimum or limiting soil conditions for crop production. It is beyond
doubt that the soil condition cannot be adequately characterized by a single
soil property. The inability of pore space, bulk density or equivalent properties
to unambiguously describe the soil condition can be derived from Figs. 1 and
2, by comparing the soil qualities of "dry" and "wet" compacted soil.

The quantification of the traffic-induced effects on soil condition by the
concept of soil qualities is an attempt to widen the usefulness of information
obtained from prediction and to provide means to link relevant knowledge of
adjacent soil, crop and machine related disciplines.

The accuracy of the prediction function determines the deviation between
the predicted values (Y_{pr}) and the observed values (Y_{obs}) of the respective soil
qualities. The composite diagrams in Figs. 1 and 2 show a considerable degree
of deviation between Y_{pr} and Y_{obs}. A major factor causing this deviation is the
variation in the soil type between the sites that were sampled (Lerink, 1990).
Factors of minor importance are the preceding crop, weather factors, the soil
condition at the preceding field operation and sampling and measurement er-
rors. From the shape of the prediction curves it is inferred that the gravimetric
moisture content at compaction is a dominant soil factor in determining the
effect of a specific field operation on the resulting field soil condition.

The practicability of the prediction method presented here is greatly ham-
pered by the large number of observations required to develop the prediction
function expressed by the curves in Figs. 1 and 2. To overcome this problem, a
simple laboratory method has been developed (Dawidowski and Lerink, 1990)
to determine the shape of the curves expressing the effect on soil qualities as a
function of the moisture content at compaction and the compactive load. Thus,

196

a limited number of field observations suffice to coordinate the positions of the respective curves.

CONCLUSION

The comparative prediction method, based on a limited domain, has proved to be a useful tool to predict the immediate effect of field traffic during distinct field operations on the soil condition.

The main assumption that underlies the prediction method is whether the soil condition of a given field soil, at the time a specific field operation is carried out, is adequately characterized by the gravimetric moisture content, so as to allow the prediction function to be unique. The experimental data presented here validate this assumption.

REFERENCES

Akram, M. and Kemper, W.D., 1979. Infiltration of soils as affected by the pressure and water content at the time of compaction. Soil Sci. Soc. Am. J., 43: 1080–1086.
Barnes, K.K., Carleton, W.M., Taylor, H.M., Throckmorton, R.I. and Vanden Berg, G.E. (Editors), 1971. Compaction of Agricultural Soils. ASAE, St. Joseph, MI, 471 pp.
Black, C.A. (Editor), 1965. Methods of Soil Analysis. I. Agronomy No. 9, Part 1. ASA, Madison, WI, 770 pp.
Beekman, F., 1987. Soil Strength and Forest Operations. Ph.D. Thesis, Wageningen Agricultural University, The Netherlands, 168 pp.
Chancellor, W.J., 1976. Compaction of soil by agricultural equipment. Bull. 1881, Div. Agric. Sci., Univ. California, Davis, CA, 53 pp.
Dawidowski, J.B. and Koolen, A.J., 1987. Changes in soil water suction, conductivity and dry strength during deformation of wet undisturbed samples. Soil Tillage Res., 9: 169–180.
Dawidowski, J.B. and Lerink, P., 1990. The effect of quick uni-axial compaction of prepared soil on soil physical and mechanical properties. Soil Tillage Res., in press.
De Wit, C.T. and Van Keulen, H., 1987. Modeling production of field crops and its requirements. Geoderma, 40: 253–265.
Gupta, S.C. and Larson, W.E., 1982. Modeling soil mechanical behavior during tillage. ASA Spec. Publ. 44, pp. 151–178.
Kirkham, D., De Boodt, M.F. and De Leenheer, L., 1959. Modulus of rupture determination on undisturbed soil core samples. Soil Sci., 87: 141–144.
Koolen, A.J., 1978. The influence of a soil compaction process on subsequent soil tillage processes. A new research method. Neth. J. Agric. Sci., 26: 191–199.
Koolen, A.J., 1987. Deformation and compaction of elemental soil volumes and effects on mechanical soil properties. Soil Tillage Res., 10: 5–19.
Koolen, A.J. and Kuipers, H., 1983. Agricultural Soil Mechanics. Springer, Heidelberg, 241 pp.
Koolen, A.J. and Kuipers, H., 1989. Soil deformation under compressive forces. In: W.E. Larson, G.R. Blake, R.R. Allmarar, W.B. Vonheer and S.C. Gupta (Editors), Mechanics and Related Processes in Structured Agricultural Soils, NATO ASI Series, Series E: Applied Sciences, vol. 172. Kluwer, Dordrecht, pp. 37–53.
Koolen, A.J. and Van Ouwerkerk, C., 1988. Pedotechnique – inventory of predictive methods, and unlocking of relevant input data. Proc. 11th Conf. Int. Soil Tillage Res. Org. (ISTRO), 11–15 July 1988, Edinburgh, pp. 721–726.

Lerink, P., 1990. Prediction of the Immediate Effect of Traffic on Field Soil Condition. Ph.D. Thesis, Wageningen Agricultural University, The Netherlands, in preparation.

Perdok, U.D. and Hendrikse, L.M., 1982. Workability test procedure for arable land. Proceedings of the 9th Conf. Int. Soil Tillage Res. Org. (ISTRO), Osijek, Yugoslavia, pp. 511-519.

Soane, B.D., 1985. Traction and transport systems as related to cropping systems. Proc. Int. Conf. Soil Dynamics, Auburn, AL, Vol. 5, pp. 863-935.

Soane, B.D., Blackwell, P.S., Dickson, J.W. and Painter, D.J., 1981a. Compaction by agricultural vehicles: a review. I. Soil and wheel characteristics. Soil Tillage Res., 1: 207-237.

Soane, B.D., Blackwell, P.S., Dickson, J.W. and Painter, D.J., 1981b. Compaction by agricultural vehicles: a review. II. Compaction under tyres and other running gear. Soil Tillage Res., 1: 373-400.

Soane, B.D., Dickson, J.W. and Campbell, D.J., 1982. Compaction by agricultural vehicles: a review. III. Incidence and control of compaction in crop production. Soil Tillage Res., 2: 3-36.

Tijink, F.G.J., 1988. Load-bearing processes in agricultural wheel-soil systems. Ph.D. Thesis, Wageningen Agricultural University, The Netherlands, 173 pp.

Van Lanen, H.A.J. and Boersma, O.H., 1988. Use of soil-structure type data in a soil-water model to assess the effects of traffic and tillage on moisture deficit, aeration and workability of sandy loam and clay loam soils. Proceedings of the 11th Conf. Int. Soil Tillage Res. Org. (ISTRO), 11-15 July 1988, Edinburgh, pp. 415-420.

Vermeulen, G.D., Arts, W.B.M. and Klooster, J.J., 1988. Perspective of reducing soil compaction by using a low ground pressure farming system: selection of wheel equipment. Proceedings of the 11th Conf. Int. Soil Tillage Res. Org. (ISTRO), 11-15 July 1988, Edinburgh, pp. 329-334.

Voorhees, W.B., Senst, C.G. and Nelson, W.W., 1978. Compaction and soil structure modification by wheel traffic in the northern Corn Belt. Soil Sci. Soc. Am. J., 42: 344-349.

Technical Note

The kneading distortion apparatus

P. Lerink

Tillage Laboratory of the Wageningen Agricultural University, Diedenweg 20, 6703 GW, Wageningen (The Netherlands)

ABSTRACT

Lerink, P., 1990. The kneading distortion apparatus. *Soil Tillage Res.*, 17: 173–179.

A relatively simple apparatus was developed to impose controlled, homogeneous kneading distortion (deformation at constant volume) on wet soil. By contrast with the triaxial apparatus, the kneading distortion apparatus allows virtually unlimited distortion at soil-apparatus system defined stress states. The kneading distortion apparatus is primarily designed to study the effects of distortion on soil physical properties.

INTRODUCTION

In agriculture, the loading of soil under wet soil conditions by machinery or cattle may cause large soil deformation. As soil water hampers considerable volumetric strain (compaction), deformation mainly features distortion (deformation at constant volume). Soil distortion is of practical importance because it requires energy and it modifies soil physical properties which are important for soil use. In continuum mechanics, distortion refers to the change of the shape of a geometrical element upon loading.

In the laboratory, distortional strains can be imposed on a soil specimen by the triaxial apparatus (Koolen and Kuipers, 1983). The degree of distortion that can be obtained by the triaxial apparatus is limited. Furthermore, the triaxial apparatus is expensive and the test is time consuming. In order to enable virtually unlimited soil distortion, the kneading distortion apparatus was developed. The kneading distortion apparatus was primarily designed to study the effects of distortion on soil physical properties.

THE KNEADING DISTORTION APPARATUS

The main parts of the kneading distortion apparatus are the sample holder, the piston–annulus unit and the adaptor to alter the kneading mode (Fig. 1).
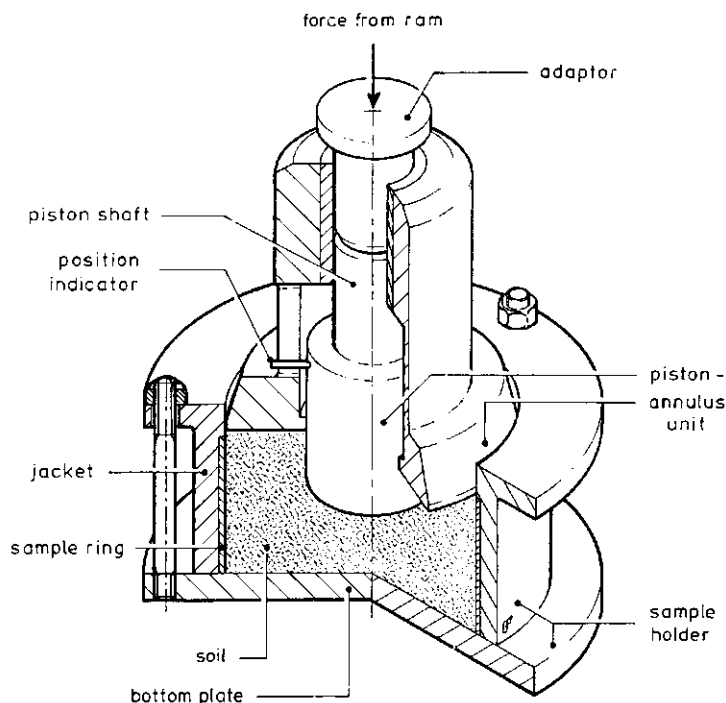
Fig. 1. The kneading distortion apparatus.

A soil sample in a steel cylinder (height 50.0 mm; inner diameter 98.6 mm) is tightly fitted between the jacket and the bottom plate by screwing down the nuts. In order to prevent drainage, the bottom plate is furnished with a rubber seal.

At the start of the test, the piston–annulus unit is placed on top of the sample. A loading ram forces the piston at constant speed into the sample. The ram speed should be high enough to prevent soil water transport over macroscopic distances. We tested at a ram speed, during the piston down stroke, of 500 mm min^{-1}. During the down stroke of the piston, the force exerted via the adaptor on the piston and the displacement of the piston are simultaneously recorded. The maximum displacement of the piston is approximately 15 mm. As a result of the penetration of the piston, the soil between the piston circumference and the inner circumference of the sample ring bulges and lifts the annulus. The piston shaft is greased in order to minimize friction.

The load is removed when the piston has travelled the pre-set travel distance (Δh). After removal of the adaptor, distortion is continued by forcing the shaft of the annulus downward. The down stroke of the annulus forces the soil to lift the piston. The load on the annulus is removed once a flush sample surface is retained, as is indicated by the position indicator of the piston (see

200

Fig. 1). The force needed for the down stroke of the annulus is not measured because it is irrelevant owing to the frictional forces that are likely to occur between the annulus and the sample ring at this part of the loading cycle. In order to obtain the desired degree of distortion, the 'two stroke' kneading distortion is continued by repeating the procedure as described above.

The distorted soil sample can be used for further experimentation by taking a cylindrical sub-sample of the soil between the piston and the bottom plate. To do so, a cylindrical steel cylinder, with a sharpened rim and an inner diameter that equals the diameter of the piston, is forced into the soil sample until the bottom plate is reached. After the bottom plate has been removed, the cylindrical sub-sample can be obtained by removing the soil between the two steel cylinders.

SAMPLE PREPARATION

Soil deformation at negligible volume change occurs when the volume percentage of entrapped air is approximately 5% (v/v) or less. The remolded or undisturbed soil sample in the steel cylinder can be brought to this condition by adjusting the moisture content and/or by pre-compaction. To prevent friction, the sample ring is greased prior to filling.

ANALYSIS OF KNEADING DISTORTION

The strain field of a soil sample in a cylindrical soil bin, resulting from the penetration of a piston with a diameter which is considerably smaller than the diameter of the soil bin, was studied by Chancellor and Schmidt (1962). It was shown, that the strain field on the soil body between the piston and the bottom of the soil bin mainly featured downward and lateral strain, whereas the strain field of the surrounding soil body mainly featured lateral and upward strain. In order to describe the soil behaviour in the kneading distortion apparatus quantitatively, the following assumptions were made: (1) during the piston down stroke, the cylindrical soil body between the piston and the bottom plate, with an initial diameter which equals the diameter of the piston, and an initial height which equals the height of the soil sample prior to distortion, exhibits downward and lateral strain only. Similarly, the surrounding, hollow cylindrical soil body exhibits lateral and upward strain only; (2) both soil bodies exhibit homogeneous strain; (3) the direction of the first principal strain (ϵ_1) of both soil bodies is vertical; (4) the strain fields around the vertical axis through the center of the soil sample are radially symmetric; (5) strain occurs at constant volume; (6) the soil physical phenomena which underlie distortion are independent of the directions of the principal strains. Thus, according to this assumption, distortion can be adequately quantified by the scalar quantities, ϵ_1, ϵ_2 and ϵ_3. (7) The soil physical phenomena are
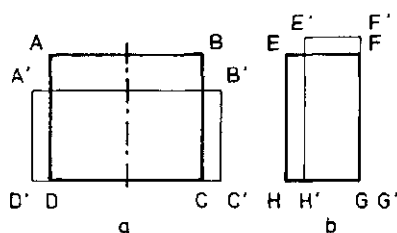
Fig. 2. Free body diagram of soil distortion during the piston down stroke, (a) refers to the cylindrical soil body under the piston, while (b) refers to the hollow cylindrical soil body under the annulus.

independent of whether strain is the result of axial shortening or axial elongation.

According to these simplifying assumptions, the change of shape of the cylindrical and hollow cylindrical soil bodies can be expressed by the free body diagrams in Fig. 2a,b, respectively. Upon penetration of the piston, it is assumed that the vertical cross-section of the cylindrical soil body, denoted as ABCD, changes to A'B'C'D' (Fig. 2a), while the vertical cross-section of the hollow cylindrical soil body, denoted as EFGH, changes to E'F'G'H' (Fig. 2b).

Large strains are commonly quantified using the natural strain concept. The degree of strain of the cylindrical soil body resulting from a pre-set piston displacement Δh is uniquely defined by $\bar{\epsilon}_1$, since $\bar{\epsilon}_2 = \bar{\epsilon}_3$ (according to assumption (4) and $\bar{\epsilon}_1 + \bar{\epsilon}_2 + \bar{\epsilon}_3 = 0$ (according to assumption (5)). The degree of distortion of the cylindrical soil body, resulting from a pre-set piston down stroke Δh thus equals

$$\bar{\epsilon}_1(\Delta h) = -\ln(1 - \Delta h/h_0) \qquad (1)$$

where $\bar{\epsilon}_1(\Delta h)$ is the natural largest principal strain, resulting from the pre-set piston down stroke Δh, and h_0 is the initial height of the cylindrical soil body. (Axial shortening is defined as positive strain.) The degree of distortion of the hollow cylindrical soil body under the annulus is not considered as it is of little importance here.

After the piston has travelled the pre-set distance Δh, the load on the piston via the adaptor is removed and distortion is continued by loading the annulus. The annulus down stroke is stopped once a flush sample surface is retained, as is indicated by the position indicator (Fig. 1). At this part of the test, it is assumed that A'B'C'D' changes to ABCD, while E'F'G'H' changes to EFGH (i.e. the initial shape is retained). Since vertical shortening and radial expansion of the cylindrical soil body is replaced by vertical elongation and radial shrinking, respectively, distortion resulting from one loading cycle (a piston down stroke followed by an annulus down stroke) is referred to as kneading distortion.

202

The degree of distortion of $A'B'C'D'$ resulting from the annulus down stroke until a flush sample surface is retained equals $-\bar{\epsilon}_1(\Delta h)$. Assumption (7) and the description of distortion by the natural strain concept allows summation of the absolute values of strain resulting from the piston down stroke and the annulus down stroke. The total distortion of the cylindrical soil body under the piston resulting from n loading cycles is thus

$$\bar{\epsilon}_1(n,\Delta h) = -2n\ln(1-\Delta h/h_0) \tag{2}$$

where $\bar{\epsilon}_1(n,\Delta h)$ is the natural largest principal strain, resulting from n loading cycles, with a pre-set travel distance Δh of the piston.

The true strain path of the cylindrical soil body under the piston deviates from the assumed strain path, in that the initial cylindrical shape changes into a barrel shape during the piston down stroke, as was visualized by Dawidowski et al. (1990) and which is in agreement with the earlier findings of Söhne (1953). This indicates that distortion of the soil body is not completely homogeneous. In order to limit the heterogeneity, the maximum travel distance of the piston (Δh) should not exceed approximately a quarter of the initial height of the soil sample.

ANALYSIS OF STRESS

The stress analysis is comparable to the strain analysis. In order to describe the state of stress acting on the soil bodies during a piston down stroke, the following simplifying assumptions were made: (1) the soil bodies are isotropic; (2) the stress distribution in the soil bodies is uniform; (3) shear stresses at the boundaries of the soil bodies are absent; (4) the directions of σ_1, σ_2 and σ_3 correspond with the directions of ϵ_1, ϵ_2 and ϵ_3, respectively; (5) the soil bodies behave in a perfectly plastic manner (non-work hardening and non-work softening), and the soil has no internal friction.

According to the assumptions, the state of stress of the cylindrical and hollow cylindrical soil bodies during the piston down stroke is expressed by the free body diagrams in Fig. 3a,b, respectively. The assumed instantaneous ma-
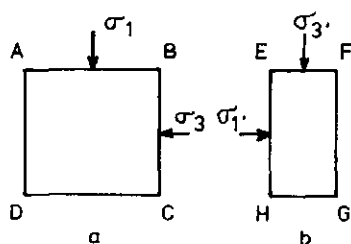

Fig. 3. Free body diagram of the stress system during the piston down stroke, (a) refers to the soil body under the piston, while (b) refers to the soil body under the annulus.

jor principal stress σ_1 (Fig. 3a) equals F/A, where F is the force exerted by the piston on the cylindrical soil body and A is the horizontal, cross-sectional area of the soil body. As opposed to the triaxial test, σ_3 in the kneading distortion test can not be controlled. For perfectly plastic, non-frictional soils, the Coulomb–Mohr Criterion states

$$\sigma_1 - \sigma_3 = 2c \tag{3}$$

where c is cohesion.
Similarly (Fig. 3b):

$$\sigma_{1'} - \sigma_{3'} = 2c \tag{4}$$

The confining pressure on the hollow cylindrical soil body ($\sigma_{3'}$) stems from the weight of the annulus and equals approximately 3.4 kPa. Since $\sigma_{1'}$ equals σ_3, it follows from eqns. (3) and (4) that

$$\sigma_3 = (\sigma_1 + \sigma_{3'})/2 \tag{5}$$

Despite the rigorous idealization, limited experimental evidence is available (Dawidowski et al., 1990) to support the stress analysis presented here.

Similar considerations can be applied to evaluate the stress state of the soil sample during the annulus down stroke. It can be expected however, that the simplifying assumptions proposed so far are less justified owing to soil-sample ring friction and adhesion at this part of the test.

CLOSING REMARKS

Current laboratory research methods on the effect of loading on the soil conditions primarily concern soil compaction, i.e. volumetric strain and the associated effects on soil physical properties. Knowledge on the effects of large distortional strains, which are likely to occur in wet soil conditions, on soil physical properties is still fragmentary. The kneading distortion apparatus may be a useful tool to widen this field of knowledge. The kneading distortion test is a cheap and quick test and enables virtually unlimited distortional strain. The effectiveness of the kneading distortion test to simulate the effect on the soil condition in terms of soil physical properties, as a function of the degree of distortion and the type of stress system that induced distortion, was experimentally verified by Dawidowski et al. (1990).

REFERENCES

Chancellor, W.J. and Schmidt, R.H., 1962. Soil deformation beneath surface loads. Trans. ASAE, 5: 240–246, 249.
Dawidowski, J.B., Lerink, P. and Koolen, A.J., 1990. Controlled distortion of soil samples with reference to soil physical effects. Soil Tillage Res, 17: 15–30.
Koolen, A.J. and Kuipers, H., 1983. Agricultural Soil Mechanics. Advanced Series in Agricultural Sciences 13, Springer Verlag, Berlin, 241 pp.
Söhne, W., 1953. Druckverteilung im Boden und Bodenverformung unter Schlepperreifen. Grundl. Landtechnik, 5: 49–63.

Prediction of aspects of soil–wheel systems

A.J. Koolen[a], P. Lerink[b], D.A.G. Kurstjens[a], J.J.H. van den Akker[c] and W.B.M. Arts[d]

[a]*Tillage Laboratory of the Wageningen Agricultural University, Diedenweg 20, 6703 GW Wageningen, Netherlands*
[b]*Rumptstad Industries, Stad aan het Haringvliet, Netherlands*
[c]*The Winand Staring Centre for Integrated Land, Soil and Water Research (SC), Wageningen, Netherlands*
[d]*Institute of Agricultural Engineering (IMAG), Wageningen, Netherlands*

(Accepted 7 October 1991)

ABSTRACT

Koolen, A.J., Lerink, P., Kurstjens, D.A.G., van den Akker, J.J.H. and Arts, W.B.M., 1992. Prediction of aspects of soil–wheel systems. *Soil Tillage Res.*, 24: 381–396.

A simple formula is given which predicts maximum stress–depth relationships under wheels from vertical wheel load and the tyre inflation pressure. Predictions were compared with stress measurements at a depth of 30 cm under a wide range of vehicles, for zero rut depth, non-significant horizontal wheel force, and soil top layers overlaying more rigid subsoil. A very wide diagonal rubber tyre and a very wide radial polyurethane tyre were compared with respect to their contact stress distributions. Stress measurements at a depth of 15 cm showed that the former tyre produced higher peak stresses. If values of soil cohesion and angle of internal friction are available, the model SOCOMO can predict size and location of plastic regions in soil under tyres. If only specific types of field traffic and given pieces of land are considered, it is possible to measure useful relationships between soil water content at traffic event and traffic-induced change of any soil physical property.

INTRODUCTION

Recently, in the Netherlands, a research project was carried out to investigate the benefits of a low ground pressure farming system (Vermeulen and Klooster, 1992). The core of the project was a 4 year field experiment on an 'average' Dutch soil (10 ha), with a machinery fleet representative of a 60 ha arable farm in the Netherlands with 55 and 82 kW tractors. In order to aid transfer of the findings to other conditions, the project also included research to establish prediction methods.

A soil–wheel system has many aspects worthy of prediction. Prediction may concern vehicle aspects, topsoil or subsoil aspects. As complexity and types of questions vary among these categories, approaches to find answers also vary.

Correspondence to: A.J. Koolen, Tillage Laboratory of the Wageningen Agricultural University, Diedenweg 20, 6703 GW Wageningen, Netherlands.

The impact of a vehicle pass is greatest near the ruts. In principle, the vehicle-induced changes in the physical conditions of a soil near a rut would be found by solving a set of equations that account for equilibrium of forces, the boundary conditions and the stress–strain relationships, and by translating the calculated stress and strain fields into changes in soil physical condition. We considered that this exact method is not feasible for zones near ruts because the soil here is very often severely deformed. Instead, a prediction method was developed (Lerink, 1990), based on observations of relationships between relevant soil and wheel characteristics (the independent variables) and process aspects (the dependent variables). The dependent variables reflect the physical conditions of the soil that prevail in rut centres at shallow depths immediately after a field traffic event. These variables include measures of water holding capacity, of exchange possibilities for gases, of conductivity, and of soil strength. The independent variables included type of field traffic and soil water content at a considered depth at time of traffic. Some of the results are presented in Vermeulen and Klooster (1992). This prediction method may be classified as a comparative method (Koolen and Kuipers, 1983), and is based on a strongly reduced domain. The domain of the soil and wheel characteristics is confined to one piece of land, two levels of tyre inflation pressure and a few types of field operations that may be very compactive (seedbed operations, harvesting root crops, ploughing). The work of Lerink (1990) provides a strategy that can be followed when the physical condition of soil severely deformed in field operations is to be predicted, especially when prediction has to account for field soil water content at time of field operation.

Where greater zones under wheels are considered, the question arises whether wheel-induced strains are elastic or permanent (plastic). Because permanent deformations may mean permanent worsening of the soil physical condition, it is important to know the locations of elastic and plastic zones under tyres. Elastic strains and strains in a transitional stage are rather small. This may explain why many research workers have used elastic theory to calculate stress fields under tyres. In the Netherlands, expertise was built up by Van den Akker (1988), who developed the soil compaction model SO-COMO. At the start of the research project, it was decided to apply SO-COMO. As both σ_1 and σ_3 fields have been calculated, the Mohr–Coulomb failure criterion could be used. This criterion needs values for soil cohesion (c) and angle of internal friction (ϕ). Values of c and ϕ were measured by triaxial tests and used to find shape, size and location of plastic regions in soil under tyres (Van den Akker and Lerink, 1990). Relations between plastic region size, wheel characteristics and soil cohesion are shown in Fig. 1. Cohesion of unsaturated agricultural soil is largely determined by soil water tension and soil water content. Van den Akker and Lerink (1990) concluded that reducing tyre inflation pressures may be a good soil structure improving
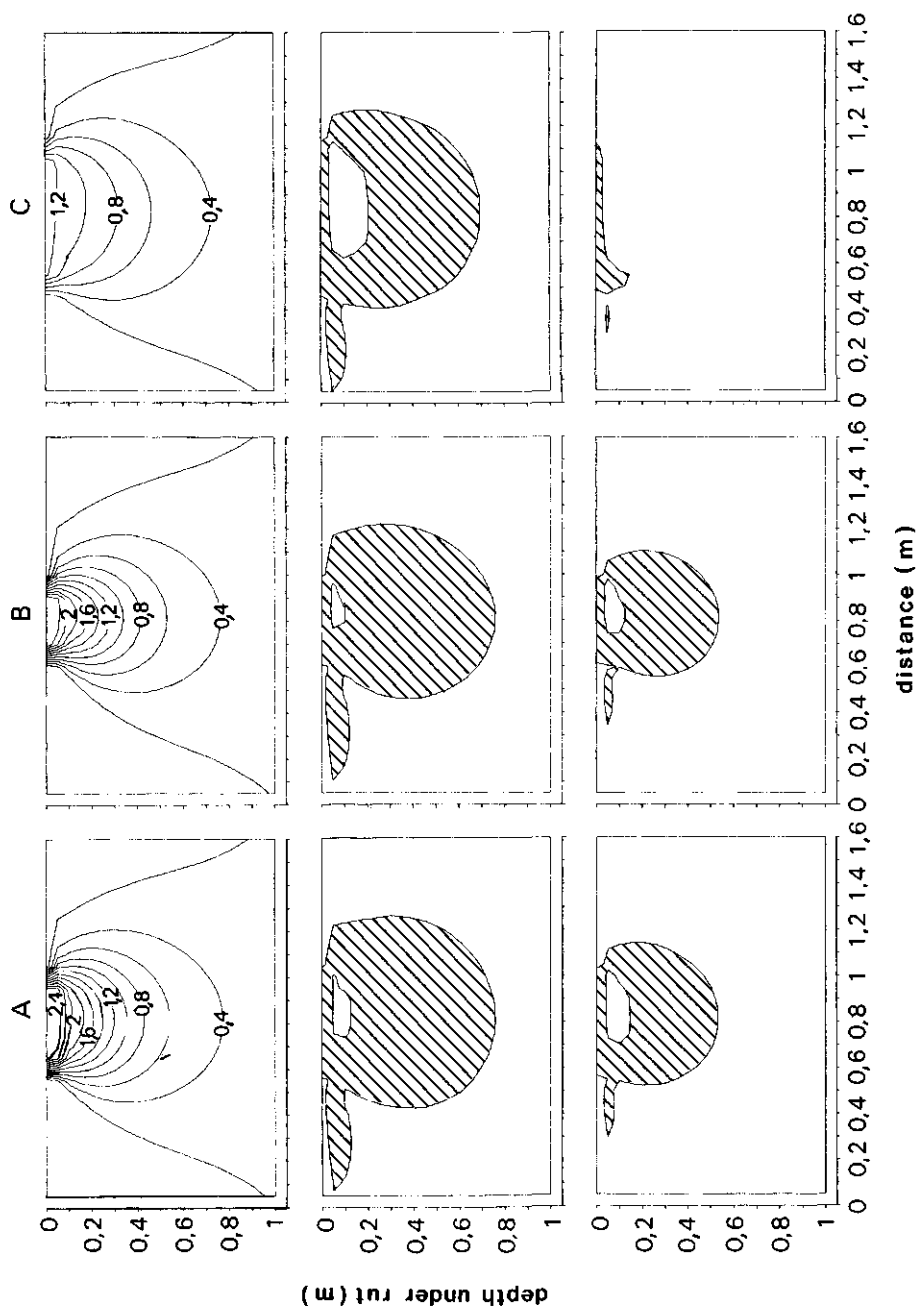
207

Fig. 1. Major principal stresses σ_1 and plastic areas in a longitudinal cross-section through rut centres under tyres: A, tyre width 0.42 m, tyre inflation pressure 170 kPa; B, tyre width 0.55 m, inflation pressure 170 kPa; C, tyre width 0.55 m, inflation pressure 80 kPa. In all cases, wheel load is 30 kN vertically and 6 kN horizontally. The towed wheel moves from the left to the right. Top: major principal stresses σ_1 (kPa). Centre: plastic areas caused by the loading, soil angle of internal friction $\phi = 31°$ and cohesion $c = 6$ kPa. Bottom: plastic areas if c is increased to 12 kPa, e.g. by drying of the soil (ϕ remains at 31°).

strategy at normal soil conditions in field traffic. At very wet soil conditions, it is difficult, even with this strategy, to prevent traffic-induced damage to the subsoil. Of course, the solutions in Fig. 1 are only estimates: perfectly elastic behaviour of soil is very rare, and the presence of plastic regions changes the stress and strain fields found by assuming complete elastic behaviour. The finite element method (FEM) which is very promising (Kirby, 1989) is less sensitive to non-elastic phenomena.

The above methods need information on soil: the selection of a piece of land in the first method and c and ϕ values in the second. Methods that only provide stress fields, irrespective of soil properties, are also useful, because the stress level that a tyre produces in the soil is generally considered to be a measure of the hazard to soil structure in field traffic. The following sections present soil stresses underneath tyre centres which have been calculated from vertical wheel load and tyre inflation pressure, and stresses which have been measured.

MEASURED AND PREDICTED STRESSES UNDER TYRES

General

The stress on a surface element of the contact surface between a deflecting tyre and a rigid soil will have a vertical normal component and a horizontal shear component. The normal component is related to vertical wheel load through tyre inflation pressure and carcass stiffness. The shear component arises from the ever existing relative movements between the rolling and deflecting tyre and the rigid soil and from wheel slip. These stress components cause a state of stress at each point in the soil near the interface. The assumption of rigidity of the soil means that such stress states nowhere equal soil resistance to plastic deformation. In many cases, soil strength cannot resist these stress states and soil is permanently deformed.

Burt et al. (1987) installed stress transducers in tyres to measure normal and shear stresses in the soil–tyre contact surface of tractor tyres. Aiming at information on many tyres, we followed an alternative approach and measured soil stresses at a certain distance below the soil–tyre interface. Schoenmakers and Koolen (1987) demonstrated in a laboratory experiment that this can be achieved in an accurate way at the interface of soil layers of contrasting stiffness if flat-box type transducers are placed in the harder layer and have their sensitive surfaces flush with the boundary between the hard and soft layers. Their test programme included soil–wheel systems in which rut depths were virtually zero, intermediate, or very large. Van den Akker and Carsjens (1989) applied this approach in field conditions and concluded that stresses measured in this way are sufficiently accurate. We made stress measurements with transducers placed in a rigid horizontal plate, which was installed at depths of 15 or 30 cm in field soils that were always strong enough

209

to prevent tyre rut formation. It was assumed that the measurements made at a depth of 30 cm mainly reflected effects of wheel load and tyre inflation pressure, and that measurements at a depth of 15 cm provided information on contact stress distribution, especially with large tyre sizes and high wheel loads.

The theory to predict stress level below tyres may be simple when vertical wheel load and tyre inflation pressure are the only variables considered and prediction is confined to soil–wheel systems with significant tyre deflection and zero or near-zero rut depths. We used the elastic solution for a uniformly loaded circular area (stress q) on a medium, modified by Fröhlich's concentration factor ν (Koolen and Kuipers, 1983, p. 36), and tried to have a correct stress level near the surface by relating the stress q to tyre inflation pressure, tyre carcass stiffness, and tyre–soil interface shear stresses via a simple rule of thumb. Predicted stresses were compared with the stresses measured at a depth of 30 cm.

The normal stress distributions that were measured at a depth of 15 cm were intended to provide insight into the normal stress distribution in the contact surface of large tyres. We related the normal stresses measured at a depth of 15 cm to tyre contact normal stresses via the summation procedure followed by Söhne (1953).

Theory

Applying soil–rubber friction theory and Mohr–Coulomb soil failure theory, Koolen and Kuipers (1983, pp. 88–90) deduced for an 'average' soil–tyre system that the major principal stresses in the soil near the contact surface are not perpendicular to the contact surface and equal 1.4 times the normal stresses at the contact surface. Bailey and Burt (1988) measured an average ratio of 1.46 in a test programme including different slip percentages and multiple tyre passes. Therefore, we stated that the major principal stresses at the contact surface can be approximated by 1.4–1.5 times the normal stresses. To account for carcass stiffness, we assumed that mean normal stress in the contact surface of a deflected tyre equals 1.2–1.3 times tyre inflation pressure. Combining both approximations gives the following rule of thumb: mean major principal stress at the contact surface can be approximated as twice the tyre inflation pressure. As the approximations are rough, this rule of thumb also gives rough estimates: it can only provide the level of stress near the contact surface.

The contact surface is usually arched and without clear boundaries. We assumed that the contact surface is: (i) plane, horizontal and circular; (ii) loaded by a stress distribution consisting of uniformly distributed normal stresses q equal to the level of the major principal stresses near the contact surface; (iii) of such a size that the product of its size and the normal stress q

equals the vertical load that is exerted by the tyre on the soil. If the above assumptions are introduced in the elastic solution for a uniformly loaded circular area (stress q) on a medium with concentration factor v, then

$$\sigma_z = q \cdot (1 - \cos^v \{\arctan [(1/z) \cdot (P/\pi q)^{1/2}]\}) \tag{1}$$

where σ_z is the major principal stress σ_1 under wheel centre at depth z and P is vertical wheel load. This formula correctly estimates: (i) the stress level under the tyre at shallow depths (for zero depth, $\sigma_z = q$; the stress level by definition); (ii) the stress level in soil at great depths because the deeper soil experiences the wheel as a vertical point load (P) equal to q multiplied by the contact surface area (it is known that influence of wheel pull, or towing force, vanishes relatively rapidly with depth). Therefore it may be expected that the formula also gives acceptable estimates for intermediate depths.

Using the rule of thumb that q equals twice the tyre inflation pressure p_i, and giving v a value of four, we calculated σ_z–z relationships by applying eqn. (1) to a wide range of wheel loads and tyre inflation pressures. The calculation results are presented in Fig. 2. The curves account for tyre size implicitly because one of the assumptions was that contact size multiplied by normal contact stress equals vertical wheel load.

Stress distribution in the tyre–soil contact surface is manifested in the stress distribution on any imaginary horizontal plane under the tyre if, relatively, plane depth is shallow and tyre size is great. We calculated stress distributions on such a plane for a number of assumed contact surface stress distributions with Söhne's summation procedure. Comparison of these calculated distri-
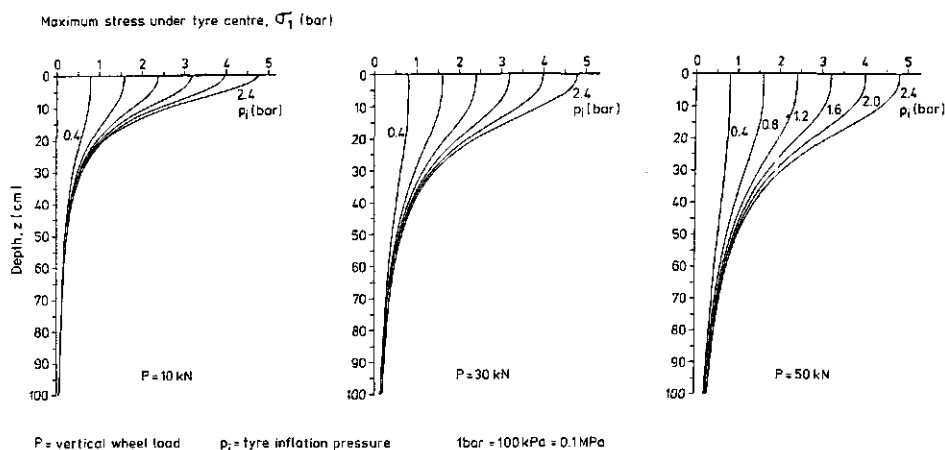

Fig. 2. Calculated maximum stresses under tyres as a function of depth, for different wheel loads and tyre inflation pressures.

butions with a measured distribution on such an imaginary plane will show which assumed soil–tyre contact stress distribution is closest to reality.

Experiments

Five stress transducers were installed in the upper part of a rigid plate with their sensitive areas flush with the upper plate surface (see Fig. 3). Each transducer (Model SA-E, Sensotec, Columbus, OH) had a 5 cm diameter sensitive area with a capacity of 0–3.5 bar. The signals of the strain gauge-type transducers were led to a computer (measuring frequency: 100 or 330 Hz) or to a U-V recorder. The rigid plate with transducers was placed horizontally at a certain depth in field soil. Soil near and above the plate was compacted in order to avoid rut formation by passes of test vehicles. The measuring programme included two plate depths: one at which depth of sensitive areas was about 30 cm, and one at which this was about 15 cm. Vehicle test runs were performed in such a way that one wheeling was approximately above the plate centre, and perpendicular to the row of transducers. We used different plate sizes and spacings between transducers, depending on tyre size and measur-
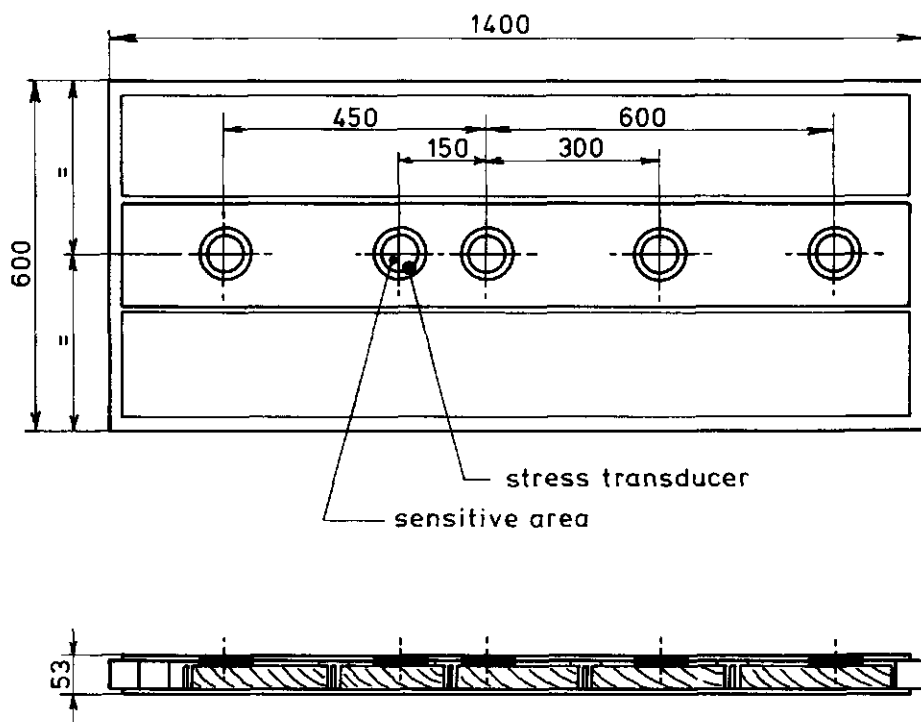

Fig. 3. Measuring plate with stress transducers (all measurements are in millimetres).

212

TABLE 1

Measurements of peak stress at a depth of 30 cm under tyres of commercial agricultural vehicles

Test no.	Location[1]	Type of traffic[2]	Vehicle weight (kg)	Wheel no.	Tyre size	Wheel load (kg)	Inflation pressure (bar)	Measured stress (bar)	Predicted stress (bar)	No. of measurements
1	A	Small Veenhuis tank, full load, low pressure	10660	1	Michelin 12.4 R 28	760	1.5	0.35	0.47	5
				2	Michelin 16.9 R 38	2185	1.4	0.95	1.07	3
				3,4	Vredestein 20/70-20 16 pr	2385	1.2	1.4	1.07	6
2	A	Small Veenhuis tank, full load, high pressure	10660	1	Michelin 12.4 R 28	760	1.5	0.35	0.47	5
				2	Michelin 16.9 R 38	2185	1.9	1.2	1.6	1
				3,4	Vredestein 20/70-20 16 pr	2385	2.7	1.85	1.34	2
3	A	Terra Gator 2004, full load	22220	1	Good Year 66×43-25 STG 10 pr	4260	0.7	1.05	1.07	1
				2	Good Year 66×43-25 STG 10 pr	6850	1	1.3	1.58	2
4	A	JKG 22-3, half load, low pressure	19114	1	Kleber 13.6 R 28	1242	1.5	0.6	0.71	4
				2	Good Year 18.4 R 38	2737	1.1	1	1.13	2
				3,4,5	Michelin 24 R 20.5 XS	2789	0.8	0.8	0.98	6
5	A	JKG 22-3, full load, low pressure	36354	1	Kleber 13.6 R 28	1477	1.5	0.7	0.81	3
				2	Good Year 18.4 R 38	3356	1.3	1.8	1.36	1
				3,4,5	Michelin 24 R 20.5 XS	4448	1	1.5	1.36	3
6	A	JKG 22-3, full load, high pressure	36354	1	Kleber 13.6 R 28	1245	1.5	0.55	0.71	3
				2	Good Year 18.4 R 38	2148	1.7	1.25	1.11	1
				3,4,5	Michelin 24 R 20.5 XS	4928	1.7	2.2	1.9	3
7	A	Ginaf truck 8×8, full load	39300	1	Michelin 24 R 20.5 XS	3950	3.1	1.7	2.04	1
				2	Michelin 24 R 20.5 XS	3950	3.1	1.7	2.04	1
				3	Michelin 24 R 20.5 XS	6670	3.5	2.7	3.05	1
				4	Michelin 24 R 20.5 XS	5080	3.1	2.2	2.44	1
8	B	L combination, not loaded	9890	1	Pirelli TM 300 S 16.9 R 24	1140	0.8	0.50	0.58	3
				2	Pirelli 300 S 18.4 R 38	1980	0.8	0.77	0.83	3
				3	Vredestein 20.0/70-20 16 pr	735	0.8	0.51	0.42	3
				4	Vredestein 20.0/70-20 16 pr	1090	0.8	0.58	0.56	3

213

No.	System[1]	Description	Total weight	Axle	Tyre	Load				Passes
9	B	H combination, not loaded	9350	1	Pirelli TM 200 13.6 R 24	1110	1.6	0.55	0.66	3
				2	Pirelli TM 300 S 14.9 R 38	1920	1.6	0.98	1.02	3
				3	Vredestein 16.0/70-20 10 pr	605	2.4	0.51	0.40	3
				4	Vredestein 16.0/70-20 10 pr	1040	2.4	0.65	0.66	3
10	B	L combination, loaded	17840	1	Pirelli TM 300 S 16.9 R 24	995	0.8	0.47	0.52	3
				2	Pirelli 300 S 18.4 R 38	2725	0.8	0.93	0.98	3
				3	Vredestein 20.0/70-20 16 pr	2350	0.8	1.20	0.91	3
				4	Vredestein 20.0/70-20 16 pr	2850	0.8	1.20	1.00	3
11	B	H combination, loaded	17270	1	Pirelli TM 200 13.6 R 24	940	1.6	0.45	0.57	3
				2	Pirelli TM 300 S 14.9 R 38	2660	1.6	1.19	1.29	3
				3	Vredestein 16.0/70-20 10 pr	2295	2.4	1.61	1.29	3
				4	Vredestein 16.0/70-20 10 pr	2740	2.4	1.54	1.48	3
12	C	Caterpillar Challenger 65	14060		Mobil Track System	Wheel peak stress:		0.62		18
						Between wheels:		0.4		15
13	D	Farmer-tank 6800 l, one axle		3	De Molen 21.080×20	3705	2.7	2.4	2.07	1
14	D	Kaweco 8000 l, one axle		3	LIM lgp 66×43-25	5900	1.4	1.5	1.97	1
15	D	Kaweco 13000 l, two axles		3,4	Trelleborg 700×26.5 8pr	3950	1.4	1.8	1.65	2
16	D	Kaweco 16000 l, two axles		3,4	Michelin 24 R 20.5	5600	2.4	2.5	2.56	2
17	D	Kaweco 18000 l, three axles		3,4,5	Michelin 24 R 20.5	4300	1.7	2	1.9	3

[1] A, Grubbenvorst; B, Slootdorp; C, Lelystad; D, Heelsum.

[2] L and H refer to traffic systems used in Vermeulen and Klooster (1992).

ing depth. Figure 3 shows the plate dimensions and transducer positions for the measurements at a depth of 15 cm. During a vehicle pass, the stress on each transducer was continuously measured as a function of time. These stress–time relationships could be transformed into stress distributions under tyres on the horizontal plane at the measuring depth, using the vehicle speeds which were also measured. Evaluation of the measurements at a depth of 30 cm was limited to the peak vertical normal stress; evaluation of the measurements at a depth of 15 cm considered the complete distribution.

Four test series with commercial types of field traffic were run, each at a different location (Grubbenvorst (A), Slootdorp (B), Lelystad (C), Heelsum (D)). Soils were sandy at A, B, and D, and clayey at C. Measuring depth was about 30 cm. The measuring plate was buried at the boundary between the top layer that is ploughed each year and the ploughpan in the subsoil. Although the refilled soil was compacted to avoid significant rut formation, the subsoil and the plate were more rigid than the refill, making the stress measurements reliable. Table 1 presents test number, location, type of traffic, vehicle weight (summed weight in the case of vehicle combination), wheel number (front wheel is 1, etc.), tyre size, wheel load, inflation pressure, peak stress determined from the stress distribution measured at a depth of approximately 30 cm. Numbers 1, 2, 4, 5, 6, 13, 14, 15, 16 and 17 were tests with trailed slurry tankers pulled by tractors. Numbers 8, 9, 10 and 11 involved trailed agricultural dumpers. The trailers had one, two, or three axles. The test runs 13–17 did not include measurements from beneath tractor tyres. Test numbers 3 and 7 were run with self-propelled tankers. Test numbers 4, 5 and 6 involved a tractor–slurry tanker combination equipped with CTIS (central tyre inflation system). Also, the tank of this combination was shifted 90 cm forward in order to transfer weight to the tractor ('field mode'). The table includes, for comparison, measurements at a depth of 30 cm from a test run (12) with a Caterpillar Challenger 65 with a Mobil Track System (Caterpillar, Peoria, IL).

One test series was run with large and wide tyres, using the IMAG single-wheel tester (Institute of Agricultural Engineers, Wageningen, Netherlands). This series, in which stress measurements were taken from the 15 cm depth, included runs with a Good Year 66×43-25 Terra Tire Super terra grip (diagonal nylon carcass, 6 ply rating) and a LIM LGP 66×43-25 polyurethane tyre (radial carcass). Because lug effects were significant for this measuring depth, lug effects in the measuring results were eliminated by an averaging procedure applied to repeated wheel passes with different lug positions. In all test series, travelling speed was about 5 km h^{-1}.

215

30 cm depth measurements

The peak vertical normal stress, derived from a measured stress distribution, will be nearly equal to the maximum of σ_1 at the measuring depth, because no significant horizontal forces acted on the wheels in these tests (a horizontal wheel force occurs where a driven wheel has to pull or where a towed wheel has a non-zero rolling resistance). Table 1 presents vertical normal peak stresses measured under tyres at a depth of approximately 30 cm. The table also presents predicted stresses for corresponding depths. These stresses were calculated from vertical wheel load and tyre inflation pressure using eqn. (1), with $q = 2p_i$, and $\nu = 4$. The calculated stresses are plotted against measured stresses in Fig. 4. Deviations tended to be relatively large with very stiff or very flexible tyre carcasses and 'over-inflated' tyres. The degree of confirmation between the measured and predicted stresses may be considered as very reasonable. This may have occurred because the effects of some disturbing factors counteracted each other: one would expect that the measured stress would be greater than the predicted stress owing to the presence of a relatively rigid subsoil.

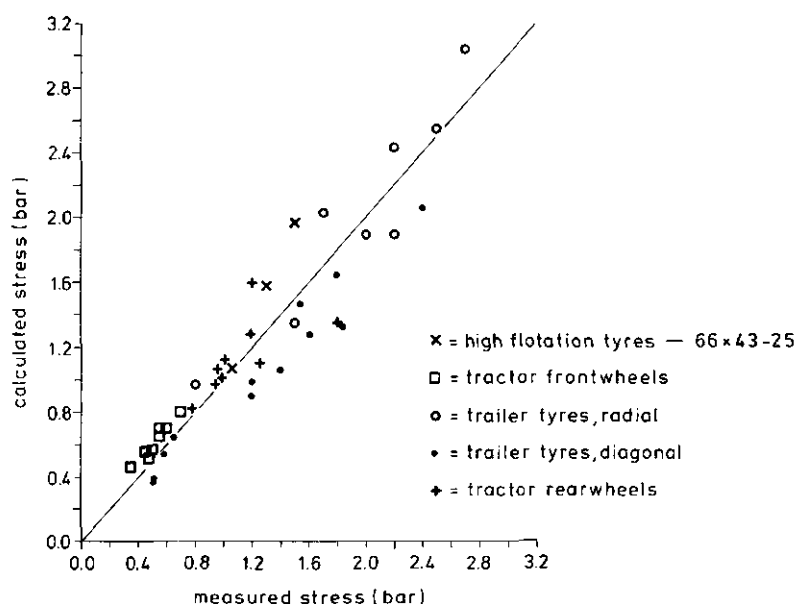The choice of a concentration factor $\nu = 4$ is rather arbitrary. We examined

Fig. 4. Measured and calculated peak stresses for the 30 cm depth under tyres of commercial agricultural vehicles.
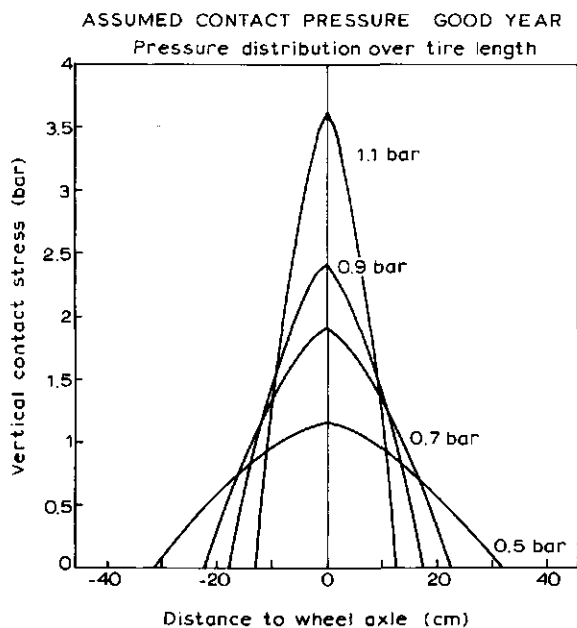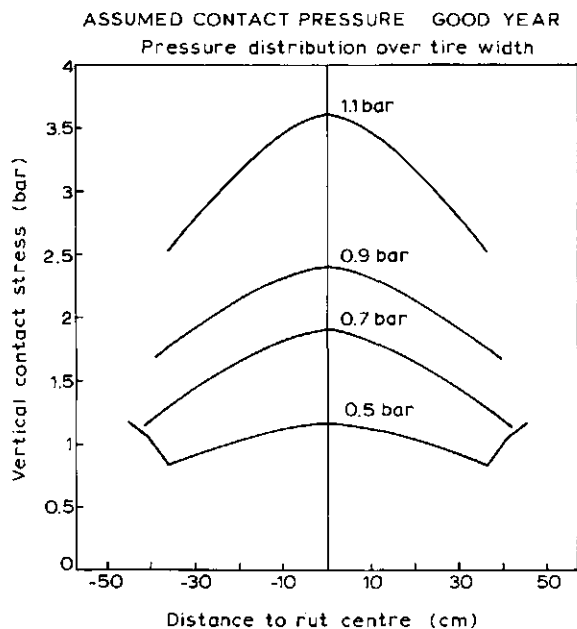
216

Fig. 5. Estimated contact stress distributions of a Good Year 66×43-25 Terra Tire at a wheel load of 4000 kg and inflation pressures of 0.5, 0.7, 0.9 and 1.1 bar (see text).
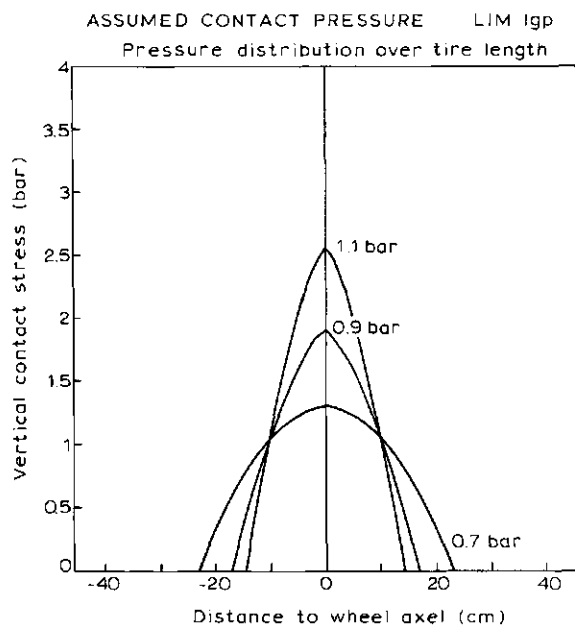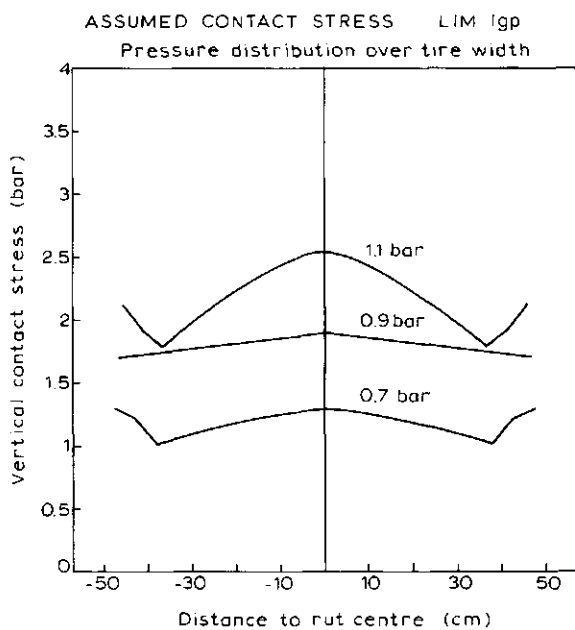
217

Fig. 6. Estimated contact stress distributions of a LIM LGP 66 × 43-25 polyurethane tyre at a wheel load of 4000 kg and inflation pressures of 0.7, 0.9 and 1.1 bar (see text).
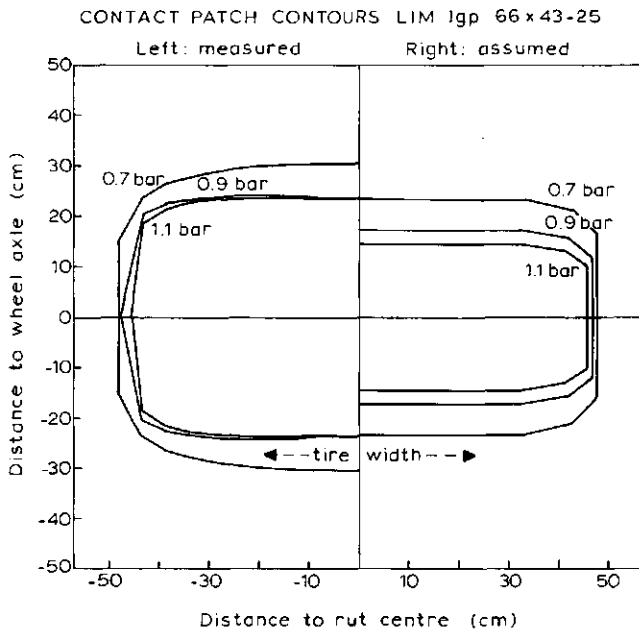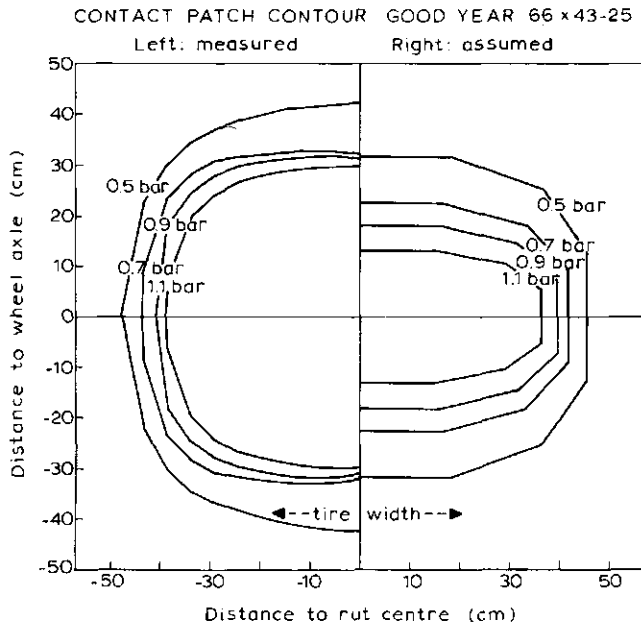
218

Fig. 7. Contact surfaces: measured on concrete (left); assumed in the estimations presented in Figs. 5 and 6 (right).

219

this choice by calculating the mean (absolute) difference between predicted and measured stress values as a percentage of the calculated stress values, for a range of ν values. The resulting ν vs. mean difference relationship had a minimum (13.5%) at $\nu=3.9$. The mean difference at $\nu=4$ was 13.8%.

We also made calculations for q/p_i ratios other than two. It became apparent that the calculated results for the 30 cm depth were not very sensitive to this ratio.

15 cm depth measurements

The ratio of measuring depth to contact surface size is small in this test series, so that the measured distribution of vertical normal stresses reflects the distribution of the vertical normal stresses at the contact surface rather than the distribution of σ_1 at the contact surface. The measurements made at the 15 cm depth are more influenced by the presence of the measuring plate than the 30 cm depth measurements because the plate was not placed at the interface of soil layers of contrasting stiffness. The measurements showed significant lug effects. We smoothed the measured 15 cm depth distributions to eliminate these lug effects.

Because of the above disturbances, the following results are more qualitative than quantitative. Using Söhne's summation procedure, we derived by trial and error, hypothetical tyre–soil contact stress distributions that were compatible with the measured 15 cm depth distributions. Figures 5 and 6 present these hypothetical tyre–soil contact stress distributions. The shapes of the assumed contact surfaces in these calculation procedures were derived from contact area measurements from tyres on a concrete surface (Fig. 7). The sizes of the assumed contact surfaces had to be selected smaller than the measured contact surfaces in order to obtain compatibility. This indicates the existence of near-zero contact stresses at a front part and a rear part of the contact surface. It may be concluded from Figs. 5 and 6 that the diagonal rubber tyre produces higher peak contact stresses than the radial polyurethane tyre.

CONCLUSION

Equation (1) predicts the maximum stress–depth relationship under wheels from the input parameters vertical wheel load and tyre inflation pressure. Prediction was satisfactory for $q/p_i=2$, $\nu=4$, zero rut depth, non-significant horizontal wheel force, and soil top layers overlaying more rigid subsoil. Vertical wheel load and tyre inflation pressure are not the only variables of soil–wheel systems. These systems also depend on factors such as tyre deformation–contact stress relations, tyre dimensions, pull, rolling resistance and soil stress–strain–strength behaviour as a function of depth.

The interesting question of what is the most important parameter after vertical wheel load and tyre inflation pressure?, is still not answered. Figures 5 and 6 show that contact stress distributions can differ much for different tyre constructions.

REFERENCES

Bailey, A.C. and Burt, E.C., 1988. Soil stress states under various tire loadings. Trans. ASAE, 31: 672–676, 682.
Burt, E.C., Bailey, A.C. and Wood, R.K., 1987. Effects of soil and operational parameters on soil–tire interface stress vectors. J. Terramech., 24: 235–246.
Kirby, J.M., 1989. Shear damage beneath agricultural tyres: a theoretical study. J. Agric. Eng. Res., 44: 217–230.
Koolen, A.J. and Kuipers, H., 1983. Agricultural Soil Mechanics: Advanced Series in Agricultural Sciences 13. Springer, Heidelberg, 241 pp.
Lerink, P., 1990. Prediction of the immediate effect of traffic on field soil qualities. Soil Tillage Res., 16: 153–166.
Schoenmakers, A.J.J.M. and Koolen, A.J., 1987. Measuring traffic-induced stresses at the interface of soil layers of contrasting stiffness. Proceedings of the 9th International Conference of the International Society for Terrain-Vehicle Systems, Barcelona, Vol. 1, pp. 267–274.
Söhne, W., 1953. Druckverteilung im Boden und Bodenverformung unter Schlepperreifen. Grundlagen Landtechnik, 5: 49–63.
Van den Akker, J.J.H., 1988. Model computation of subsoil stress distribution and compaction due to field traffic. Proceedings of the 11th International Conference of ISTRO, Edinburgh, UK, Vol. 1, pp. 403–407.
Van den Akker, J.J.H. and Carsjens, G.J., 1989. Reliability of pressure cells to measure traffic-induced stress in the topsoil–subsoil interface. Proceedings of the 4th European Conference of the International Society for Terrain-Vehicle Systems, Wageningen, Netherlands, Vol. 1, pp. 1–7.
Van den Akker, J.J.H. and Lerink, P., 1990. Verandering van bodemkwaliteiten door berijding. (Change of soil qualities by traffic). Themaboekje Management Bodemstructuur. IMAG, Wageningen, pp. 25–44 (in Dutch).
Vermeulen, G.D. and Klooster, J.J., 1992. The potential for application of a low ground pressure traffic system to reduce soil compaction on a clayey loam soil. Soil Tillage Res., 24: 337–358.